# Roles of Post-Transcriptional Gene Silencing

in the Functional Regulation of

Neuronal Gene Expression and Plasticity

Belinda Jane Goldie

BBiomedSci (Hons)

Doctor of Philosophy (Medical Biochemistry)

University of Newcastle, Australia

August 2014

THE UNIVERSITY OF
NEWCASTLE
AUSTRALIA

<u>DECLARATION</u>

Statement of Originality

This thesis contains no material which has been accepted for the award of any other degree or diploma in any university or other tertiary institution and, to the best of my knowledge and belief, contains no material previously published or written by another person, except where due reference has been made in the text. I give consent to this copy of my thesis, when deposited in the University Library, being made available for loan and photocopying subject to the provisions of the Copyright Act 1968.

Statement of Collaboration

I hereby certify that the work embodied in this thesis has been done in collaboration with other researchers, or carried out in other institutions. I have included as part of the thesis a statement clearly outlining the extent of collaboration, with whom and under what auspices.

Statement of Authorship

I hereby certify that the work embodied in this thesis contains published papers of which I am a joint author. I have included as part of the thesis a written statement, endorsed by my supervisor, attesting to my contribution to the joint publications.

Thesis by Publication

I hereby certify that this thesis is submitted in the form of a series of published papers of which I am a joint author. I have included as part of the thesis a written statement from each co-author; and endorsed by the Faculty Assistant Dean (Research Training), attesting to my contribution to the joint publications.

_____   _____

Belinda J Goldie   **Date**

ABSTRACT

The phenomenon of synaptic plasticity in neurons is poorly understood, but is known to rely on appropriate temporo-spatial availability of mRNA. The complexity of neuronal cytoarchitecture necessitates an exquisite regulatory matrix that begins with the establishment of subcellular compartments during differentiation, however the molecular mechanisms that support trafficking and translational control are not well defined. The class of short, non-coding RNA molecules known as microRNA (miRNA) have well-established roles in neuronal differentiation and development, and growing evidence suggests that miRNA-mediated post-transcriptional gene silencing (PTGS) may be an important mediator of synaptic plasticity. To investigate this in a human genetic context, techniques were established for isolating distinct subcellular fractions of the SH-SY5Y neuroblastoma cell line and examining genome-wide miRNA and mRNA responses to neuronal cues such as differentiation and depolarisation. These studies identified a pattern of activity-associated miRNA expression changes unique to the neurites that was revealed to be connected to the release of exosomes from this compartment. Interestingly, some miRNA were found to be preferentially enriched in the nucleus. A motif detected within these sequences lead to the unexpected identification of putative transcription factor binding elements within their precursors, showing support for novel roles of miRNA outside PTGS. Connecting these findings was the unanticipated contribution of primate-specific miRNA, resulting in significant ontological enrichment of neuronal functionality. This demonstrates the importance and relevance of these cells as a vehicle for explicating the mechanisms underlying higher brain functions. Ultimately, substantial evidence was obtained to support a role for miRNA and the components of PTGS in the functional compartmentalisation of neurons and the response to activity, though further methodological developments are required to elaborate the novel mechanisms of miRNA function and investigate the direct contribution of miRNA-mediated PTGS to enabling real-time, activity-driven synaptic modification.

ACKNOWLEDGEMENTS

TABLE OF CONTENTS

LIST OF ABBREVIATIONS

3' UTR	3' Untranslated Region
AChE	acetylcholinesterase
AEBSF	4-(2-aminoethyl)benzenesulfonyl fluoride hydrochloride
Ago	argonaute
ALS	amyotrophic lateral sclerosis
ANOVA	Analysis of Variance
ATRA	all-trans retinoic acid
BDNF	brain-derived neurotrophic factor
Ca2+	Calcium
cAMP	cyclic adenosine mono-phosphate
CNS	central nervous system
co-IP	co-immunoprecipitation
CRM1	exportin-1 (XPO1)
CV	coefficient of variability
DABG	detection above background
DAVID	Database for annotation, visualization and integrated discovery
DCt	change in cycle threshold value (delta Ct)
DE	differential expression
DGCR8	DiGeorge syndrome critical region 8
DLPFC	dorso-lateral pre-frontal cortex
DMEM	Dulbecco's modified eagle medium
DTT	dithiothreitol
EDTA	ethylenediaminetetraacetic acid
eIF4b	elongation initiation factor 4b
ES	enrichment score
FAC	functional annotation clustering
FCS	fetal calf serum
FDR	false discovery rate
FOS	FBJ murine osteosarcoma viral oncogene homolog
GAP43	growth-associated protein 43
GATHER	gene annotation tool to help explain relationships

GPCR	g-protein coupled receptor
GRIA3/4	glutamate receptor, ionotropic, AMPA 3/4
GUSB	glucuronidase, beta
IPA	Ingenuity pathway analysis
iPSC	induced pluripotent stem cell
K+	Potassium
kDa	kiloDaltons
LAMP1	lysosome-associated membrane protein 1
LC-MS/MS	liquid chromatography-mass spectrometry
LDCV	large dense core vesicle
LE	localisation element
LTD	long-term depression
LTP	long-term potentiation
MAP1b	microtubule-associated protein 1b
MASCOT	Matrix Software program for protein identification from peptide mass
MAZ	myc-associated zinc finger protein
MEME	multiple EM for motif elicitation
miRNA	microRNA
MRE	miRNA recognition element
mRNA	messenger RNA
NGF	nerve growth factor
NPC	neural progenitor cell
NPY	neuropeptide Y
NTRK2	neurotrophic tyrosine kinase, receptor, type 2
p	p-value
P-body	processing body
PBMC	peripheral blood mononuclear cell
PBS	phosphate buffered saline
PCIAA	phenol chloroform isoamyl alcohol
PFC	pre-frontal cortex
pre-miRNA	precursor miRNA
pri-miRNA	primary miRNA
PSD	post-synaptic density
PTGS	post-transcriptional gene silencing

qPCR/qRT-PCR/RT-PCR	quantitative real-time PCR
RAR	retinoic acid receptor
RARE	retinoic acid response element
RBM4/10	RNA binding motif protein 4/10
RIN	RNA integrity number
RIP	RNA co-immunoprecipitation
RIP-seq	RNA co-immunoprecipitation followed by RNAseq
RISC	RNA-induced silencing complex
RMA	robust multichip algorithm
RNAi	RNA interference
RNAPII	RNA polymerase II
RNAseq	mRNA next-generation sequencing
RNP	ribonucleoprotein
ROBO1/2	roundabout, axon guidance receptor, homolog 1/2
RRM	RNA recognition motif
rRNA	ribosomal RNA
SDS-PAGE	sodium dodecylsulfate polyacrylamide gel electrophoresis
snoRNA	small nucleolar RNA
STG	superior temporal gyrus
SYP	synaptophysin
TPA	phorbolester
TRBP/TARBP	trans-activation-responsive region RNA-binding protein
trkB	tyrosine receptor kinase B, encoded by NTRK2 gene

CHAPTER 1

Introduction

Thesis Overview

This dissertation is a thesis by publication, comprising the original intellectual contributions I have made to the literature during my candidature. Presented and discussed herein are the publications to which I have made extensive methodological, experimental and analytical contributions.

This introductory chapter describes the structure of the thesis and defines the scope of my project by presenting the rationale, hypotheses and aims that have directed and motivated my research since commencement of my candidature in 2011. My scientific vision was born from a simple statement I read during a literature review for my final year undergraduate research project, which investigated miRNA in relation to schizophrenia: that the cognitive defects associated with the disorder could be ascribed to failures in synaptic plasticity. It did not require much further investigation to realise that the mechanisms underlying synaptic plasticity are poorly understood. However the concept that temporo-spatial regulation of mRNA availability was critical piqued my interest, as the growing understanding of miRNA functionality suggested that these molecules could be uniquely poised to support this complex neuronal system.

These concepts are developed in the literature review included as the second chapter of this thesis. The opening section describes the sequence of discoveries that shaped our understanding of the synaptic specialisation, and the idea that the mechanisms regulating this complexity remain obscure. This is followed by an in-depth exploration of the current knowledge of the molecular mechanisms underpinning miRNA-mediated post-transcriptional gene silencing. The review closes with an integration of these concepts, proposing a hypothesis postulating miRNA as adapter molecules providing both flexibility and functional redundancy. It is thus the desire to understand miRNA within the context of functioning neuronal systems, and the molecular components that could support this biology, that have informed the hypotheses and experiments across my candidature.

The third chapter is methodology based and addresses a key issue in the field of molecular neurobiology: the human genetic context. The SH-SY5Y neuroblastoma

cell line is widely used, and misused, as a model of human neuronal function. Moreover, the results of cell culture based studies are often downplayed in favour of animal studies. This perspective article, which includes a systematic review of the SH-SY5Y literature, presents work I conducted to investigate the strength of these cells as a neuronal model, and functionally integrates genome-wide gene and miRNA expression profiled throughout differentiation, along with biochemical analysis of maturation. These findings, in combination with those from Chapter 4, provide compelling evidence of the robustness of the SH-SY5Y system.

Chapter 4 is the major publication arising from my candidature. Underlying the findings of this work, I established several key bench methodologies for subcellular neuronal miRNA analysis through adaptation and extensive validation, as well as strategies for analysing genome-wide data generated from disparate subcellular fractions. The latter were also integral to the work presented in Chapter 5. Using these techniques I was able to identify fraction-specific patterns of miRNA response to depolarisation, importantly involving many human- or primate-specific miRNA. I also showed for the first time that these cells release miRNA-enriched exosomes when depolarised and, through a collaboration I initiated, conducted a full proteomic analysis of these vesicles.

In Chapter 5 the focus changes to the nucleus, a compartment not conventionally associated with mature miRNA function. The transcriptional composition of the nucleus and cytoplasm are very different, and as such I hypothesised that a traditional differential expression analysis incorporating normalisation would obscure these differences. I therefore undertook three alternative bioinformatic analyses with validation to determine the most accurate method for analysing genome-wide data from distinct subcellular compartments. Furthering this analysis, I investigated two further hypotheses: the existence of a common sequence motif directing nuclear import; and that Argonaute-directed mechanisms might not entirely explain the nuclear miRNA abundance. To test the latter, I established a co-immunoprecipitation protocol along with RNAseq and devised methods to analyse these data.

The thesis discussion in Chapter 6 draws the findings from all chapters together in the context of the themes underlying my research. Importantly, the implications of depolarisation-associated miRNA dynamics are considered in the context of what is known about the biology of these molecules in schizophrenia, and the potential for future studies based on these findings is discussed. The findings regarding subcellular miRNA compartmentalisation are evaluated in terms of potential functional contributions, firstly to neuron-specific mechanisms such as synaptic plasticity, and then in the broader sense of non-canonical collaborations involving Ago-independent processes.

Following on from these chapters, appendices are included to provide supplementary materials relevant to each publication, where necessary. The final element to the thesis is a full bibliography, cataloguing each citation in the order they appear.

Rationale and Hypothesis

To create permanent change at the synapse, neurons require a mechanism for effecting more than just acute changes in protein synthesis, necessitating greater real-time control of mRNA availability at the synapse. Intracellular mRNA traffic and translation is highly regulated in eukaryotes, providing a complex temporo-spatial expression pattern within discrete subcellular compartments. The structures and mechanisms that support this complexity are not well understood. Initial studies of mRNA trafficking within neurons identified regulatory elements in the 3'-UTRs of transcripts that facilitated the attachment of carrier proteins as being the primary means by which targeted localisation is achieved. However in some cases it was identified that these localisation elements alone were not sufficient to direct appropriate trafficking, and it was postulated that other "unknown", trans-acting regulatory mechanisms must exist.

Also acting on the 3'UTR of mRNA, miRNA-mediated gene silencing is a compelling candidate for providing this regulation. The employment of a nucleic acid-driven system presents an alternative with considerable advantages over a protein-based system, where studies indicated a unique transporter protein is required for each individual mRNA. In particular, the requirement of only 7-8 nucleotides of sequence complementarity for target recognition provides the economy of a small number of molecules with the ability to regulate many transcripts, supporting the development of regulatory networks with common functional outputs. Moreover, the reversible interaction between the miRNA and its carrier Argonaute protein both delivers a flexible, reusable framework, and enables the components to respond to synaptic activation signals.

There is evidence to suggest that miRNA and the RNA interference pathway are integral in supporting functional compartmentalisation of neurons. This project was thus designed to test the hypothesis that miRNA are functionally compartmentalised in neurons, and are key regulators of activity-related neuronal functions including synaptic plasticity and communication.

Research Aims

Since their discovery, the contribution of individual miRNA to the development of specific diseases has been the subject of intense investigation. However the one-to-many nature of miRNA-target relationships suggests that, particularly in the complex intracellular environment of neurons, a systems biology approach to investigating broader regulatory networks may be more informative. It is also becoming apparent that the prevailing dogma of miRNA biogenesis and function may be incomplete. The importance of non-conserved targets and positively correlated miRNA-mRNA associations, two dimensions that are typically excluded from analyses, has recently been shown [1]; while studies have also indicated that processing of primary miRNA may occur outside the nucleus [2,3], and mature miRNA function may not be exclusive to the cytoplasm [4,5]. Thus, non-canonical aspects of miRNA function must also be considered.

Next generation sequencing has identified many genes and transcriptional networks unique to the human brain and enriched for neuronal processes [6]. In support of a key role for miRNA in assisting this functionality, brain specific miRNA have been shown to be involved in key aspects of neuronal development [7] and disease [8], and many of these are expressed only in primates or, even more narrowly, only in humans [9]. It is therefore important to develop an understanding of genome-wide, subcellular miRNA dynamics within a human model of neuronal function.

Aim 1

The first aim of this project was to establish techniques for purifying and analysing subcellular structures and protein complexes associated with RNA-directed trafficking and post-transcriptional regulation of post-synaptic translation.

The SH-SY5Y neuroblastoma cell line is commonly used as a model of human neuronal function, as it can be chemically induced to differentiate into populations closely resembling neurons [10-12]; for optimal emulation of cortical neurons this

is achieved through sequential treatment with ATRA and BDNF [13]. The dendritic fraction, termed neurites in these cells, has been isolated by differential centrifugation [14] and demonstrates neuron-like subcellular sorting of proteins [15]. Importantly, two vesicle populations have been identified in SH-SY5Y [16], one of which is characterised as neurotransmitter-containing large dense-core vesicles (LDCVs) [17]. The other smaller population has not been investigated, however their reported size suggests they may be exosomes, vesicles of approximately 100nm diameter that are known to contain miRNA and are receiving increasing attention in the fields of intercellular communication and neurobiology [18-20]. The first component of this aim was to establish and validate all these methodologies.

The second part of this aim required establishment of a method to identify post-transcriptionally regulated mRNA. Co-immunopreciptiation is used to identify mRNA transcripts associated with a specific protein; in the context of miRNA-mediated gene silencing this method can be employed to identify mRNAs that are paired with a miRNA through purification of Ago1- and/or Ago2-bound molecules [21,22]. The distinction between these proteins is important, as Ago2 contains an active slicer domain and is associated with transcript degradation, while Ago1 lacks this activity [23] and is associated with reversible gene silencing.

Aim 2
After establishing these techniques, the second aim was to investigate the relationship between activity-dependent mRNA translation and miRNA-mediated gene silencing in the post-synaptic compartment of neurons in vitro, and the functional significance of activity-associated miRNA and their protein targets in neurotransmission and memory formation.

With the ability to isolate various subcellular compartments, genome wide expression, and responses to cues such as differentiation and depolarisation, can be profiled by microarray or next generation sequencing. Normalised analysis and

validation of these results by more quantitative methods such as real-time qPCR are complicated by the uncertain subcellular distribution of genes normally used as reference [24]. Thus, analytical approach becomes an important dimension of this project.

List of Publications Included as part of thesis

Goldie BJ and Cairns MJ: **Post-transcriptional trafficking and regulation of neuronal gene expression.** *Molecular Neurobiology* 2012, **45**(1):99-108.

Goldie BJ, Barnett MM, Cairns MJ: **BDNF and the maturation of post-transcriptional regulatory networks in human neuroblast differentiation.** *Frontiers in Cellular Neuroscience* 2014, October 15;8:325.

Goldie BJ, Dun MD, Lin M, Smith ND, Verrills NM, Dayas CV and Cairns MJ: **Activity-associated miRNA are packaged in Map1b-enriched exosomes released from depolarised neurons**. *Nucleic Acids Research* 2014, 42(14):9195-208.

Goldie BJ, Atkins JR, Weidenhofer J and Cairns MJ: **A consensus miRNA sequence motif is associated with Ago2-specific nuclear localisation of neuronal mRNAs in human neuroblasts**. *Submitted.*

List of additional publications throughout candidature

Gupta P, Liu B, Wu JQ, Soriano V, Vispo E, Carroll AP, <u>Goldie BJ</u>, Cairns MJ and Saksena NK: **Genome-wide mRNA and miRNA analysis of peripheral blood mononuclear cells (PBMC) reveals different miRNAs regulating HIV/HCV co-infection**. *Virology* 2014, **450-451**(C):336-49.

Quinn R, Brown A, <u>Goldie BJ</u>, Levi E, Dickson P, Smith D, Cairns MJ and Dayas CV: **Distinct miRNA Expression in the Dorsal Striatal Subregions Associated with Risk for Addiction in Rats.** *Translational Psychiatry*, In Press*.*

Hollins SL, <u>Goldie BJ</u>, Carroll AP, Mason EA, Walker FR, Eyles DW and Cairns MJ: **Ontogeny of small RNA in the regulation of mammalian brain development.** *BMC Genomics* 2014, Sep 9;15:777.

CHAPTER 2

Literature Review

STATEMENT OF CONTRIBUTION OF OTHERS

<u>Goldie BJ</u> and Cairns MJ: **Post-transcriptional trafficking and regulation of neuronal gene expression.** *Mol Neurobiol* 2012, **45**(1):99-108.

*I attest that Research Higher Degree candidate **Belinda Goldie** was the primary contributor to the development of this publication. This extensive contribution included: synthesising and developing the intellectual scope of the literature review, and writing the manuscript in full.*

_____

Belinda J Goldie (candidate)

_____

Murray J Cairns (supervisor)

_____   _____   __05/08/2014_____

Professor Robert Callister   **Date**

Assistant Dean Research Training (ADRT)

Post-Transcriptional Trafficking and Regulation of Neuronal Gene Expression

Belinda J. Goldie · Murray J. Cairns

Abstract Intracellular messenger RNA (mRNA) traffic and translation must be highly regulated, both temporally and spatially, within eukaryotic cells to support the complex functional partitioning. This capacity is essential in neurons because it provides a mechanism for rapid input-restricted activity-dependent protein synthesis in individual dendritic spines. While this feature is thought to be important for synaptic plasticity, the structures and mechanisms that support this capability are largely unknown. Certainly specialized RNA binding proteins and binding elements in the 3′ untranslated region (UTR) of translationally regulated mRNA are important, but the subtlety and complexity of this system suggests that an intermediate "specificity" component is also involved. Small non-coding microRNA (miRNA) are essential for CNS development and may fulfill this role by acting as the guide strand for mediating complex patterns of post-transcriptional regulation. In this review we examine post-synaptic gene regulation, mRNA trafficking and the emerging role of post-transcriptional gene silencing in synaptic plasticity.

Keywords MicroRNA · Gene silencing · Synaptic plasticity · Dendritic spines · Memory

B. J. Goldie · M. J. Cairns (✉)
School of Biomedical Sciences and Pharmacy,
Faculty of Health and the Hunter Medical Research Institute,
The University of Newcastle,
University Drive,
Callaghan, NSW 2308, Australia
e-mail: murray.cairns@newcastle.edu.au

B. J. Goldie · M. J. Cairns
Schizophrenia Research Institute,
405 Liverpool St,
Darlinghurst, NSW 2010, Australia

Introduction

Through its network of dendritic and axonal connections, an individual neuron may integrate information from thousands of cells. How it accomplishes this amazing feat of engineering remains a great unknown of neurobiology. What is known is that the establishment of long-term potentiation (LTP) or long-term depression (LTD) at these connections involves a combination of post-translational modification of synaptic protein and subtle changes in gene expression. While real-time changes in protein structure and function are easily reconciled, it is more difficult to imagine how a single transcriptional apparatus could respond to discrete stimuli from so many connections in a timely manner. We now know that to overcome this problem, a significant proportion of activity-associated expression is post-transcriptionally regulated in the dendritic spines of post-synaptic neurons. Understanding how this complex and dynamic temporospatial pattern can be established and encoded in functioning neurons represents a challenging biological problem. In this review, evidence and mechanisms for post-transcriptional regulation of post-synaptic gene expression are examined in the context of new information about the role of small non-coding RNA, known as microRNA.

Part I—Gene Expression and Synaptic Plasticity

In a functioning neural network, individual post-synaptic termini require the capacity to respond to direct stimuli with high specificity in real-time. While a small supply of inactive protein precursors can be maintained in the synaptic compartment, the logistics of managing activity-dependent post-translational modification of a large number of polypeptides has significant

13

limitations. A more elegant solution is to have encoded messages present with localized translational machinery, such that peptides can be synthesized as required.

Post-synaptic Protein Synthesis

Early evidence of localized synaptic protein synthesis, the visualization of clustered ribosomes (polyribosomes) associated with the bases of dendritic spines [1], was later confirmed within isolated synaptosomes by the incorporation of radio-labeled amino acids into nascent peptides synthesized within this fraction [2]. Appearance of the labeled peptides in the synaptic membrane and post-synaptic density within 15 min of activity supported the local synthesis hypothesis, since proteins synthesized deep in the soma of a neuron could take hours to arrive at the synapse [3]. Mitochondria, themselves capable of protein synthesis, were excluded as the source of the newly synthesized peptides by differential treatment with eukaryotic and mitochondrial protein synthesis inhibitors, confirming that translation of these new peptides is indeed driven by ribosomes [4, 5].

Together these findings provide strong support for localized, on-demand synaptic protein synthesis, and to confirm that this is triggered in response to biologically relevant stimuli, Feig and Lipton demonstrated de novo dendritic protein synthesis after electrical excitation [6]. Further investigation of LTP suggested that the same signals driving axon guidance and synapse formation during development might also be involved in activity-dependent synaptic plasticity in the adult brain [7]. Supporting this hypothesis, the level of BDNF messenger RNA (mRNA) was found to increase markedly in response to electrical activity [8], evoking a proportional increase in electrical potentiation, with more rapid onset of potentiation and decreased time to elicit a 25% increase in synaptic strength [9]. This reciprocal relationship between electrical and neurotrophic signals was found to be associated with both short-term and long-term regulation of neuronal signaling (reviewed in [8]), making the neurotrophins good candidates for ongoing modulators of synaptic strength.

While these observations support the hypothesis that mRNA is actively translated into protein in dendritic spines, how is untranslated mRNA made available at the synapse in response to incoming signals?

Neuronal mRNA Traffic

Transcription, with the exception of mitochondrial encoded genes, takes place almost exclusively in the nucleus, such that synaptic mRNA must be transported large distances from this central organelle, through the dendritic tree to the dendritic spines. This poses several key logistical questions: What regulatory mechanisms are in place to ensure the correct transcripts arrive at the appropriate spines? What cellular machinery enables the mRNA to be trafficked? And importantly, how is translation suspended until the destination is reached? Detailed observation of hippocampal neurons in culture has revealed evidence of mRNA sorting even at early developmental stages (Fig. 1) [10, 11]. During the first 24 h, growing neurons sprout several minor processes in vitro that are not discernible as either axons or dendrites. The axon is the first process to extend, and its growth is rapid compared with that of dendrites. As such, polyA mRNA is found extensively at the active growth cone; there is little or no labeling of dendrites. After the axon is completed, elaboration of the dendritic tree begins. Compartmentation becomes obvious, as mRNA is no longer detectable in the axon, while labeling over the dendrites increases as the tree continues to expand.

The appropriate redistribution of selective mRNA in response to specific stimuli requires an address sequence encoding the destination, and a chaperone to prevent ectopic translation en-route to the synapse. In support of this hypothesis, Steward and colleagues [12] followed the induction of mRNA for the immediate-early gene (IEG) Arc (activity-regulated cytoskeleton-associated protein) in response to synaptic activity. Arc mRNA was found to localize specifically in electrically stimulated post-synaptic dendrites, but more importantly this targeting continued when protein synthesis was abolished, suggesting the localization was signaled from within the mRNA sequence [13]. Address sequences known as *cis*-acting, or localization, elements (LEs) have been established for several other compartmentally enriched mRNA by observing disrupted localization resulting from specific deletions or antisense molecules. A 54-nucleotide conserved element in the 3′-untranslated region (UTR) of the β-actin transcript was found to direct the localization of the mRNA to growth cones of cultured neurons in response to neurotransmitter (NT-3) stimulation. With anti-sense inhibition of the zipcode sequence, the neurotransmitter still elicited an increase in β-actin mRNA synthesis; however, this RNA interference prevented the formation of a *trans*-acting ribonucleoprotein (RNP) complex with Zipcode Binding Protein-1 (ZBP1), and the transcript was confined to the soma [14].

Similar *cis*-acting elements have been reported in the 3′-UTRs of other spatially regulated transcripts including myelin basic protein (MBP) in oligodendrocytes [15], elongation factor 1α [16], microtuble-associated protein 2 (MAP2) [17], and the α-subunit of calmodulin-dependent protein kinase 2 (CaMKIIα) [18]. In the latter two cases, however, the targeting element identified is not the sole determinant of localization, suggesting the existence of a more complex system for regulating the expression of genes after transcription. LEs of 640 and 94 nucleotides in the 3′-UTRs of MAP2 and CaMKIIα, respectively, were found to

Fig. 1 Development of compartmentation in neurons. Neurons establish compartments very early during differentiation. Rapid growth of the axonal process results in heavy labelling of polyA mRNA over the growth cone during this period, but this is redistributed into the dendritic arbor when branching begins. In mature neurons, several protein markers can be used to identify the different types of process, demonstrating that each of the compartments has cultivated unique translational requirements
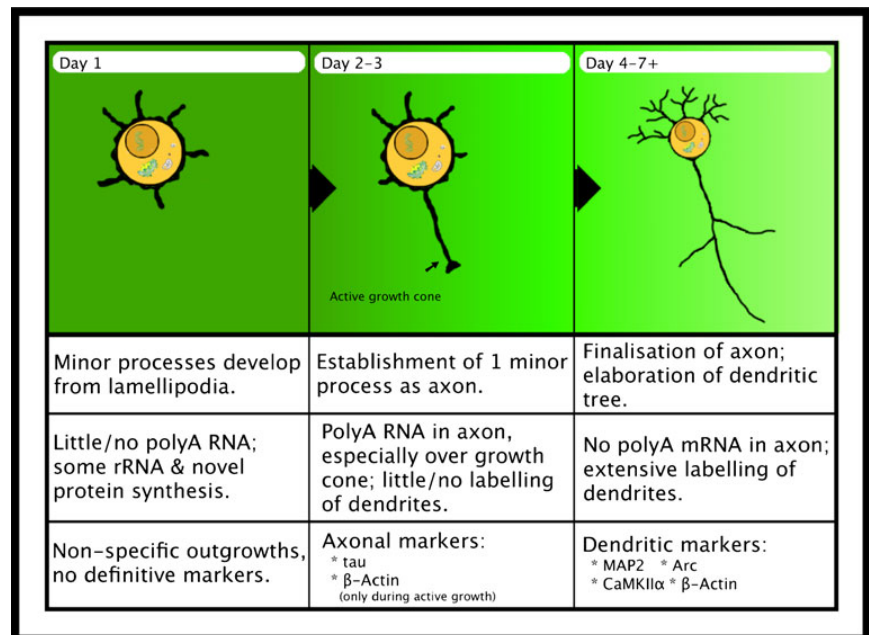
be sufficient for dendritic localization. In the case of MAP2, cells expressing a 3′-UTR with the LE deleted exhibited slightly reduced targeting compared with those expressing shorter partial UTRs, which the authors proposed could arise from alteration of the UTR's secondary structure after specific deletion of the LE [17]. Furthermore, while the 94-nt *cis*-acting element found in CaMKIIα successfully targeted the mRNA to dendrites, partial deletions of this region, which retained the LE, failed to localize. However, targeting of this construct was restored by depolarization with BDNF, implying the involvement of a second, inhibitory *cis*-acting element that functions to suppress transport in resting cells [18]. Microarray analysis of mRNA differentially associated with polysomes after BDNF stimulation agreed with this finding and identified several other candidates for dendritic targeting and translation, including *N*-methyl D-aspartate (NMDA) receptor subunit 3 (NR3), and the PSD scaffolding protein Homer2, which were validated in preparations of rat forebrain synaptoneurosomes [19].

Although the mechanisms are different, findings regarding CaMKII and MAP2 are suggestive of external interference acting upon the 3′-UTRs of dendritically active mRNA. One method by which the secondary structure of MAP2 could be altered is by the reversible binding of silencing protein or RNA entities within the LE, which could be removed in response to activity and restore functionality. This same strategy could explain the activity-induced de-repression exhibited by the secondary *cis*-acting element of the CaMKIIα UTR. Moreover, it is interesting to

note that both mRNA were co-localized with distinct moving granules. Together these observations suggest a system of reversible suppression, perhaps utilizing the RNA interference (RNAi) pathway and post-transcriptional gene silencing (PTGS).

Part II—Post-transcriptional Gene Silencing

Within the last 10 years, the discovery of endogenous small non-coding RNA known as microRNA (miRNA) has sparked a flurry of research and dramatically changed our understanding of gene regulation. miRNA employ complimentary base pairing and the RNA induced silencing complex (RISC) to bind and either suppress translation or facilitate degradation of their target mRNA. A large proportion of these molecules are enriched or specifically expressed in the mammalian brain, and many of these also co-purify in neurons with actively translating polyribosomes [20], thereby potentially regulating protein expression at the synapse in response to changing requirements.

MicroRNA

miRNA are 19–22-nucleotide RNA fragments derived primarily from non-coding regions of the genome, although some are embedded within the coding regions of known genes [21]. miRNA are transcribed into long

primary transcripts (pri-miRNA) forming hairpin structures that are cleaved in the nucleus by the microprocessor complex consisting primarily of Drosha and DGCR8, to form shorter (~ 70 nt) precursor hairpins known as pre-miRNA (Fig. 2). Exportin-5 transfers pre-miRNA to the cytoplasm for further cleavage by Dicer to yield the mature, double-stranded miRNA (~ 20 nt). The mature miRNA becomes active after it is assembled into the RISC with proteins from the Argonaute (Ago) family. After selective removal and degradation of the passenger strand [22–24], the RISC-associated guide strand directs the complex in search of its mRNA targets.

The base pairing of miRNA and mRNA in vertebrates only requires partial homology, with a preference for contiguous pairing only occurring at the "seed" region, located at nucleotides two through seven of the guide strand. The lack of stringency results in a many-to-many relationship between miRNA and mRNA targets, with the consequence that as much as 60% of the genome may be regulated post-transcriptionally by a comparatively small cohort of miRNA [23]. The guide strand binds to the complimentary region in the 3′ UTR of its target by Watson–Crick base pairing of the seed residues. Several alternative seed binding arrangements have been observed (Fig. 3), and these are believed to confer

Fig. 2 miRNA biogenesis pathway. Primary miRNA (*pri-miR*) are transcribed from genomic DNA in the nucleus where they are cleaved by Drosha, complexed with DGCR8, to shorter precursor transcripts (*pre-miR*) ~ 80–100 nucleotides in length. Exportin-5 transports pre-miRs to the cytoplasm where Dicer cleaves them to a duplex structure (~ 20 nucleotides) that is loaded into the RISC. The passenger strand is ejected from the RISC and degraded, while the guide strand identifies the mRNA target and binds it, resulting in deadenylation and degradation, or translational repression, of the transcript

Fig. 3 miRNA-target binding. Canonical binding (**a**–**c**) includes the seed residues (2–7) and either (**a**, **b**) or both (**c**) residues 1 and 8. Marginal binding is only 6-mer, involving only the seed residues (**d**) or an offset including residue 8 (**e**). Canonical binding is considered stronger and more effective for target recognition compared with marginal binding. (Adapted from [25])

differential target affinity, proportional to the number of nucleotides involved [25]. There is no specific binding between the Ago domains and the miRNA; rather the strand is held in place by energetically favorable pi-stacking bonds between the aromatic rings of the nucleotides and conserved phenylalanine residues in the binding pocket [26], suggesting that if the RISC were disassembled its cargo would be freed without modification. This raises the possibility of miRNA recycling since some enzymes employ this method of engagement to participate transiently in catalytic reactions. The potential for de-repression suggests a possible role for miRNA in reversible and cyclic transcript silencing.

miRNA in Neural Structure and Function

A key role for processed miRNA in neuronal differentiation is demonstrated by significantly increased Dicer expression in response to differentiation in both neuroblastoma cell lines [27] and cultures of cerebellar granule neurons [28]. These models have identified miRNA that are both up-regulated and down-regulated by the differentiation process. Importantly, enhanced expression of known brain-specific and brain-enriched miRNA including miR-124a was reported, while down-regulation of the miR-17 family, whose targets are enriched for pathways involving LTP,

17

axon guidance and regulation of the actin cytoskeleton [29], is consistent with the expectation that these mRNA would be in high demand during this period. Further, miR-125b also exhibited up-regulation during differentiation and was shown to be both necessary and sufficient for neurite out-growth in the differentiating cells by both gain- and loss-of-function studies [30].

The impact of miRNA on development is exemplified in studies where miRNA maturation was ablated by Dicer knock-out [31, 32]. Although miRNA depletion appears to have little effect on uncommitted progenitor cells, which retain their ability to proliferate [32], differentiation and morphogenesis are clearly affected. The resulting pheno-types are grossly abnormal, exhibiting improper differentia-tion, incomplete neural patterning including reduced arealization and layering, lack of interneurons, and impaired connectivity, dendritic targeting and arborization [31–33], suggesting that miRNA assist in providing a biologically robust environment during development [34, 35]. With an emerging role in neural development, it is not surprising that alterations in miRNA biogenesis and expression are also associated with neurodevelopmental disorders such as schizophrenia [29, 36–38].

Arguably one of the most studied CNS-specific miRNA is miR-124, which has been shown to regulate the switch from progenitor cell to committed neuron, acting in one instance through Sox9 to switch off glial function and promote cell cycle exit leading to activation of the differen-tiation process [39]. Along with miR-9*, miR-124 is sup-pressed in neural progenitors by the repressor-element-1-silencing transcription factor (REST). When differentiation is initiated, REST suppression is lifted, and the miRNA targets the 3′-UTR of chromatin remodeling factor BAF53a, thereby epigenetically mediating the switch to a differenti-ated pattern of gene expression [40]. Interestingly, ectopic expression of miR-124 in association with dFMR1, the homolog of fragile-X mental retardation protein (FMRP) in *Drosophila*, decreased dendritic branching in dendritic arborization sensory neurons [41].

This intricacy and diversity of miR-124's activities dur-ing neural development underscores several key points re-garding the current understanding of miRNA biology. Firstly, while many brain-specific and brain-enriched miRNA are critical for correct development of the brain and nervous system, very few have been characterized in detail. Secondly, neural miRNA have many targets and participate in a range of complexes to achieve their regula-tory goals. Thirdly, and perhaps most importantly, miRNA can promote the neuronal phenotype while at the same time negatively regulating some neural functions, such as miR-124 and dendritic branching. This is to be expected as the influence of miRNA is a continuum that "fine-tunes" mRNA expression rather than switching it on and off, where

the balance of activity may vary spatially within the cell at any given time.

Part III—Could miRNA and PTGS Provide a Mechanism for Activity-dependent mRNA Translation at the Synapse?

Remodeling of discreet post-synaptic membranes in re-sponse to activity requires mechanisms that facilitate real-time control of protein synthesis. An important aspect of this control is defined by the local availability and activity of mRNA. While this is supported by a plethora of sequence specific solutions, the evolution of nucleic acid-dependent gene silencing pathways has also provided neurons with an opportunity to employ a more universal system for achiev-ing these objectives.

The key advantage of using nucleic acids over proteins to implement cellular trafficking is the flexibility provided by the level of functional redundancy built into the system. Using individual carrier proteins to chaperone each tran-script around the cell is a fairly limited solution, which becomes a very difficult problem in complex systems. By utilizing an RNA-encoded adapter molecule such as miRNA, the post-transcriptional regulatory systems are pro-vided with the potential for extraordinary autonomy, econ-omy and scalability that may enable them to manage the complexity required for sophisticated neural systems.

miRNA and Post-synaptic Gene Regulation

Studies of miRNA expression in synaptoneurosomes sug-gest enrichment and depletion of subsets of miRNA in the vicinity of synapses [42, 43], where they have demonstrated key roles regulating spine morphology and excitability [43–47], briefly summarized in Table 1. Pre-miRNA and an inactive form of Dicer have additionally been observed localized to the PSD [42, 48]. This is significant in the context of synaptic function because increased intracellular Ca^{2+} driven by NMDA stimulation has been shown to induce calpain-directed cleavage and activation of Dicer, which can subsequently process pre-miRNA into function-ally active mature miRNA.

Conversely, excitation may also lift the repression im-posed on synaptically localized RISC-associated mRNA. In support of this hypothesis the RISC protein Armitage has been shown to decompose in response to LTP-inducing stimuli in *Drosophila* neurons, releasing CaMKII mRNA and other memory-associated transcripts for immediate translation [49]. While the CaMKII 3′-UTR was shown to be regulated by miR-280 and miR-289, it seems unlikely that these are the only miRNA regulating this transcript. Like many dendritically localized mRNA such as MAP2,

Table 1 Targets and demonstrated functions of identified synaptically enriched miRNA

miR	Target	Function	Reference
134	Limk1	Negative regulator of spine volume. BDNF lifted repression, reinstating Limk1.	[47]
134	Pumilio2	K^+ or BDNF increase transcription of miR379–410 cluster (contains miR-134) by Mef2 binding. miR-134 binds Pum2, promoting dendritogenesis. Moreover, miR-134 buffers Pum2 within a narrow range critical for activity-dependent dendritogenesis.	[45]
138	APT1	Negative regulator of spine size. miR-138 binds APT1 → increased palmitoylation of $G\alpha_{13}$ and relocation of subunit to membrane → increase RhoA signaling → spine shrinkage.	[43]
124	CREB	Negative regulation of CREB → reduced LTP in response to serotonin stimulation.	[46]
125b	NR2A	Overexpression results in longer, thinner spines → decreased EPSP.	[44]
132		Overexpression results in shorter, stubby spines → increased EPSP.	[44]

CaMKIIα has a long 3′-UTR with many predicted miRNA binding sites. The secondary structure of the MAP2 3′-UTR was proposed to be responsible for its dendritic localization [17], and based on understanding of miRNA function, it is possible that miRNA bind to the 3′ UTR and transport MAP2, and potentially other plasticity-associated mRNA, to the dendrites. Interestingly, many of these transcripts co-localize with neuronal granules. These ribonucleoprotein complexes are associated with synapto-dendritic transport and trafficking. As these structures also contain miRNA, they are likely to play a role in post-synaptic gene silencing.

Neuronal Granules

Several classes of neuronal granule have been shown to co-localize with miRNA, mRNA and other known protein and enzyme components of RNAi (reviewed in [50]). Granules were originally discovered as GW bodies and are marked by the RNA-binding protein GW182. Their primary role appears to be the spatial control of mRNA availability via 5′-3′ mediated decay, and they are associated with various mRNA-degrading enzymes. GW bodies are now more commonly referred to as processing bodies (P-bodies) and are known in many cell types as post-transcriptional regulators of gene expression [51], chiefly facilitating pathways such as nonsense mediated decay, RNA degradation and miRNA-mediated silencing [52]. Another major group of granule detected in the cytoplasm of neurons is transport RNPs (tRNPs) whose markers include Staufen1 and 2, FMRP and ZBP1, and which are chiefly involved in redistribution of translationally arrested mRNA [53]. A group of heterogeneous nuclear RNPs (hnRNPs) is also active in the nucleus. These nuclear granules interact with their cytoplasmic counterparts via nuclear export factor 7 (NXF7) to coordinate mRNA sorting, transport and storage [54].

The heterogeneity of neuronal granules and relative paucity of known markers has led to conflict in their elaboration, with some studies reporting tRNPs to be similar in structure and function to P-bodies [55], while others report them distinct [56]. Some of this confusion might be explained by reports of transient physical association between P-bodies and stress granules [57], and more recent video-microscopic reports of docking events between tRNPs and P-bodies [56]. These have been observed with varying time-courses and could certainly confound observations depending on the labeling and timing protocols employed. The addition of Ago-containing miRNA-induced RNPs (miRNPs) further supports a model involving diverse, functionally distinct granules. Not only are the Ago proteins themselves functionally distinct, but expression profiling of miRNA obtained after incubation with Ago1-specific antibodies selected target mRNA that were enriched for long 3′-UTRs, demonstrating a selection process in the loading of targets into Ago1 miRNPs, the significance of which is not yet understood [58].

A neuron-specific sub-class of granule known as dlP-bodies has recently been identified and also contains ribosomes and enzymes required for localized protein translation, while being depleted of XRN1 normally associated with P-bodies that induce RNA decay [59]. DlP-bodies exhibit directed movement towards distant synapses in response to BDNF stimulation where they subsequently disassemble, freeing the mRNA for potential translation, and indeed neurons have been demonstrated to increase localized mRNA translation at the synapse in response to BDNF. Similar results have been observed in other sub-types of P-body in response to NMDA and glutamate [56], with the

different depolarization agents shown to affect overall composition of P-body and tRNP subpopulations. Together these findings suggest that neuronal granules play an important role in miRNA-associated dendrito-synaptic trafficking of mRNA, as well as real-time, post-synaptic, activity-dependent regulation of translation in response to incoming signals.

Functional Integration

The evidence discussed strongly supports the existence of a deliberate, highly sophisticated and coordinated system of mRNA sorting, transportation and localization in mammalian neurons. To ensure the smooth running of such a network undoubtedly requires extensive inter-compartmental communication. The nature of much of this signaling remains undetermined; however, as a common participant in all compartments, miRNA undoubtedly play a key role. The recent detection of docking events between tRNPs and P-bodies provides an interesting mechanism by which communication could be facilitated. Docking was observed over periods up to 1 min, during which time it is conceivable that mRNA could be "rescued" from degradation by transferring from P-body to tRNP; conversely, transcripts that are no longer required may be moved from tRNP to P-body for disposal. Alternatively, it may be that the different classes of granules dock on some occasions to exchange information "updates" regarding the transcriptional requirements of the cell. Given that new classes of granule continue to be identified, the protein markers of the various classes remain largely undefined, and the contents (and therefore potential functions)

differ greatly between granules, this area of research is likely to yield interesting insights into intracellular communication.

Could miRNA Compartmentalization Regulate Activity-driven Synaptic Gene Expression and Memory Formation?

In this review we have drawn on the current evidence that supports an integrated model of the synaptic response to excitation (Fig. 4). In the resting state (Fig. 4, left panel), translationally repressed transcripts are localized near the bases of dendritic spines, along with ribosomes, while inactive Dicer and pre-miRNA are anchored in the PSD. In response to stimulation by neurotransmitters or neurotrophic factors, several cascades of activity are initiated in the post-synaptic cell (Fig. 4, center panel). The rapid increase in intracellular calcium activates calpain, which cleaves Dicer from the PSD; pre-miRNA are also released, although the mechanism driving this is unknown. Stimulation causes mRNA-associated RISCs to decompile, allowing the transcripts to be translated by polyribosomes. As depolarization continues (Fig. 4, right panel), active Dicer is deployed, cleaving pre-miRNA to provide more mature miRNA to perhaps sequester free translating mRNA and provide some attenuation to the stimulus pulse.

It should be emphasized that not all these events need occur in response to a discrete excitation. Rather, these mechanisms are more likely employed as needed to modulate what can be regarded as the translational homeostasis of each individual synapse, and this will necessarily vary between synapses depending on the number and nature of their connections. The participation of miRNA and other
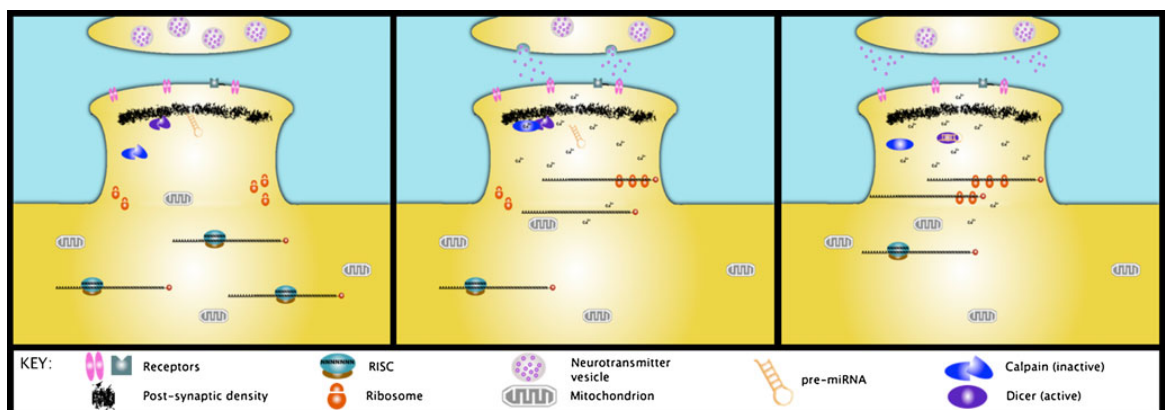
Fig. 4 Involvement of PTGS in synaptic plasticity. In the resting synapse (*left panel*), the key role of PTGS is the silencing of mRNA functionally localized here but not yet required for translation; however, inactive elements of the miRNA pathway may also be present and tethered in the PSD, such as Dicer and pre-miRNA. When a stimulus arrives (*center panel*), the increase in calcium (Ca^{2+}) triggers events that alter the translational equilibrium of the synapse. These may include de-repression and translation of RISC-bound mRNA, activation of Dicer and release of pre-miRNA. As depolarisation continues (*right panel*), Dicer may cleave new mature miRNA to counterbalance freed mRNA as the new equilibrium of the synapse is realized

107

elements of post-transcriptional gene silencing in so many aspects of the synaptic response to excitation indicates that these small regulatory molecules may be key modulators of mRNA availability and protein synthesis in post-synaptic termini. Some aspects of this integrated model have been demonstrated in response to patterns of stimulation normally associated with the formation of long-term and/or short-term memory; however, of almost 1000 known human miRNA, very few have begun to be characterized, with many studies restricting their focus to targets of individual miRNA or related family members. In this respect, broader studies of the subcellular redirection of both mRNA and miRNA in response to physiological stimuli may prove more informative in the full elaboration of the contribution of reversible gene silencing to synaptic plasticity in the context of functioning neurons and the pathophysiology of neurological disorders.

References

1. Steward O, Levy WB (1982) Preferential localization of polyribosomes under the base of dendritic spines in granule cells of the dentate gyrus. J Neurosci 2(3):284–291
2. Rao A, Steward O (1991) Evidence that protein constituents of postsynaptic membrane specializations are locally synthesized: analysis of proteins synthesized within synaptosomes. J Neurosci 11(9):2881–2895
3. Steward O, Pollack A, Rao A (1991) Evidence that protein constituents of postsynaptic membrane specializations are locally synthesized: time course of appearance of recently synthesized proteins in synaptic junctions. J Neurosci Res 30(4):649–660
4. Torre ER, Steward O (1992) Demonstration of local protein synthesis within dendrites using a new cell culture system that permits the isolation of living axons and dendrites from their cell bodies. J Neurosci 12(3):762–772
5. Kang H, Schuman EM (1996) A requirement for local protein synthesis in neurotrophin-induced hippocampal synaptic plasticity. Science 273(5280):1402–1406
6. Feig S, Lipton P (1993) Pairing the cholinergic agonist carbachol with patterned Schaffer collateral stimulation initiates protein synthesis in hippocampal CA1 pyramidal cell dendrites via a muscarinic, NMDA-dependent mechanism. J Neurosci 13(3):1010–1021
7. Goodman CS, Shatz CJ (1993) Developmental mechanisms that generate precise patterns of neuronal connectivity. Cell 72 (Suppl):77–98
8. Lo DC (1995) Neurotrophic factors and synaptic plasticity. Neuron 15(5):979–981
9. Kang H et al (1996) Determinants of BDNF-induced hippocampal synaptic plasticity: role of the Trk B receptor and the kinetics of neurotrophin delivery. Learn Mem 3(2–3):188–196
10. Dotti CG, Sullivan CA, Banker GA (1988) The establishment of polarity by hippocampal neurons in culture. J Neurosci 8(4):1454–1468
11. Kleiman R, Banker G, Steward O (1994) Development of subcellular mRNA compartmentation in hippocampal neurons in culture. J Neurosci 14(3 Pt 1):1130–1140
12. Steward O et al (1998) Synaptic activation causes the mRNA for the IEG Arc to localize selectively near activated postsynaptic sites on dendrites. Neuron 21(4):741–751
13. Dahm R, Kiebler M, Macchi P (2007) RNA localisation in the nervous system. Semin Cell Dev Biol 18(2):216–223
14. Zhang HL et al (2001) Neurotrophin-induced transport of a beta-actin mRNP complex increases beta-actin levels and stimulates growth cone motility. Neuron 31(2):261–275
15. Ainger K et al (1997) Transport and localization elements in myelin basic protein mRNA. J Cell Biol 138(5):1077–1087
16. Huang F, Chotiner JK, Steward O (2005) The mRNA for elongation factor 1alpha is localized in dendrites and translated in response to treatments that induce long-term depression. J Neurosci 25(31):7199–7209
17. Blichenberg A et al (1999) Identification of a cis-acting dendritic targeting element in MAP2 mRNAs. J Neurosci 19(20):8818–8829
18. Mori Y et al (2000) Two cis-acting elements in the 3′ untranslated region of alpha-CaMKII regulate its dendritic targeting. Nat Neurosci 3(11):1079–1084
19. Schratt GM et al (2004) BDNF regulates the translation of a select group of mRNAs by a mammalian target of rapamycin-phosphatidylinositol 3-kinase-dependent pathway during neuronal development. J Neurosci 24(33):7366–7377
20. Kim J et al (2004) Identification of many microRNAs that copurify with polyribosomes in mammalian neurons. Proc Natl Acad Sci USA 101(1):360–365
21. Zhu Y et al (2009) A microRNA gene is hosted in an intron of a schizophrenia-susceptibility gene. Schizophr Res 109(1–3):86–89
22. Bicker S, Schratt G (2008) MicroRNAs: tiny regulators of synapse function in development and disease. J Cell Mol Med 12 (5A):1466–1476
23. Filipowicz W, Bhattacharyya SN, Sonenberg N (2008) Mechanisms of post-transcriptional regulation by microRNAs: are the answers in sight? Nat Rev Genet 9(2):102–114
24. Konecna A, et al. 2009 What are the roles of microRNAs at the mammalian synapse? Neurosci Lett
25. Bartel DP (2009) MicroRNAs: target recognition and regulatory functions. Cell 136(2):215–233
26. Jinek M, Doudna JA (2009) A three-dimensional view of the molecular machinery of RNA interference. Nature 457 (7228):405–412
27. Potenza N, Papa U, Russo A (2009) Differential expression of Dicer and Argonaute genes during the differentiation of human neuroblastoma cells. Cell Biol Int 33(7):734–738
28. Barbato C et al (2007) Dicer expression and localization in post-mitotic neurons. Brain Res 1175:17–27
29. Beveridge NJ, et al (2009) Down-regulation of miR-17 family expression in response to retinoic acid induced neuronal differentiation. Cell Signal 21(12):1837–1845
30. Le MTN et al (2009) MicroRNA-125b promotes neuronal differentiation in human cells by repressing multiple targets. Mol Cell Biol 29(19):5290–5305
31. Giraldez AJ et al (2005) MicroRNAs regulate brain morphogenesis in zebrafish. Science 308(5723):833–838

32. De Pietri Tonelli D et al (2008) miRNAs are essential for survival and differentiation of newborn neurons but not for expansion of neural progenitors during early neurogenesis in the mouse embryonic neocortex. Development 135(23):3911–3921

33. Berdnik D et al (2008) MicroRNA processing pathway regulates olfactory neuron morphogenesis. Curr Biol 18(22):1754–1759

34. Li X et al (2009) A microRNA imparts robustness against environmental fluctuation during development. Cell 137(2):273–282

35. Stark A et al (2005) Animal microRNAs confer robustness to gene expression and have a significant impact on 3′UTR evolution. Cell 123(6):1133–1146

36. Beveridge NJ et al (2010) Schizophrenia is associated with an increase in cortical microRNA biogenesis. Mol Psychiatry 15 (12):1176–1189

37. Gardiner E, et al. 2011 Imprinted DLK1-DIO3 region of 14q32 defines a schizophrenia-associated miRNA signature in peripheral blood mononuclear cells. Mol Psychiatry. (July 5, EPUB ahead of print)

38. Santarelli DM et al (2011) Upregulation of dicer and microRNA expression in the dorsolateral prefrontal cortex Brodmann area 46 in schizophrenia. Biol Psychiatry 69(2):180–187

39. Cheng L-C et al (2009) miR-124 regulates adult neurogenesis in the subventricular zone stem cell niche. Nat Neurosci 12(4):399–408

40. Yoo A (2009) et al. MicroRNA-mediated switching of chromatin-remodelling complexes in neural development, Nature

41. Xu X-L et al (2008) The steady-state level of the nervous-system-specific microRNA-124a is regulated by dFMR1 in *Drosophila*. J Neurosci 28(46):11883–11889

42. Lugli G et al (2008) Expression of microRNAs and their precursors in synaptic fractions of adult mouse forebrain. J Neurochem 106(2):650–661

43. Siegel G et al (2009) A functional screen implicates microRNA-138-dependent regulation of the depalmitoylation enzyme APT1 in dendritic spine morphogenesis. Nat Cell Biol 11(6):705–716

44. Edbauer D et al (2010) Regulation of synaptic structure and function by FMRP-associated microRNAs miR-125b and miR-132. Neuron 65(3):373–384

45. Fiore R et al (2009) Mef2-mediated transcription of the miR379-410 cluster regulates activity-dependent dendritogenesis by fine-tuning Pumilio2 protein levels. EMBO J 28(6):697–710

46. Rajasethupathy P et al (2009) Characterization of small RNAs in aplysia reveals a role for miR-124 in constraining synaptic plasticity through CREB. Neuron 63(6):803–817

47. Schratt GM et al (2006) A brain-specific microRNA regulates dendritic spine development. Nature 439(7074):283–289

48. Lugli G et al (2005) Dicer and eIF2c are enriched at postsynaptic densities in adult mouse brain and are modified by neuronal activity in a calpain-dependent manner. J Neurochem 94(4):896–905

49. Ashraf SI et al (2006) Synaptic protein synthesis associated with memory is regulated by the RISC pathway in *Drosophila*. Cell 124 (1):191–205

50. Eulalio A, Behm-Ansmant I, Izaurralde E (2007) P bodies: at the crossroads of post-transcriptional pathways. Nat Rev Mol Cell Biol 8(1):9–22

51. Jakymiw A et al (2007) The role of GW/P-bodies in RNA processing and silencing. J Cell Sci 120(Pt 8):1317–1323

52. Eulalio A et al (2007) P-body formation is a consequence, not the cause, of RNA-mediated gene silencing. Mol Cell Biol 27 (11):3970–3981

53. Kiebler MA, Bassell GJ (2006) Neuronal RNA granules: movers and makers. Neuron 51(6):685–690

54. Katahira J et al (2008) Nuclear RNA export factor 7 is localized in processing bodies and neuronal RNA granules through interactions with shuttling hnRNPs. Nucleic Acids Res 36(2):616–628

55. Barbee SA et al (2006) Staufen- and FMRP-containing neuronal RNPs are structurally and functionally related to somatic P bodies. Neuron 52(6):997–1009

56. Zeitelhofer M et al (2008) Dynamic interaction between P-bodies and transport ribonucleoprotein particles in dendrites of mature hippocampal neurons. J Neurosci 28(30):7555–7562

57. Kedersha N et al (2005) Stress granules and processing bodies are dynamically linked sites of mRNP remodeling. J Cell Biol 169 (6):871–884

58. Hong X, et al. 2009 Immunopurification of Ago1 miRNPs selects for a distinct class of microRNA targets. Proc Natl Acad Sci USA.

59. Cougot N et al (2008) Dendrites of mammalian neurons contain specialized P-body-like structures that respond to neuronal activation. J Neurosci 28(51):13793–13804

CHAPTER 3

Methodological considerations for

in-vitro neuronal modelling

STATEMENT OF CONTRIBUTION OF OTHERS

Goldie BJ, Barnett MM and Cairns MJ: **BDNF and the maturation of post-transcriptional regulatory networks in human neuroblast differentiation.** *Frontiers in Cellular Neuroscience*, 2014, October 15; 8:325, doi: 10.3389/fncel.2014.00325.

I attest that Research Higher Degree candidate **Belinda Goldie** *was the primary contributor to the development of this publication. This extensive contribution included: driving the initial study design and intellectual development of the study; establishing, optimising, executing, analysing and interpreting all experiments contained within this study; performing all gene expression, bioinformatic and statistical analyses; and writing the manuscript in full. Michelle Barnett performed the review of the literature.*

_____

Belinda J Goldie (candidate)

_____

Michelle M Barnett

_____

Murray J Cairns (supervisor)

_____   ____05/08/2014_____

Professor Robert Callister   **Date**

Assistant Dean Research Training (ADRT)

BDNF and the maturation of posttranscriptional regulatory networks in human SH-SY5Y neuroblast differentiation

Belinda J. Goldie[1,2], Michelle M. Barnett[1] and Murray J. Cairns[1,2]*

[1] *The Centre for Translational Neuroscience and Mental Health, School of Biomedical Sciences and Pharmacy, University of Newcastle, Callaghan, NSW, Australia*
[2] *Schizophrenia Research Institute, Sydney, NSW, Australia*

The SH-SY5Y culture system is a convenient neuronal model with the potential to elaborate human/primate-specific transcription networks and pathways related to human cognitive disorders. While this system allows for the exploration of specialized features in the human genome, there is still significant debate about how this model should be implemented, and its appropriateness for answering complex functional questions related to human neural architecture. In view of these questions we sought to characterize the posttranscriptional regulatory structure of the two-stage ATRA differentiation, BDNF maturation protocol proposed by Encinas et al. (2000) using integrative whole-genome gene and microRNA (miRNA) expression analysis. We report that ATRA-BDNF induced significant increases in expression of key synaptic genes, brain-specific miRNA and miRNA biogenesis machinery, and in AChE activity, compared with ATRA alone. Functional annotation clustering associated BDNF more significantly with neuronal terms, and with synaptic terms not found in ATRA-only clusters. While our results support use of SH-SY5Y as a neuronal model, we advocate considered selection of the differentiation agent/s relative to the system being modeled.

Keywords: neuronal differentiation, MicroRNAs, gene expression profiling, cell culture techniques, SH-SY5Y cells

INTRODUCTION

The nervous system, and in particular the brain, arguably represents the most complex area of human biology. Many different cell types are present, interacting in multiplexed combinations, and every circuit is uniquely wired by individual patterns of experience. This complexity continues down to the subcellular level with intricate transportation systems and biomolecular partitioning. Temporo-spatial specificity of mRNA translation in particular is critical for localized protein synthesis as it supports the synaptic remodeling required for synaptic plasticity.

Recent studies have suggested that small, non-coding RNA species known as microRNA (miRNA) play a role in supporting temporo-spatial traffic of neuronal mRNA (Goldie and Cairns, 2012). Many miRNA demonstrate brain-specific (Smirnova et al., 2005; Krichevsky et al., 2006) and region-specific (Hollins et al., 2014) expression and have been shown to regulate key aspects of brain development and neuronal morphology (Giraldez et al., 2005), including patterning and arealisation, dendritic branching (Xu et al., 2008) and spine volume (Schratt et al., 2006). The presence of miRNA in exosomes suggests they may also play a role in activity-driven communication (Fauré et al., 2006).

A key limitation in studies of the nervous system is that ethical considerations and availability of tissue generally restrict these investigations to animal models, relying on *in-vitro* or *ex-vivo* preparations, typically of mouse or rat, to extrapolate human function. Although the composition of the post-synaptic density is well conserved among mammals (Bayés et al., 2010), the dynamic component of plasticity provided by mRNA and miRNA

is quite divergent. Human transcription networks have evolved a complexity that drives species-specific gene expression in the pre-frontal (PFC) and frontal cortices (Konopka et al., 2012). Among transcripts that are subject to human-specific developmental remodeling, miRNA in the PFC exhibit the greatest and most rapid divergence from other primates with an average evolutionary length 24 times that of other transcript types (Somel et al., 2011). These findings suggest that animal models, while informative, may not provide full understanding of the molecular mechanisms underlying neuronal function in higher primates and humans.

NEURONAL DIFFERENTIATION OF NEUROBLASTOMAS

To overcome this limitation, several human immortalized cell lines are available which for some purposes can model human neuron behavior. Among these, neuroblastoma cell lines are highly accessible and can be matured into terminally differentiated, neuron-like cells using agents such as retinoic acid (RA), enabling clearer determination of molecular and morphological changes induced by differentiation. Treatment with RA is associated with inhibition of proliferation, extension of processes commonly termed neurites (Stio et al., 2001), increased acetylcholinesterase (AChE) activity (Sidell et al., 1984), and enhanced production of synaptic vesicles (Sarkanen et al., 2007); features consistent with neuronal maturation.

In the SH-SY5Y cell line, a sympathetic line containing noradrenaline and neuropeptide Y in dense-core vesicles (Goodall et al., 1997; Ou et al., 1998), three stereoisomers of RA, *all-trans*

25

(ATRA), *9-cis* and *13-cis*, are all observed to induce this phenotype, however differential activity at the receptor level appears to impact the differentiation process. ATRA acts at the native retinoic acid receptor (RAR), which binds to retinoic acid response elements (RAREs) in the DNA to alter transcription of RA-activated genes, while the *9-cis* isomer acts in a similar manner on the retinoid X receptor (RXR). This difference could explain the observation that although *9-cis* RA induces stronger morphological and transcriptional responses these changes are reversed after washout, while the response to ATRA is permanent (Redfern et al., 1994). This finding suggests that ATRA may be a more suitable agent for studying the effects of commitment to a neuronal lineage.

NEURONAL MATURATION WITH BDNF
In the developing brain, the final connectivity of a neuron is determined largely by signals received from the neurotrophin family of proteins, which are expressed in a laminar-specific pattern and influence the growth and complexity of the dendritic tree (McAllister et al., 1995). Of this family, brain-derived neurotrophic factor (BDNF) has a profound effect on pyramidal neurons in cortical layers 4 and 5, in addition to which it has demonstrated the capacity to target mRNAs to the synapse (Tongiorgi et al., 1997; Righi et al., 2000) and stimulate their local translation (Miyata et al., 2005). In particular, polysome profiling of active translation conducted by Schratt and colleagues demonstrated that BDNF is required to stimulate local translation of key synaptic components such as CamKII, NMDA receptors NR1, and NR3, PSD93 and LIMK-1 (Schratt et al., 2004). These findings suggest the employment of BDNF for *in vitro* neuronal maturation may produce cells more closely matching the phenotype and, importantly, gene expression profile of neurons *in vivo*.

BDNF is active at the *trkB* receptor (gene name NTRK2), which is absent from naïve SH-SY5Y cells; its expression can be induced by differentiation with ATRA (Kaplan et al., 1993), and some studies have employed a 5–6 day protocol of concurrent ATRA and BDNF treatments. However, in an arguably seminal paper published in 2000, Encinas and colleagues demonstrated that *trkB* does not reach peak expression in this cell line until 5 days' exposure to ATRA (Encinas et al., 2000); thus these short-duration, dual-agent protocols may bear limited similarity to mature neurons: a model of sequential treatment with ATRA for 5 days followed by BDNF, that yields neurotrophin-dependent mature cells, may be more physiological.

RATIONALE AND METHODS
We performed a comprehensive review of the literature to understand the use of differentiation protocols for the maturation of SH-SY5Y cells. Specifically, for *in vitro* research work attempting to emulate mature neuronal behavior, we wanted to know to what extent the sequential treatment with ATRA followed by BDNF was being utilized compared with other differentiation protocols or undifferentiated cells. A search of the PubMed literature for "SH-SY5Y" identified 3419 papers published in English between the publication of the Encinas protocol (2000) and the time of writing (April 2014), from which 410

papers studying the neuroblastoma disease itself were excluded. This list was narrowed to 2307 papers by searching for words associated with differentiation, neurodegeneration and mental health conditions (see Supplementary Figure S1 for full description of review inclusion/exclusion criteria). Surprisingly, 1914 of 2307 papers (83%) did not utilize a differentiation protocol at all, nor was an explanation for using undifferentiated cells given.

Among 393 studies employing a differentiation protocol, the most common differentiation agent was ATRA only (283 of 393 papers, 72%, or 12% of all studies); approximately 16% (65 papers, 3% of all studies) utilized other differentiating agents such as the phorbolester 12-O-tetradecanoylphorbol-13-acetate (TPA), which has been shown to generate an adrenergic phenotype (Påhlman et al., 1983). Moreover, a remarkably small proportion (45 papers, 11 or 2% of all studies) utilized Encinas' sequential protocol of ATRA differentiation followed by BDNF, despite its compelling evidence: The switch from ATRA to BDNF on day 5 coincides with peak expression of its receptor *trkB*, however the biochemical impact of this transition has not previously been reported, nor has the gene expression profile been extensively characterized. Moreover, the importance of post-transcriptional regulation of gene expression by miRNA in the control of neuronal differentiation, development, connectivity, and synaptic function is now well established, as reviewed in Goldie and Cairns (2012); a thorough investigation of this two-stage neuronal model in this light is therefore timely.

We undertook comparative genome-wide gene and miRNA expression analyses of naïve, 5-day ATRA-treated and 5-day ATRA- + 7-day BDNF-treated SH-SY5Y using Affymetrix Exon v1.0 and miRNA v2.0 microarrays. Data were analyzed with Genespring Gx 12 software (Agilent) to identify differentially expressed transcripts with Benjamini-Hochberg correction for multiple testing and a corrected *p*-value cut-off of 0.05. Microarray results were confirmed by examination of a selection of significantly altered transcripts by qPCR with random-primed cDNA for gene expression and specific mature miRNA primers for miRNA expression as described previously (Santarelli et al., 2011). Functional analysis of gene expression changes was conducted using the Functional Annotation Clustering (FAC) tool of the DAVID bioinformatics suite (Huang et al., 2008) on lists of genes having significantly different expression (as defined above) at each timepoint. Integrated analysis of altered miRNA expression was conducted using QIAGEN's Ingenuity Pathways Analysis software (IPA, QIAGEN Redwood City, www.qiagen.com/ingenuity). A target analysis was performed on significantly up- and down-regulated miRNA, and the list of targets refined by expression pairing with the list of altered genes. Core analysis was carried out on negatively correlated pairings to investigate significantly altered pathways and functional networks.

To report on biochemical neuronal maturity, we measured the acetylcholinesterase (AChE) activity of samples collected at various timepoints during differentiation and maturation using the Amplex Red AChE assay kit according to the manufacturer's instructions (Invitrogen).

SEQUENTIAL DIFFERENTIATION WITH ATRA THEN BDNF YIELDS A MORE NEURONAL CELL POPULATION

MORPHOLOGY

Neuroblast cultures were imaged at each stage of treatment at 10X magnification with an Axiovert inverted microscope (Zeiss) (**Figure 1**). In line with the results of Encinas and colleagues, cells visually appeared more neural across the two-stage differentiation process. Compared with naïve cells (**Figure 1A**), cells treated with ATRA for 5 days appeared to have reduced proliferation, took on a more polar morphology and began to extend longer, more robust neurites (**Figure 1B**). During 7 days subsequent BDNF exposure, cell bodies began to migrate into clusters, some a large as ∼110 μm diameter, while neurites increased in number, size and complexity (**Figure 1C**).

GENE EXPRESSION

Differentiation with ATRA significantly altered the expression of 46 genes; remarkably, 38 of these were up regulated, characterizing neuronal differentiation as the "switching on" of a genetic programme. BDNF maturation had a much bigger effect on gene expression, significantly altering 265 genes (189 up, 76 down) compared with controls and importantly, 387 genes (123 up, 264 down) compared with ATRA differentiated samples. As shown in **Figure 1D**, the genes most strongly induced by ATRA were down regulated by BDNF maturation, while a group showing only mild ATRA induction were further strengthened by BDNF. These included many neuronal genes and components of the miRNA biogenesis machinery (**Table 1A**), a panel of which were validated by qPCR (**Figure 1F**). Strikingly, neuropeptide Y (NPY), which has been reported as non-responsive to ATRA (Påhlman et al., 1995), demonstrated 146-fold increase in expression in response to sequential ATRA + BDNF.

Genes "activated" by each of the ATRA differentiation and BDNF maturation processes were functionally analyzed using the DAVID FAC tool. In ATRA-treated samples the only cluster terms to remain significant after *p*-value correction related to retinoid metabolism. This is perhaps not surprising given the subsequent down regulation of genes induced by ATRA treatment. In contrast, when compared with both control and ATRA-treated cohorts, BDNF-matured samples were strikingly enriched for neuronally relevant clusters including "neuron projection" (*ES* = 4.83, corrected *p* = 0.00027) and "synaptic transmission" (*ES* = 2.33, corrected *p* = 0.03). Although some of these terms were present in the ATRA results, they were not significant (**Table 1B**).

miRNA EXPRESSION

In response to ATRA differentiation, 36 miRNA demonstrated significantly different expression. Unlike gene expression there was no clear directional bias with 20 up and 16 down regulated. Also in contrast to the gene expression results, the miRNA most strongly induced by ATRA were further strengthened by BDNF maturation (**Figure 1E**). BDNF induced differential expression of 70 miRNA compared to undifferentiated cells (42 down, 28 up). Notably, differentiation dramatically increased the expression of miR-132, a key regulator of dendritic growth and arborisation, as well as known brain-specific miRs −210 and −212, the latter

of which inhibits a locus with miR-132. Significant increase in expression of miRs −132 and −212 by BDNF maturation was confirmed by qPCR (**Figure 1F**). We also observed ATRA-mediated decrease in miR-17 family expression, consistent with previous observations (Beveridge et al., 2009); all members of this family were further down-regulated by BDNF maturation.

FUNCTIONAL INTEGRATION

The importance of BDNF in shaping the regulatory environment of matured cells was investigated using IPA software. Genes showing two-stage activation (173 genes, **Figure 1E**, red line) were paired with a target analysis of 44 negatively correlated miRNA (10 miRNA with 42 target genes). Core analysis of these molecules showed a strong enhancement of neuronal functionality, with top functional terms "neurotransmission" (*p* = 1.97e-07, APP, GRIK2, KCNMB4, PCDHB10, PCDHB14, PCDHB5, PSEN1), "neurological disease" (*p* = 7.41e-07, APP, BCL2, CHGB, DPYSL3, ESRRG, GABRA3, GRIK2, LGR5, NTRK2, PLK2, PSEN1, SCN3A, VCAN), "synaptic transmission of cells" (*p* = 1.52e-06, APP, GRIK2, PCDHB10, PCDHB14, PCDHB5, PSEN1), and "synaptogenesis" (*p* = 1.93e-06, APP, PCDHB10, PCDHB14, PCDHB5). Full results are presented in Supplementary Table S1. Visual representation of this analysis revealed that many of these genes encode proteins that reside in the synaptic membrane (Supplementary Figure S2). Moreover, four families of miRNA (miR-18a,b, miR-17,20a,b, miR-130, and miR-1275) were found to be key hubs providing regulatory support to this functionality.

ACETYLCHOLINESTERASE ACTIVITY

Only modest changes in AChE activity were observed during ATRA-induced differentiation, however maturation with BDNF caused sharp increases in activity (**Figure 1G**). Strikingly, AChE activity in cells treated with ATRA for 5 days followed by 1 day of BDNF exposure was higher than in those treated for 7 days with ATRA alone, highlighting the importance of the neurotrophin in development of the neuronal phenotype. Moreover, the magnitude of the response increased with ATRA concentration used to induce differentiation (Supplementary Figure S3), possibly due to the expression of more BDNF receptors at higher ATRA concentrations.

DISCUSSION

Human neuroblast cultures, particularly the SH-SY5Y line, are used extensively to model the basic biology of neurons. They may also have application in high-throughput screening assays of neuroactive compounds. The literature is controversial regarding the need to differentiate SH-SY5Y, as exemplified by an exchange between Luchtman and Song (2010) regarding the latter's conclusions with respect to the applicability of SH-SY5Y differentiation in studying neurotoxicity and neuroprotection in Parkinson's disease (Cheung et al., 2009). What is clear from this exchange is the need to carefully consider experimental methodology and applicability of the cell model used within the context of the research question.

Our results presented here suggest that the sequential ATRA differentiation-BDNF maturation program yields a cell

FIGURE 1 | Comparison of single-stage (ATRA) and two-stage (ATRA + BDNF) differentiation of SH-SY5Y. Compared with **(A)** 5 DIV untreated cultures, cells **(B)** treated with ATRA for 5 days demonstrate reduced proliferation and take on a more polar appearance, with neurites being extended and networks beginning to develop. **(C)** After further maturation with BDNF, cell bodies migrate into clusters and the neurite networks become increasingly complex. **(D)** Heat map (*k*-means, 4 clusters) clustering genes and miRNA significantly differentially expressed (blue = low expression, yellow = high) during sequential differentiation. C = control, R = ATRA, B = BDNF. Four clusters reveal key expression patterns, in particular the strength of BDNF induction (star). These are summarized as trend lines showing average expression of constituent **(E)** genes and **(F)** miRNA; the groups of transcripts demonstrating two-stage induction (red lines) clustered significantly for neuronal functional terms (see **Table 1A**) and contained many key neuronal peptides, receptors and miRNA (see **Table 1B**).

(Continued)

28

FIGURE 1 | Continued
Symbols delineate differing two-stage expression patterns. **(G)** A selection of these transcripts examined by qPCR confirmed that maturation with BDNF drove increased expression (red bars) compared with ATRA differentiation alone (black bars). *$p < 0.05$; **$p < 0.01$; ***$p < 0.001$. **(H)** AChE activity was measured after 1, 3, 5, and 7 days' ATRA treatment, or 5 days' ATRA treatment followed by 1, 3 or 5 days' treatment with BDNF. Increases in AChE activity were most strongly elicited by BDNF maturation; notably, 5 day ATRA + 1 day BDNF evoked more response than an extended 7 day ATRA treatment (red box). Treatments were 10 μM ATRA and 50 ng/ml BDNF throughout.

Table 1A | Neuronal genes and miRNA demonstrating increased expression after BDNF maturation of ATRA-differentiated SH-SY5Y.

Gene symbol	Gene name	Fold-change (BDNF/ATRA)
NPY[a,c]	Neuropeptide Y	146
RELN[a,b,d,e]	Reelin	9.01
NTRK2[b,d]	Neurotrophic tyrosine kinase, receptor, type 2	2.0
GRIK3[a,d,f]	Glutamate receptor, ionotropic, kainate 3	3.3
GRIN2B[a,b,c,d]	Glutamate receptor, NMDA, subunit 2B	3.28
CHRM1[a,b]	Cholinergic receptor, muscarinic 1	3.23
HTR3C[a]	Serotonin receptor 3C	3.28
HTR5A[a,d,e]	Serotonin receptor 5A	3.3
DRD2[a,c,f]	Dopamine receptor D2	3.3
HCRTR1[d,e]	Hypocretin (orexin) receptor 1	3.1
CACNA1C[a,b,d,e]	Calcium channel, voltage-dependent, 1C subunit	3.3
NRG1[a,b,d]	Neuregulin 1	3.25
DICER1	Dicer 1, ribonuclease type III	2.56
DROSHA[a]	Drosha, ribonuclease type III	2.94
DGCR8[a]	DiGeorge syndrome critical region gene 8	3.04
XPO5	Exportin 5	3.48
MIR132	Hsa-miR-132	3.04
MIR212	Hsa-miR-212	1.78

Disease associations:
[a] *schizophrenia.*
[b] *Alzheimer.*
[c] *Huntington's.*
[d] *bipolar/mood disorders.*
[e] *autism spectrum disorders*
[f] *Parkinson's.*

Table 1B | Comparison of significance of neuronal terms derived from functional clustering of genes altered by sequential differentiation and maturation of SH-SY5Y.

Term	Corrected *p*-value		
	ATRA vs. CTRL	BDNF vs. CTRL	BDNF vs. ATRA
Neuron development	0.238	0.037	5.19E-03
Neuron differentiation	0.397	3.05E-03	6.24E-03
Axon	0.557	3.04E-05	0.019
Axonogenesis	0.750	0.046	2.40 E-03
Cell morphogenesis involved in neuron differentiation	0.763	0.066	2.31 E-03
Neuron projection	0.769	2.52E-05	2.65E-04
Neuron projection development	0.812	0.065	3.94E-03
Synaptic transmission	n/a	1.25E-04	0.031
Synapse	n/a	7.92E-05	0.079

population with significantly more characteristics of mature neurons compared with ATRA treatment alone. We observed obvious morphological similarities with neurons, including intricate and complex neurite structure and evidence of migration with cell bodies organizing into clusters. The cells also displayed substantial enhancement of neuron-associated gene expression, in particular induction of NPY, NTRK2, and CHRM2. There was also evidence of increased posttranscriptional regulation, with elevated expression of miRNA biogenesis machinery including, DROSHA, DGCR8, DICER, and XPO5. This capacity was realized through significantly elevated expression of many miRNA, including key neuronal miRs −132 and −212, supporting the critical roles these molecules play in developing and mature neurons. These individual findings were corroborated at the systems level by the abundance of terms related to neuronal operation and synapse formation derived from the integrated functional analysis. Moreover we have recently shown that miRNA expression and distribution in these cells is rapidly altered in response to

potassium-induced depolarisation (Goldie et al., 2014). A substantial component of this depolarisation-associated change in miRNA was found to be mediated by release of miRNA-enriched exosomes.

These higher orders of neural differentiation and function are dependent on neurotrophin signaling. The importance of BDNF and the expression of the *trk* receptors in shaping the neuronal specialization have been demonstrated from development through maturity and plasticity. In particular, during cortical development this neurotrophin exerts profound effects on layer 4 and 5 neurons, where it significantly increases the number and complexity of dendritic branches (McAllister et al., 1995), axonal length (Labelle and Leclerc, 2000), as well as the number of spines (Bamji et al., 2006) and therefore potential synaptic connectivity. BDNF maturation of SH-SY5Y clearly reproduced this effect in terms of neurite morphology; however it is generally considered that these cells do not form synapses. Studies in neurons have shown that the trkB receptor is required for synapse formation, and ablation of trkB resulted in deficits of synapse formation (Luikart et al., 2005). Further, the interaction between BDNF and the trkB receptor plays an important role in neuronal development (Cheng et al., 2011; Dong et al., 2012), and is important for synaptic plasticity (Kang et al., 1996).

Our systematic review revealed only 2% (45 of 2307) of papers used sequentially differentiated cells, and only 35 of these studies allowed sufficient exposure to ATRA (5 days) to allow for maximal expression of trkB. Without the interaction between BDNF and trkB, which is optimally induced by exposing the cells to ATRA for 5 days, synapse formation is unlikely and has not been reported in conventional culture. However, by pre-treating these cells with ATRA, Agholme and colleagues were able to detect

synaptic structures and vesicular transport in a 3D gel culture. Synapses were found in samples matured in BDNF alone, however were more numerous when matured with a cocktail containing BDNF, neuregulin β1, nerve growth factor and vitamin D₃ (Agholme et al., 2010). Although more work needs to be done to fully characterize these structures, this finding indicates that with more development this culture technique may provide a system for unraveling some of the complexities of the human neuron maturation and connectivity.

CONCLUSIONS

SH-SY5Y is a flexible culturing system that can be differentiated into several mature neuronal phenotypes, depending on the differentiation agent selected. In our investigation of gene expression and the posttranscriptional regulatory environment of these cells, we found that differentiation combined with BDNF maturation is optimal for generating a phenotype approaching mature neurons. By contrast, the changes induced by ATRA alone appeared to produce an intermediate phenotype between immature neuroblasts and mature neurons, and may be a suitable analog for the study of developing neurons. This system provides a robust *in vitro* alternative to animal models for investigating some aspects of neuronal function with the advantage of the human genetic context for revealing species-specific higher order complexity.

SUPPLEMENTARY MATERIAL

The Supplementary Material for this article can be found online at: http://www.frontiersin.org/journal/10.3389/fncel.2014.00325/abstract

REFERENCES

Agholme, L., Lindström, T., Kågedal, K., Marcusson, J., and Hallbeck, M. (2010). An *in vitro* model for neuroscience: differentiation of SH-SY5Y cells into cells with morphological and biochemical characteristics of mature neurons. *J. Alzheimers Dis.* 20, 1069–1082. doi: 10.3233/JAD-2010-091363

Bamji, S. X., Rico, B., Kimes, N., and Reichardt, L. F. (2006). BDNF mobilizes synaptic vesicles and enhances synapse formation by disrupting cadherin-beta-catenin interactions. *J Cell Biol* 174, 289–299. doi: 10.1083/jcb.200601087

Bayés, À., van de Lagemaat, L. N., Collins, M. O., Croning, M. D. R., Whittle, I. R., Choudhary, J. S., et al. (2010). Characterization of the proteome, diseases and evolution of the human postsynaptic density. *Nat. Neurosci.* 14, 19–21. doi: 10.1038/nn.2719

Beveridge, N. J., Tooney, P. A., Carroll, A. P., Tran, N., and Cairns, M. J. (2009). Down-regulation of miR-17 family expression in response to retinoic acid induced neuronal differentiation. *Cell. Signal.* 21, 1837–1845. doi: 10.1016/j.cellsig.2009.07.019

Cheng, P.-L., Song, A.-H., Wong, Y.-H., Wang, S., Zhang, X., and Poo, M.-M. (2011). Self-amplifying autocrine actions of BDNF in axon development. *Proc. Natl. Acad. Sci. U.S.A.* 108, 18430–18435. doi: 10.1073/pnas.1115907108

Cheung, Y.-T., Lau, W. K.-W., Yu, M.-S., Lai, C. S.-W., Yeung, S.-C., So, K.-F., et al. (2009). Effects of all-trans-retinoic acid on human SH-SY5Y neuroblastoma as *in vitro* model in neurotoxicity research. *Neurotoxicology* 30, 127–135. doi: 10.1016/j.neuro.2008.11.001

Dong, Q., Ji, Y.-S., Cai, C., and Chen, Z.-Y. (2012). LIM kinase 1 (LIMK1) interacts with tropomyosin-related kinase B (TrkB) and Mediates brain-derived neurotrophic factor (BDNF)-induced axonal elongation. *J. Biol. Chem.* 287, 41720–41731. doi: 10.1074/jbc.M112.405415

Encinas, M., Iglesias, M., Liu, Y., Wang, H., Muhaisen, A., Ceña, V., et al. (2000). Sequential treatment of SH-SY5Y cells with retinoic acid and brain-derived neurotrophic factor gives rise to fully differentiated, neurotrophic factor-dependent, human neuron-like cells. *J. Neurochem.* 75, 991–1003. doi: 10.1046/j.1471-4159.2000.0750991.x

Fauré, J., Lachenal, G., Court, M., Hirrlinger, J., Chatellard-Causse, C., Blot, B., et al. (2006). Exosomes are released by cultured cortical neurones. *Mol. Cell. Neurosci.* 31, 642–648. doi: 10.1016/j.mcn.2005.12.003

Giraldez, A. J., Cinalli, R. M., Glasner, M. E., Enright, A. J., Thomson, J. M., Baskerville, S., et al. (2005). MicroRNAs regulate brain morphogenesis in zebrafish. *Science* 308, 833–838. doi: 10.1126/science.1109020

Goldie, B. J., and Cairns, M. J. (2012). Post-transcriptional trafficking and regulation of neuronal gene expression. *Mol. Neurobiol.* 45, 99–108. doi: 10.1007/s12035-011-8222-0

Goldie, B. J., Dun, M. D., Lin, M., Smith, N. D., Verrills, N. M., Dayas, C. V., et al. (2014). Activity-associated miRNA are packaged in Map1b-enriched exosomes released from depolarized neurons. *Nucleic. Acids. Res.* 42, 9195–9208. doi: 10.1093/nar/gku594

Goodall, A. R., Danks, K., Walker, J. H., Ball, S. G., and Vaughan, P. F. (1997). Occurrence of two types of secretory vesicles in the human neuroblastoma SH-SY5Y. *J. Neurochem.* 68, 1542–1552.

Hollins, S. L., Goldie, B. J., Carroll, A. P., Mason, E. A., Walker, F. R., Eyles, D. W., et al. (2014). Ontogeny of small RNA in the regulation of mammalian brain development. *BMC Genomics* 15:777. doi: 10.1186/1471-2164-15-777

Huang, D., Sherman, B., and Lempicki, R. (2008). Bioinformatics enrichment tools: paths toward the comprehensive functional analysis of large gene lists. *Nucleic Acids Res.* 2, 428–430. doi: 10.1093/nar/gkn923

Kang, H., Jia, L. Z., Suh, K. Y., Tang, L., and Schuman, E. M. (1996). Determinants of BDNF-induced hippocampal synaptic plasticity: role of the Trk B receptor and the kinetics of neurotrophin delivery. *Learn. Mem.* 3, 188–196.

Kaplan, D. R., Matsumoto, K., Lucarelli, E., and Thiele, C. J. (1993). Induction of TrkB by retinoic acid mediates biologic responsiveness to BDNF and differentiation of human neuroblastoma cells. Eukaryotic Signal Transduction Group. *Neuron* 11, 321–331.

Konopka, G., Friedrich, T., Davis-Turak, J., Winden, K., Oldham, M. C., Gao, F., et al. (2012). Human-specific transcriptional networks in the brain. *Neuron* 75, 601–617. doi: 10.1016/j.neuron.2012.05.034

Krichevsky, A. M., Sonntag, K.-C., Isacson, O., and Kosik, K. S. (2006). Specific microRNAs modulate embryonic stem cell-derived neurogenesis. Stem Cells 24, 857–864. doi: 10.1634/stemcells.2005-0441

Labelle, C., and Leclerc, N. (2000). Exogenous BDNF, NT-3 and NT-4 differentially regulate neurite outgrowth in cultured hippocampal neurons. *Brain Res. Dev. Brain Res.* 123, 1–11. doi: 10.1016/S0165-3806(00)00069-9

Luchtman, D. W., and Song, C. (2010). Why SH-SY5Y cells should be differentiated. *Neurotoxicology* 31, 164–5. doi: 10.1016/j.neuro.2009.10.015

Luikart, B. W., Nef, S., Virmani, T., Lush, M. E., Liu, Y., Kavalali, E. T., et al. (2005). TrkB has a cell-autonomous role in the establishment of hippocampal Schaffer collateral synapses. *J. Neurosci.* 25, 3774–3786. doi: 10.1523/JNEUROSCI.0041-05.2005

McAllister, A. K., Lo, D. C., and Katz, L. C. (1995). Neurotrophins regulate dendritic growth in developing visual cortex. *Neuron* 15, 791–803.

Miyata, S., Mori, Y., Fujiwara, T., Ikenaka, K., Matsuzaki, S., Oono, K., et al. (2005). Local protein synthesis by BDNF is potentiated in hippocampal neurons exposed to ephrins. *Brain Res. Mol. Brain Res.* 134, 333–337. doi: 10.1016/j.molbrainres.2004.10.034

Ou, X. M., Partoens, P. M., Wang, J. M., Walker, J. H., Danks, K., Vaughan, P. F., et al. (1998). The storage of noradrenaline, neuropeptide Y and chromogranins in and stoichiometric release from large dense cored vesicles of the undifferentiated human neuroblastoma cell line SH-SY5Y. *Int. J. Mol. Med.* 1, 105–112.

Påhlman, S., Hoehner, J. C., Nånberg, E., Hedborg, F., Fagerström, S., Gestblom, C., et al. (1995). Differentiation and survival influences of growth factors in human neuroblastoma. *Eur. J. Cancer.* 31A, 453–458.

Påhlman, S., Ruusala, A. I., Abrahamsson, L., Odelstad, L., and Nilsson, K. (1983). Kinetics and concentration effects of TPA-induced differentiation of cultured human neuroblastoma cells. *Cell Differ.* 12, 165–170.

Redfern, C. P., Lovat, P. E., Malcolm, A. J., and Pearson, A. D. (1994). Differential effects of 9-cis and all-trans retinoic acid on the induction of retinoic acid receptor-beta and cellular retinoic acid-binding protein II in human neuroblastoma cells. *Biochem. J.* 304 (Pt 1), 147–154.

Righi, M., Tongiorgi, E., and Cattaneo, A. (2000). Brain-derived neurotrophic factor (BDNF) induces dendritic targeting of BDNF and tyrosine kinase B mRNAs in hippocampal neurons through a phosphatidylinositol-3 kinase-dependent pathway. *J. Neurosci.* 20, 3165–3174.

Santarelli, D. M., Beveridge, N. J., Tooney, P. A., and Cairns, M. J. (2011). Upregulation of dicer and microRNA expression in the dorsolateral prefrontal cortex Brodmann area 46 in schizophrenia. *Biol. Psychiatry* 69, 180–187. doi: 10.1016/j.biopsych.2010.09.030

Sarkanen, J.-R., Nykky, J., Siikanen, J., Selinummi, J., Ylikomi, T., and Jalonen, T. O. (2007). Cholesterol supports the retinoic acid-induced synaptic vesicle formation in differentiating human SH-SY5Y neuroblastoma cells. *J. Neurochem.* 102, 1941–1952. doi: 10.1111/j.1471-4159.2007.04676.x

Schratt, G. M., Nigh, E. A., Chen, W. G., Hu, L., and Greenberg, M. E. (2004). BDNF regulates the translation of a select group of mRNAs by a mammalian target of rapamycin-phosphatidylinositol 3-kinase-dependent pathway during neuronal development. *J. Neurosci.* 24, 7366–7377. doi: 10.1523/JNEUROSCI.1739-04.2004

Schratt, G. M., Tuebing, F., Nigh, E. A., Kane, C. G., Sabatini, M. E., Kiebler, M., et al. (2006). A brain-specific microRNA regulates dendritic spine development. *Nature* 439, 283–289. doi: 10.1038/nature04367

Sidell, N., Lucas, C. A., and Kreutzberg, G. W. (1984). Regulation of acetylcholinesterase activity by retinoic acid in a human neuroblastoma cell line. *Exp. Cell. Res.* 155, 305–309.

Smirnova, L., Gräfe, A., Seiler, A., Schumacher, S., Nitsch, R., and Wulczyn, F. G. (2005). Regulation of miRNA expression during neural cell specification. *Eur. J. Neurosci.* 21, 1469–1477. doi: 10.1111/j.1460-9568.2005.03978.x

Somel, M., Liu, X., Tang, L., Yan, Z., Hu, H., Guo, S., et al. (2011). MicroRNA-driven developmental remodeling in the brain distinguishes humans from other primates. *PLoS Biol* 9:e1001214. doi: 10.1371/journal.pbio.1001214

Stio, M., Celli, A., and Treves, C. (2001). Synergistic anti-proliferative effects of vitamin D derivatives and 9-cis retinoic acid in SH-SY5Y human neuroblastoma cells. *J. Steroid Biochem Mol. Biol.* 77, 213–222. doi: 10.1016/S0960-0760(01)00059-0

Tongiorgi, E., Righi, M., and Cattaneo, A. (1997). Activity-dependent dendritic targeting of BDNF and TrkB mRNAs in hippocampal neurons. *J. Neurosci.* 17, 9492–9505.

Xu, X.-L., Li, Y., Wang, F., and Gao, F.-B. (2008). The steady-state level of the nervous-system-specific microRNA-124a is regulated by dFMR1 in Drosophila. *J. Neurosci.* 28, 11883–11889. doi: 10.1523/JNEUROSCI.4114-08.2008

CHAPTER 4

Investigation of activity-associated subcellular miRNA dynamics

<u>STATEMENT OF CONTRIBUTION OF OTHERS</u>

<u>Goldie</u> BJ, Dun MD, Lin M, Smith ND, Verrills NM, Dayas CV and Cairns MJ:
Activity- associated miRNA are packaged in Map1b-enriched exosomes released from depolarised neurons. *Nucleic Acids Research*, 2014, 42(14):9195-208, doi: 10.1093/nar/gku594.

*I attest that Research Higher Degree candidate **Belinda Goldie** was the primary contributo r to the development of this publication. This extensive contribution included: driving the initial study design and intellectual development of the study; establishing, optimising,*

executing, analysing and interpreting all experiments contained within this study (excludin g EM, MS and western blotting); performing all gene expression, bioinformatic (including

proteomic) and statistical analyses; and writing the manuscript in full.

_____

Belinda J Goldie (candidate)

_____

Minjie Lin

_____

Nicole M Verrills

_____

Murray J Cairns (supervisor)

_____

Matthew D Dun

_____

Nathan D Smith

_____

Christopher V Dayas

_____   ____05/08/2014____

Professor Robert Callister   **Date**

Assistant Dean Research Training (ADRT)

Activity-associated miRNA are packaged in Map1b-enriched exosomes released from depolarized neurons

Belinda J. Goldie[1,2,3], Matthew D. Dun[1,4], Minjie Lin[5], Nathan D. Smith[6], Nicole M. Verrills[1,4], Christopher V. Dayas[1,3] and Murray J. Cairns[1,2,3,*]

[1]School of Biomedical Sciences and Pharmacy, Faculty of Health and Medicine, University of Newcastle, Callaghan, NSW 2308, Australia, [2]Schizophrenia Research Institute, Sydney, Australia, [3]Centre for Translational Neuroscience and Mental Health, Hunter Medical Research Institute, University of Newcastle, Callaghan, NSW 2308, Australia, [4]Hunter Cancer Research Alliance, Hunter Medical Research Institute, University of Newcastle, Callaghan, NSW, 2308, Australia, [5]School of Environmental and Life Sciences, University of Newcastle, Callaghan, NSW 2308, Australia and [6]ABRF, Research Services, University of Newcastle, Callaghan, NSW 2308, Australia

ABSTRACT

Rapid input-restricted change in gene expression is an important aspect of synaptic plasticity requiring complex mechanisms of post-transcriptional mRNA trafficking and regulation. Small non-coding miRNA are uniquely poised to support these functions by providing a nucleic-acid-based specificity component for universal-sequence-dependent RNA binding complexes. We investigated the subcellular distribution of these molecules in resting and potassium chloride depolarized human neuroblasts, and found both selective enrichment and depletion in neurites. Depolarization was associated with a neurite-restricted decrease in miRNA expression; a subset of these molecules was recovered from the depolarization medium in nuclease resistant extracellular exosomes. These vesicles were enriched with primate specific miRNA and the synaptic-plasticity-associated protein MAP1b. These findings further support a role for miRNA as neural plasticity regulators, as they are compartmentalized in neurons and undergo activity-associated redistribution or release into the extracellular matrix.

INTRODUCTION

Post-synaptic excitation triggers a localized and temporally regulated cascade of protein synthesis, modification and other molecular activity, which culminates in the remodelling of dendritic spines' size, shape and receptor density. These processes ultimately modify the strength of the neural connection, changing its potential for subsequent excitation from the same inputs, and are essential for encoding experience in the cellular networks of the brain. At the molecular level, this process is facilitated by the neurons' capacity to organize localized, input-restricted protein synthesis within dendrites and dendritic spines (1). While mRNA coding these proteins are transcribed from DNA in the nucleus and distributed and stored locally throughout the soma until needed, little is known about the mechanisms directing dendritic mRNA transport and, more importantly, how translation is suspended until required (2). Evidence from the study of key neuronal genes such as CamKIIα (3), MAP2 (4), MBP (5) and β-actin (6) has demonstrated the role of localization elements (LEs) encoded in the 3′ UTR of the mRNA for binding proteins that "chaperone" the transcript through the cell. In each case, the RNA binding protein identified was unique to its target transcript; however with so much mRNA trafficking in neurons it seems unlikely that each one will have its own "personal" chaperone. It would be less cumbersome to have more redundant systems where multiple transcripts destined for the same location could be recognized by small "adaptors" to each transcript, which associate reversibly with their cargo and potentially respond to dendritic location and synaptic activation.

A strong candidate to provide this logistic support to mRNA trafficking is the class of 17–22 nucleotide short, non-coding transcripts known as microRNA (miRNA). These post-transcriptional regulators recognize their target mRNA by signatures in their 3′ UTRs known as miRNA Recognition Elements (MREs) that are only 6–8 nucleotides long; thus a single miRNA has the flexibility to regulate the expression of many mRNAs. In support of a neuron-specific trafficking role, many miRNAs are brain specific or brain enriched, and play critical roles in neuronal differentiation and morphogenesis (7,8). In ex-

*To whom correspondence should be addressed. Email: murray.cairns@newcastle.edu.au

periments where miRNA biogenesis is impaired or ablated, the resulting phenotypes are grossly abnormal, exhibiting improper differentiation, incomplete neural patterning including reduced arealization and layering, lack of interneurons, and impaired connectivity, dendritic targeting and arborization (8–10).

miRNA utilize the Argonaute (Ago) family of RNA-binding proteins and provide the specificity component for their protein complex known as an RNA-induced silencing complex (RISC). Activated RISC molecules have been associated with a range of functions particularly gene silencing and RNA interference mediated by RNA destabilization (11). However, they are also thought to mediate interactions with the 5′ cap of mRNA, or even arrest ribosomes, to confer translational repression (12). The RISC has been demonstrated to play an important role in long-term potentiation (LTP) in *Drosophila*, as it decompiles in response to stimuli, releasing memory-associated transcripts that are subsequently actively translated (13); similarly in the rat, memory-associated transcripts were shown to be de-repressed at the synapse in an activity-dependent manner (14).

To further investigate the putative role of miRNA in regulating and segregating dendritic gene expression in mammalian systems, we examined the redistribution of miRNA and their mRNA targets in differentiated human neuroblasts in response to a stimulating concentration of K$^+$ ions. These analyses revealed K$^+$-associated changes in both miRNA and mRNA expressions; strikingly, modulation of miRNA was confined to the synapto-dentritic compartment, while mRNA followed no consistent pattern. Down regulation of miRNAs in the neurite fraction was accompanied by a corresponding release of MAP1b-containing microvesicles enriched for primate-specific mature miRNA. These data also suggest that small RNA species are subject to a functionally specific selection process for transmission or disposal in these vesicles.

MATERIALS AND METHODS

Cell culture

Populations of SH-SY5Y human neuroblastoma cells (ATCC, kindly provided by Jean-Marie Sontag, University of Newcastle) were maintained at 37°C, 5% CO$_2$, 90% humidity in Dulbecco's Modified Eagle's Medium (DMEM, Hyclone) supplemented with 10% Fetal Calf Serum (FCS, Sigma Aldrich), 2% HEPES and 1% L-glutamine. Cells were routinely passaged and harvested by washing with phosphate buffered saline (PBS) followed by brief incubation with trypsin.

Differentiation

To obtain neuronal cells, populations were seeded as noted in individual methods and differentiation was induced as follows. After 24 h (Day 0), medium was replaced with medium supplemented with 10 μM *all-trans* retinoic acid (ATRA, Sigma). Flasks were incubated wrapped in foil for 5 days; media was changed on Day 3. On Day 5, ATRA was removed by washing 3 times with DMEM before continuing with methods as described.

Depolarization

Depolarization was induced by 3-min room temperature incubation in stimulating HBS (35 mM NaCl, 100 mM KCl, 0.6 mM MgSO$_4$.7H$_2$O, 2.5 mM CaCl$_2$.2H$_2$O, 10 mM HEPES, 6 mM Glucose) (15). After depolarization, HBS was replaced with warm complete medium and cells were allowed to recover for 10 min under culturing conditions.

Two depolarization regimens were employed using the above strategy. These included a single stimulus + recovery and four consecutive stimulus + recovery cycles, designed to mimic patterns of electrical activation required to induce early-phase and late-phase LTP respectively (16). In addition, sham-depolarized controls were prepared using a non-stimulating HBS from which KCl was omitted and NaCl was increased to 140 mM.

Separation of neurites from cell bodies

Cells were seeded into high-yield flasks (HY flasks, Millipore) with a growth area of 600 cm^2 to ensure enough RNA would be produced from the fractions. To obtain active neurites during differentiation, cells were harvested after four days of ATRA treatment, using a method modified from Meyerson (17). Depolarization conditions were prepared as described, harvested and washed twice with ice-cold EDTA buffer (0.54 mM EDTA, 137 mM NaCl, 10 mM Na$_2$HPO$_4$, 2.7 mM KCl, 0.15 mM KH$_2$PO$_4$ pH 7.4, 100 U/ml RNase inhibitor). Individual samples were resuspended in 10 ml ice-cold EDTA buffer and homogenized with 6 strokes at 60 rpm with a teflon/glass homogenizer (Potter-Elvehjem). The homogenate was then loaded onto a 3.5 ml cushion of 20% sucrose in EDTA buffer and centrifuged at 500 g for 4 min, 4°C. The "neurite" fraction was collected from the load/20% sucrose interface, and the pellet retained as the "cell body" fraction. Intact cells (1 ml) were also collected prior to fractionation as a whole-cell control. Fractions and whole-cell controls were purified by centrifugation at 15 500 g for 40 min, 4°C, and the pellets used for RNA extraction. Neurite fractions were characterized by quantitative real-time PCR (qPCR) enrichment of transcripts for synaptophysin (SYP) and GAP43 compared with cell body fractions, as described in Supplementary Materials (Supplementary Figure S1).

Exosome purification

To achieve the large populations necessary to obtain enough vesicular RNA for multiple avenues of analysis, cells were seeded in high-yield flasks (HY flasks, Millipore) with a growth area of 1000 cm^2. After differentiation, cells were depolarized once and the buffer retained for vesicle collection. Non-stimulating HBS from sham-depolarized controls was retained and processed alongside depolarization buffer to confirm that the release of vesicles was a direct result of depolarization and not residual from other sources such as fetal bovine serum. Cells were not allowed a recovery, and instead were immediately harvested and lysed in TRIzol for profiling of cellular miRNA remaining acutely after depolarization.

Exosome ultra-concentrate was obtained from the depolarization buffer by centrifugation through Amicon Ultra-

15 100kD centrifugal filters (Millipore) as described ([18]). Briefly, buffer was centrifuged in 15 ml aliquots at 4000 rpm for 3 min at RT to a final volume of approximately 100 µl, which was passed through a 0.1 µm syringe filter to remove debris. Ultra-concentrate was then DNaseI treated (Invitrogen) and washed 3×15 ml (with centrifugation as before) with PBS before 1 ml of TRIzol was added for RNA extraction.

Exosome collection from separated neurites and cell bodies

Neurite and cell body fractions were prepared as described above to the point of fraction collection. Separated fractions were then depolarized for 3 min with 100 mM KCl as described above before proceeding with the final 40 min centrifugation step. The supernatant was processed as described above for exosome purification. Exosomal RNA was extracted as described below, while exosomal protein was quantified using a bicinchoninic acid protein assay kit (Pierce) according to the manufacturer's instructions.

Electron microscopy

Ultra-concentrated exosomes, prepared as described above, were fixed in 3% glutaraldehyde in 0.1 m phosphate buffer (pH 7.3) overnight at 4°C. The samples were air-dried on copper grids coated with formvar membrane made from 1% polyvynilformal 15/95 in ethylene dichloride, and stained with 0.5% uranyl acetate in 30% ethanol for 10 min and further stained with lead citrate for 10 min. Lead precipitates on grid sections were removed by rinsing in 0.05 M NaOH before further rinsing in distilled H_2O. Grids were left at room temperature to dry and the stained sections were examined using a JEOL-1200EX transmission electron microscope (JEOL, Tokyo, Japan) operating at 80 kV.

Western blotting

Western blotting was performed on exosomal protein extracted using modified RIPA buffer (1% SDS, 1% Triton X-100, 500 mM sodium fluoride, 50 mM EDTA, 10 mM sodium orthovanadate, 0.05% sodium deoxycholate) containing a protease inhibitor cocktail (Roche) at 100°C for 5 min, vortexed vigorously and centrifuged at 10 000 *g* for 15 min at 4°C. Quantification of the isolated protein supernatant was achieved using a bicinchoninic acid protein assay kit (Pierce) according to the manufacturer's instructions. 20 µg of exosmome protein was boiled in NuPAGE LDS Sample Buffer (4X) (Invitrogen) supplemented with 2% 2-mercaptoethanol for 5 min and resolved on 4–12% NuPAGE Bis-Tris Gels polyacrylamide gels (Invitrogen). The resolved proteins were then transferred onto nitrocellulose membranes under a constant current of 350 mA for 1 h. The nitrocellulose membranes were blocked overnight in 5% skim milk powder in TBS (Tris-buffered saline: 100 mM Tris/HCl, pH 7.6, and 150 mM NaCl) (pH 7.4) supplemented with 0.1% Tween 20 (TBST). Membranes were rinsed in TBST and probed overnight with primary antibodies against LAMP1 (1:1000) and FLOT1 (1:1000) (both Abcam) in 1% skim milk powder in TBST. Membranes were then further probed for 1 h with a 1:5000 dilution of

horseradish peroxidase-conjugated secondary antibody at room temperature. Following a further 3 washes in TBST, cross-reactive proteins were visualized using an ECL (enhanced chemiluminescence) kit (GE Healthcare) according to the manufacturer's instructions.

Mass spectrographic analyses

Cells and exosomes were lysed in RIPA buffer supplemented with protease and phosphatase inhibitors (as mentioned above) before resolution on 4–12% Bis-Tris acrylamide gels. The gels were then silver stained and bands excised. Peptides were generated using trypsin by in-gel digestion of excised bands of interest ([19,20]). Proteins were digested for 18 h at room temperature and peptides then analysed by tandem mass spectrometry (LC-MS/MS). Peptides sequenced using AmaZon ETD Ion Trap (Bruker Daltonik GmbH, Preston, VIC, Australia) with peptide separation achieved prior by PRLC using Dionex Ultimate 3000 RSLCnano (Dionex, Idstein, Germany). Files were converted into MASCOT Generic Format and imported into Bruker's ProteinScape platform (Bruker Daltonics, Bremen, Germany) for database searching. Searches were performed against the SwissProt database (version 57.15) using in house licensed MASCOT server (version 2.3.02, Matrix Science), with the species set to Homo sapiens and the number of allowed trypsin missed cleavages set to 2. Carbamidomethylation of Cysteine was set as a fixed modification, whereas oxidation of Methionine and phosphorylation of Serine, Threonine and Tyrosine were set as variable modifications. The parent ion tolerance was set to 1.4 Da with fragment ion set to 0.7 Da. Peptide thresholds were set requiring false positive rate less than 0.05% and a MASCOT score greater than 40. Those spectra meeting these criteria were validated by manual inspection to ensure accurate y- and b-ion detection with overlapping sequence coverage. MS was conducted from 3 separate experiments and peptides identified in each run are presented meeting the criteria above.

RNA Extraction and QA

Total RNA was extracted using TRIzol (Invitrogen), with an enhanced overnight $-30°C$ precipitation using glycogen (Sigma) as co-precipitant. RNA quality was checked via Bioanalyzer RNA 6000 Nano chip, while small RNA composition was determined by Bioanalyzer Small RNA chip (both Agilent).

Expression Analysis

For miRNA expression, total RNA was labelled using a FlashTag Biotin HSR RNA labelling kit (Genisphere), hybridized to Genechip miRNA 2.0 microarrays (Affymetrix) and scanned with Affymetrix GeneChip Scanner 3000 7G. For exon/gene expression, total RNA was transcribed to cDNA and amplified using the Applause WT-Amp Plus ST kit, then fragmented and labelled with the Encore Biotin module (both NuGEN). Labelled cDNA was hybridized to GeneChip Exon ST microarrays and scanned as before. QC of microarray data was performed as per manufacturer's recommendations.

Data were analysed using Genespring GX software to determine differentially expressed mRNA and miRNA. Initial functional analysis was conducted on predicted targets of candidate miRNA using the functional annotation clustering (FAC) tool on the DAVID bioinformatics portal (21). FAC reports the significance of functionally related clusters via an Enrichment Score (ES), which is calculated as –log of the geometric mean of P-values of the terms in that cluster. Thus, an ES of 1.3 is equivalent to a mean P-value of 0.05, and $P < 0.01$ is indicated by ES > 2. We therefore considered clusters with ES>2 to be significant. Integrated functional analysis was then undertaken using Integrated Pathways Analysis (IPA) software. A target analysis was performed on the lists of miRNA altered in each condition; this was then paired with experimentally observed changes in mRNA expression in the same condition. Using fold-change data, inversely correlated miRNA–mRNA pairings were filtered and subjected to pathways and other functional analyses.

For vesicular samples, presence/absence of transcripts was determined by limits of experimental detection. From our experience, the limit of detection by qPCR for validation purposes corresponds to a raw signal intensity of approximately 30 on these arrays; however, we set the cut-off at 40 to allow a margin of error. Selected transcripts were confirmed by qPCR as outlined below; expression was defined as the level of detection above background (DABG) readings from no-template control wells.

Quantitative real-time PCR (qPCR)

Forty cycles of real-time PCR was performed as previously described (22). Briefly, multiplex oligo(dT)-primed or specific miRNA-primed reverse transcription was carried out on 500 ng DNase-treated total RNA using Superscript II reverse transcriptase (both Invitrogen) in a final volume of 20 μl. Real-time PCR was performed in triplicate 12.5 μl reactions on diluted cDNA with Power SYBRGreen master mix using an ABI Prism 7500 sequence detection system (both Applied Biosystems). For vesicle samples, 50 ng was reverse transcribed in half-volume reactions and treated as 1:5 dilution of cDNA in the PCR, which was carried out as above.

Normalization

Gene expression qPCR was normalized to GUSB. The small RNAs used to normalize miRNA expression studies, however, are preferentially enriched in the nucleus, precluding conventional normalization. We therefore assessed data reproducibility by calculating the Co-efficient of Variation (CV) for each of the reference small RNAs (U6, U44, U49) and test miRNA in both cell body and neurite fractions. The CV is calculated as $\sigma/\bar{x}$ and expressed as a percentage, and is a normalized measure of the spread of data. Variability ranged between 0.016 and 0.183 cycles; as a single PCR cycle relates to a 2-fold change in expression, this translated to 1.005-fold to 1.065-fold variability in expression. We then compared the variability within the reference small RNAs to the test miRNA and found no significant difference either in the cell bodies ($P = 0.72$) or neurites ($P = 0.47$). Finally,
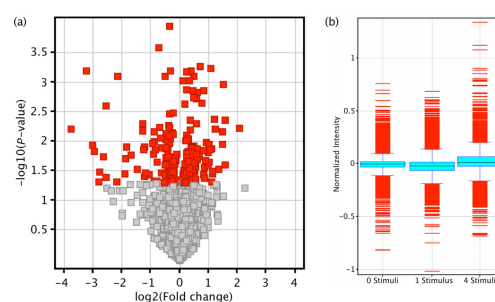

Figure 1. miRNA and mRNA responses to depolarization in whole cells. miRNA and mRNA microarrays were performed on 3 biological replicates of resting cells and cells subjected to one single or four sequential K$^+$ depolarizations. (**a**) Volcano plot comparing miRNA expression between resting and single-depolarized cells demonstrates the bias for down regulation of miRNA in response to activity. Each square represents a single miRNA plotted by fold change (x-axis) and significance (y-axis). (**b**) Boxplot of mRNA microarray data. Compared with resting cells (left), the mRNA profile of cells was reduced by a single stimulus (centre). After 4 successive depolarizations (∼1 h), mRNA levels had recovered, and in fact exceeded that of resting cells (right).

we confirmed the tightness of the data by checking for outliers using Grubb's test. No outliers were detected in either fraction at a significance cut-off of 0.01.

RESULTS

miRNA are down-regulated in response to depolarization in whole cells

Differentiated human SH-SY5Y neuroblast cultures were depolarized with stimulating levels of K$^+$, either once or four times sequentially prior to fractionation and genome-wide miRNA and mRNA analysis. In whole cells, a single stimulus significantly altered the expression of 154 mature miRNA ($P < 0.05$), with a strong trend towards down regulation (71%) (Figure 1a). After 4 stimuli this was reduced to 99 altered miRNA, with 60% down-regulated. Between the 2 modes of depolarization, only 15 altered miRNA were common, and these also showed a bias for down regulation (66% down).

Neurite-associated miRNA are down-regulated after depolarization

To further investigate the subcellular distribution of this depolarization-associated change in miRNA expression, we also analysed the somato-dendritic fraction and dendrite depleted cell bodies from resting and depolarized cells. These analyses reveal that miRNA appear to be compartmentalized in neurites with significant enrichment and depletion of 29 ($P < 0.05$) and 40 molecules ($P < 0.05$) respectively, including all 3 miR-124 precursor hairpins (Figure 2a). qPCR closely validated the array expression of miRNA tested (Figure 2b, miR-1973 representative) with $R^2 = 0.88$ (Figure 2c). Interestingly, the neurite compartment responded to depolarization by up- or down-regulating
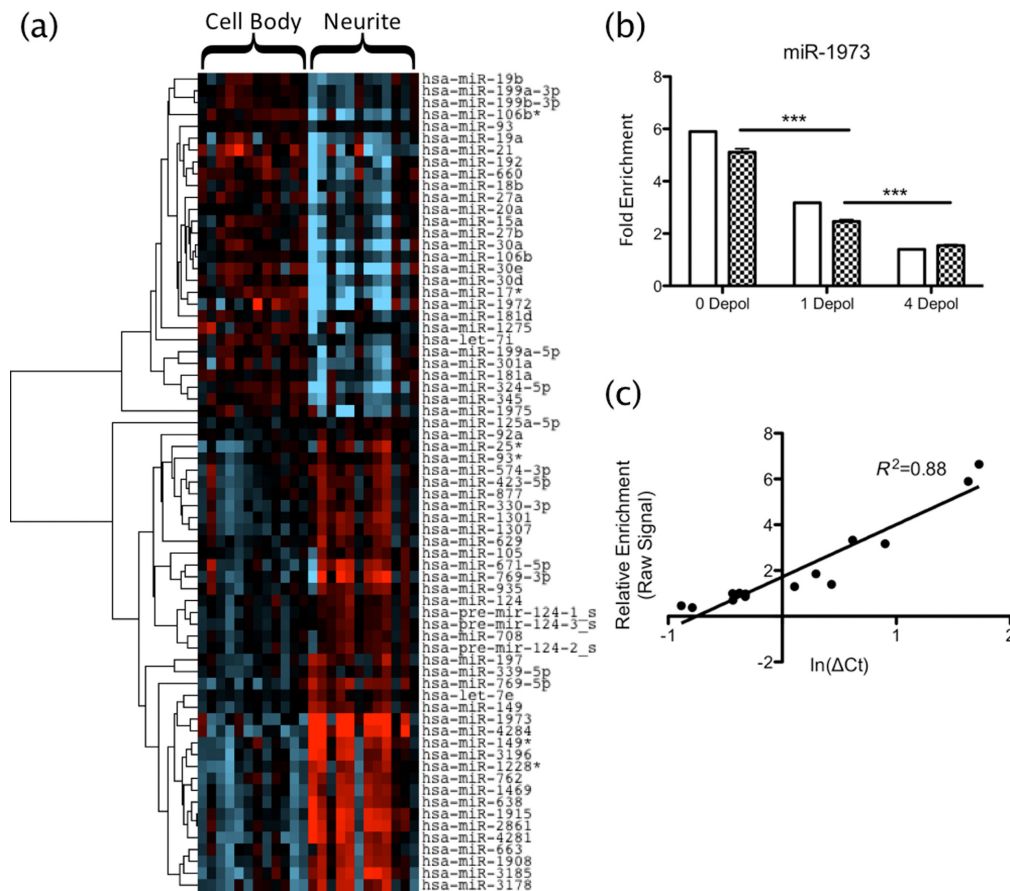
Figure 2. miRNA compartmentalization in neurites. (**a**) T-test was used to find miRNA differentially expressed between compartments ($P < 0.05$), independent of depolarization. Heat map shows supervised clustering of miRNA expression in neurites versus cell bodies. Two main clusters are revealed, indicating miRNA with low (blue) and high (red) expressions in neurites compared with cell bodies. (**b**) qRT-PCR results (chequered bars) closely matched those seen by microarray (open bars), both in enrichment and response to depolarization; miR-1973 shown is representative of 5 miRNA validated across 3 depolarization statuses (15 samples total). (**c**) Correlation of microarray and qPCR expression had $R^2 = 0.88$, validating the microarrays.

miRNA expression (Figure 3a), in contrast to the cell body fraction, which did not display a significant response to stimulation with K+ ions (Figure 3b).

miRNA are released from the neurite fraction in exosomes during depolarization

The apparent depletion of somato-dentritic miRNA following depolarization did not lead to redistribution deeper in the soma as the abundance of individual miRNAs tested did not increase in this fraction (Figure 3). We thus speculated that these miRNA are degraded or disposed of in some other manner. One possibility is that miRNA are released from the dendrites as encapsulated microvesicles or

exosomes in response to excitation (23). Analysis of the depolarization media supported this hypothesis, with EM revealing the presence of distinct vesicles (Figure 4a) of average diameter (106 ± 7.62 nm), which is at the upper end of the size range reported for exosomes (24,25). However, since the vesicles passed through a 0.1 μm filter their actual size is likely smaller and thus within range. The vesicles were positive for exosome markers LAMP1 and Flotillin1 (Figure 4b and c), and contained ribosomal RNA (Figure 5a) and a small RNA population significantly enriched for miRNA (Figure 5b–d).

Importantly, 50% of the miRNA detected in the exosomes were enriched in neurites compared with cell bodies (Table 1). In particular, 4 of these miRNA (miR-638,
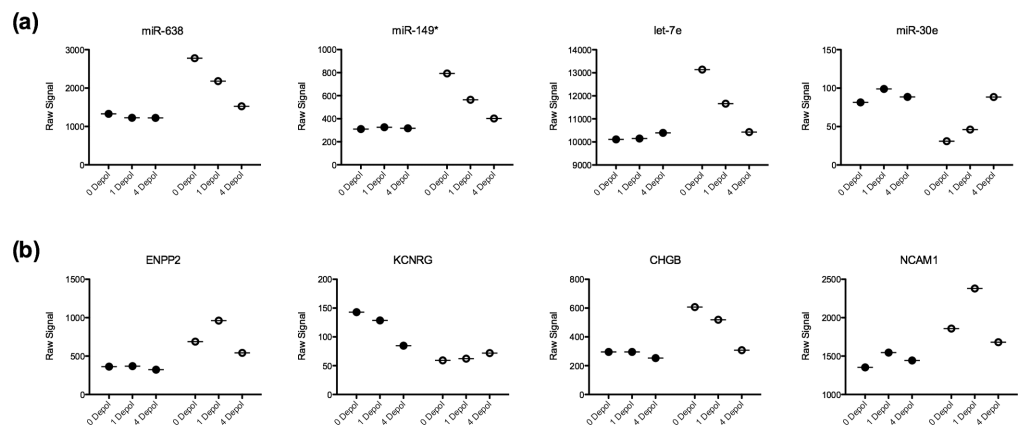
Figure 3. Different subcellular miRNA and mRNA responses to depolarization. Microarray data were analysed by two-way ANOVA on compartment and depolarization pattern to investigate the subcellular response to depolarization. (**a**) miRNA showed little response to depolarization in the cell bodies, however there were clear up- and down- regulation patterns in the neurites. (**b**) Comparatively, mRNA expression followed no consistent pattern in either fraction with successive depolarizations. Closed circles represent cell body samples; open circles represent neurites. 0 depol, 1 depol and 4 depol indicate resting, single depolarized and 4 sequential depolarized cells, respectively.
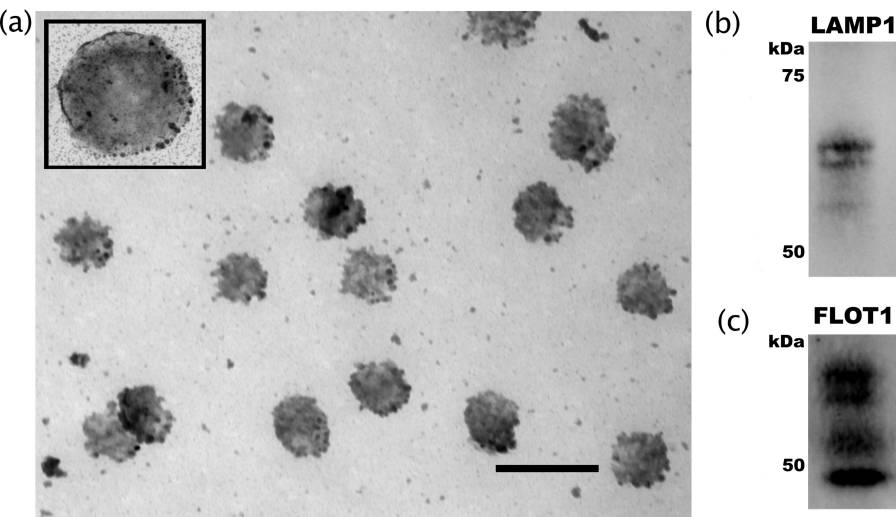
Figure 4. Structural characterization of vesicles as exosomes. Characterization of vesicles released from neurites following potassium-induced depolariza-tion. (**a**) Glutaraldehyde-fixed samples were sliced and photographed using a JEOL-1200EX transmission electron microscope. Scale bar = 200 nm for main photo, 100 nm for inset. Analysis of particle size using ImageJ software found the average diameter of these vesicles to be 106 ± 7.62 nm. (**b**) Western blot analysis of exosome markers LAMP1 and (**c**) Flot1. Each experiment was replicated 3 times and representative blots are depicted.

39
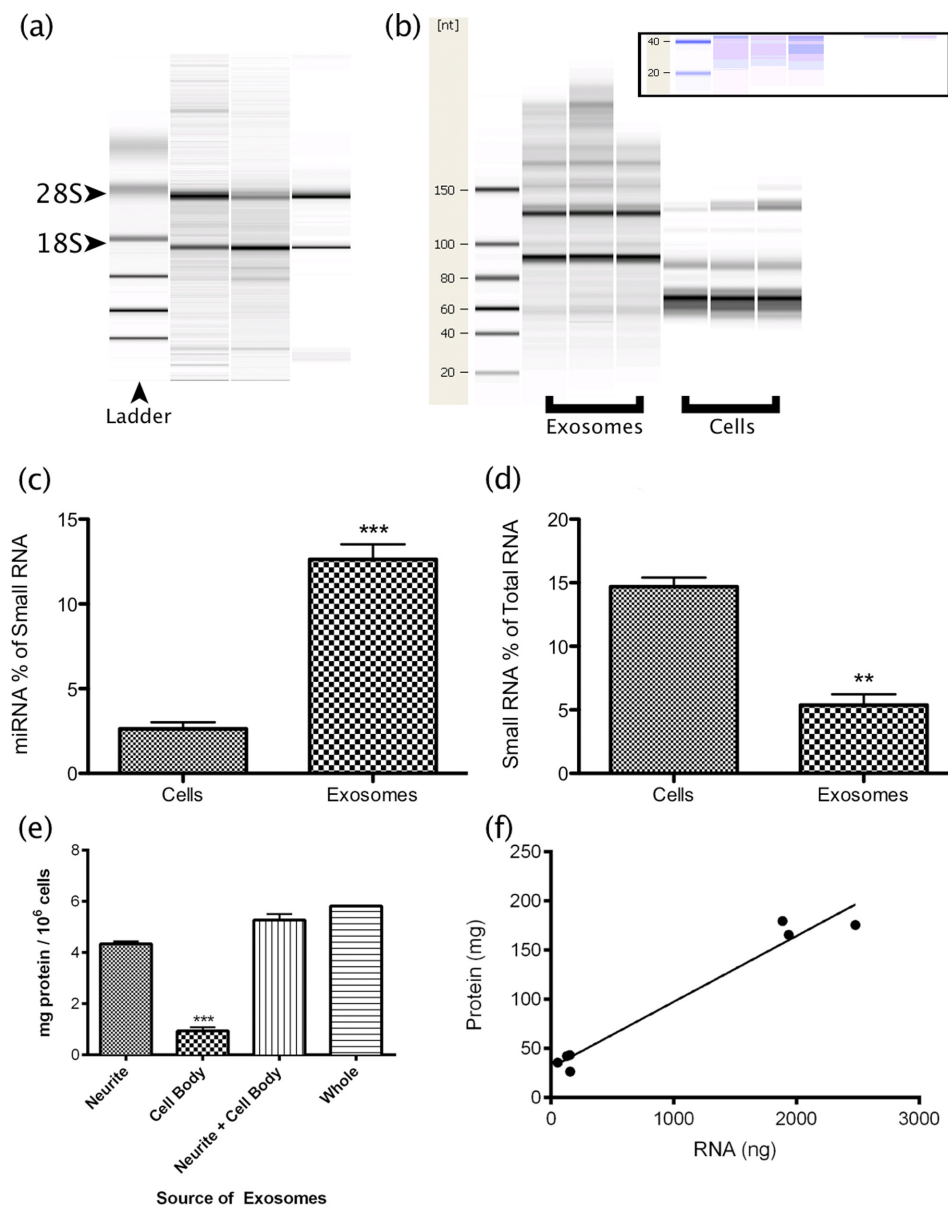
Figure 5. Vesicular nucleic acid composition is consistent with exosomes. (**a**) Bioanalyzer analysis of triplicate samples revealed the presence ribosomal RNA. (**b**) Bioanalyzer comparison of small RNAs derived from vesicles and cells. The vesicular samples appeared enriched for small RNAs (inset). (a and b) Lanes represent individual samples. (**c**) Quantitative analysis of Bioanalyzer data confirmed that miRNA comprised a significantly greater proportion of small RNA in the vesicles, despite (**d**) a reduced overall contribution of small RNA to total RNA. (**e**) Neurites and cell bodies were separated prior to depolarization. Quantitation of protein from vesicle fractions obtained indicated that the neurites are the primary source of depolarization-associated vesicle release. (**f**) Correlation of protein and RNA yields from neurite- and cell body-derived vesicles ($R^2 = 0.96$).

-149*, -4281 and let-7e) were negatively regulated by repeated depolarization in this compartment. The vesicular miRNA cohort was also enriched (10/24) with primate-specific molecules (Table 1), which suggested that these depolarization-associated vesicles might have functional significance in the primate brain.

Investigation of localization of vesicular release by separate depolarization of the neurites and cell bodies implicated the neurites as the primary source of RNA-containing vesicles. On average, 4.68-fold more vesicular protein was obtained from neurites (Figure 5e). RNA yield correlated significantly with protein ($R^2 = 0.96$, $P < 0.0001$, Figure 5f), however neurite-derived samples contained 3.1 times as much RNA/mg protein, suggesting the possibility of a fraction-specific packaging mechanism. Supporting this, LAMP1 mRNA was significantly enriched in the neurite fraction and depleted from this fraction by depolarization (Supplementary Figure S2), suggesting site-specific synthesis of the exosomes.

Exosomes are enriched with synapto-dendritic proteins depleted from depolarized cells

Total protein from resting cells, depolarized cells and exosomes was visualized by silver-stained SDS-PAGE to investigate relative composition. The constitution of exosomes was unique compared with cells, while depolarized cells showed strong homology with resting cells. Strikingly, a band of approximately 250 kDa, present in resting cells, was strongly depleted by depolarization and appeared enriched in exosomes (Figure 6a, bands a and b). These bands were excised and analysed by mass spectrometry, identifying 15 proteins in the depolarized cell sample and 13 in the exosomes (Supplementary Table S1). Among these, 8 proteins were common, the most significant of which was microtubule-associated protein 1b (MAP1B, MAS-COT score 4962). MAP1b is associated with synaptic plasticity, highly localized in the axon growth cone and dendritic spines, and displays activity-dependent pattern of translation in neurons (26–29). Interesting among proteins unique to the exosomal band were the two filamins, A and B (MAS-COT scores 421.7 and 152.6 respectively). Filamins remodel the actin cytoskeleton, and filamin A is localized to the dendritic shaft (30), while filamin B has been associated with PSD95 (31).

Proteomic characterization of exosomes by mass spectrometry

Twenty bands corresponding to the most abundant exosomal proteins (enumerated Figure 6a) were subjected to liquid chromatography mass spectrometry, positively identifying 1329 peptides representing 387 redundant proteins, approximately one third of which have been previously associated with exosomes (Supplementary Data S1); including the exosomal marker LAMP1 (Figure 4b). Gene ontology analysis (Supplementary Data S2) revealed markedly significant enrichment of the 'De novo' post-translational protein synthesis ($q = 6.0e-35$), proteasome complex ($q = 2.5e-19$) and translational elongation ($q = 2.1e-12$) pathways (Figure 6b). In particular, a strong bias was observed towards

HSP90-CCT chaperone complex constituent proteins as well as known peptide clients of this structure (Supplementary Data S1, highlighted). Exosomal constituents were also significantly associated with a variety of neurological disorders including Parkinson's ($p = 1.93e-08$), Alzheimer's ($p = 7.43e-04$) and dementia ($p = 5.19e-04$), and IPA functional analysis generated a highly connected neuronal network among these proteins (Supplementary Figure S3).

Convergent influence among depolarization-associated miRNA from whole cells

To determine whether the change in miRNA availability would have functional relevance in depolarized neuroblasts, functional analysis of predicted targets for all 5 common (single and multiple) up-regulated miRNA was performed. The intersection of these 5 predictions contained 24 genes, which were then subjected to FAC. Similarly, this analysis was also carried out for the 10 common down-regulated miRNA (192 target genes). This very stringent analysis of putative convergent miRNA influence among the up-regulated miRNA revealed tissue specificity for the brain (13/24 genes, $P = 0.036$), which also ranked top among targets for the 10 common down-regulated miRNA (94/192 genes, $P = 0.006$). The small gene list sizes restricted the number of significant clusters, however functionally relevant terms such as "post-transcriptional regulation of gene expression" ($P = 0.003$) and "central nervous system axonogenesis" ($P = 0.008$) were significant among targets of the down-regulated miRNA. These included key neuronal genes such as glutamate (GRIN2A) and GABA (GABRA1) receptors, neurexin3 (NRXN3) and doublecortin (DCX), as well as the schizophrenia-associated gene DISC1. Interestingly, the miRNA biogenesis gene DICER was the most strongly regulated predicted target of the down-regulated miRNA.

Acute activation alters regulation of GPCR signalling pathway; chronic activation modulates regulation of transcription and translation

A single K^+-induced depolarization also resulted in an acute reduction in whole-cell mRNA levels, with 251 changed genes after 1 depolarization, 74% of which were significantly down-regulated ($P < 0.05$, FDR). After 4 stimuli, cellular mRNA levels recovered and exceeded resting levels with 89% of 1168 differentially expressed genes being up-regulated (Figure 1b). FAC analysis of genes altered by 1 depolarization found only 1 functional cluster with ES>2, which was represented by terms involving GPCR signalling (ES = 3.19). After 4 depolarizations, 6 clusters had ES>2, and the focus shifted to the nucleus (ES = 7.3), RNA processing and splicing (ES = 4.4), ribosome biogenesis (ES = 3.1) and regulation of translation (ES = 3.1).

IPA software was used to integrate miRNA and mRNA expression to determine functional clusters of miRNA–mRNA regulatory relationships that are altered by depolarization. In response to single stimulus, this analysis confirmed the FAC results, demonstrating significant alteration of a regulatory network involving G-protein coupled receptor signalling ($p = 1.36e-03$, Supplementary Figure S4a),

Table 1. miRNA detected in exosome samples

miRNA[a]	Sample Ranking			Relative Abundance[b] (%)
	A	B	C	
hsa-miR-638	2	1	1	13
hsa-miR-1915	1	2	2	12
*hsa-miR-149**	4	3	3	9
hsa-miR-2861	3	4	5	9
hsa-miR-3196	5	5	4	9
hsa-let-7b	6	6	7	5
hsa-miR-1975	8	7	6	3
hsa-miR-1281	9	8	8	3
hsa-miR-762	7	9	10	5
hsa-miR-1908	10	10	9	4
hsa-miR-23b	11	11	11	4
*hsa-miR-1228**	12	13	12	4
hsa-miR-320b	14	14	14	2
hsa-miR-320c	17	12	13	2
hsa-miR-92a	15	15	15	2
hsa-miR-320a	16	16	16	2
hsa-miR-1469	13	17	23	3
hsa-miR-99b	18	18	19	1
hsa-miR-191	21	19	17	1
hsa-miR-1184	22	20	20	2
hsa-miR-23a	20	22	22	1
hsa-miR-24	24	23	18	1
hsa-miR-4281	23	21	21	1
hsa-let-7e	19	24	24	1

[a]miRNA list in declining abundance by rank sum of 3 replicates (A,B,C). miRNA in *italics* were enriched in neurites. miRNA shown in **bold** are currently only known in humans or primates (hsa only or hsa+ptr+ppy). miRNA shown in red are primate-specific AND enriched in neurites.
[b]Relative abundance as determined by averaged microarray fluorescence across samples A, B, C, divided by total signal obtained from miRNA detected on the microarray and expressed as a percentage.
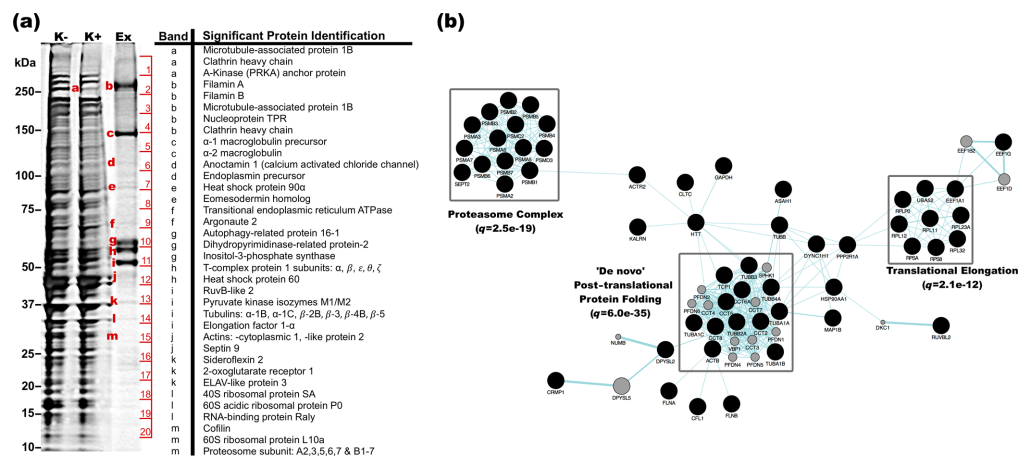
Figure 6. Proteomic analysis of exosomes. (**a**) Protein from resting cells (K$^-$), depolarized cells (K$^+$) and exosomes was solubilized and resolved by SDS-PAGE. Bands of interest (enumerated) were excised and sequenced by mass spectrometry. (**b**) Pathways analysis of 387 proteins identified by mass spectrometry. Analysis was performed using the Genemania plugin for Cytoscape software. Clusters representing the most significantly enriched functions are indicated by grey boxes, and indicative *q*-values shown.

importantly indicating modulation of the cascade from receptor to nucleus. This finding was elaborated by revealing the significance of calcium-induced cAMP signalling via Gs-coupled receptors ($p = 5.65e-06$, Supplementary Figure S4b). Analysis of the response to repeated stimuli also agreed with the FAC analysis. A highly connected "DNA transcription" regulatory network (Supplementary Figure S5), centred on miRs-548 and -506, was identified among negatively correlated genes and miRNA (genes up, miRNA down).

miRNA appear functionally compartmentalized in neurites

Predicted targets of miRNA that appeared compartmentalized within or excluded from neurites were submitted to DAVID for FAC as before. Targets of neurite-enriched miRNA comprised 5 functional clusters with ES>2, and suggested a compartmental requirement for increased regulation of transcripts whose products are involved in GTP and PKC signalling (ES = 3.7 and 3.0 respectively), axon guidance and development (ES = 2.5) and secretion of vesicles (ES = 2.4 and 2.3). Neurite-depleted miRNA also demonstrated functional specificity to this compartment with 3 functional clusters having ES>2. Predicted targets were enriched for regulation of pre- and post-translational modulation, specifically RNA-mediated gene silencing (ES = 2.4), and ATP-driven phosphorylation processes (ES = 2.4), including MAPK- and CAMK- family members and BDNF receptor NTRK2.

Functional annotation of dendritic miRNA–mRNA interactions in response to depolarization

We next examined the subcellular response to activity by 2-way ANOVA. Depolarization significantly altered both the miRNA and mRNA composition of the neurites ($P < 0.05$, FDR), but strikingly the modulation of miRNA expression appeared localized to the neurites. Over successive depolarizations, the abundance of significantly changed miRNA transcripts remained almost unchanged in the cell body fractions while either increasing or decreasing in the neurites (Figure 3a). However, this was not the case for mRNA expression, which varied in both compartments (Figure 3b).

Integrated analysis with IPA found functionally relevant regulatory networks after 1 and 4 depolarizations. Most interesting among these was a "neuronal signalling" network, comprising 4 miRNA and many neurotransmitter receptors with negatively correlated response (mRNA up, miRNA down) after 1 stimulus (Supplementary Figure S6).

Exosomes released during depolarization are enriched with primate specific miRNA

Since exosomal vesicles have been shown to contain various RNA species, we extracted and analysed total RNA to characterize this population. Strong ribosomal RNA bands were detected (Figure 5a), while the small RNA composition of these vesicles proved quite different from that of whole cells (Figure 5b), with stronger bands apparent at the sizes of transfer RNA and/or precursor miRNA transcripts. Moreover, miRNA comprised a significantly higher

proportion of small RNA isolated from vesicles (Figure 5c, and visible in Figure 5b enhanced gel inset), despite a significantly smaller proportion of small RNA being present (Figure 5d).

Vesicular RNA from three separate cell populations was then analysed by microarray to investigate the profile of miRNA packaged in these particles. We detected the same 23 mature miRNA in all replicates, 9 (39%) of which were specific to humans or primates (hsa only, or hsa+ptr+ppy), and 14 (61%) were preferentially enriched in the neurites of their parent cells (Table 1). Moreover, 6 miRNA (26% of the vesicular cohort) fulfilled both criteria, suggesting that these dendrite-derived activity-associated exosomal miRNA have emerged recently in evolutionary history (Table 1).

For further confirmation of the microarray analysis, we examined the expression of 18S rRNA and miR-638, the most abundant miRNA detected in the exosomes by qPCR. This analysis included two additional samples that were not profiled by microarray. The transcripts were detected significantly above background ($P < 0.0001$), with 18S rRNA and miR-638 emerging at cycles 26.2 and 10.5 respectively, confirming the presence of both transcripts in the vesicles analysed by microarray as well as the novel samples.

miRNA responding negatively to depolarization in neurites were released in exosomes, and target functionally relevant mRNA

More than 60% of the miRNA detected in exosomes were enriched in neurites compared with cell bodies, suggesting that they were derived from the dendritic fraction of the parent cells. In particular, 4 of these miRNA (miR-638, -149*, -4281 and let-7e) were negatively regulated by repeated depolarization in this compartment. We therefore wondered what the functional significance of encapsulating and releasing these 4 miRNA would have for the parent cells or surrounding cells that are the likely recipients of this molecular cargo? A list of mRNA potentially regulated by these miRNA collectively was compiled. This list comprising 95 transcripts, a significant proportion of which demonstrated tissue specificity for the brain (57/95, corr. $P = 0.022$), was submitted for FAC. Enrichment scores were slightly lower due to the small list used for analysis, however the terms significantly enriched (ES = 1.92–1.14) all related to synaptic function including synapse, post-synaptic density and regulation of neuronal synaptic plasticity.

DISCUSSION

The findings presented here demonstrate that K^+-induced depolarization significantly alters the miRNA composition of cultured human neurons at both the cellular and subcellular levels. The over representation of down-regulated miRNA expression suggests that neural activity leads to global reduction in post-synaptic gene silencing which could facilitate a rapid increase in local translation. This finding is supported by the work of Konopka and colleagues, which demonstrated enhancements of learning and memory in mice via miRNA depletion (32). Although fewer in number, a proportion of miRNA was also increased in depolarized cells and the somato-dendritic fraction suggesting
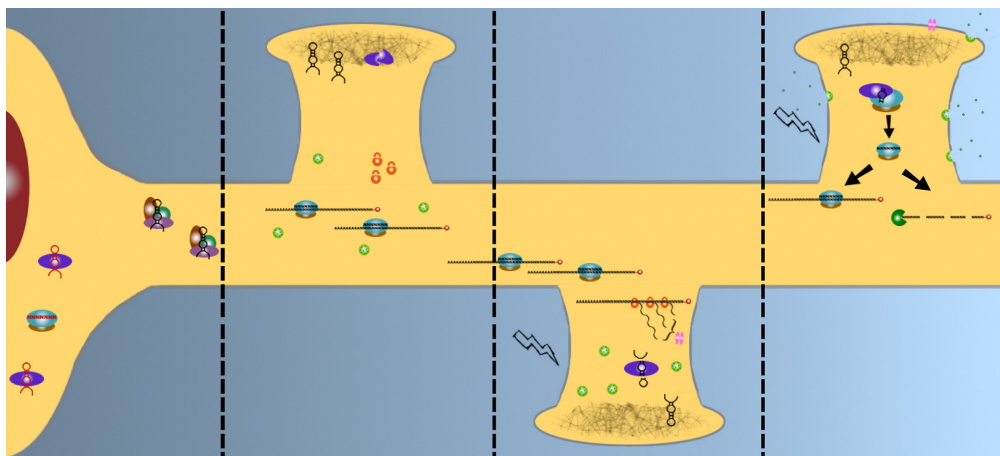
Figure 7. Integrated model of PTGS and synaptic plasticity. Dendritically-targeted miRNA (black) are sorted from cell body restricted transcripts (red), and transported either as precursor hairpins by RNP complexes (panel 1) for storage in the PSD along with inactive DICER (panel 2), or as part of an active RISC (panel 2). miRNA-enriched exosomes, packaged into multivesicular bodies (MVBs, green, panel 2), and ribosomes (orange) are scattered throughout the dendritic tree. When a spine is depolarized (panel 3), the RISC decompiles, freeing its mRNA cargo for translation, while DICER is activated and cleaves required hairpins from the PSD. As activity continues (panel 4), MVBs fuse with the cell membrane, releasing exosomes, while newly synthesized proteins are inserted into the membrane/PSD. The cleaved mature miRNA are loaded into an awaiting RISC, and may "mop-up" excess mRNAs to attenuate the response, either by silencing or degradation.

that there is also some selective increase in gene silencing. Indeed, specific miRNA have been shown to be down- and up-regulated in neuronal plasticity in response to different stimuli (33). The predicted targets of both the down- and up- regulated miRNA were functionally clustered, revealing enrichment of genes involved in plasticity-related processes including synaptic activity, protein localization and neuron morphogenesis. The functionality of predicted target genes was supported by the observed genome-wide changes in gene expression.

These observations raise important questions about miRNA partitioning within the differentiated neuron and how it is so rapidly altered within minutes of depolarization. In respect to compartmentalization, the literature suggests that mature miRNA are transported to dendritic spines and the post-synaptic milieu within ribonucleoprotein complexes or granules—perhaps associated with their synaptically localizing mRNA targets (34,35). They may also become localized to the synapse in their inactive precursor form and become activated by maturation through dendritically localized Dicer protein that has been shown to itself be activated after excitation-dependent proteolysis by the calcium-dependent protease Calpain (36). More recently, the same group have shown that there is also post-synaptic localization of microprocessor complex proteins Drosha and DGCR8 capable of localized processing of primary miRNA transcripts (37). While it is unlikely that the changes we observed are due to changes in ribonucleoprotein trafficking of miRNA, an elevation of functional Dicer in the post-synaptic compartment could lead to the production of more mature miRNA in a matter of minutes after depolarization. As most of the miRNA were decreased af-

ter depolarization, it is plausible that these molecules were degraded by nuclease, perhaps as a secondary consequence of RISC decomposition brought about to facilitate activity-associated induction of translation (13,14).

An alternative explanation is that these molecules are packaged and released from the depolarized cells in vesicles. To test this hypothesis, we collected and analysed exosomal miRNA and identified a number of molecules that were enriched in the synaptodendritic fraction and depleted from this fraction in the parent cells after depolarization. The vesicular RNA was found to be enriched with small RNA, and surprisingly rich with recently evolved primate-specific miRNA. Depolarization of SH-SY5Y has previously been shown to trigger formation and release of synaptic vesicles (LDCVs, 200nm diameter), as well as a population of smaller, uncharacterized vesicles (60 nm diameter) (38–40). Combined with the present findings, these smaller vesicles are most likely exosomes, which have been found to be released from cultured cortical rat neurons (23), and are increasingly associated with intercellular miRNA trafficking, the establishment of polarity (reviewed in (24,41)) and extracellular distribution of mRNA and proteins (42), and have been shown to effect changes in target cell phenotype and activation (43).

These vesicles were only released from cells upon stimulation, suggesting an activity-specific function. This interpretation was supported by the target gene pathway analysis of the vesicular miRNA that was enriched with synaptic processes including synapse, post-synaptic density and regulation of neuronal synaptic plasticity. While it has been known for some time that recycling endosomes contribute to spine growth in response to LTP-inducing stimuli (44),

the mechanisms of synaptic exosome release have begun to be elaborated in more detail in the *Drosophila* nervous system (45). Indeed, it is broadly suggested that exosomal transfer of miRNA may contribute to the function of neural systems by modifying local neurons and supporting cells such as astrocytes, oligodendrocytes and microglia. In support, Morel et al. (2013) have recently shown that miR 124a is released from neuronal exosomes and can regulate the expression of astroglial glutamate transporter (GLT1) (46). Moreover, exosomes originating from the pre-synaptic terminal were found to regulate retrograde signalling in their post-synaptic partners at the *Drosophila* neuromuscular junction via transfer of synaptotagmin4 (47). Their potential significance in synaptic function is supported by the MS-observed enrichment of MAP1B in these vesicles. MAP1B positive post-synaptic terminals were reported by Kawakami et al. to contain clear vesicles (26) and by Kitamura and colleagues as being associated with increased synaptogenesis (27). If these exosomes were transferred to neighbouring synapses during depolarization, the infusion of MAP1B and other substrates for spine remodelling, such as actin, tubulin and cofilin, would foster strengthening of the post-synaptic membrane. This is reinforced by the presence of Filamins A and B in exosomes. Although the Filamins have been shown to decrease in expression during development, the decrease is modest and they are still well expressed in the mature brain, in particular in the cortex (30,48). Filamin A has been shown to be localized to the dendritic shaft, but absent from dendritic spines, which has been suggested to enable the flexibility required for plasticity, and is also associated with surface localization of certain receptors, in particular several subtypes of potassium channel (30), which is interesting in the current context of potassium depolarization.

Conversely, it is possible that activity-associated exosomal release provides a means for cells to rapidly eliminate regulatory and structural molecules that are limiting or repressing the expansion of their post-synaptic function. This concept accords with the view that exosomes perform a role in cellular waste disposal (24). Regardless of the mechanism, our observation that these depolarization-associated vesicles were enriched with functionally significant primate-specific miRNA is fascinating and urges further investigation of exosomal release and transfer in the mammalian nervous system.

More broadly, the apparent functional specificity of miRNA compartmentalization, both in terms of their target analyses and the experimentally observed response to depolarization, lends support to the hypothesis that this process is involved with neural plasticity-associated translational regulation (Figure 7). In further support of this hypothesis, we recently demonstrated that while most target gene transcripts are inversely correlated with intracellular miRNA concentration, a substantial proportion are positively correlated (49). Functional annotation of the transcripts positively correlated with miRNA levels in SH-SY5Y cells suggested that these were involved in highly localized neural processes including neuroactive ligand-receptor interaction and adherens junctions. These observations further suggest that miRNA are delivered or generated with dynamic patterns of intracellular localization

that enable them to collectively orchestrate even more complex combinatorial patterns of localized activity-dependent translation. Interestingly, the localization of the depolarization response to the neurite compartment was unique to miRNA, whereas mRNAs were modulated in both the neurites and cell bodies. Investigation of predicted targets of neurite-enriched, depolarization-responsive miRNA found enrichment of neuronally relevant genes, pathways and ontologies, suggesting that the expression changes identified are a deliberate response to stimulation of neuronally differentiating cells. Since both the up- and down-regulated cohorts are predicted to regulate expression of neuronal genes, these findings also suggest that depolarization selectively regulates the abundance of miRNA that directly modulate the response to this event and ultimately fine-tunes translational homeostasis.

In summary, we observed rapid depolarization-associated redistribution of miRNA in neurons, suggesting that they are an important regulatory component in the dynamics of normal synaptic function. As synaptic function is thought to be compromised in neurodegenerative and neuropsychiatric conditions, it is plausible that these molecules and their role in translational homeostasis are disrupted in these neuropathologies. This is supported by our postmortem investigation of schizophrenia, where we identified elevation of cortical miRNA expression that contrasted with the bias towards reduction of miRNA in response to depolarization observed in this study (22,50). If a reduction in PTGS is a requisite mechanism for synaptic plasticity and the over-abundance of miRNA in this pathology is insurmountable, the signal may be muted or lost. This mechanism warrants further investigation, as currently available therapeutics fail to provide improvement of cognitive symptoms. Interestingly, a large proportion of the depolarization-associated changes could be attributed to the release of exosomes containing synaptic protein MAP1b, and enriched with recently evolved miRNA. While the full implications are yet to be determined, it is tempting to speculate that these molecules and the associated mechanism could be involved in facilitating greater synaptic complexity and cognitive efficiency.

SUPPLEMENTARY DATA

Supplementary Data are available at NAR Online.

FUNDING

REFERENCES

1. Steward,O., Pollack,A. and Rao,A. (1991) Evidence that protein constituents of postsynaptic membrane specializations are locally synthesized: time course of appearance of recently synthesized proteins in synaptic junctions. *J. Neurosci. Res.*, **30**, 649–660.

2. Goldie,B.J. and Cairns,M.J. (2012) Post-transcriptional trafficking and regulation of neuronal gene expression. *Mol. Neurobiol.*, **45**, 99–108.

3. Mori,Y., Imaizumi,K., Katayama,T., Yoneda,T. and Tohyama,M. (2000) Two cis-acting elements in the 3' untranslated region of alpha-CaMKII regulate its dendritic targeting. *Nat. Neurosci.*, **3**, 1079–1084.

4. Blichenberg,A., Schwanke,B., Rehbein,M., Garner,C.C., Richter,D. and Kindler,S. (1999) Identification of a cis-acting dendritic targeting element in MAP2 mRNAs. *J. Neurosci.*, **19**, 8818–8829.

5. Ainger,K., Avossa,D., Diana,A.S., Barry,C., Barbarese,E. and Carson,J.H. (1997) Transport and localization elements in myelin basic protein mRNA. *J. Cell Biol.*, **138**, 1077–1087.

6. Hüttelmaier,S., Zenklusen,D., Lederer,M., Dictenberg,J., Lorenz,M., Meng,X., Bassell,G.J., Condeelis,J. and Singer,R.H. (2005) Spatial regulation of beta-actin translation by Src-dependent phosphorylation of ZBP1. *Nature*, **438**, 512–515.

7. Beveridge,N.J., Tooney,P.A., Carroll,A.P., Tran,N. and Cairns,M.J. (2009) Down-regulation of miR-17 family expression in response to retinoic acid induced neuronal differentiation. *Cell Signal.*, **21**, 1837–1845.

8. Giraldez,A.J., Cinalli,R.M., Glasner,M.E., Enright,A.J., Thomson,J.M., Baskerville,S., Hammond,S.M., Bartel,D.P. and Schier,A.F. (2005) MicroRNAs regulate brain morphogenesis in zebrafish. *Science*, **308**, 833–838.

9. Berdnik,D., Fan,A.P., Potter,C.J. and Luo,L. (2008) MicroRNA processing pathway regulates olfactory neuron morphogenesis. *Curr. Biol.*, **18**, 1754–1759.

10. De Pietri Tonelli,D., Pulvers,J.N., Haffner,C., Murchison,E.P., Hannon,G.J. and Huttner,W.B. (2008) miRNAs are essential for survival and differentiation of newborn neurons but not for expansion of neural progenitors during early neurogenesis in the mouse embryonic neocortex. *Development*, **135**, 3911–3921.

11. Caudy,A.A., Myers,M., Hannon,G.J. and Hammond,S.M. (2002) Fragile X-related protein and VIG associate with the RNA interference machinery. *Genes Dev.*, **16**, 2491–2496.

12. Eulalio,A., Huntzinger,E. and Izaurralde,E. (2008) Getting to the root of miRNA-mediated gene silencing. *Cell*, **132**, 9–14.

13. Ashraf,S.I., McLoon,A.L., Sclarsic,S.M. and Kunes,S. (2006) Synaptic protein synthesis associated with memory is regulated by the RISC pathway in Drosophila. *Cell*, **124**, 191–205.

14. Banerjee,S., Neveu,P. and Kosik,K.S. (2009) A coordinated local translational control point at the synapse involving relief from silencing and MOV10 degradation. *Neuron*, **64**, 871–884.

15. Géraldine,M., Stéphanie,D., Bénédicte,L., Isabelle,D., Monique,L. and Sylvie,V. (2010) DHA enhances the noradrenaline release by SH-SY5Y cells. *Neurochem. Int.*, **56**, 94–100.

16. Huang,Y.Y. and Kandel,E.R. (1994) Recruitment of long-lasting and protein kinase A-dependent long-term potentiation in the CA1 region of hippocampus requires repeated tetanization. *Learn. Mem.*, **1**, 74–82.

17. Meyerson,G., Pfenninger,K.H. and Påhlman,S. (1992) A complex consisting of pp60c-src/pp60c-srcN and a 38 kDa protein is highly enriched in growth cones from differentiated SH-SY5Y neuroblastoma cells. *J. Cell Sci.*, **103**, 233–243.

18. Miranda,K.C., Bond,D.T., McKee,M., Skog,J., Păunescu,T.G., Da Silva,N., Brown,D. and Russo,L.M. (2010) Nucleic acids within urinary exosomes/microvesicles are potential biomarkers for renal disease. *Kidney Int.*, **78**, 191–199.

19. Dun,M.D., Anderson,A.L., Bromfield,E.G., Asquith,K.L., Emmett,B., McLaughlin,E.A., Aitken,R.J. and Nixon,B. (2012) Investigation of the expression and functional significance of the novel mouse sperm protein, a disintegrin and metalloprotease with thrombospondin type 1 motifs number 10 (ADAMTS10). *Int. J. Androl.*, **35**, 572–589.

20. Dun,M.D., Smith,N.D., Baker,M.A., Lin,M., Aitken,R.J. and Nixon,B. (2011) The chaperonin containing TCP1 complex (CCT/TRiC) is involved in mediating sperm-oocyte interaction. *J. Biol. Chem.*, **286**, 36875–36887.

21. Huang,D.W., Sherman,B.T., Tan,Q., Kir,J., Liu,D., Bryant,D., Guo,Y., Stephens,R., Baseler,M.W., Lane,H.C. *et al.* (2007) DAVID Bioinformatics Resources: expanded annotation database and novel algorithms to better extract biology from large gene lists. *Nucleic Acids Res.*, **35**, W169–W175.

22. Beveridge,N.J., Gardiner,E., Carroll,A.P., Tooney,P.A. and Cairns,M.J. (2010) Schizophrenia is associated with an increase in cortical microRNA biogenesis. *Mol. Psychiatry*, **15**, 1176–1189.

23. Fauré,J., Lachenal,G., Court,M., Hirrlinger,J., Chatellard-Causse,C., Blot,B., Grange,J., Schoehn,G., Goldberg,Y., Boyer,V. *et al.* (2006) Exosomes are released by cultured cortical neurones. *Mol. Cell. Neurosci.*, **31**, 642–648.

24. Lakkaraju,A. and Rodriguez-Boulan,E. (2008) Itinerant exosomes: emerging roles in cell and tissue polarity. *Trends Cell Biol.*, **18**, 199–209.

25. Théry,C., Zitvogel,L. and Amigorena,S. (2002) Exosomes: composition, biogenesis and function. *Nat. Rev. Immunol.*, **2**, 569–579.

26. Kawakami,S.-I., Muramoto,K., Ichikawa,M. and Kuroda,Y. (2003) Localization of microtubule-associated protein (MAP) 1B in the postsynaptic densities of the rat cerebral cortex. *Cell. Mol. Neurobiol.*, **23**, 887–894.

27. Kitamura,C., Shirai,K., Inoue,M. and Tashiro,T. (2007) Changes in the subcellular distribution of microtubule-associated protein 1B during synaptogenesis of cultured rat cortical neurons. *Cell. Mol. Neurobiol.*, **27**, 57–73.

28. Tortosa,E., Montenegro-Venegas,C., Benoist,M., Härtel,S., González-Billault,C., Esteban,J.A. and Avila,J. (2011) Microtubule-associated protein 1B (MAP1B) is required for dendritic spine development and synaptic maturation. *J. Biol. Chem.*, **286**, 40638–40648.

29. Zervas,M., Opitz,T., Edelmann,W., Wainer,B., Kucherlapati,R. and Stanton,P.K. (2005) Impaired hippocampal long-term potentiation in microtubule-associated protein 1B-deficient mice. *J. Neurosci. Res.*, **82**, 83–92.

30. Noam,Y., Phan,L., McClelland,S., Manders,E.M., Ehrengruber,M.U., Wadman,W.J., Baram,T.Z. and Chen,Y. (2012) Distinct regional and subcellular localization of the actin-binding protein filamin A in the mature rat brain. *J. Comp. Neurol.*, **520**, 3013–3034.

31. Arbuckle,M.I., Komiyama,N.H., Delaney,A., Coba,M., Garry,E.M., Rosie,R., Allchorne,A.J., Forsyth,L.H., Bence,M., Carlisle,H.J. *et al.* (2010) The SH3 domain of postsynaptic density 95 mediates inflammatory pain through phosphatidylinositol-3-kinase recruitment. *EMBO Rep.*, **11**, 473–478.

32. Konopka,W., Kiryk,A., Novak,M., Herwerth,M., Parkitna,J.R., Wawrzyniak,M., Kowarsch,A., Michaluk,P., Dzwonek,J., Arnsperger,T. *et al.* (2010) MicroRNA loss enhances learning and memory in mice. *J. Neurosci.*, **30**, 14835–14842.

33. Krol,J., Busskamp,V., Markiewicz,I., Stadler,M.B., Ribi,S., Richter,J., Duebel,J., Bicker,S., Fehling,H.J., Schubeler,D. *et al.* (2010) Characterizing light-regulated retinal microRNAs reveals rapid turnover as a common property of neuronal microRNAs. *Cell*, **141**, 618–631.

34. Hillebrand,J., Pan,K., Kokaram,A., Barbee,S., Parker,R. and Ramaswami,M. (2010) The Me31B DEAD-Box helicase localizes to postsynaptic foci and regulates expression of a CaMKII reporter mRNA in dendrites of Drosophila olfactory projection neurons. *Front. Neural. Circuits*, **4**, 121.

35. Barbee,S.A., Estes,P.S., Cziko,A.-M., Hillebrand,J., Luedeman,R.A., Coller,J.M., Johnson,N., Howlett,I.C., Geng,C., Ueda,R. *et al.* (2006) Staufen- and FMRP-containing neuronal RNPs are structurally and functionally related to somatic P bodies. *Neuron*, **52**, 997–1009.

36. Lugli,G., Larson,J., Martone,M.E., Jones,Y. and Smalheiser,N.R. (2005) Dicer and eIF2c are enriched at postsynaptic densities in adult mouse brain and are modified by neuronal activity in a calpain-dependent manner. *J. Neurochem.*, **94**, 896–905.

37. Lugli,G., Larson,J., Demars,M.P. and Smalheiser,N.R. (2012) Primary microRNA precursor transcripts are localized at post-synaptic densities in adult mouse forebrain. *J. Neurochem.*, **123**, 459–466.

38. Goodall,A.R., Danks,K., Walker,J.H., Ball,S.G. and Vaughan,P.F. (1997) Occurrence of two types of secretory vesicles in the human neuroblastoma SH-SY5Y. *J. Neurochem.*, **68**, 1542–1552.

39. Ou,X.M., Partoens,P.M., Wang,J.M., Walker,J.H., Danks,K., Vaughan,P.F. and De Potter,W.P. (1998) The storage of noradrenaline, neuropeptide Y and chromogranins in and stoichiometric release from large dense cored vesicles of the undifferentiated human neuroblastoma cell line SH-SY5Y. *Int. J. Mol. Med.*, **1**, 105–112.

40. Sarkanen,J.-R., Nykky,J., Siikanen,J., Selinummi,J., Ylikomi,T. and Jalonen,T.O. (2007) Cholesterol supports the retinoic acid-induced synaptic vesicle formation in differentiating human SH-SY5Y neuroblastoma cells. *J. Neurochem.*, **102**, 1941–1952.

41. Smalheiser,N.R. (2007) Exosomal transfer of proteins and RNAs at synapses in the nervous system. *Biol. Direct.*, **2**, 35.

42. Valadi,H., Ekström,K., Bossios,A., Sjöstrand,M., Lee,J.J. and Lötvall,J.O. (2007) Exosome-mediated transfer of mRNAs and microRNAs is a novel mechanism of genetic exchange between cells. *Nat. Cell. Biol.*, **9**, 654–659.

43. Nazarenko,I., Rana,S., Baumann,A., McAlear,J., Hellwig,A., Trendelenburg,M., Lochnit,G., Preissner,K.T. and Zöller,M. (2010) Cell surface tetraspanin Tspan8 contributes to molecular pathways of exosome-induced endothelial cell activation. *Cancer Res.*, **70**, 1668–1678.

44. Park,M., Salgado,J.M., Ostroff,L., Helton,T.D., Robinson,C.G., Harris,K.M. and Ehlers,M.D. (2006) Plasticity-induced growth of dendritic spines by exocytic trafficking from recycling endosomes. *Neuron*, **52**, 817–830.

45. Koles,K., Nunnari,J., Korkut,C., Barria,R., Brewer,C., Li,Y., Leszyk,J., Zhang,B. and Budnik,V. (2012) Mechanism of evenness

interrupted (Evi)-exosome release at synaptic boutons. *J. Biol. Chem.*, **287**, 16820–16834.

46. Morel,L., Regan,M., Higashimori,H., Ng,S.K., Esau,C., Vidensky,S., Rothstein,J. and Yang,Y. (2013) Neuronal exosomal miRNA-dependent translational regulation of astroglial glutamate transporter GLT1. *J. Biol. Chem.*, **288**, 7105–7116.

47. Korkut,C., Li,Y., Koles,K., Brewer,C., Ashley,J., Yoshihara,M. and Budnik,V. (2013) Regulation of postsynaptic retrograde signaling by presynaptic exosome release. *Neuron*, **77**, 1039–1046.

48. Sheen,V.L., Feng,Y., Graham,D., Takafuta,T., Shapiro,S.S. and Walsh,C.A. (2002) Filamin A and Filamin B are co-expressed within neurons during periods of neuronal migration and can physically interact. *Hum. Mol. Genet.*, **11**, 2845–2854.

49. Carroll,A.P., Tran,N., Tooney,P.A. and Cairns,M.J. (2012) Alternative mRNA fates identified in microRNA-associated transcriptome analysis. *BMC Genomics.*, **13**, 561.

50. Santarelli,D.M., Beveridge,N.J., Tooney,P.A. and Cairns,M.J. (2011) Upregulation of dicer and microRNA expression in the dorsolateral prefrontal cortex Brodmann area 46 in schizophrenia. *Biol. Psychiatry*, **69**, 180–187.

CHAPTER 5

A putative novel aspect of

miRNA biology in neurons

STATEMENT OF CONTRIBUTION OF OTHERS

Goldie BJ, Atkins JR, Weidenhofer J and Cairns MJ: **A consensus miRNA sequence motif is associated with Ago2-specific nuclear localisation of neuronal mRNAs in human neuroblasts.** *Submitted.*

*I attest that Research Higher Degree candidate **Belinda Goldie** was the primary contributor to the development of this publication. This extensive contribution included: driving the initial study design and intellectual development of the study; establishing, optimising, executing, analysing and interpreting all experiments contained within this study; performing all gene expression and statistical analyses, and some bioinformatic analysis; and writing the manuscript in full. Joshua Atkins assisted with bioinformatic analysis.*

_____

Belinda J Goldie (candidate)

_____

Joshua R Atkins

_____

Judith Weidenhofer

_____

Murray J Cairns (supervisor)

_____   ___05/08/2014_____

Professor Robert Callister   **Date**

Assistant Dean Research Training (ADRT)

A consensus miRNA sequence motif is associated with Ago2-specific nuclear localisation of neuronal mRNAs in human neuroblasts

Belinda J Goldie[1,2,3], Joshua R Atkins[1,2,3], Judith Weidenhofer[1,3], Murray J Cairns[1,2,3]

[1] School of Biomedical Sciences and Pharmacy, and the Centre for Translational Neuroscience and Mental Health, University of Newcastle, Callaghan, NSW 2308, Australia.

[2] Schizophrenia Research Institute, Sydney, Australia.

[3] Hunter Medical Research Institute.

Abstract

Complex intracellular patterns of mRNA translation are integral to supporting the organisation of large polar interconnected neurons. How these cells establish and manage the dynamic temporo-spatial partitions guiding the traffic and ultimate function of RNA is an important question. We recently demonstrated that microRNA (miRNA) are functionally compartmentalised in neurons and most likely play a role in chaperoning their target transcripts in these intracellular microenvironments. We now show that a group of miRNA in cultured neuroblasts are preferentially enriched in the nucleus. Most of these molecules were primate specific and shared a sequence motif with homology to the MAZ transcription factor binding element. RISC-protein RNA co-immunoprecipitation and RNA-Seq (RIP-Seq) suggested that most of the transcripts in the nucleus associated with Ago2 may also be regulated by MAZ promoter elements. Functional annotation of these nuclear Ago2 transcripts identified significant enrichment of neural pathways in contrast to those associated with Ago1.

Highly specific post-transcriptional management of mRNA is important for defining a four dimensional intracellular matrix in the development and function of complex eukaryotic cells. This feature and the mechanisms that support it are particularly important within neurons, where the availability of appropriate transcripts for input-restricted postsynaptic translation is integral to the synthesis of new proteins in response to excitation. While there has been significant advances in our understanding of post-transcriptional regulation of mRNA traffic, translation and degradation, there remains much to learn about the mRNA lifecycle and its relationship to the patterns that help define the intracellular topography and intercellular relationships.

Integral to intracellular mRNA patterning in neurons are the mechanisms supporting compartmentation. Compartments represent subcellular microdomains with common localisation and/or functional goals, and it has been shown that as much as 71% of mRNA undergo subcellular localisation prior to translation [1]. The importance in neurobiology is highlighted by the fact that compartmental establishment begins less than 24 hours after the commencement of differentiation, when the presence or absence of particular mRNAs is sufficient to discern the axon from developing dendrites [2,3]. Compartmental separation may be delineated by physical barriers, such as the nuclear envelope, or in the case of remote dendritic spines may be implied by geographical distance. To overcome these barriers, hardware networks must develop to facilitate interaction and communication, and to ensure precise temporo-spatial availability of the mRNA software. However, the diversity of hardware and software comprising the intracellular landscape suggests a requirement for a streamlined system, with flexible regulatory molecules mediating these interactions.

A group of mRNA regulators demonstrating increasing importance in cell biology in general, and neurobiology in particular, are the 19-22 nucleotide non-coding transcripts known as microRNA (miRNA). Neuronal differentiation and development are reliant on appropriate miRNA expression, which has been shown to provide the timing for key switches in gene expression [4,5] and trigger alternate splicing to include neuron-specific exons [6]. It is perhaps not surprising considering their mode of biogenesis and canonical function as translational regulators, that miRNA function is typically associated with the cytoplasm; however a growing body of evidence supports deliberate partitioning and/or transport of miRNA into the nucleus in a variety of neuronal and non-neuronal cell types [7-11]. Importantly, the roles of miRNA in the nucleus appear to be broader than their established function as post-transcriptional silencers, and could include transcriptional control via interaction of RISC proteins with several chromatin remodelling factors [12,13]; regulation of non-coding RNA activity by targeting endogenous anti-sense and sense transcripts [14]; and co-regulatory transcriptional relationships between intronic miRNA and their host genes [15,16]. We have recently shown functional compartmentalisation of activity-responsive miRNA in the neurites of differentiated SH-SY5Y human neuroblastoma cells [17], and we wanted to investigate the presence of miRNA in the nucleus of this neuronal model. Here we report that mature miRNA are present in the nucleus of these cells and in fact some miRNA demonstrate compartmental preference, having more than 70% of total expression there, many of which were primate-specific transcripts. Among these sequences, a common four-nucleotide motif was found that was absent from nucleus-depleted miRNA and associated significantly with subcellular location. Using RNA co-immunoprecipitation (RIP) we show that

this motif discriminates between Ago1 and Ago2 for functional enrichment among targets, and reveal a putative regulatory network in the undifferentiated cells that could contribute to neuronal maturation.

Results

Nuclear and cytoplasmic RNA fractionation

Nuclear and cytoplasmic fractions were prepared in triplicate from SH-SY5Y cells by hypo-osmotic lysis. After confirming that the fractionation process did not adversely impact either nuclear (Fig. 1a) or RNA integrity, successful separation of the fractions was inspected by qPCR examination of the distribution of nucleus-specific transcripts snoRNA U44 and U49 relative to whole cells. Significant depletion of U44 (p=0.03) and U49 (p=0.04) from the cytoplasmic fractions was observed, while expression in the nuclear fractions was consistent with that observed in intact cells (Fig. 1b).

Microarray analysis of subcellular fractions

Nuclear and cytoplasmic expression of 847 human miRNA was measured by microarray. Conventionally, microarray data is normalised prior to analysis to minimise the effect of RNA loading and intensity variation. Because of the significant difference between the two compartments being analysed and the subtlety of miRNA expression, it was a concern for the analysis of these experiments that conventional normalisation would be not be appropriate for subcellular fractions, and important expression changes would be lost or distorted. We therefore compared the analyses from 3 approaches to this problem including: (1) normalised by the Affymetrix standard RMA with linear Bayesian differential expression and subsequent p-value correction; (2) pseudo-normalised via a

recently published signal ranking method [11]; and (3) un-normalised. Nucleus-enriched miRNA were identified using the 3 methods.
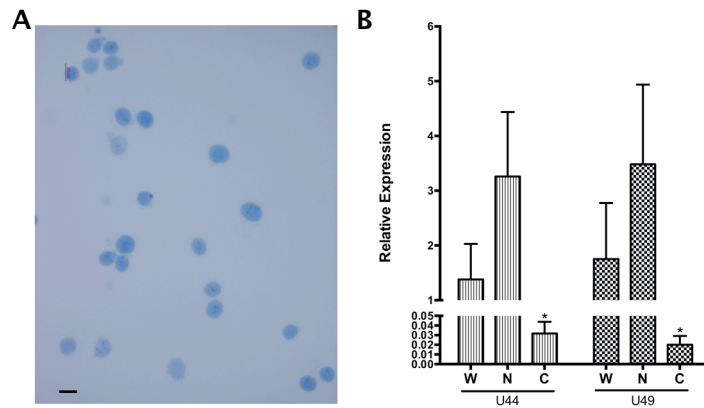

Figure 1. Purification of SH-SY5Y nuclei. qPCR was performed on total RNA extracted from (a) nuclear and cytoplasmic fractions of SH-SY5Y. Scale bar = 20μm. (b) Relative expression of small nucleolar RNAs (snoRNAs) U44 (p=0.03) and U49 (p=0.04) was significantly lower in cytoplasmic fractions compared with whole cells by student's t-test, while no significant difference was observed between nuclear and whole cell expression. Fold change is calculated as the mean cycle threshold (Ct) for each snoRNA and that produced by U6 in the same sample (ΔCt). Error bars indicate mean ± s.e.m. **Note the split y-axes.**

Surprisingly, although the un-normalised and RMA normalised analyses reported similar numbers of nucleus-enriched miRNA (30 and 49 respectively), the signal-rank analysis found 191 mature miRNAs. This seamed unrealistic as it suggested that 71% of all miRNA included in the analysis were preferentially enriched in the nucleus. A selection of top-ranked miRNA detected by each method was probed by qRT-PCR as validation. Transcripts selected as nuclear by the signal-rank normalisation validated poorly (Fig. 2a), with 6 of the 7 demonstrating no significant difference in expression between the compartments. The only exception was miR-107, however this transcript was significantly associated with the cytoplasmic fraction (p=0.0377, t-test). Similar results arose from the canonical Bayesian DE analysis (Fig. 2b). The un-normalised data validated well, with miRNA

detected as both enriched and depleted validating significantly (Fig. 2c). Interestingly, the results from the signal-rank and linear Bayesian validations agreed more closely with those expected based on the un-normalised analysis (Fig. 2d,e). Correlation of un-normalised microarray and qPCR data for validated miRNA revealed a strong linear relationship between the methods, with a correlation coefficient R^2=0.7634 (Fig. 2f). Before continuing based on the results of this analysis, we confirmed robustness of the data by verifying consistency of housekeeping snoRNAs within the same fraction across samples and ensuring no samples were outliers, as described previously [17] (Supplementary Fig. S1).

Some mature miRNA are preferentially localised in the nucleus

Successful validation of the un-normalised data led us to continue with a deeper investigation of data generated from this mode of analysis. We found that many miRNA have at least some expression in the nucleus (Supplementary Table 1), however there were 13 miRNAs registering more than 70% of total mature expression in the nucleus; interestingly most of these were not conserved (Table 1). We were initially surprised to find both strands of a single miRNA, miR-768, registering >90% nuclear enrichment, however miRBase has re-designated the transcript from this locus as a snoRNA and thus it was excluded from further analyses.
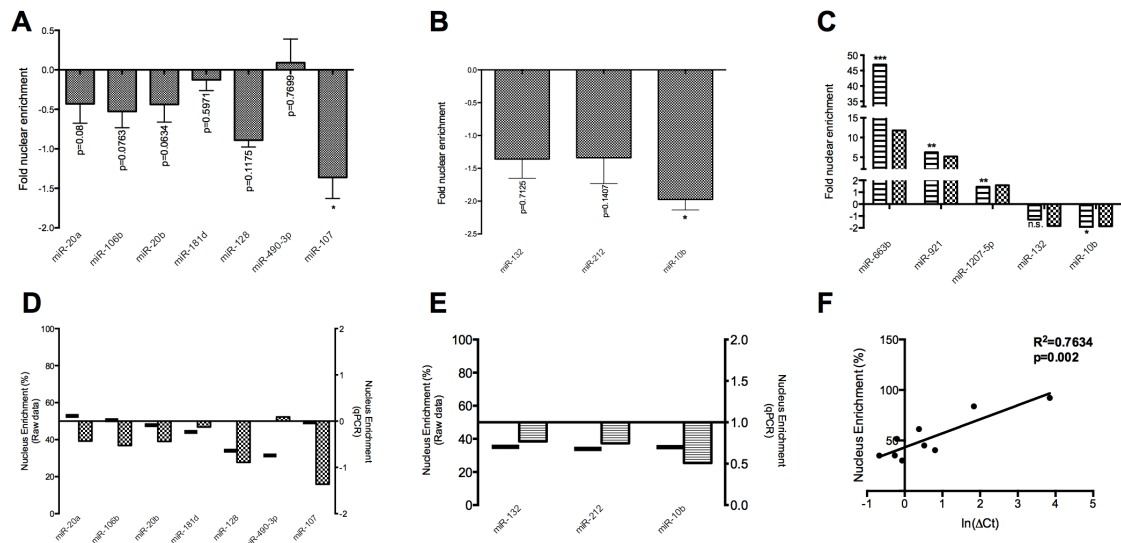
Figure 2. qPCR validation of comparative microarray analyses. Expression of putative nucleus-enriched miRNA from (a) signal-rank normalised and (b) linear Bayesian analyses was probed by qRT-PCR. Validation found no significant difference between nuclear and cytoplasmic levels of these miRNA (p-values shown, t-test), except miR-107 and miR-10b, however these were enriched in the cytoplasm. (c) Fold nuclear enrichment was calculated as (nucleus/cytoplasm) from raw array intensity (chequered bars) and compared against ΔCt for the same miRNA probed by qRT-PCR (striped bars) for selected nucleus-enriched and – depleted transcripts. (d,e) qRT-PCR expression of the miRNA identified by the signal-rank and linear Bayesian methods (chequered bars, right Y-axes) was more accurately reflected by the un-normalised % nuclear expression (black bars, right Y-axes). (f) Un-normalised microarray % nuclear enrichment and linearised qRT-PCR values demonstrated a strong correlation with R^2=0.7634. Asterisks indicate significance of the difference between nuclear and cytoplasmic expression (*, $p < 0.05$; **, $p < 0.01$; ***, $p < 0.0001$).

Detection of a putative 4-nucleotide nuclear miRNA motif

Internal sequence "signals" are often responsible for determining localisation of mRNAs, and it has previously been reported that miR-29b is imported into the nucleus under direction of a hexanucleotide element [10]. We therefore wondered whether a common motif might exist among nucleus-enriched miRNA identified by this study. After filtering out very lowly expressed miRNA (raw signal < 30), the mature sequences for the most nucleus-enriched miRNA (Table 2) were submitted

to the MEME motif investigation tool. A 4-nucleotide motif was found, with all but one miRNA containing "G[AU]GG" (Fig. 3). The only discordant miRNA, miR-297, contained the slightly divergent "GUGC", and stands out as the only conserved miRNA among those analysed for the motif.

Calculation of expected motif frequency in MEME is determined by default from nucleotide frequencies across the entire genome, so to enable a more accurate representation of the frequency within the human miRNA-ome, we downloaded all mature human miRNA sequences from the current version of miRBase (miRBase 17) and created a background Markov model with the actual nucleotide frequencies within this population (G=0.281, C=0.226, A=0.229, U=0.263). Rerunning the MEME analysis with these parameters improved the E-value by 5 orders of magnitude, from 1.3e06 in the initial analysis to 3.6e01, however this algorithm still relies on the entire genome as a background.
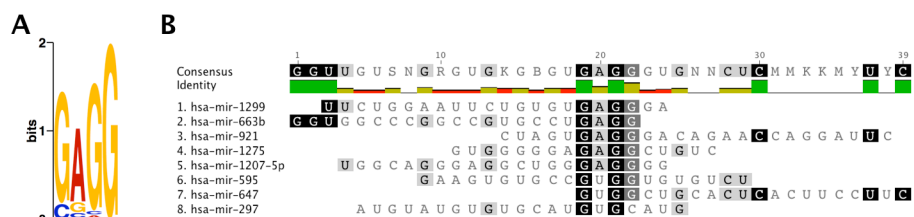

Figure 3. Putative motif detected in nucleus-enriched miRNA. (a) Motif logo generated by MEME suite. (b) Alignment of mature miRNA sequences (5'-3') demonstrating location of motif within individual sequences.

Table 1. miRNA with highest % nuclear expression

miRNA name	Nuclear %	Conservation*
hsa-miR-768-5p ^	94.17	n/a
hsa-miR-768-3p ^	93.71	n/a
hsa-miR-1299	93.17	No (hsa, ptr, ppy)
hsa-miR-297	92.72	Yes
hsa-miR-663b	92.17	No (hsa, ptr, ppy)
hsa-miR-647	89.19	No (hsa, ppy)
hsa-miR-595	88.09	No (hsa, ptr, mml, ppy)
hsa-miR-921	83.82	No (hsa, ppy, efu)
hsa-miR-593*	80.62	No (hsa, ptr, mml, ppy)
hsa-miR-1183	78.28	No (hsa, ptr, ppy)
hsa-miR-664*	75.44	Yes
hsa-miR-1275	73.87	No (hsa, ptr, ppy)
hsa-miR-574-5p	71.94	Yes

***Species identifiers:** hsa, Homo sapiens; ptr, Pan troglodytes; mml – Macaca mulatta; ppy – Pongo pygmaeus; efu, Eptesicus fuscus.*

Table 2. Nuclear miRNA analysed for motif.

miRNA name	Nuclear %	Mature Sequence
hsa-miR-1299	93.17	UUCUGGAAUUCUGUGUGAGGGA
hsa-miR-297	92.72	AUGUAUGUGUGCAUGUGCAUG
hsa-miR-663b	92.17	GGUGGCCCGGCCGUGCCUGAGG
hsa-miR-647	89.19	GUGGCUGCACUCACUUCCUUC
hsa-miR-595	88.09	GAAGUGUGCCGUGGUGUGUCU
hsa-miR-921	83.82	CUAGUGAGGGACAGAACCAGGAUUC
hsa-miR-1275	73.87	GUGGGGGAGAGGCUGUC
hsa-miR-1207-5p	61.33	UGGCAGGGAGGCUGGGAGGGG

Returning to the miRBase data, examination of the mature sequences for all miRNAs revealed that approximately 25% of all known human miRNAs contain this motif (Table 3). We then collated the sequences of 30 miRNA whose nuclear expression accounted for <25% of their total expression (nucleus-depleted). By chance we would expect 7-8 of these miRNA to contain the motif, however none did (Table 4). Contingency analysis indicated that expression of this motif is significantly correlated with nuclear enrichment (Fisher's exact test, $p<0.0001$). It is interesting to note that the "GAGG" motif detected here is similar to the GA-box motif recognised in DNA by the transcription factor Myc-associated zinc finger protein (MAZ). Investigation of the pre-miR hairpin sequences for the motif-containing miRNA found putative MAZ binding elements ("GGGAGGG") in pre-miR-1207 and pre-miR-647, and the shorter "GGAGG" in pre-miR-595.

Table 3. Frequency of putative nuclear motif within the human miRNA-ome.

Number of human miRNA (miRBase 17)	1727
Number of miRNA containing "GAGG" or "GUGG"	439
Frequency of motif within miRNA-ome	**0.254**

Table 4. Motif analysis of nucleus-depleted miRNA (<25% total expression)

miRNA name	Mature sequence	Contains motif?
hsa-miR-342-5p	AGGGGUGCUAUCUGUGAUUGA	N
hsa-miR-25*	AGGCGGAGACUUGGGCAAUUG	N
hsa-miR-129-3p	AAGCCCUUACCCCAAAAAGCAU	N
hsa-miR-602	GACACGGGCGACAGCUGCGGCCC	N
hsa-miR-572	GUCCGCUCGGCGGUGGCCCA	N
hsa-miR-30b*	UGUAAACAUCCUACACUCAGCU	N
hsa-miR-598	UACGUCAUCGUUGUCAUCGUCA	N
hsa-miR-148b	UCAGUGCAUCACAGAACUUUGU	N
hsa-miR-200c	UAAUACUGCCGGGUAAUGAUGGA	N
hsa-miR-218-2*	CAUGGUUCUGUCAAGCACCGCG	N
hsa-miR-130b*	ACUCUUUCCCUGUUGCACUAC	N
hsa-miR-135a*	UAUAGGGAUUGGAGCCGUGGCG	N
hsa-miR-92b*	AGGGACGGGACGCGGUGCAGUG	N
hsa-miR-874	CUGCCCUGGCCCGAGGGACCGA	N
hsa-miR-379	UGGUAGACUAUGGAACGUAGG	N
hsa-miR-941	CACCCGGCUGUGUGCACAUGUGC	N
hsa-miR-767-5p	UGCACCAUGGUUGUCUGAGCAUG	N
hsa-miR-346	UGUCUGCCCGCAUGCCUGCCUCU	N
hsa-miR-1225-5p	GUGGGUACGGCCCAGUGGGGGG	N
hsa-miR-409-5p	AGGUUACCCGAGCAACUUUGCAU	N
hsa-miR-92a-1*	AGGUUGGGAUCGGUUGCAAUGCU	N
hsa-miR-1303	UUUAGAGACGGGGUCUUGCUCU	N
hsa-miR-26b	UUCAAGUAAUUCAGGAUAGGU	N
hsa-miR-720	UCUCGCUGGGGCCUCCA	N
hsa-miR-532-3p	CCUCCCACACCCAAGGCUUGCA	N
hsa-miR-1301	UUGCAGCUGCCUGGGAGUGACUUC	N
hsa-miR-23b*	UGGGUUCCUGGCAUGCUGAUUU	N
hsa-miR-1270	CUGGAGAUAUGGAAGAGCUGUGU	N
hsa-miR-1292	UGGGAACGGGUUCCGGCAGACGCUG	N
hsa-miR-193a-5p	UGGGUCUUUGCGGGCGAGAUGA	N

Analysis of nucleus-enriched mRNA

For initial investigation of miRNA regulation in the nucleus, RNA from the same cells used for miRNA expression was amplified, labelled and hybridised to Affymetrix Human Exon 1.0 ST microarrays. Data were summarised for both gene-level and exon-level expression. Nucleus-enriched mRNAs were identified in the same manner as for miRNA, yielding a group of 91 transcripts having greater abundance in the nucleus (compared with 2035 with cytoplasmic enrichment). This list was used to refine a target filter applied to the 8 nucleus-enriched miRNA,

yielding a group of 23 mRNAs and 26 miRNA-mRNA pairings. GPCR signalling (p<0.0001), nucleic acid metabolism (p=0.01) and RNA processing (p=0.002) were significant GO terms, and this functional analysis derived a well-connected network of mRNAs regulated by the nucleus-enriched miRNA (Fig. 4).
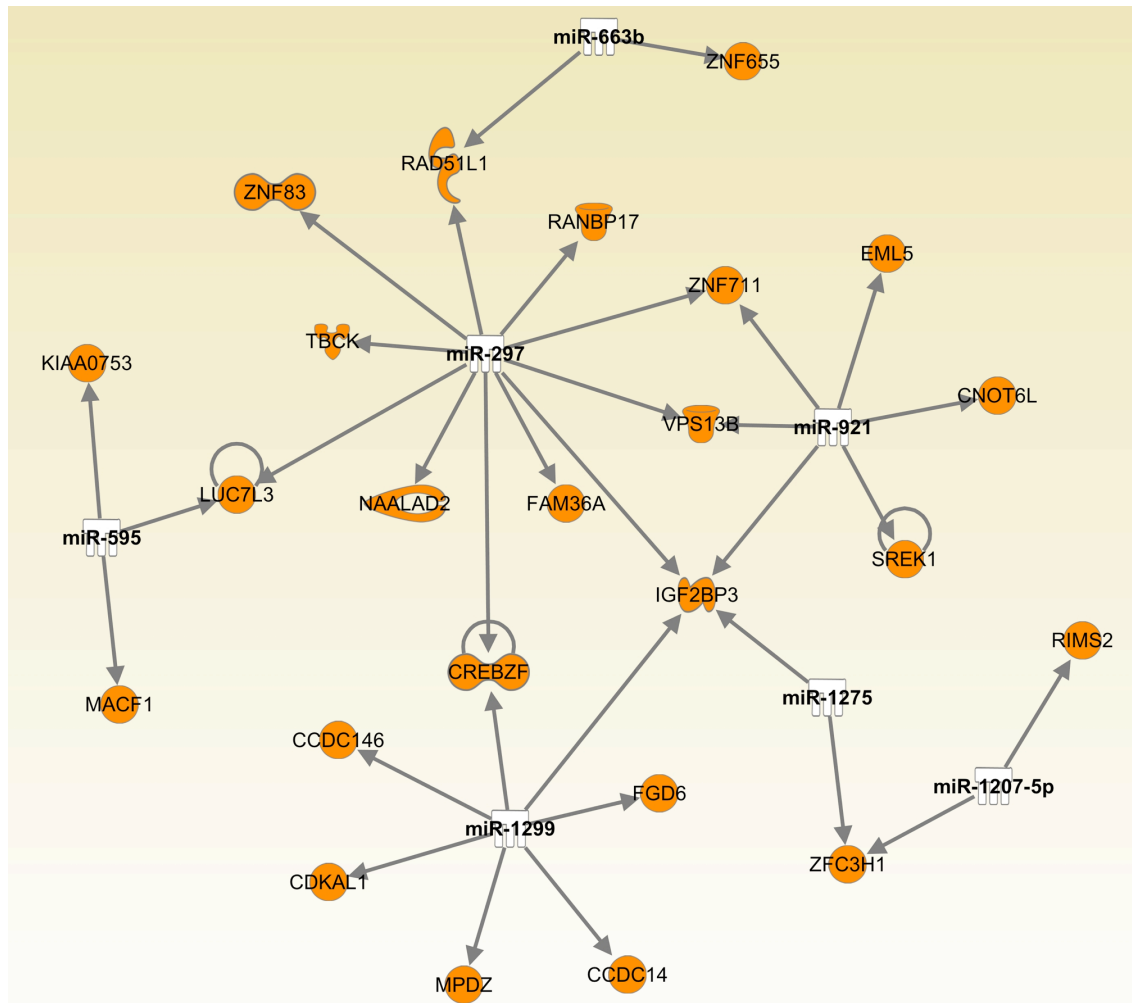
Figure 4. Nucleus-enriched miRNA-mRNA regulatory network. Using IPA software, nucleus enriched miRNA were matched with nucleus-enriched mRNA based on predicted targeting. This network focuses on "nucleic acid metabolism" and "mRNA processing".

Nucleus-enriched miRNA may influence nuclear retention of alternate splice variants

A splicing ANOVA was carried out on exon-level expression data using Genespring GX12 software to identify mRNAs demonstrating significantly different (FDR <

0.01) splicing between nuclear and cytoplasmic compartments. This analysis found 1207 transcripts having splicing index > 2, of which approximately one third (473) were identified by IPA as targets of the nucleus-enriched miRNA, yielding 637 miRNA-mRNA regulatory pairings. IPA core functional analysis of these genes showed significant enrichment of "nervous system development and function" (p = 5.4E-12 – 1.18e-4). Filtering the pairings for "nervous system signalling" identified a tight network comprising 7 miRNA and 54 mRNA that was highly connected with axon guidance signalling (Supplementary Figure S2).

Nuclear enrichment of RISC-associated mRNA

To determine whether nuclear miRNA enrichment was associated with canonical Ago-mediated mechanisms in the nucleus, we performed RIP on nuclear lysates followed by RNA-Seq of Ago-associated transcripts. Because Ago2 contains an active slicer domain and is associated with degradation, while Ago1 lacks this activity and is associated with translational repression [18], these pull-downs were performed individually to enable assessment of inherent functional differences. A comprehensive list of miRNAs targeting positive reads was filtered for nucleus-enriched miRNAs and compared between samples, yielding 189 mRNAs unique to Ago1, 435 unique to Ago2 and 657 transcripts detected in both pull-downs (Supplementary Table 2); these lists were functionally analysed using GATHER and the DAVID FAC tool.

Excitingly, in these undifferentiated neuronal cells, GATHER found that Ago2-associated transcripts were significantly enriched with neuronal terms including axonogenesis (p<0.0001) and neurogenesis (p0.0003), while the most significant FAC clusters (ES=3.9 and ES=3.2) related to neuron development, neuron differentiation, neuron projection, axonogenesis, and axon guidance (complete FAC

analyses are contained in supplementary information). Genes contributing to this functionality included the plasticity-associated cytoskeleton regulator ARC, glutamate receptors GRIA3 and GRIA4, and axon guidance receptors ROBO1 and ROBO2. A transcription factor analysis, also carried out using GATHER, identified MAZ as a common driver (Bayes factor = 20) of 301 out of the 435 genes uniquely associated with Ago2, however it was not linked to transcripts unique to Ago1 nor those common to both. In contrast, mRNAs associated with Ago1 were functionally linked to more general cellular processes and enrichment of functional domains.

Convergent functions of Ago1/2 in transcriptional regulation

Interestingly, transcripts common to both Ago1 and Ago2 were very strongly linked by FAC to the nucleus (ES=6.3), transcriptional regulation (ES=6.4) and chromatin modification (ES=4.5). Also enriched in this list were molecules containing RNA recognition motifs capable of binding RNAs (ES=5.2). GATHER identified gene ontologies including GPCR signalling, protein modification and nucleotide metabolism (all $p<0.0001$). Important among this list was LIN28A, the human homolog of pluripotency factor Lin-28. This transcription factor contains both DNA and RNA binding domains, and has been shown to interfere with pre-miR processing, both negatively regulating pre-let-7 maturation and being itself negatively regulated by the mature let-7 to control differentiation of neural stem cells [19].

Discussion

The question of miRNA subcellular localisation has particularly important implications for the complex regulatory requirements of neurons. Indeed, specific enrichment of miRNA, elements of the miRNA biogenesis pathway, and RISC-

mediated transcript silencing have been found to play an integral role in synapse formation and synaptic plasticity [7,9]. The present study sought to investigate the question of neuronal nuclear miRNA localisation in a human genetic context using SH-SY5Y human neuroblast cells. A recent study in this cell line found that stable overexpression of Ago1, but not Ago2, resulted in slowing of the cell cycle and induction of apoptosis, while over expression of either resulted in significant enhancement of the neuronal phenotype during retinoic acid differentiation [12]. This suggests that although there may be some mechanistic convergence between the two, it is likely there will be some functional outcomes unique to each.

We performed genome-wide analysis of subcellular mature miRNA expression in the nuclear and cytoplasmic fractions and identified a group that were preferentially enriched in the nucleus. When we aligned these molecules we found a four-nucleotide sequence motif that was significantly associated with the nuclear fraction suggesting that it may be a functionally significant signal for directing nuclear import, or nuclear retention of the miRNA. A similar profiling study conducted in rat neurons observed miRs-25 and -92a as specifically enriched in the nucleus, but no consensus sequence was observed [20]. While these two miRNA were not among nucleus-enriched transcripts in our study, we mostly observed non-conserved miRNA associated with primates.

Although it has been shown that the nucleotide sequences of some miRNAs contain a putative nuclear localisation sequence [10], the biological function of this is not clear. While the mechanism for this localisation is not known, CRM1 (exportin1) has been shown to import mature miRNA into the nucleus in large complexes associated with topoisomerase and helicase [13]. Mature miRNA in the cytoplasm are known to be associated with Ago1 or Ago2 in the RISC, so we wondered if these

mature miRNA in the nucleus are also associated with RISC proteins. Using Ago1 and Ago2 RIP and RNA-Seq, we identified that both proteins were present in the nucleus and associated with mRNA transcripts. However, while the miRNA-effector complex is conventionally localised in the cytoplasm, alternative functions for miRISCs in the nucleus cannot be overlooked. One possibility is that RISC-associated miRNA bind the to target pre-mRNA preventing its export from the nucleus. Another is that these RISC-associated miRNA facilitate translocation of their target mRNA back into the nucleus, again sequestering it away from its translational apparatus. In support of the latter hypothesis, Ago2 has been found to associate with several proteins containing RNA recognition motifs (RRMs), including RBM4, RBM10 and eIF4b, and RBM4 in particular is required for Ago2-mediated gene silencing [24]. As RRMs participate in bidirectional nucleus-cytoplasmic shuttling of RNA-binding proteins [25], it is possible that this motif causes cytoplasmic RISCs to enter the nucleus or causes nuclear RISCs to be retained there. The latter is supported by our FAC and ontological analyses, which showed that mRNAs associated with nuclear Ago2 in these undifferentiated neuronal cells were enriched for transcripts specific to a mature neuronal phenotype.

A further possibility supported by our data is the involvement of miRNA in nuclear retention of particular splice variants. miRNAs have been linked to splicing regulation through feedback networks involving SF2/ASF in cells including SH-SY5Y [26,27]. However, as nucleocytoplasmic differences between splice variants have been shown to have significant association with differential 3' UTR exon expression [28], it is probable that this regulatory relationship extends to compartmental discrimination. In particular our analysis showed significant

neuronal functionality among differentially spliced targets of nucleus-enriched miRNA, and miRNA have been shown to differentially regulate splice variants of key neuronal genes in neuronal cells [29,30].

Nuclear enrichment of miRNP complexes may also assist with transcriptional control. Ago1 has been shown to directly regulate transcriptional gene silencing in human cells via recruitment of histone methyltransferase for H3K9me2 [31]. In these experiments, Kim and colleagues showed that Ago1 was interacting directly with TARBP2, a constituent of the RISC, and RNA polymerase II (RNAPII). Spliced transcripts with long 3' UTRs associated with RNAPII can interact with chromatin to maintain a transcriptionally open state [32]; taken in context with our findings of an emphasis on cellular metabolism in Ago1 unique transcripts, and transcriptional regulation and chromatin modification amongst the Ago1/2 common transcripts, this is supportive of a role for miRNA-mediation of Ago1/TARBP2/RNAPII transcriptional control complexes.

Perhaps the most interesting aspect of the nuclear localisation of miRNA was the discovery of a consensus motif with similarity to the MAZ recognition sequence. Despite its annotation as a transcription factor, MAZ was identified in the mRNA interactome of human cell lines HEK [33] and HeLa [34], suggesting it can interact with RNA transcripts. While MAZ does not contain canonical RNA binding domains, its six C_2H_2 zinc fingers, which have been variously shown to bind to GA boxes ranging from "G5AG5" to "G2AG2" [21-23], could potentially bind to the cognate sequence in RNA. We identified full-length binding elements in the pre-miRNA sequences for nucleus-enriched miRs-647 and -1207-5p, and a shorter version in pre-miR-595. Additionally, two non-conserved MREs for miR-647 and one for miR-1299 are predicted in the MAZ 3' UTR.

Piriyapongsa et al recently observed significant enrichment of transcription factor binding sites within the sequences of precursor miRNAs compared with randomised sequence or other genomic regions such as introns, suggesting that more direct interaction or cross-talk with miRNA at different levels, may be a conserved function of these regulatory molecules [35]. The non-conserved nature of both the miRNA and MREs, taken together with the enrichment of MAZ driven neuronal functionality among Ago2-specific targets of these miRNA, support the idea of a neuron-specific miRNA-Ago2-MAZ regulatory circuit involved in neuronal differentiation, in a similar manner to let-7, miR-125 and lin-28 regulation of neural stem cell differentiation [19]. In such a system the pre-miRNA could act as a decoy for MAZ protein, down regulating transcription of its targets, while the mature miRNA acted on the 3' UTR of these nascent mRNA to prevent nuclear export and translation. Interestingly, Ugai and colleagues found MAZ throughout the cytoplasm of retinoic acid differentiated PC19 cells, and particularly enriched in the neurites, compared with immature cells where MAZ localised to the nucleus [36]. It is plausible that MAZ could interact with miRNA or their precursor forms in the periphery of neurons and become translocated to the nucleus with or without the associated miRNA in response to environmental or developmental cues.

Finally, MAZ may be altering or inhibiting Ago2-associated, Dicer-independent miRNA maturation [37]. Using the pre-miR-451 system, which is known to be dependent on the slicer activity of Ago2 for maturation, Yang and colleagues demonstrated several functional parameters required for Ago2-associated pre-miR processing [38] in human cervical cancer (HeLa) and mouse embryonic fibroblast (MEF) lines. Among our nucleus-enriched miRNA only pre-miR-297 fulfils the requirements of base-pairing at most positions within the hairpin and short

hairpin length, and has a uracil at the 5' position which is associated with more efficient Ago2 pre-miR processing. This is an interesting observation considering that miR-297 was the only conserved miRNA in this list, and miR-451 is itself well conserved, however neither of these homologs was identified among a list of Ago2-dependent miRNA in the mouse striatum [39], suggesting that the mechanism, or at least the miRNA may be cell-type specific.

The functional repertoire of miRNA is rapidly expanding from their initial role as post-transcriptional regulators, and we have demonstrated here and elsewhere that, at least in neurons, subcellular location is just as important for miRNA as for mRNA. Moreover, our findings in the nucleus and neurites have revealed substantial enrichment of primate-specific miRNA in these critical compartments, suggesting these molecules may make a pivotal contribution to the development of higher brain functions. In our view, shifting the focus of miRNA studies from individual gene-miRNA regulatory relationship to systems level analyses, along with broadening consideration from conserved-only targets to include non-conserved, will assist further elucidation of miRNA biology and could facilitate understanding of much that is currently unknown about human neural complexity.

Methods

Cell Culture

SH-SY5Y cells were obtained from ATCC. Populations were maintained at 37°C, 5% CO_2, 90% humidity in DMEM (Hyclone) supplemented with 10% Fetal Bovine Serum (Sigma Aldrich), 2% HEPES and 1% L-glutamine (both Hyclone). Cells were routinely passaged and harvested by washing with Phosphate-Buffered Saline

(PBS, Gibco) followed by brief incubation with trypsin. Assays were carried out on cells at passage 10.

Subcellular fractionation

Cells were harvested and fractionated by hypotonic lysis as described by Wang and colleagues [40] with some modifications. Briefly, cells were washed 3 times with ice-cold PBS and pelleted at 4,000rpm for 3 minutes. The pellet was resuspended in 1ml ice-cold RSB Resuspension Buffer (10mM Tris, pH 7.4, 10mM NaCl, 3mM MgCl$_2$), incubated on ice 3 minutes, and centrifuged as before. The supernatant was removed, pellet volume estimated, then resuspended in 4x volume of RSBG40 Lysis Buffer (10mM Tris, pH 7.4, 10mM NaCl, 3mM MgCl2, 10% glycerol, 0.5% NP-40, 0.5mM DTT, 100U/ml RNase inhibitor) by slow pipetting. Nuclei were pelleted at 7,000rpm for 3 minutes, and the supernatant kept as the cytoplasmic fraction. Nuclei were resuspended in RSBG40, and one-tenth volume of detergent (3.3% wt/wt sodium deoxycholate, 6.6% vol/vol Tween 40, diluted 1:5) was added by gentle vortexing. Nuclei were pelleted as before, and the supernatant pooled with the cytoplasmic fraction. The nuclear pellet was washed with RSBG40 and collected at 10,000rpm for 5 minutes and the pellet used for nuclear RNA extraction. Nuclear integrity was checked by light microscopic examination of samples, diluted 1:2 with trypan blue, at 40X magnification. Whole cells from the same samples were used as controls where appropriate.

RNA extraction, quantification and quality assessment

Total RNA was extracted using TRIzol reagent per manufacturer's instructions (Invitrogen), with the modification of 2μl of glycogen (20mg/ml, Sigma) added to the isopropanol precipitation step, which was allowed to proceed overnight at -30°C. The following day, samples were centrifuged for 30 minutes at 10,000rpm,

4°C, before completion of the standard procedure. Purified RNA was quantified using the Qubit fluorometer and Quant-IT RNA assay kit per manufacturer's instructions (Invitrogen). RNA quality was checked using Bioanalyzer RNA 6000 Nano chips per manufacturer's instructions (Agilent).

Genome-wide analysis of miRNA expression

Total RNA was labelled using a FlashTag Biotin HSR RNA labelling kit according to manufacturer's instructions (Genisphere). Labelled RNA was hybridised to Genechip miRNA 1.0 microarrays, washed, stained and scanned per the manufacturer's instructions (Affymetrix).

Genome-wide analysis of gene expression

Total RNA was transcribed to cDNA and amplified using the Applause WT-Amp Plus ST kit, then fragmented and labelled with the Encore Biotin module, both according to the manufacturer's instructions (NuGEN). Labelled cDNA was hybridised to GeneChip Exon 1.0 ST microarrays, washed, stained and scanned as above. Data analyses were conducted at gene and exon expression (splicing) levels.

Analysis of microarray expression from different subcellular compartments

We expected great variation between nuclear and cytoplasmic expression, and it has not been well established whether normalisation would preserve or mask the differences. We therefore undertook to analyse the data by three methods and perform validation on candidate miRNA from each.

Method 1 – RMA (across-sample) normalisation. Data were normalised using the Affymetrix standard Robust Multichip Algorithm (RMA) with p-value correction for multiple testing, and differentially compartmentalised genes were identified by empirical linear Bayesian model [41].

<u>Method 2 – Signal rank (in-sample) normalisation</u>. Data were analysed as recently described by Jeffries et al for nucleus-cytoplasmic fractionation of NPCs [11]. Briefly, probe signals from each sample were sorted in descending order and a rank calculated based on the distance of each signal from the median signal in that sample. Compartmental enrichment was defined as every sample from one compartment having higher rank than every sample from the other.

<u>Method 3 – No normalisation</u>. Raw signals from each sample were averaged across replicates, and probes with low expression in all samples (raw signal < 30) removed. The nuclear proportion of expression was calculated as the percentage that nuclear signal contributed to total array signal from each condition (nucleus + cytoplasm). A miRNA was considered enriched in the nucleus if its "Nuclear % expression" was greater than 70%.

Quantitative real-time PCR (qPCR)

Multiplex reverse transcription was performed on 500ng of DNaseI-treated total RNA using oligo(dT) primer and, where appropriate, specific primers for individual miRNAs. All primers were added to a final concentration of 40nM. Reactions were performed using Superscript II reverse transcriptase in 5X first-strand buffer per manufacturer's instructions (Invitrogen). Real-time PCR was performed in triplicate on diluted cDNA (1:40) combined with Power SybrGreen master mix (Applied Biosystems) with 10µM of the appropriate forward and reverse primers, in a final volume of 12.5µl, using an ABI prism 7500 sequence detection system (Applied Biosystems). Forty cycles of PCR were applied; for gene expression, the annealing temperature was set at 60°C, while for miRNA the annealing step was at 50°C.

Functional integration of miRNA and gene expression

A list of nucleus-enriched miRNA was loaded into Ingenuity Pathway Analysis (IPA) software. A target filter analysis was performed on miRNA to identify target mRNA; this list was refined by pairing with nucleus-enriched mRNA, or mRNAs demonstrating significantly different splicing between nucleus and cytoplasm, and Core Analysis performed on gene lists generated from target gene-miRNA pairings.

RNA co-immunoprecipitation (RIP)

Nuclei were isolated as described above, lysed in IP Lysis Buffer (150mM KCl, 25mM Tris-HCl ph7.5, 2mM EDTA, 1mM NaF, 0.5% NP-40, 0.5mM DTT, 0.5mM AEBSF) by vortexing and the lysate cleared by centrifugation at 16,000g for 10 minutes, 4°C. Co-immunoprecipitation (co-IP) of Ago1 and Ago2 was carried out as described by [42] and [43] respectively, using antibodies obtained from that group. Briefly, protein G-sepharose beads were prepared by washing with IP Lysis Buffer. Beads were then coupled to 10μg of Ago1 or Ago2 antibody in IP Lysis Buffer for 2 hours, 4°C under constant rotation. Excess antibody was removed by washing twice with IP Lysis Buffer. Cleared lysate was incubated with coupled beads for 3 hours, 4°C under constant rotation. Beads were then pelleted and washed 3x with IP Wash Buffer (300mM NaCl, 50mM Tris pH7.5, 1mM NaF, 0.01% NP-40, 5mM $MgCl_2$) with RNase inhibitor before digestion with proteinase K for 1 hour at 42°C. Finally, RNA was extracted using PCIAA with overnight precipitation at -30°C and glycogen co-precipitant.

RNA-Seq

RNA yields from nuclear RIP were very low, and samples were sent unquantified, along with whole nucleus controls, to Beijing Genomics Institute for RNA-Seq. RIP samples were amplified using the SMARTer method before the standard Illumina

library prep. Paired-end reads were aligned to the genome using TopHat (v2.0.11) [44] and counted using HTSeq (v0.6.1) [45]. Genes with low read count (<10) were filtered out to avoid false positives resulting from amplification. Remaining genes were scanned for miRNA target sites against the TargetScan conserved database (Release 6.1). Downstream analyses were performed in Excel, and final gene lists underwent functional analysis using the Gene Annotation Tool to Help Explain Relationships (GATHER) [46] the DAVID Functional Annotation Clustering (FAC) tool [47].

References

1. Lécuyer E, Yoshida H, Parthasarathy N, Alm C, Babak T, et al. (2007) Global analysis of mRNA localization reveals a prominent role in organizing cellular architecture and function. Cell 131: 174–187. doi:10.1016/j.cell.2007.08.003.

2. Dotti CG, Sullivan CA, Banker GA (1988) The establishment of polarity by hippocampal neurons in culture. J Neurosci 8: 1454–1468.

3. Kleiman R, Banker G, Steward O (1994) Development of subcellular mRNA compartmentation in hippocampal neurons in culture. J Neurosci 14: 1130–1140.

4. Cheng L-C, Pastrana E, Tavazoie M, Doetsch F (2009) miR-124 regulates adult neurogenesis in the subventricular zone stem cell niche. Nat Neurosci 12: 399–408. doi:10.1038/nn.2294.

5. Yoo A, Staahl B, Chen L, Crabtree G (2009) MicroRNA-mediated switching of chromatin-remodelling complexes in neural development. Nature. doi:10.1038/nature08139.

6. Makeyev EV, Zhang J, Carrasco MA, Maniatis T (2007) The MicroRNA miR-124 promotes neuronal differentiation by triggering brain-specific alternative pre-mRNA splicing. Mol Cell 27: 435–448. doi:10.1016/j.molcel.2007.07.015.

7. Lugli G, Larson J, Martone ME, Jones Y, Smalheiser NR (2005) Dicer and eIF2c are enriched at postsynaptic densities in adult mouse brain and are modified by neuronal activity in a calpain-dependent manner. J Neurochem 94: 896–905. doi:10.1111/j.1471-4159.2005.03224.x.

8. Politz JCR, Hogan EM, Pederson T (n.d.) MicroRNAs with a nucleolar location. RNA-A PUBLICATION OF THE RNA SOCIETY {15}: {1705–1715}. doi:{10.1261/rna.1470409}.

9. Schratt GM, Tuebing F, Nigh EA, Kane CG, Sabatini ME, et al. (2006) A brain-specific microRNA regulates dendritic spine development. Nature 439: 283–289. doi:10.1038/nature04367.

10. Hwang H-W, Wentzel EA, Mendell JT (2007) A hexanucleotide element directs microRNA nuclear import. Science 315: 97–100. doi:10.1126/science.1136235.

11. Jeffries CD, Fried HM, Perkins DO (2011) Nuclear and cytoplasmic localization of neural stem cell microRNAs. RNA 17: 675–686. doi:10.1261/rna.2006511.

12. Parisi C, Giorgi C, Batassa EM, Braccini L, Maresca G, et al. (2011) Ago1 and Ago2 differentially affect cell proliferation, motility and apoptosis when overexpressed in SH-SY5Y neuroblastoma cells. FEBS Lett 585: 2965–2971.

doi:10.1016/j.febslet.2011.08.003.

13. Castanotto D, Lingeman R, Riggs AD, Rossi JJ (2009) CRM1 mediates nuclear-cytoplasmic shuttling of mature microRNAs. Proc Natl Acad Sci USA {106}: {21655–21659}. doi:{10.1073/pnas.0912384106}.

14. Hansen TB, Wiklund ED, Bramsen JB, Villadsen SB, Statham AL, et al. (2011) miRNA-dependent gene silencing involving Ago2-mediated cleavage of a circular antisense RNA. EMBO J 30: 4414–4422. doi:10.1038/emboj.2011.359.

15. Janas MM, Khaled M, Schubert S, Bernstein JG, Golan D, et al. (2011) Feed-Forward Microprocessing and Splicing Activities at a MicroRNA–Containing Intron. PLoS Genetics 7: e1002330. doi:10.1371/journal.pgen.1002330.g005.

16. Ballarino M, Pagano F, Girardi E, Morlando M, Cacchiarelli D, et al. (2009) Coupled RNA processing and transcription of intergenic primary miRNAs. Mol Cell Biol. doi:10.1128/MCB.00664-09.

17. Goldie BJ, Dun MD, Lin M, Smith ND, Verrills NM, et al. (2014) Activity-associated miRNA are packaged in Map1b-enriched exosomes released from depolarized neurons. Nucleic Acids Res. doi:10.1093/nar/gku594.

18. Meister G (2013) Argonaute proteins: functional insights and emerging roles. Nat Rev Genet 14: 447–459. doi:10.1038/nrg3462.

19. Rybak A, Fuchs H, Smirnova L, Brandt C, Pohl EE, et al. (2008) A feedback loop comprising lin-28 and let-7 controls pre-let-7 maturation during neural stem-cell commitment. Nat Cell Biol 10: 987–993. doi:10.1038/ncb1759.

20. Khudayberdiev SA, Zampa F, Rajman M, Schratt G (2013) A comprehensive characterization of the nuclear microRNA repertoire of post-mitotic neurons. Front Mol Neurosci 6: 43. doi:10.3389/fnmol.2013.00043.

21. Komatsu M, Li HO, Tsutsui H, Itakura K, Matsumura M, et al. (1997) MAZ, a Myc-associated zinc finger protein, is essential for the ME1a1-mediated expression of the c-myc gene during neuroectodermal differentiation of P19 cells. Oncogene 15: 1123–1131. doi:10.1038/sj.onc.1201283.

22. Tsutsui H, Geltinger C, Murata T, Itakura K, Wada T, et al. (1999) The DNA-binding and transcriptional activities of MAZ, a myc-associated zinc finger protein, are regulated by casein kinase II. Biochem Biophys Res Commun 262: 198–205. doi:10.1006/bbrc.1999.1130.

23. Bossone SA, Asselin C, Patel AJ, Marcu KB (1992) MAZ, a zinc finger protein, binds to c-MYC and C2 gene sequences regulating transcriptional initiation and termination. Proc Natl Acad Sci USA 89: 7452–7456.

24. Höck J, Weinmann L, Ender C, Rüdel S, Kremmer E, et al. (2007) Proteomic and functional analysis of Argonaute-containing mRNA-protein complexes in

human cells. EMBO Rep 8: 1052–1060. doi:10.1038/sj.embor.7401088.

25. Cassola A, Noé G, Frasch AC (2010) RNA recognition motifs involved in nuclear import of RNA-binding proteins. RNA Biol 7: 339–344.

26. Meseguer S, Mudduluru G, Escamilla JM, Allgayer H, Barettino D (2010) Micro-RNAs-10a and -10b contribute to retinoic acid-induced differentiation of neuroblastoma cells and target the alternative splicing regulatory factor SFRS1 (SF2/ASF). J Biol Chem. doi:10.1074/jbc.M110.167817.

27. Wu H, Sun S, Tu K, Gao Y, Xie B, et al. (2010) A splicing-independent function of SF2/ASF in microRNA processing. Mol Cell 38: 67–77. doi:10.1016/j.molcel.2010.02.021.

28. Chen L (2009) A global comparison between nuclear and cytosolic transcriptomes reveals differential compartmentalization of alternative transcript isoforms. Nucleic Acids Res. doi:10.1093/nar/gkp1136.

29. Guidi M, Muiños-Gimeno M, Kagerbauer B, Martí E, Estivill X, et al. (2010) Overexpression of miR-128 specifically inhibits the truncated isoform of NTRK3 and upregulates BCL2 in SH-SY5Y neuroblastoma cells. BMC Mol Biol 11: 95. doi:10.1186/1471-2199-11-95.

30. Laneve P, Di Marcotullio L, Gioia U, Fiori ME, Ferretti E, et al. (2007) The interplay between microRNAs and the neurotrophin receptor tropomyosin-related kinase C controls proliferation of human neuroblastoma cells. Proc Natl Acad Sci USA 104: 7957–7962. doi:10.1073/pnas.0700071104.

31. Kim DH, Villeneuve LM, Morris KV, Rossi JJ (2006) Argonaute-1 directs siRNA-mediated transcriptional gene silencing in human cells. Nat Struct Mol Biol 13: 793–797. doi:10.1038/nsmb1142.

32. Caudron-Herger M, Müller-Ott K, Mallm J-P, Marth C, Schmidt U, et al. (2011) Coding RNAs with a non-coding function: Maintenance of open chromatin structure. nucleus 2: 410–424. doi:10.4161/nucl.2.5.17736.

33. Baltz AG, Munschauer M, Schwanhäusser B, Vasile A, Murakawa Y, et al. (2012) The mRNA-bound proteome and its global occupancy profile on protein-coding transcripts. Mol Cell 46: 674–690. doi:10.1016/j.molcel.2012.05.021.

34. Castello A, Fischer B, Eichelbaum K, Horos R, Beckmann BM, et al. (2012) Insights into RNA biology from an atlas of mammalian mRNA-binding proteins. Cell 149: 1393–1406. doi:10.1016/j.cell.2012.04.031.

35. Piriyapongsa J, Jordan IK, Conley AB, Ronan T, Smalheiser NR (2011) Transcription factor binding sites are highly enriched within microRNA precursor sequences. Biol Direct 25: 3181–3182. doi:10.1093/bioinformatics/btp554.

36. Ugai H, Li HO, Komatsu M, Tsutsui H, Song J, et al. (2001) Interaction of Myc-

associated zinc finger protein with DCC, the product of a tumor-suppressor gene, during the neural differentiation of P19 EC cells. Biochem Biophys Res Commun 286: 1087–1097. doi:10.1006/bbrc.2001.5469.

37. Diederichs S, Haber DA (2007) Dual Role for Argonautes in MicroRNA Processing and Posttranscriptional Regulation of MicroRNA Expression. Cell 131: 1097–1108. doi:10.1016/j.cell.2007.10.032.

38. Yang JS, Maurin T, Lai EC (2012) Functional parameters of Dicer-independent microRNA biogenesis. RNA 18: 945–957. doi:10.1261/rna.032938.112.

39. Schaefer A, Im HI, Veno MT, Fowler CD, Min A, et al. (2010) Argonaute 2 in dopamine 2 receptor-expressing neurons regulates cocaine addiction. Journal of Experimental Medicine 207: 1843–1851. doi:10.1038/ng1744.

40. Wang Y, Zhu W, Levy DE (2006) Nuclear and cytoplasmic mRNA quantification by SYBR green based real-time RT-PCR. Methods 39: 356–362. doi:10.1016/j.ymeth.2006.06.010.

41. Smyth GK (2004) Linear models and empirical bayes methods for assessing differential expression in microarray experiments. Stat Appl Genet Mol Biol 3: Article3. doi:10.2202/1544-6115.1027.

42. Beitzinger M, Peters L, Zhu JY, Kremmer E, Meister G (2007) Identification of human microRNA targets from isolated argonaute protein complexes. RNA Biol 4: 76–84.

43. Rüdel S, Flatley A, Weinmann L, Kremmer E, Meister G (2008) A multifunctional human Argonaute2-specific monoclonal antibody. RNA 14: 1244–1253. doi:10.1261/rna.973808.

44. Kim D, Pertea G, Trapnell C, Pimentel H, Kelley R, et al. (2013) TopHat2: accurate alignment of transcriptomes in the presence of insertions, deletions and gene fusions. Genome Biol 14: R36. doi:10.1186/gb-2013-14-4-r36.

45. Anders S, Pyl PT, Huber W (2014) HTSeq–A Python framework to work with high-throughput sequencing data. bioRxiv.

46. Chang JT, Nevins JR (2006) GATHER: a systems approach to interpreting genomic signatures. Bioinformatics 22: 2926–2933. doi:10.1093/bioinformatics/btl483.

47. Huang DW, Sherman BT, Tan Q, Kir J, Liu D, et al. (2007) DAVID Bioinformatics Resources: expanded annotation database and novel algorithms to better extract biology from large gene lists. Nucleic Acids Res 35: W169–W175. doi:10.1093/nar/gkm415.

CHAPTER 6

Thesis Discussion

Introduction

Although neuropathologies such as schizophrenia report failures of synaptic plasticity in relation to cognitive deficits, the relative mystery surrounding the functioning of plasticity in the healthy brain represents a distinct obstacle in treating such disorders. Understanding the phenomenon of neuronal plasticity is thus an important problem in molecular neurobiology. Functional compartmentalisation of mRNA enables the specificity required to refine responses to a single activated synapse, but little is known about how this complex system could be regulated in functioning neurons.

While the discovery of miRNA and PTGS has enabled scientists to establish a functional model of synaptic plasticity that displays an intrinsically dynamic and flexible infrastructure, the modes of study employed within these research fields impose two key limitations. In neuroscience, the reliance on animal models and limitations associated with studying post-mortem brain tissue impedes the elaboration of this machinery within functioning human neurons; while in miRNA research, the disease-driven impetus to define individual regulatory partners of each miRNA precludes understanding of overall system-level trends. To address these limitations, the studies contained in this thesis employed a human neuroblastoma-based cell culture model in conjunction with genome-wide approaches to investigate the subcellular compartmentalisation of miRNA and the dynamics of their involvement in the response to neuronal activity at both the cellular and subcellular level.

The importance of SH-SY5Y as an in-vitro model of human neuronal function

Many of the miRNA that were identified in Chapter 4 of this thesis as being functionally relevant to neuronal activity (i.e. enriched in neurites, responsive to

depolarisation and released in exosomes), and in Chapter 5 as being preferentially enriched in the nucleus, were not conserved. That is, their expression is restricted to either humans alone, or humans and higher-order primates. This suggests that even the mass profiling of miRNA expression in animal models such as rats or mice would give limited insights into the regulatory capacity of these molecules in the human brain. In support of this, Chapter 5 of this thesis proposed a putative novel mechanism of dual transcriptional and translational control by primate-specific neuronal miRNA involving the transcription factor MAZ through the identification of a four-nucleotide motif. A similar profiling study conducted in rat neurons was unable to derive a motif among nucleus-enriched miRNA [145]. Moreover, many aspects of neurocognitive disorders are difficult to adequately establish or measure in animal models, making them of limited utility in elaborating these disorders. It is therefore important to institute and give credence to human-derived cell culture models to provide access to this missing layer of information.

The SH-SY5Y neuroblastoma line has been extensively cultured since its establishment in the 1970s [10], and is very versatile as a neuronal model system due to the plurality of neuronal phenotypes inducible depending on the differentiation agent employed [11]. The major criticism of this model has been the lack of synapse development in culture, however recent evidence suggests that this might be due to an incompletely conducive environment. When we consider the life of a cultured primary cortical or hippocampal neuron, these cells have differentiated and matured in a brain, exposed to a cocktail of signalling molecules, in contact with neighbouring cells including astrocytes and glia in addition to other neurons; the formation of synaptic connections is the integration of all these factors, accompanied by experience-dependent patterns of activity. It seems, then,

relatively naïve to expect that the addition of a single neurotrophic factor to cells that are being induced to be neurons would be sufficient to stimulate synapse formation. This idea is supported by the paper published in 2010 reporting a culture system were synaptic structures were observed in SH-SY5Y cultures [104]. The system was based on pre-differentiation with ATRA, and a neuronal maturation cocktail that included BDNF, NGF, neuregulin1 and vitamin D_3. In conjunction with these chemical cues, the cells were provided with a three-dimensional growth matrix, enabling them to develop growth conformations more reminiscent of *in vivo*.

However, despite the development of increasingly faithful neuronal emulations, new SH-SY5Y usage paradigms are underemployed. A comprehensive review of the SH-SY5Y literature conducted in Chapter 3 revealed that, most surprisingly, approximately 83% of studies use undifferentiated cells to model neuronal function (and dysfunction). In some instances these investigations were not supported by other lines of enquiry such as primary cultures or *in vivo* animal experiments, thus relying on observations from a model that is likely to be functionally inappropriate.

Integrating findings from all studies comprising this thesis supports the validity of the SH-SY5Y neuronal model. The differentiated cells demonstrate strong similarity to neurons in terms of morphology, gene expression and miRNA expression, and are increased in activation capacity as evidenced by elevated levels of AChE. In response to depolarisation, gene expression changes mimicked those of primary neurons creating early- and late-phase LTP in culture, including significantly increased FOS expression, and exosomes were released from the neurite fraction. Importantly, the cells demonstrated functional

compartmentalisation of mRNA; thus, the finding that miRNA are also compartmentalised suggests that the subcellular miRNA responses to depolarisation observed here may reflect their importance in the synaptic fraction of functioning neurons *in vivo*.

Neuronal Compartmentalisation of miRNA: the importance of location

Functional partitioning of the subcellular space is critical to the establishment of polarity in cells generally; the complexity of neurons is highlighted by the fact that this delineation begins less than 24 hours after commencement of differentiation. During this process, the presence or absence of particular mRNA transcripts is sufficient to discern the axon from dendrites, as well as indicating progress toward terminal differentiation. Post-differentiation, an intricate mRNA transportation network culminates in deposition of translationally silenced transcripts at the bases of dendritic spines, and translation is initiated in response to activation of the local synapse.

How this functionality is controlled remains unknown. As evidence supporting the importance of miRNA in neuronal function continues to accumulate it seems likely that these short, regulatory transcripts play an integral role. Although several studies have identified individual miRNA as being present in the nucleus or dendrites, experiments presented in this thesis addressed a gap in the knowledge and investigated genome-wide patterns of subcellular miRNA expression. The studies contained herein have demonstrated that, like mRNA, neurons compartmentalise miRNA in a manner that supports functional neurobiology. Further, they revealed the importance of non-conserved, primate-specific miRNA in the brain, and particularly in the response to depolarisation where repeated activity resulted in cumulative down-regulation of particular molecules. Although

some of this was attributable to exosomal release, for those miRNA not detected in exosomes an alternative fate must be determined.

As postulated in the literature review in Chapter 2, miRNAs participating in post-transcriptional silencing of mRNA in the dendritic tree could become dissociated from their cargo in response to activity and subsequently degraded, however this has not been conclusively shown. Visual indications of miRNA expression and targeting activity are typically assessed by methods such as in-situ hybridisation or luciferase assay. These methods require sacrifice of the living tissue, and as such lack the ability to convey the temporal dynamics of translational regulation in a complex system such as the neuron. Since mRNAs are typically directed to their destination by *cis*-acting signals within the 3' UTR it could be hypothesised that a fluorescent protein associated with the UTR would be similarly trafficked, revealing the transcript's location. Such a construct could be encoded in a vector and transfected into cells in culture, however if the UTR is under miRNA regulation the fluorescence will not be visible, and thus successful transfection unclear, until the repression is lifted. This limitation could be overcome by employing 2 fluors – one independent of the UTR to report transfection, and the other UTR-associated to "sense" whether the transcript is currently under the regulation of miRNA. A future direction of this project is thus to determine whether such a construct can be used to visualise mRNA localisation and miRNA activity in functioning neuronal cells at rest and in response to depolarisation, in real time.

An important subcellular compartment to consider is the sequestration of miRNA in exosomes, as these are released by depolarisation into the extracellular space and as such could form an important part of the synaptic milieu. Exosomes were initially considered to perform a waste disposal role that, in the neuronal context,

could dispose of miRNA that are inhibiting the synaptic goals of the source cell. Once released into the extracellular environment, however, they could potentially be taken up by surrounding neurons, astrocytes and glia. This would enable the post-synaptic cell to modulate expression and/or signalling in those cells, communicating either what the cell of origin is trying to achieve in a positive way, or pushing that cell's agenda in a competitive sense by using inhibitory miRNA to reduce the resting potential of surrounding synapses.

The communication power of exosomes extends to transformation, whereby target cells are induced to phenotypically resemble source cells, or to modify the content of their own exosomes to emulate that of the exogenous vesicles [169]. In this regard, exosomes hold the possibility of being a vehicle for therapeutics, and indeed delivery of synthetic small RNAs to the brain has been demonstrated via targeted exosomes [170]. In order to better understand the transformative potential of SH-SY5Y-derived exosomes, experiments extending the work in this thesis are investigating the effects of repeated depolarisation and stage of differentiation/maturation on exosomal miRNA. Future experiments could attempt to achieve trans-differentiation, or phenotypic modulation, of target cells. A good target for these experiments would be the HEK293 human embryonic kidney line, as the kidney and brain arise developmentally from the same tissue, and this line has been shown to be related to neurons [171]. The results from the investigations outlined above will assist in directing these experiments by indicating the influence of neuronal maturation on the miRNA content of the exosomes, and thus how exosomes should be prepared to achieve optimal phenotypic modulation.

Activity-associated miRNA dynamics and implications for schizophrenia

Dysregulation of miRNA expression is now well established in the context of schizophrenia. Indeed, our research group has shown global up-regulation of miRNA in the dorsolateral prefrontal cortex (DLPFC) and superior temporal gyrus (STG) associated with increased expression of miRNA biogenesis components DGCR8 and DICER, and, along with altered target gene expression in the same samples, functionally convergent on pathways associated with synaptic plasticity, axon guidance and LTP [60,62].

Studies performed in Chapter 4 of this thesis found global down regulation of whole cell miRNA expression in response to single and repeated depolarisations, and this finding was recapitulated in the neurite compartment suggesting that reduction of miRNA-mediated silencing is integral to the responsiveness of the post-synaptic compartment to synaptic activity. Indeed reduction of miRNA expression has been shown to enhance memory formation in mice [123]. Taken together, these two findings intimate that an inability to adequately attenuate miRNA expression in response to synaptic activation could underlie the impairments to executive function observed in schizophrenia. This mechanism could be tested in part using the SH-SY5Y model described in these studies by employing the fluoroquinoline enoxacin to drive increased miRNA expression [172], although it is not certain that over expression directed by an exogenous compound would reflect endogenous over expression given that this antibiotic acts by stabilising the DICER/TRBP complex, while in schizophrenia all major components of miRNA biogenesis are themselves increased in expression.

In this regard, a powerful tool in the elaboration of cognitive disorders lies in neural induction of patient-derived induced pluripotent stem cells (iPSCs). This

technique has demonstrated disease phenotype-dependent differential drug responsiveness using dermal-derived, functional cortical neurons in Alzheimer's patients [173]; while spinal neurons derived from Amyotrophic Lateral Sclerosis patients exhibited morphological and biochemical characteristics consistent with disease pathophysiology, and were successfully used to screen several compounds for potential to reverse symptomology [174]. In fact iPSC-derived neurons may also have the capacity to treat diseases involving loss of neurons, as autologous cells can undergo re-implantation into the primate brain with minimal loss due to their reduced immunogenicity [175].

Developing techniques in this field are focusing on derivation of iPSCs from peripheral blood, as this tissue is less invasive to obtain. Combining this method with the successful outcomes described above from dermal-derived neurons indicates great promise in the application of these techniques to schizophrenia in particular, and to greater understanding of human neuronal cell biology more generally.

Expect the unexpected: the future of miRNA research

Despite being first identified in 2001 [176], there is still much that remains unknown about miRNA and their overall contributions to cell biology. In part this is due to rapid discovery of new miRNA through next-generation sequencing. Since its creation in 2002, the miRNA annotation database miRBase (http://www.mirbase.org) has jumped from around 200 entries to almost 36000 mature miRNA in 223 species, with the current version (v. 21) annotating 1881 precursor and 2588 mature human miRNA. miRNA are recognised primarily as post-transcriptional regulators of gene expression, and as such the expression of mature miRNA is considered to be restricted to the cytoplasm.

The work described in Chapter 5 of this thesis supports a growing body of evidence suggesting that the roles of miRNA are not restricted to PTGS, nor their expression to the cytoplasm. This study found that some mature miRNA are actually preferentially enriched in the nucleus, raising the questions of whether these mature miRNA transcripts were actively imported into the nucleus or if they were processed and retained there, and even more pertinently, what function these miRNAs are fulfilling. Ago co-IP suggested that, at least in part, a canonical RISC may be involved, however through functional and motif analyses a novel relationship between miRNA, Ago2 and the transcription factor MAZ was proposed. Novel nuclear relationships have been found in feedback loops that have been demonstrated to regulate miRNA splicing [152] and maturation [144]. Co-operative interactions with transcription factors, some of which have both DNA and RNA binding domains, could extend the functions of miRNA to transcriptional control directly through interactions with transcription complexes, and indirectly through participation in histone modifications. Indeed the latter has been implicated by involvement of RISC proteins with chromatin remodelling factors [138].

In a rat neuronal model, MAZ was reported to translocate from the nucleus to the neurites after cells were differentiated with ATRA [160]. This finding places MAZ in a powerful position, as the presence of a transcription factor at the synapse could enable a direct signal transduction mechanism for communicating permanent plasticity-associated expression changes into the nucleus. Experiments following on from this work will aim to confirm the interaction of miRNA with MAZ and investigate the subcellular localisation of MAZ in human neurons. The MAZ RNA binding repertoire will be elaborated in the nucleus and neurites by co-IP,

while direct interactions proposed with the precursor miRNA identified in this study will be investigated by electro-mobility shift assay (EMSA) using custom oligonucleotides that have been designed to retain the key secondary structure of these transcripts. Techniques are also being developed within our research laboratory for culturing the SH-SY5Y cells on glass slides to enable visual inspection of MAZ expression by confocal microscopy.

Conclusions

This thesis sought to test the hypothesis that miRNA are functionally compartmentalised in neurons, and that they serve as key regulators of activity-related neuronal functions including synaptic plasticity and communication. Through the establishment of techniques for subcellular fractionation, exosome purification and co-immunoprecipitation, and addressing the challenges associated with analysing data derived from these experiments, the studies contained herein have revealed several unique aspects of miRNA expression in functioning human neurons. In particular, the unexpected finding unifying these studies demonstrated the significance of non-conserved, human- and primate-specific miRNA in supporting functional neurobiology, and highlighted the importance of considering the relevance of the model employed in studies of synaptic plasticity. This finding also holds crucial implications for studies of neuropsychiatric disorders such as schizophrenia where no complete animal model currently exists, as it suggests that it may only be through the development of novel approaches, such as studying neurons derived from patients' own cells, that we may finally begin to understand the failures of synaptic plasticity that underlie these devastating disorders.

It seems clear that miRNA networks fulfil critical regulatory requirements in neurons, support functional compartmentalisation, and are key contributors to

intra- and inter-cellular communication in the brain. Future studies focused on elaborating the structures and interactions participant in these networks, and developing novel methods for investigating these systems in living human cells, could hold the keys to unlocking the complexities of memory formation and plasticity.

APPENDIX I

Chapter 3 Additional Files

ADDITIONAL FILE 1

Goldie et al, Review of SH-SY5Y Literature
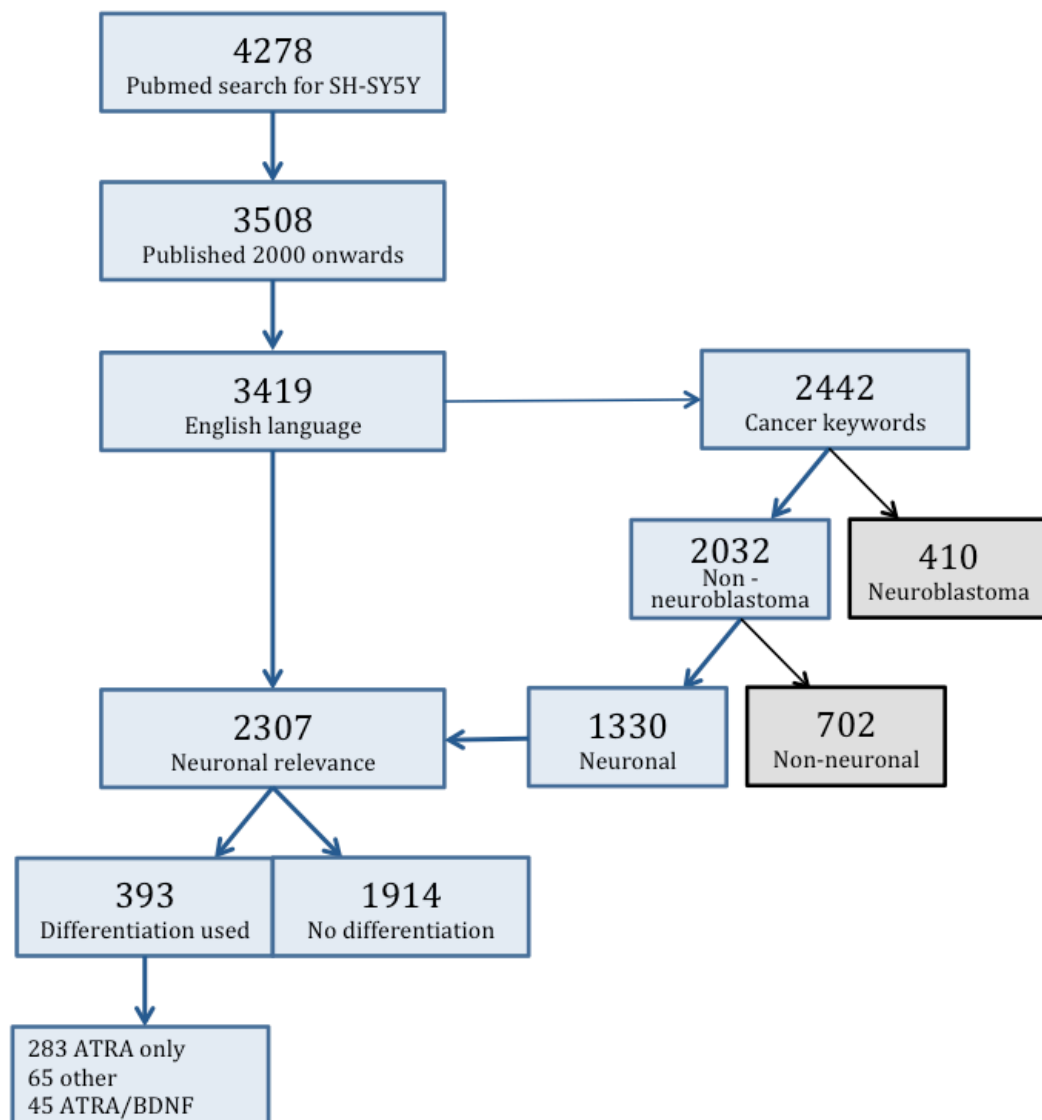
Supplementary Figure S1. Schematic of criteria for SH-SY5Y literature review.

ADDITIONAL FILE 2
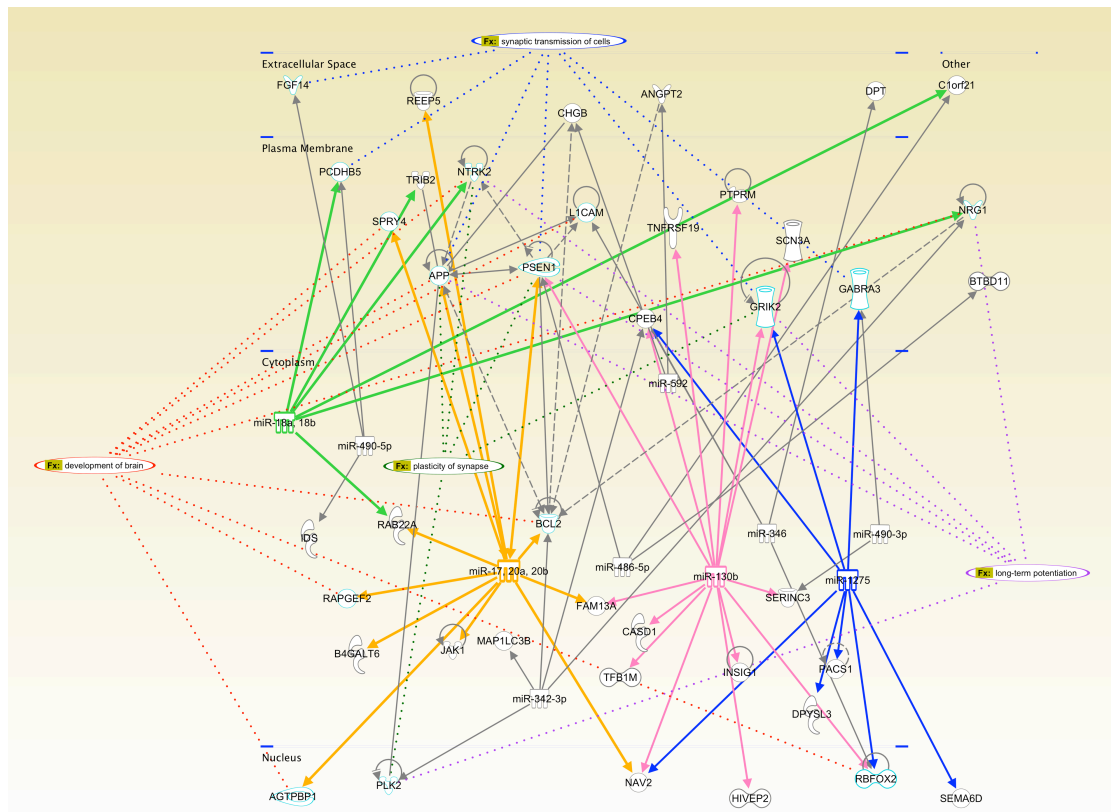
Supplementary Figure S2. Down-regulation of key miRNA accompanies up-regulation of genes integral to neuronal phenotype. IPA target analysis of miRNA incrementally down regulated during two-stage differentiation was integrated with up-regulated mRNA and overlaid with cellular functions statistically over-represented among targeted genes. This sub-cellular layout demonstrates the functional importance of four families of miRNA in regulating many mRNA central to neuron development, with an emphasis on the composition of the synaptic membrane.

ADDITIONAL FILE 3
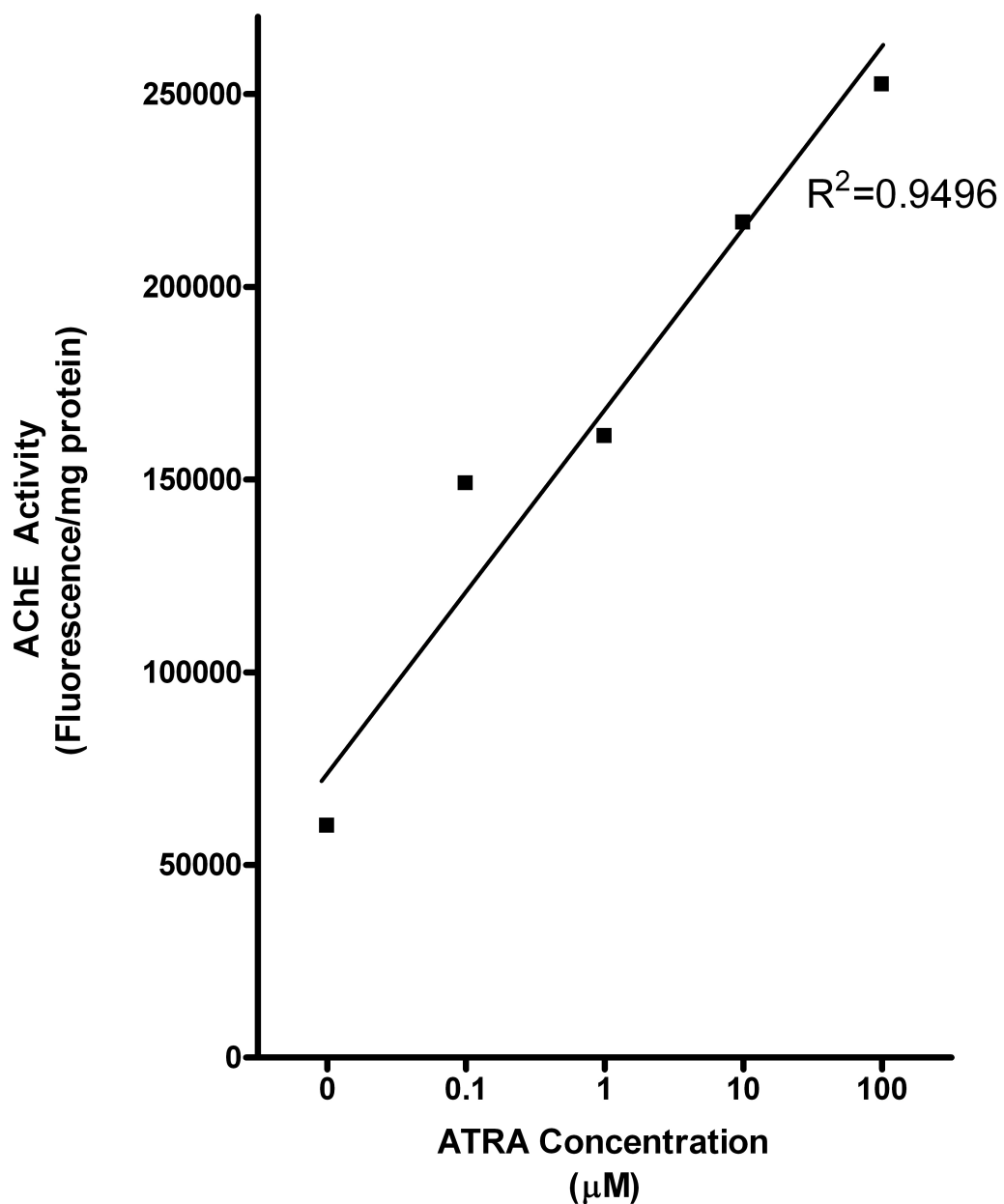
Supplementary Figure S3. Enhanced neuronal maturity is primed by ATRA concentration. Cells were differentiated with titrated concentrations of ATRA followed by maturation with the same concentration of BDNF. Neuronal maturity was assayed by AChE activity at various timepoints during BDNF maturation and the values averaged. A very strong correlation was observed between concentration of ATRA used for differentiation and the level of BDNF induced activity, suggesting that the production of more BDNF receptors enhances neuronal maturity.

Supplementary Table S1. IPA Core Analysis of integrated miRNA and target mRNA expression altered by two stage differentiation (miRNA down, mRNA up).

Category	Diseases or Functions Annotation	p-Value	# Molecules	Molecules
Cell-To-Cell Signaling and Interaction	neurotransmission	1.97E-07	7	APP,GRIK2,KCNMB4,PCDHB10,PCDHB14,PCDHB5,PSEN1
Nervous System Development and Function	neurotransmission	1.97E-07	7	APP,GRIK2,KCNMB4,PCDHB10,PCDHB14,PCDHB5,PSEN1
Neurological Disease	neurological signs	7.41E-07	13	APP,BCL2,CHGB,DPYSL3,ESRRG,GABRA3,GRIK2,LGR5,NTRK2,PLK2,PSEN1,SCN3A,VCAN
Cell-To-Cell Signaling and Interaction	synaptic transmission of cells	1.52E-06	6	APP,GRIK2,PCDHB10,PCDHB14,PCDHB5,PSEN1
Nervous System Development and Function	synaptic transmission of cells	1.52E-06	6	APP,GRIK2,PCDHB10,PCDHB14,PCDHB5,PSEN1
Cellular Assembly and Organization	function of mitochondria	1.83E-06	3	BCL2,NTRK2,PSEN1
Cellular Function and Maintenance	function of mitochondria	1.83E-06	3	BCL2,NTRK2,PSEN1
Cell-To-Cell Signaling and Interaction	synaptogenesis	1.93E-06	4	APP,PCDHB10,PCDHB14,PCDHB5
Nervous System Development and Function	synaptogenesis	1.93E-06	4	APP,PCDHB10,PCDHB14,PCDHB5
Cellular Assembly and Organization	synaptogenesis	1.93E-06	4	APP,PCDHB10,PCDHB14,PCDHB5
Cellular Function and Maintenance	synaptogenesis	1.93E-06	4	APP,PCDHB10,PCDHB14,PCDHB5
Tissue Development	synaptogenesis	1.93E-06	4	APP,PCDHB10,PCDHB14,PCDHB5
Neurological Disease	Movement Disorders	2.29E-06	15	APP,BCL2,CHGB,DPYSL3,ESRRG,FGF14,GABRA3,GRIK2,LGR5,NRG1,NTRK2,PLK2,PSEN1,SCN3A,VCAN
Neurological Disease	Huntington's Disease	2.38E-06	12	BCL2,CHGB,DPYSL3,ESRRG,GABRA3,GRIK2,LGR5,NTRK2,PLK2,PSEN1,SCN3A,VCAN
Hereditary Disorder	Huntington's Disease	2.38E-06	12	BCL2,CHGB,DPYSL3,ESRRG,GABRA3,GRIK2,LGR5,NTRK2,PLK2,PSEN1,SCN3A,VCAN
Psychological Disorders	Huntington's Disease	2.38E-06	12	BCL2,CHGB,DPYSL3,ESRRG,GABRA3,GRIK2,LGR5,NTRK2,PLK2,PSEN1,SCN3A,VCAN
Neurological Disease	Huntington's Disease	2.38E-06	12	BCL2,CHGB,DPYSL3,ESRRG,GABRA3,GRIK2,LGR5,NTRK2,PLK2,PSEN1,SCN3A,VCAN
Skeletal and Muscular Disorders	disorder of basal ganglia	2.74E-06	14	APP,BCL2,CHGB,DPYSL3,ESRRG,GABRA3,GRIK2,LGR5,NRG1,NTRK2,PLK2,PSEN1,SCN3A,VCAN
Neurological Disease	disorder of basal ganglia	2.74E-06	14	APP,BCL2,CHGB,DPYSL3,ESRRG,GABRA3,GRIK2,LGR5,NRG1,NTRK2,PLK2,PSEN1,SCN3A,VCAN
Psychological Disorders	disorder of basal ganglia	2.74E-06	14	APP,BCL2,CHGB,DPYSL3,ESRRG,GABRA3,GRIK2,LGR5,NRG1,NTRK2,PLK2,PSEN1,SCN3A,VCAN
Cancer	digestive organ tumor	1.10E-05	36	AGTPBP1,ANGPT2,BAZ2B,BCL2,BTBD11,CASD1,CDC42BPA,CDH2,CHGB,CPEB4,DHRS7,EPHA6,FGF14,GRIK2,HIVEP2,INSIG1,JAK1,L1CAM,LGR5,NRG1,NTRK2,PCDH9,PCDHB5,PI15,PLK2,PSEN1,PTPRM,PVRL3,RAPGEF2,RGS7,SCN3A,SEMA6D,SLC8A3,SPRY1,TNFRSF19,TSPAN8
Gastrointestinal Disease	digestive organ tumor	1.10E-05	36	AGTPBP1,ANGPT2,BAZ2B,BCL2,BTBD11,CASD1,CDC42BPA,CDH2,CHGB,CPEB4,DHRS7,EPHA6,FGF14,GRIK2,HIVEP2,INSIG1,JAK1,L1CAM,LGR5,NRG1,NTRK2,PCDH9,PCDHB5,PI15,PLK2,PSEN1,PTPRM,PVRL3,RAPGEF2,RGS7,SCN3A,SEMA6D,SLC8A3,SPRY1,TNFRSF19,TSPAN8
Cancer	colorectal cancer	1.17E-05	33	AGTPBP1,ANGPT2,BAZ2B,BCL2,BTBD11,CASD1,CDC42BPA,CDH2,CHGB,CPEB4,DHRS7,EPHA6,FGF14,GRIK2,HIVEP2,INSIG1,JAK1,L1CAM,LGR5,NRG1,NTRK2,PCDH9,PCDHB5,PI15,PLK2,PTPRM,PVRL3,RAPGEF2,SCN3A,SLC8A3,SPRY1,TNFRSF19,TSPAN8
Gastrointestinal Disease	colorectal cancer	1.17E-05	33	AGTPBP1,ANGPT2,BAZ2B,BCL2,BTBD11,CASD1,CDC42BPA,CDH2,CHGB,CPEB4,DHRS7,EPHA6,FGF14,GRIK2,HIVEP2,INSIG1,JAK1,L1CAM,LGR5,NRG1,NTRK2,PCDH9,PCDHB5,PI15,PLK2,PTPRM,PVRL3,RAPGEF2,SCN3A,SLC8A3,SPRY1,TNFRSF19,TSPAN8
Neurological Disease	neuromuscular disease	1.26E-05	14	APP,BCL2,CHGB,DPYSL3,ESRRG,GABRA3,GRIK2,LGR5,NRG1,NTRK2,PLK2,PSEN1,SCN3A,VCAN
Skeletal and Muscular Disorders	neuromuscular disease	1.26E-05	14	APP,BCL2,CHGB,DPYSL3,ESRRG,GABRA3,GRIK2,LGR5,NRG1,NTRK2,PLK2,PSEN1,SCN3A,VCAN
Behavior	associative memory	1.43E-05	2	APP,PSEN1
Nervous System Development and Function	associative memory	1.43E-05	2	APP,PSEN1
Neurological Disease	formation of senile plaques	1.43E-05	2	APP,PSEN1
Cellular Assembly and Organization	formation of senile plaques	1.43E-05	2	APP,PSEN1
Tissue Development	formation of senile plaques	1.43E-05	2	APP,PSEN1
Cancer	breast or colorectal cancer	1.55E-05	37	AGTPBP1,ANGPT2,BAZ2B,BCL2,BTBD11,CASD1,CDC42BPA,CDH2,CHGB,CPEB4,DHRS7,EPHA6,ESRRG,FGF14,GRIK2,HIVEP2,INSIG1,JAK1,L1CAM,LGR5,MAP1LC3B,NRG1,NTRK2,PCDH9,PCDHB5,PI15,PLK2,PTPRM,PVRL3,RAPGEF2,SCN3A,SLC8A3,SPRY1,TNFRSF19,TSPAN8,VCAN
Cell-To-Cell Signaling and Interaction	assembly of synapse	1.87E-05	3	PCDHB10,PCDHB14,PCDHB5
Nervous System Development and Function	assembly of synapse	1.87E-05	3	PCDHB10,PCDHB14,PCDHB5
Cellular Assembly and Organization	assembly of synapse	1.87E-05	3	PCDHB10,PCDHB14,PCDHB5
Cellular Function and Maintenance	assembly of synapse	1.87E-05	3	PCDHB10,PCDHB14,PCDHB5
Tissue Development	assembly of synapse	1.87E-05	3	PCDHB10,PCDHB14,PCDHB5
Cancer	epithelial neoplasia	4.05E-05	50	AGTPBP1,ANGPT2,APP,BAZ2B,BCL2,BTBD11,CASD1,CDC42BPA,CDH2,CHGB,DHRS7,DPT,EPHA6,ESRRG,FAM13A,FGF14,GRIK2,HIVEP2,IDS,INSIG1,JAK1,KCNMB4,L1CAM,LGR5,MAP1LC3B,NAV2,NRG1,NTRK2,PACS1,PCDH9,PCDHB10,PCDHB14,PCDHB5,PI15,PLK2,PSEN1,PTPRM,RAPGEF2,RBFOX2,RGS7,SCN3A,SDCBP,SEMA6D,SLC8A3,SPRY4,SPRY1,TMEM66,TRIB2,TSPAN8,VCAN
Neurological Disease	autosomal dominant familial Alzheimer's disease	4.28E-05	2	APP,PSEN1
Hereditary Disorder	autosomal dominant familial Alzheimer's disease	4.28E-05	2	APP,PSEN1
Psychological Disorders	autosomal dominant familial Alzheimer's disease	4.28E-05	2	APP,PSEN1
Metabolic Disease	autosomal dominant familial Alzheimer's disease	4.28E-05	2	APP,PSEN1
Neurological Disease	juvenile onset Huntington disease	4.28E-05	2	GRIK2,NTRK2
Hereditary Disorder	juvenile onset Huntington disease	4.28E-05	2	GRIK2,NTRK2
Psychological Disorders	juvenile onset Huntington disease	4.28E-05	2	GRIK2,NTRK2
Skeletal and Muscular Disorders	juvenile onset Huntington disease	4.28E-05	2	GRIK2,NTRK2
Cell-To-Cell Signaling and Interaction	long-term potentiation of hippocampus	4.28E-05	2	APP,NRG1
Nervous System Development and Function	long-term potentiation of hippocampus	4.28E-05	2	APP,NRG1
Behavior	spatial memory	4.28E-05	2	APP,PSEN1
Nervous System Development and Function	spatial memory	4.28E-05	2	APP,PSEN1
Cell-To-Cell Signaling and Interaction	synaptic transmission of hippocampal neurons	4.28E-05	2	APP,PSEN1

Category	Function/Disease	p-value	Count & Genes
Nervous System Development and Function	synaptic transmission of hippocampal neurons	4.28E-05	2 APP,PSEN1
Cell Death and Survival	apoptosis of brain cells	4.90E-05	3 APP,BCL2,PSEN1
Cancer	carcinoma	5.08E-05	49 AGTPBP1,ANGPT2,APP,BAZ2B,BCL2,BTBD11,CASD1,CDC42BPA,CDH2,CHGB,DHRS7,DPT,EPHA6,ESRRG,FAM13A,FGF14,GRIK2,HIVEP2,INSIG1,JAK1,KCNMB4,L1CAM,LGR5,MAP1LC3B,NAV2,NRG1,NTRK2,PACS1,PCDH9,PCDHB10,PCDHB14,PCDHB5,PI15,PLK2,PSEN1,PTPRM,RAPGEF2,RBFOX2,RGS7,SCN3A,SDCBP_SEMA6D,SLC8A3,SPRY1,SPRY4,TMEM66,TRIB2,TSPAN8,VCAN
Neurological Disease	Alzheimers disease type 3	8.54E-05	2 APP,PSEN1
Hereditary Disorder	Alzheimers disease type 3	8.54E-05	2 APP,PSEN1
Psychological Disorders	Alzheimers disease type 3	8.54E-05	2 APP,PSEN1
Metabolic Disease	Alzheimers disease type 3	8.54E-05	2 APP,PSEN1
Cell Death and Survival	apoptosis of Schwann cells	8.54E-05	2 BCL2,NRG1
Post-Translational Modification	heterodimerization of protein	8.54E-05	2 BCL2,NRG1
Cell Death and Survival	cell death of cortical neurons	8.87E-05	3 APP,BCL2,PSEN1
Cell-To-Cell Signaling and Interaction	adhesion of melanoma cell lines	1.01E-04	3 L1CAM,NRG1,VCAN
Tissue Development	adhesion of melanoma cell lines	1.01E-04	3 L1CAM,NRG1,VCAN
Cell Death and Survival	cell death of neuroglia	1.15E-04	3 APP,BCL2,NRG1
Cancer	abdominal cancer	1.32E-04	44 AGTPBP1,ANGPT2,APP,BAZ2B,BCL2,BTBD11,CASD1,CDC42BPA,CDH2,CHGB,CPEB4,DHRS7,DPT,EPHA6,ESRRG,FAM13A,FGF14,GRIK2,HIVEP2,INSIG1,JAK1,L1CAM,LGR5,NAV2,NRG1,NTRK2,PCDH9,PCDHB10,PCDHB5,PI15,PLK2,PSEN1,PTPRM,PVRL3,RAPGEF2,RBFOX2,SCN3A,SEMA6D,SLC8A3,SPRY1,TNFRSF19,TRIB2,TSPAN8,VCAN
Cell Death and Survival	apoptosis of cortical neurons	1.42E-04	2 APP,PSEN1
Cancer	cylindroma	1.42E-04	2 BCL2,NTRK2
Nervous System Development and Function	growth of neurites	1.63E-04	4 APP,BCL2,L1CAM,NRG1
Cellular Assembly and Organization	growth of neurites	1.63E-04	4 APP,BCL2,L1CAM,NRG1
Tissue Development	growth of neurites	1.63E-04	4 APP,BCL2,L1CAM,NRG1
Cellular Development	differentiation of brain cancer cell lines	2.12E-04	2 BCL2,PSEN1
Cell Death and Survival	cell death of neuroblastoma cell lines	2.28E-04	5 APP,BCL2,NTRK2,PSEN1,XPR1
Cell Death and Survival	cell death of germ cell tumor cell lines	2.97E-04	2 APP,BCL2
Nervous System Development and Function	cell death of hippocampal neurons	2.97E-04	2 APP,VCAN
Cellular Movement	migration of neuroglia	2.97E-04	2 APP,VCAN
Cancer	migration of neuroglia	2.97E-04	2 L1CAM,NRG1
Cellular Movement	scattering of breast cancer cell lines	3.32E-04	27 AGTPBP1,BTBD11,CASD1,CDC42BPA,CDH2,CHGB,CPEB4,DHRS7,EPHA6,FGF14,GRIK2,HIVEP2,INSIG1,JAK1,L1CAM,NRG1,NTRK2,PCDH9,PCDHB5,PI15,PLK2,PTPRM,PVRL3,RAPGEF2,SCN3A,SLC8A3,SPRY1
Gastrointestinal Disease	colon cancer	3.32E-04	27 AGTPBP1,BTBD11,CASD1,CDC42BPA,CDH2,CHGB,CPEB4,DHRS7,EPHA6,FGF14,GRIK2,HIVEP2,INSIG1,JAK1,L1CAM,NRG1,NTRK2,PCDHB5,PI15,PLK2,PTPRM,PVRL3,RAPGEF2,SCN3A,SLC8A3,SPRY1
Cell Death and Survival	cell death of granule cells	3.95E-04	2 BCL2,PSEN1
Cell Morphology	collapse of growth cone	3.95E-04	2 L1CAM,SEMA6D
Cellular Compromise	collapse of growth cone	3.95E-04	2 L1CAM,SEMA6D
Cellular Assembly and Organization	morphology of filaments	3.95E-04	2 APP,PSEN1
Cell Morphology	morphology of filaments	3.95E-04	2 APP,PSEN1
Cellular Compromise	permeability transition of mitochondria	3.95E-04	2 APP,BCL2
Cancer	head and neck cancer	4.19E-04	11 ANGPT2,BCL2,DPT,IDS,INSIG1,KCNMB4,LGR5,NTRK2,RAPGEF2,SPRY1,TSPAN8
Cell Death and Survival	cell viability of neuroblastoma cell lines	4.38E-04	3 APP,BCL2,NTRK2
Nervous System Development and Function	cell viability of neurons	4.38E-04	3 APP,BCL2,NRG1
Cell Death and Survival	cell viability of neurons	4.38E-04	3 APP,BCL2,NRG1
Neurological Disease	seizures	5.01E-04	6 CHGB,GABRA3,NRG1,PLK2,PSEN1,SCN3A
Small Molecule Biochemistry	production of lactic acid	5.06E-04	2 BCL2,ESRRG
Cell Cycle	re-entry into cell cycle progression	5.06E-04	2 BCL2,NRG1
Cell Death and Survival	fragmentation of DNA	6.65E-04	4 APP,BCL2,NRG1,TNFRSF19
DNA Replication, Recombination, and Repair	fragmentation of DNA	6.65E-04	4 APP,BCL2,NRG1,TNFRSF19
Cell Cycle	cell cycle progression of lymphoblastoid cell lines	7.70E-04	2 BCL2,PSEN1
Cellular Assembly and Organization	formation of cytoplasmic aggregates	7.70E-04	2 APP,PSEN1
Nervous System Development and Function	growth of axons	7.70E-04	2 BCL2,NRG1
Cellular Assembly and Organization	growth of axons	7.70E-04	2 BCL2,NRG1
Tissue Development	growth of axons	7.70E-04	2 BCL2,NRG1
Neurological Disease	cerebral amyloid angiopathy	9.21E-04	2 APP,PSEN1
Psychological Disorders	cerebral amyloid angiopathy	9.21E-04	2 APP,PSEN1
Metabolic Disease	cerebral amyloid angiopathy	9.21E-04	2 APP,PSEN1
Cardiovascular Disease	cerebral amyloid angiopathy	9.21E-04	2 APP,PSEN1
Cell Death and Survival	cell viability of tumor cell lines	1.04E-03	10 ANGPT2,APP,BCL2,CDC42BPA,CDH2,JAK1,NRG1,NTRK2,PLK2,PTPRM
Cellular Function and Maintenance	autophagy of tumor cell lines	1.17E-03	4 APP,BCL2,HIVEP2,MAP1LC3B
Cell Morphology	autophagy of tumor cell lines	1.17E-03	4 APP,BCL2,HIVEP2,MAP1LC3B

Category	Function / Disease	p-value	#	Molecules
Cell Death and Survival	neuronal cell death	1.32E-03	4	APP,BCL2,NRG1,PSEN1
Nervous System Development and Function	differentiation of neurons	1.40E-03	3	APP,BCL2,PSEN1
Cellular Development	differentiation of neurons	1.40E-03	3	APP,BCL2,PSEN1
Small Molecule Biochemistry	metabolism of hydrogen peroxide	1.40E-03	3	ANGPT2,APP,BCL2
Free Radical Scavenging	metabolism of hydrogen peroxide	1.40E-03	3	ANGPT2,APP,BCL2
Cell Death and Survival	cell death of retinal cells	1.45E-03	2	APP,BCL2
Cell Death and Survival	degeneration of neurons	1.45E-03	2	APP,PSEN1
Cellular Compromise	degeneration of neurons	1.45E-03	2	APP,PSEN1
Small Molecule Biochemistry	degradation of hydrogen peroxide	1.45E-03	2	APP,BCL2
Free Radical Scavenging	degradation of hydrogen peroxide	1.45E-03	2	APP,BCL2
Cancer	colon carcinoma	1.53E-03	24	AGTPBP1,BTBD11,CASD1,CDC42BPA,CDH2,CHGB,DHRS7,EPHA6,FGF14,GRIK2,HIVEP2,INSIG1,JAK1,L1CAM,NTRK2,PCDH9,PCDHB5,PI15,PLK2,PTPRM,RAPGEF2,SCN3A,SLC8A3,SPRY1
Gastrointestinal Disease	colon carcinoma	1.53E-03	24	AGTPBP1,BTBD11,CASD1,CDC42BPA,CDH2,CHGB,DHRS7,EPHA6,FGF14,GRIK2,HIVEP2,INSIG1,JAK1,L1CAM,NTRK2,PCDH9,PCDHB5,PI15,PLK2,PTPRM,RAPGEF2,SCN3A,SLC8A3,SPRY1
Cellular Development	proliferation of neuroblastoma cell lines	1.55E-03	3	ANGPT2,BCL2,NTRK2
Cellular Growth and Proliferation	proliferation of neuroblastoma cell lines	1.55E-03	3	ANGPT2,BCL2,NTRK2
Hereditary Disorder	mucopolysaccharidoses	1.66E-03	2	HGSNAT,IDS
Metabolic Disease	mucopolysaccharidoses	1.66E-03	2	HGSNAT,IDS
Developmental Disorder	mucopolysaccharidoses	1.66E-03	2	HGSNAT,IDS
Neurological Disease	glioblastoma cancer	1.66E-03	5	ANGPT2,IDS,LGR5,RAPGEF2,TSPAN8
Cancer	glioblastoma cancer	1.66E-03	5	ANGPT2,IDS,LGR5,RAPGEF2,TSPAN8
Neurological Disease	amyotrophic lateral sclerosis	1.69E-03	5	APP,BCL2,GABRA3,SCN3A,TSPAN8
Cell Death and Survival	cell viability of cervical cancer cell lines	1.69E-03	5	BCL2,CDC42BPA,JAK1,PLK2,PTPRM
Cellular Movement	migration of melanoma cell lines	1.70E-03	3	L1CAM,NRG1,SDCBP
Cancer	prostate cancer	1.84E-03	9	BCL2,CDH2,ESRRG,FAM13A,JAK1,NTRK2,PCDHB10,PI15,VCAN
Organismal Injury and Abnormalities	prostate cancer	1.84E-03	9	BCL2,CDH2,ESRRG,FAM13A,JAK1,NTRK2,PCDHB10,PI15,VCAN
Reproductive System Disease	prostate cancer	1.84E-03	9	BCL2,CDH2,ESRRG,FAM13A,JAK1,NTRK2,PCDHB10,PI15,VCAN
Cellular Function and Maintenance	pH of cells	1.87E-03	2	BCL2,L1CAM
Cell Morphology	pH of cells	1.87E-03	2	BCL2,L1CAM
Cell Death and Survival	apoptosis of neurons	1.87E-03	3	APP,BCL2,PSEN1
Cell Death and Survival	cell viability	1.90E-03	11	ANGPT2,APP,BCL2,CDC42BPA,CDH2,JAK1,NRG1,NTRK2,PLK2,PSEN1,PTPRM
Cellular Development	differentiation of tumor cell lines	2.05E-03	5	APP,BCL2,NRG1,NTRK2,PSEN1
Cell Death and Survival	apoptosis of gonadal cells	2.10E-03	2	BCL2,CDH2
Cellular Function and Maintenance	autophagy of breast cancer cell lines	2.10E-03	2	BCL2,MAP1LC3B
Cell Morphology	autophagy of breast cancer cell lines	2.10E-03	2	BCL2,MAP1LC3B
Cancer	castration refractory prostate cancer process	2.10E-03	2	BCL2,NTRK2
Organismal Injury and Abnormalities	castration refractory prostate cancer process	2.10E-03	2	BCL2,NTRK2
Reproductive System Disease	castration refractory prostate cancer process	2.10E-03	2	BCL2,NTRK2
Cellular Movement	migration of stomach cancer cell lines	2.10E-03	2	CDH2,SDCBP
Nervous System Development and Function	outgrowth of neurites	2.13E-03	3	APP,BCL2,L1CAM
Cellular Assembly and Organization	outgrowth of neurites	2.13E-03	3	APP,BCL2,L1CAM
Tissue Development	outgrowth of neurites	2.13E-03	3	APP,BCL2,L1CAM
Cell Morphology	outgrowth of neurites	2.13E-03	3	APP,BCL2,L1CAM
Neurological Disease	Schizophrenia	2.33E-03	8	APP,CHGB,GABRA3,GRIK2,NRG1,NTRK2,PTPRM,RGS7
Hereditary Disorder	Schizophrenia	2.33E-03	8	APP,CHGB,GABRA3,GRIK2,NRG1,NTRK2,PTPRM,RGS7
Psychological Disorders	Schizophrenia	2.33E-03	8	APP,CHGB,GABRA3,GRIK2,NRG1,NTRK2,PTPRM,RGS7
Cardiovascular System Development and Function	vasculogenesis	2.36E-03	6	ANGPT2,APP,BCL2,CDH2,NRG1,PTPRM
Organismal Development	vasculogenesis	2.36E-03	6	ANGPT2,APP,BCL2,CDH2,NRG1,PTPRM
Cancer	colon adenocarcinoma	2.49E-03	23	AGTPBP1,BTBD11,CASD1,CDC42BPA,CDH2,CHGB,DHRS7,EPHA6,FGF14,GRIK2,HIVEP2,JAK1,L1CAM,NTRK2,PCDH9,PCDHB5,PI15,PLK2,PTPRM,RAPGEF2,SCN3A,SLC8A3,SPRY1
Gastrointestinal Disease	colon adenocarcinoma	2.49E-03	23	AGTPBP1,BTBD11,CASD1,CDC42BPA,CDH2,CHGB,DHRS7,EPHA6,FGF14,GRIK2,HIVEP2,JAK1,L1CAM,NTRK2,PCDH9,PCDHB5,PI15,PLK2,PTPRM,RAPGEF2,SCN3A,SLC8A3,SPRY1
Cancer	Cancer	2.63E-03	60	AGTPBP1,ANGPT2,APP,BA22B,BCL2,BTBD11,CASD1,CDC42BPA,CDH2,CDO1,CHGB,CPEB4,DHRS7,DPT,EPHA6,ESRRG,FAM13A,FGF14,GABRA3,GRIK2,HIVEP2,IDS,INSIG1,JAK1,KCNMB4,L1CAM,LGR5,MAP1LC3B,MRAP2,NAV2,NRG1,NTRK2,PACS1,PCDH9,PCDHB10,PCDHB14,PCDHB5,PI15,PLK2,PSEN1,PTPRM,PVRL3,RAPGEF2,RBFOX2,REEP5,RGS7,SCN3A,SDCBP,SEMA6D,SERINC3,SLC8A3,SPRY1,SPRY4,TFB1M,TMEM66,TNFRSF19,TRIB2,TSPAN8,VCAN,XPR1
Cell-To-Cell Signaling and Interaction	adhesion of vascular endothelial cells	2.83E-03	3	ANGPT2,CDH2,L1CAM
Tissue Development	adhesion of vascular endothelial cells	2.83E-03	3	ANGPT2,CDH2,L1CAM
Cardiovascular System Development and Function	adhesion of vascular endothelial cells	2.83E-03	3	ANGPT2,CDH2,L1CAM
Cellular Compromise	degradation of mitochondria	2.87E-03	2	BCL2,MAP1LC3B
Cell Signaling	uptake of Ca2+	2.87E-03	2	APP,BCL2

Category	Function/Disease	p-value	Count & Molecules
Molecular Transport	uptake of Ca2+	2.87E-03	2 APP,BCL2
Vitamin and Mineral Metabolism	uptake of Ca2+	2.87E-03	2 APP,BCL2
Cellular Movement	cell movement of breast cancer cell lines	3.11E-03	5 ANGPT2,CDH2,L1CAM,NRG1,SDCBP
Cancer	adenocarcinoma	3.16E-03	39 AGTPBP1,ANGPT2,APP,BAZ2B,BTBD11,CASD1,CDC42BPA,CDH2,CHGB,DHRS7,EPHA6,ESRRG,FAM13A,FGF14,GRIK2,HIVEP2,JAK1,L1CAM,LGR5,MAP1LC3B,NAV2,NRG1,NTRK2,PACS1,PCDH9,PCDHB10,PCDHB5,PI15,PLK2,PTPRM,RAPGEF2,RBFOX2,RGS7,SCN3A,SEMA6D,SLC8A3,SPRY1,TRIB2,VCAN
Molecular Transport	secretion of molecule	3.32E-03	4 ANGPT2,APP,KCNMB4,NRG1
Cell-To-Cell Signaling and Interaction	adhesion of tumor cell lines	3.49E-03	5 CDH2,L1CAM,NRG1,PVRL3,VCAN
Tissue Development	adhesion of tumor cell lines	3.49E-03	5 CDH2,L1CAM,NRG1,PVRL3,VCAN
Cell Death and Survival	apoptosis of microvascular endothelial cells	3.74E-03	2 APP,BCL2
Cell Death and Survival	condensation of chromatin	3.74E-03	2 APP,BCL2
DNA Replication, Recombination, and Repair	condensation of chromatin	3.74E-03	2 APP,BCL2
Neurological Disease	APP-related cerebral amyloid angiopathy	3.81E-03	1 APP
Hereditary Disorder	APP-related cerebral amyloid angiopathy	3.81E-03	1 APP
Psychological Disorders	APP-related cerebral amyloid angiopathy	3.81E-03	1 APP
Metabolic Disease	APP-related cerebral amyloid angiopathy	3.81E-03	1 APP
Cardiovascular Disease	APP-related cerebral amyloid angiopathy	3.81E-03	1 APP
Developmental Disorder	Alzheimer disease with spastic paraparesis and cotton wool plaques	3.81E-03	1 PSEN1
Neurological Disease	Alzheimer disease with spastic paraparesis and cotton wool plaques	3.81E-03	1 PSEN1
Hereditary Disorder	Alzheimer disease with spastic paraparesis and cotton wool plaques	3.81E-03	1 PSEN1
Psychological Disorders	Alzheimer disease with spastic paraparesis and cotton wool plaques	3.81E-03	1 PSEN1
Metabolic Disease	Alzheimer disease with spastic paraparesis and cotton wool plaques	3.81E-03	1 PSEN1
Cancer	B-cell leukemia/lymphoma type 2	3.81E-03	1 BCL2
Hematological Disease	B-cell leukemia/lymphoma type 2	3.81E-03	1 BCL2
Immunological Disease	B-cell leukemia/lymphoma type 2	3.81E-03	1 BCL2
Neurological Disease	CRASH syndrome	3.81E-03	1 L1CAM
Hereditary Disorder	CRASH syndrome	3.81E-03	1 L1CAM
Hereditary Disorder	Wagner syndrome	3.81E-03	1 VCAN
Ophthalmic Disease	Wagner syndrome	3.81E-03	1 VCAN
Neurological Disease	X-linked hydrocephalus with congenital idiopathic intestinal pseudoobstruction	3.81E-03	1 L1CAM
Hereditary Disorder	X-linked hydrocephalus with congenital idiopathic intestinal pseudoobstruction	3.81E-03	1 L1CAM
Gastrointestinal Disease	X-linked hydrocephalus with congenital idiopathic intestinal pseudoobstruction	3.81E-03	1 L1CAM
Developmental Disease	X-linked hydrocephalus with congenital idiopathic intestinal pseudoobstruction	3.81E-03	1 L1CAM
Neurological Disease	X-linked partial agenesis of corpus callosum	3.81E-03	1 L1CAM
Hereditary Disorder	X-linked partial agenesis of corpus callosum	3.81E-03	1 L1CAM
Developmental Disorder	X-linked partial agenesis of corpus callosum	3.81E-03	1 L1CAM
Organismal Injury and Abnormalities	X-linked partial agenesis of corpus callosum	3.81E-03	1 L1CAM
Cell-To-Cell Signaling and Interaction	adhesion of fibronectin matrix	3.81E-03	1 VCAN
Cellular Assembly and Organization	adhesion of fibronectin matrix	3.81E-03	1 VCAN
Tissue Development	adhesion of fibronectin matrix	3.81E-03	1 VCAN
Tissue Development	aggregation of melanoma cells	3.81E-03	1 CDH2
Cellular Compromise	aggregation of melanoma cells	3.81E-03	1 CDH2
Tumor Morphology	aggregation of melanoma cells	3.81E-03	1 CDH2
Cell Death and Survival	anoikis of leukemia cell lines	3.81E-03	1 BCL2
Cell Death and Survival	anoikis of lymphoma cell lines	3.81E-03	1 BCL2
Cell Death and Survival	apoptosis of ASE sensory neurons	3.81E-03	1 APP
Cell Death and Survival	apoptosis of oocytes	3.81E-03	1 BCL2
Cell-To-Cell Signaling and Interaction	attraction of axons	3.81E-03	1 L1CAM
Nervous System Development and Function	attraction of axons	3.81E-03	1 L1CAM
Neurological Disease	autosomal dominant mental retardation type 17	3.81E-03	1 PACS1
Hereditary Disorder	autosomal dominant mental retardation type 17	3.81E-03	1 PACS1
Developmental Disorder	autosomal dominant mental retardation type 17	3.81E-03	1 PACS1
Neurological Disease	autosomal recessive mental retardation type 6	3.81E-03	1 GRIK2
Hereditary Disorder	autosomal recessive mental retardation type 6	3.81E-03	1 GRIK2
Developmental Disorder	autosomal recessive mental retardation type 6	3.81E-03	1 GRIK2
Gene Expression	binding of CRE-like element	3.81E-03	1 NRG1
Cell Death and Survival	cell death of HCSM cells	3.81E-03	1 APP
Cellular Movement	cell movement of colon carcinoma cells	3.81E-03	1 L1CAM
Cell Death and Survival	cell viability of insect cell lines	3.81E-03	1 BCL2
Cancer	cell viability of neuroblastoma cells	3.81E-03	1 APP
Cell Death and Survival	cell viability of neuroblastoma cells	3.81E-03	1 APP

Category	Function	p-value		Gene
Tumor Morphology	cell viability of neuroblastoma cells	3.81E-03	1	APP
Cellular Growth and Proliferation	colony formation of lymphoblasts	3.81E-03	1	BCL2
Hematological System Development and Function	colony formation of lymphoblasts	3.81E-03	1	BCL2
Hematopoiesis	colony formation of lymphoblasts	3.81E-03	1	BCL2
Cell-To-Cell Signaling and Interaction	contact repulsion of axons	3.81E-03	1	L1CAM
Nervous System Development and Function	contact repulsion of axons	3.81E-03	1	L1CAM
Cellular Movement	contact repulsion of axons	3.81E-03	1	L1CAM
Behavior	contextual conditioning	3.81E-03	1	APP
Cell Morphology	contractility of dermal fibroblasts	3.81E-03	1	VCAN
Cellular Compromise	degeneration of cytoplasmic aggregates	3.81E-03	1	BCL2
Cellular Compromise	degeneration of smooth muscle cells	3.81E-03	1	APP
Cell Cycle	delay in G2 phase of breast cancer cell lines	3.81E-03	1	NRG1
Cell Death and Survival	delay in apoptosis of cervical cancer cell lines	3.81E-03	1	BCL2
Small Molecule Biochemistry	depletion of lactosylceramide	3.81E-03	1	B4GALT6
Molecular Transport	depletion of lactosylceramide	3.81E-03	1	B4GALT6
Lipid Metabolism	depletion of lactosylceramide	3.81E-03	1	B4GALT6
Neurological Disease	deposition of amyloid fibrils	3.81E-03	1	APP
Cellular Assembly and Organization	deposition of amyloid fibrils	3.81E-03	1	APP
Tissue Development	development of pyramidal tract	3.81E-03	1	L1CAM
Organismal Development	development of wing	3.81E-03	1	APP
Embryonic Development	development of wing	3.81E-03	1	APP
Skeletal and Muscular System Development and Function	development of wing	3.81E-03	1	APP
Cardiovascular System Development and Function	diameter of capillary vessel	3.81E-03	1	ANGPT2
Tissue Morphology	diameter of capillary vessel	3.81E-03	1	ANGPT2
Hereditary Disorder	dilated cardiomyopathy type 1U	3.81E-03	1	PSEN1
Cardiovascular Disease	dilated cardiomyopathy type 1U	3.81E-03	1	PSEN1
Neurological Disease	dystrophy of cholinergic fibers	3.81E-03	1	APP
Developmental Disorder	dystrophy of cholinergic fibers	3.81E-03	1	APP
Neurological Disease	early-onset Alzheimer disease with cerebral amyloid angiopathy	3.81E-03	1	APP
Psychological Disorders	early-onset Alzheimer disease with cerebral amyloid angiopathy	3.81E-03	1	APP
Metabolic Disease	early-onset Alzheimer disease with cerebral amyloid angiopathy	3.81E-03	1	APP
Cardiovascular Disease	early-onset Alzheimer disease with cerebral amyloid angiopathy	3.81E-03	1	APP
Neurological Disease	familial Alzheimer disease with spastic paraparesis and apraxia type 3	3.81E-03	1	PSEN1
Hereditary Disorder	familial Alzheimer disease with spastic paraparesis and apraxia type 3	3.81E-03	1	PSEN1
Psychological Disorders	familial Alzheimer disease with spastic paraparesis and apraxia type 3	3.81E-03	1	PSEN1
Metabolic Disease	familial Alzheimer disease with spastic paraparesis and apraxia type 3	3.81E-03	1	PSEN1
Hereditary Disorder	familial acne inversa type 3	3.81E-03	1	PSEN1
Dermatological Diseases and Conditions	familial acne inversa type 3	3.81E-03	1	PSEN1
Infectious Disease	familial acne inversa type 3	3.81E-03	1	PSEN1
Inflammatory Disease	familial acne inversa type 3	3.81E-03	1	PSEN1
Inflammatory Response	familial acne inversa type 3	3.81E-03	1	PSEN1
Neurological Disease	familial early-onset Alzheimer disease 1	3.81E-03	1	APP
Hereditary Disorder	familial early-onset Alzheimer disease 1	3.81E-03	1	APP
Psychological Disorders	familial early-onset Alzheimer disease 1	3.81E-03	1	APP
Metabolic Disease	familial early-onset Alzheimer disease 1	3.81E-03	1	APP
Cell Morphology	fluidity of Golgi membrane	3.81E-03	1	APP
Cellular Assembly and Organization	formation of Lewy bodies	3.81E-03	1	PSEN1
Cellular Compromise	formation of Lewy bodies	3.81E-03	1	PSEN1
Nervous System Development and Function	formation of nerve fascicle	3.81E-03	1	L1CAM
Tissue Development	formation of nerve fascicle	3.81E-03	1	L1CAM
Cellular Growth and Proliferation	formation of neural precursor cells	3.81E-03	1	APP
Cellular Assembly and Organization	formation of recycling endosomes	3.81E-03	1	RAB22A
Cellular Growth and Proliferation	formation of type A spermatogonia	3.81E-03	1	NRG1
Cellular Function and Maintenance	function of brain cells	3.81E-03	1	APP
Cellular Function and Maintenance	glycolysis of leukocyte cell lines	3.81E-03	1	BCL2
Carbohydrate Metabolism	glycolysis of leukocyte cell lines	3.81E-03	1	BCL2
Organismal Development	growth of limb	3.81E-03	1	APP
Embryonic Development	growth of limb	3.81E-03	1	APP
Skeletal and Muscular System Development and Function	growth of limb	3.81E-03	1	APP
Cell-To-Cell Signaling and Interaction	induction of carcinoma cell lines	3.81E-03	1	BCL2
Cellular Growth and Proliferation	induction of carcinoma cell lines	3.81E-03	1	BCL2

Category	Description	Count	Gene	p-value
Cell-To-Cell Signaling and Interaction	induction of lung cancer cell lines	1	BCL2	3.81E-03
Cellular Growth and Proliferation	induction of lung cancer cell lines	1	BCL2	3.81E-03
Infectious Disease	infectivity of Cercospora nicotianae	1	BCL2	3.81E-03
Inflammatory Response	inflammation of central nervous system	1	APP	3.81E-03
Cell Death and Survival	killing of hippocampal neurons	1	APP	3.81E-03
Molecular Transport	leakage of K+	1	BCL2	3.81E-03
Cellular Assembly and Organization	leakage of intracellular stores	1	BCL2	3.81E-03
Cell Death and Survival	leakage of intracellular stores	1	BCL2	3.81E-03
Cellular Compromise	lysis of mitochondria	1	BCL2	3.81E-03
Nervous System Development and Function	memory consolidation	1	APP	3.81E-03
Behavior	memory consolidation	1	APP	3.81E-03
Cardiovascular System Development and Function	morphology of capillary vessel	1	APP	3.81E-03
Organismal Development	morphology of capillary vessel	1	APP	3.81E-03
Tissue Morphology	morphology of capillary vessel	1	APP	3.81E-03
Hereditary Disorder	mucopolysaccharidosis, mps-iii-c	1	HGSNAT	3.81E-03
Metabolic Disease	mucopolysaccharidosis, mps-iii-c	1	HGSNAT	3.81E-03
Developmental Disorder	mucopolysaccharidosis, mps-iii-c	1	HGSNAT	3.81E-03
Hereditary Disorder	mucopolysaccharidosis, type II	1	IDS	3.81E-03
Metabolic Disease	mucopolysaccharidosis, type II	1	IDS	3.81E-03
Developmental Disorder	mucopolysaccharidosis, type II	1	IDS	3.81E-03
Neurological Disease	neuritic dystrophy of cerebral cortex cells	1	APP	3.81E-03
Inflammatory Disease	neuritic dystrophy of cerebral cortex cells	1	APP	3.81E-03
Neurological Disease	neuritic dystrophy of neurons	1	APP	3.81E-03
Inflammatory Disease	neuritic dystrophy of neurons	1	APP	3.81E-03
Psychological Disorders	obesity, hyperphagia, and developmental delay	1	NTRK2	3.81E-03
Developmental Disorder	obesity, hyperphagia, and developmental delay	1	NTRK2	3.81E-03
Nutritional Disease	obesity, hyperphagia, and developmental delay	1	NTRK2	3.81E-03
Cardiovascular Disease	occlusion of capillary vessel	1	APP	3.81E-03
Small Molecule Biochemistry	oxidation of cholesterol	1	APP	3.81E-03
Energy Production	oxidation of cholesterol	1	APP	3.81E-03
Lipid Metabolism	oxidation of cholesterol	1	APP	3.81E-03
Nervous System Development and Function	pH of neurons	1	L1CAM	3.81E-03
Cellular Function and Maintenance	pH of neurons	1	L1CAM	3.81E-03
Cell Morphology	pH of neurons	1	L1CAM	3.81E-03
Cellular Assembly and Organization	permeability of mitochondrial outer membrane	1	BCL2	3.81E-03
Cellular Function and Maintenance	permeability of mitochondrial outer membrane	1	BCL2	3.81E-03
Cell Morphology	permeability of mitochondrial outer membrane	1	BCL2	3.81E-03
Neurological Disease	progressive neurologic decline	1	APP	3.81E-03
Small Molecule Biochemistry	quantity of NADPH	1	BCL2	3.81E-03
Molecular Transport	quantity of NADPH	1	BCL2	3.81E-03
Nucleic Acid Metabolism	quantity of NADPH	1	BCL2	3.81E-03
Cardiovascular Disease	regression of blood vessel	1	ANGPT2	3.81E-03
Tissue Morphology	regression of blood vessel	1	ANGPT2	3.81E-03
Cell Morphology	regulatory volume decrease of kidney cell lines	1	BCL2	3.81E-03
Renal and Urological System Development and Function	regulatory volume decrease of kidney cell lines	1	BCL2	3.81E-03
Tissue Morphology	remodeling of basal lamina	1	ANGPT2	3.81E-03
Neurological Disease	spinocerebellar ataxia 27	1	FGF14	3.81E-03
Hereditary Disorder	spinocerebellar ataxia 27	1	FGF14	3.81E-03
Small Molecule Biochemistry	synthesis of docosahexaenoic acid	1	APP	3.81E-03
Lipid Metabolism	synthesis of docosahexaenoic acid	1	APP	3.81E-03
Small Molecule Biochemistry	synthesis of taurine	1	CDO1	3.81E-03
Amino Acid Metabolism	synthesis of taurine	1	CDO1	3.81E-03
Cancer	transformation of melanoma cell lines	1	SDCBP	3.81E-03
Small Molecule Biochemistry	turnover of phosphatidylinositol 4,5-diphosphate	1	PSEN1	3.81E-03
Carbohydrate Metabolism	turnover of phosphatidylinositol 4,5-diphosphate	1	PSEN1	3.81E-03
Lipid Metabolism	turnover of phosphatidylinositol 4,5-diphosphate	1	PSEN1	3.81E-03
Post-Translational Modification	tyrosine nitration of protein	1	APP	3.81E-03
Cellular Function and Maintenance	uptake of bone marrow cells	1	APP	3.81E-03
Cardiovascular System Development and Function	vasodilation of vascular tissue	1	APP	3.81E-03
Organismal Development	vasodilation of vascular tissue	1	APP	3.81E-03
Tissue Morphology	vasodilation of vascular tissue	1	APP	3.81E-03

Category	Diseases or Functions Annotation	p-Value	#	Molecules
Psychological Disorders	Mood Disorders	4.04E-03	7	APP,BCL2,GABRA3,GRIK2,NRG1,PSEN1,SCN3A
Cell Death and Survival	cell viability of hepatoma cell lines	4.06E-03	2	BCL2,CDH2
Cancer	esophagus tumor	4.20E-03	5	BCL2,NRG1,PCDH9,RGS7,SEMA6D
Gastrointestinal Disease	esophagus tumor	4.20E-03	5	BCL2,NRG1,PCDH9,RGS7,SEMA6D
Neurological Disease	frontotemporal dementia	4.38E-03	2	APP,PSEN1
Psychological Disorders	frontotemporal dementia	4.38E-03	2	APP,PSEN1
Cellular Movement	homing of embryonic cell lines	4.38E-03	2	APP,L1CAM
Embryonic Development	homing of embryonic cell lines	4.38E-03	2	APP,L1CAM
Cellular Movement	homing of epithelial cell lines	4.38E-03	2	APP,L1CAM
Hair and Skin Development and Function	homing of epithelial cell lines	4.38E-03	2	APP,L1CAM
Cancer	oral squamous cell carcinoma	4.74E-03	4	BCL2,DPT,KCNMB4,SPRY1
Gastrointestinal Disease	oral squamous cell carcinoma	4.74E-03	4	BCL2,DPT,KCNMB4,SPRY1
Cell Death and Survival	apoptosis of neuroblastoma cell lines	4.75E-03	3	APP,BCL2,XPR1
Cell Cycle	G1 phase	4.87E-03	5	BCL2,ESRRG,NRG1,PLK2,PSEN1
Cellular Development	differentiation of neuroblastoma cell lines	5.07E-03	2	APP,NTRK2
Small Molecule Biochemistry	synthesis of ceramide	5.07E-03	2	APP,BCL2
Lipid Metabolism	synthesis of ceramide	5.07E-03	2	APP,BCL2
Cancer	transformation of tumor cell lines	5.07E-03	2	NRG1,SDCBP
Cancer	prostatic intraepithelial neoplasia	5.37E-03	3	BCL2,ESRRG,VCAN
Organismal Injury and Abnormalities	prostatic intraepithelial neoplasia	5.37E-03	3	BCL2,ESRRG,VCAN
Reproductive System Disease	prostatic intraepithelial neoplasia	5.37E-03	3	BCL2,ESRRG,VCAN
Cellular Movement	homing of kidney cell lines	5.43E-03	2	APP,L1CAM
Renal and Urological System Development and Function	homing of kidney cell lines	5.43E-03	2	APP,L1CAM
Neurological Disease	multiple system atrophy	5.43E-03	2	APP,SCN3A
Cancer	prostatic carcinoma	5.62E-03	5	BCL2,ESRRG,FAM13A,JAK1,PCDHB10
Organismal Injury and Abnormalities	prostatic carcinoma	5.62E-03	5	BCL2,ESRRG,FAM13A,JAK1,PCDHB10
Reproductive System Disease	prostatic carcinoma	5.62E-03	5	BCL2,ESRRG,FAM13A,JAK1,PCDHB10
Free Radical Scavenging	generation of reactive oxygen species	5.70E-03	3	APP,BCL2,PSEN1
Cancer	genital tumor	5.79E-03	11	ANGPT2,BCL2,CDH2,ESRRG,FAM13A,JAK1,LGR5,NTRK2,PCDHB10,PI15,VCAN
Organismal Injury and Abnormalities	genital tumor	5.79E-03	11	ANGPT2,BCL2,CDH2,ESRRG,FAM13A,JAK1,LGR5,NTRK2,PCDHB10,PI15,VCAN
Reproductive System Disease	genital tumor	5.79E-03	11	ANGPT2,BCL2,CDH2,ESRRG,FAM13A,JAK1,LGR5,NTRK2,PCDHB10,PI15,VCAN
Cellular Movement	invasion of cells	5.92E-03	8	ANGPT2,APP,BCL2,CDH2,L1CAM,NRG1,SDCBP,VCAN
Cellular Movement	migration of fibrosarcoma cell lines	6.59E-03	2	APP,CDH2
Small Molecule Biochemistry	production of hydrogen peroxide	6.59E-03	2	ANGPT2,APP
Free Radical Scavenging	production of hydrogen peroxide	6.59E-03	2	ANGPT2,APP
Cell Death and Survival	apoptosis of brain cancer cell lines	6.94E-03	3	APP,BCL2,PSEN1
Neurological Disease	progressive motor neuropathy	6.97E-03	7	APP,BCL2,GABRA3,NRG1,NTRK2,SCN3A,TSPAN8
Neurological Disease	mental retardation	7.37E-03	4	GRIK2,PACS1,PAK3,SCN3A
Developmental Disorder	mental retardation	7.37E-03	4	GRIK2,PACS1,PAK3,SCN3A
Cancer	carcinoma in breast	7.41E-03	9	AGTPBP1,BCL2,CDC42BPA,CDH2,CHGB,ESRRG,GRIK2,MAP1LC3B,PCDHB10
Organismal Injury and Abnormalities	carcinoma in breast	7.41E-03	9	AGTPBP1,BCL2,CDC42BPA,CDH2,CHGB,ESRRG,GRIK2,MAP1LC3B,PCDHB10
Reproductive System Disease	carcinoma in breast	7.41E-03	9	AGTPBP1,BCL2,CDC42BPA,CDH2,CHGB,ESRRG,GRIK2,MAP1LC3B,PCDHB10
Neurological Disease	mild cognitive impairment	7.42E-03	2	APP,BCL2
Cancer	AIDS-related lymphoma	7.61E-03	1	BCL2
Hematological Disease	AIDS-related lymphoma	7.61E-03	1	BCL2
Immunological Disease	AIDS-related lymphoma	7.61E-03	1	BCL2
Neurological Disease	Alzheimer's disease type 4	7.61E-03	1	PSEN1
Hereditary Disorder	Alzheimer's disease type 4	7.61E-03	1	PSEN1
Psychological Disorders	Alzheimer's disease type 4	7.61E-03	1	PSEN1
Metabolic Disease	apoptosis of glioblastoma cells	7.61E-03	1	PSEN1
Tumor Morphology	apoptosis of glioblastoma cells	7.61E-03	1	BCL2
Cell Death and Survival	apoptosis of nucleus	7.61E-03	1	BCL2
Cellular Compromise	apoptosis of nucleus	7.61E-03	1	BCL2
Cell Death and Survival	apoptosis of testicular cancer cell lines	7.61E-03	1	BCL2
Cell Death and Survival	apoptosis of ventricular myocytes	7.61E-03	1	NRG1
Cell Cycle	arrest in G1/S phase transition of prostate cancer cell lines	7.61E-03	1	ESRRG
Cell Cycle	arrest in G2/M phase transition of ovarian cancer cell lines	7.61E-03	1	NRG1
Cell Cycle	arrest in M phase of lymphoma cell lines	7.61E-03	1	BCL2
Cell Cycle	arrest in S phase of lymphoma cell lines	7.61E-03	1	BCL2
Small Molecule Biochemistry	beta-oxidation of palmitic acid	7.61E-03	1	BCL2

Category	Function	p-value	#	Gene(s)
Energy Production	beta-oxidation of palmitic acid	7.61E-03	1	BCL2
Lipid Metabolism	beta-oxidation of palmitic acid	7.61E-03	1	BCL2
Cardiovascular Disease	capillary leak syndrome	7.61E-03	1	ANGPT2
Cell Death and Survival	cell death of pre-oligodendrocytes	7.61E-03	1	BCL2
Cancer	cell viability of lung cancer cells	7.61E-03	1	BCL2
Cell Death and Survival	cell viability of lung cancer cells	7.61E-03	1	BCL2
Tumor Morphology	cell viability of lung cancer cells	7.61E-03	1	BCL2
Nervous System Development and Function	development of corpus callosum	7.61E-03	1	L1CAM
Tissue Development	development of corpus callosum	7.61E-03	1	L1CAM
Organismal Development	development of corpus callosum	7.61E-03	1	L1CAM
Embryonic Development	development of corpus callosum	7.61E-03	1	L1CAM
Organ Development	development of corpus callosum	7.61E-03	1	L1CAM
Nervous System Development and Function	development of neural crest cells	7.61E-03	1	NRG1
Tissue Development	development of neural crest cells	7.61E-03	1	NRG1
Cellular Development	development of neural crest cells	7.61E-03	1	NRG1
Organismal Development	development of neural crest cells	7.61E-03	1	NRG1
Embryonic Development	development of neural crest cells	7.61E-03	1	NRG1
Tissue Development	elastogenesis of fibroblasts	7.61E-03	1	VCAN
Cellular Development	elastogenesis of fibroblasts	7.61E-03	1	VCAN
Connective Tissue Development and Function	elastogenesis of fibroblasts	7.61E-03	1	VCAN
Cell Cycle	entry into mitosis of breast cancer cell lines	7.61E-03	1	NRG1
Cell Morphology	fluidity of plasma membrane	7.61E-03	1	APP
Cell-To-Cell Signaling and Interaction	formation of cell-associated matrix	7.61E-03	1	VCAN
Cellular Assembly and Organization	formation of cell-associated matrix	7.61E-03	1	VCAN
Cellular Function and Maintenance	formation of cell-associated matrix	7.61E-03	1	VCAN
Tissue Development	formation of cell-associated matrix	7.61E-03	1	VCAN
Cellular Assembly and Organization	generation of amyloid-beta plaques	7.61E-03	1	APP
Cellular Assembly and Organization	generation of tau filament	7.61E-03	1	APP
Hereditary Disorder	gray platelet syndrome	7.61E-03	1	APP
Hematological Disease	gray platelet syndrome	7.61E-03	1	APP
Infectious Disease	infectivity of Sclerotinia sclerotiorum	7.61E-03	1	BCL2
Neurological Disease	learning deficit	7.61E-03	1	APP
Developmental Disorder	learning deficit	7.61E-03	1	APP
Cancer	metastasis of epithelial cell lines	7.61E-03	1	NTRK2
Cellular Assembly and Organization	morphology of fibrils	7.61E-03	1	PSEN1
Cell Morphology	morphology of fibrils	7.61E-03	1	PSEN1
Nervous System Development and Function	morphology of neurites	7.61E-03	1	APP
Cell Morphology	morphology of neurites	7.61E-03	1	APP
Tissue Morphology	morphology of neurites	7.61E-03	1	APP
Cancer	non-functioning adrenocortical adenoma	7.61E-03	1	BCL2
Cellular Assembly and Organization	outgrowth of filopodia	7.61E-03	1	NRG1
Cell Morphology	outgrowth of filopodia	7.61E-03	1	NRG1
Organismal Injury and Abnormalities	post essential thrombocythemia myelofibrosis	7.61E-03	1	JAK1
Hematological Disease	post essential thrombocythemia myelofibrosis	7.61E-03	1	JAK1
Cellular Assembly and Organization	quantity of amyloid fibrils	7.61E-03	1	APP
Cellular Assembly and Organization	quantity of autophagosomes	7.61E-03	1	MAP1LC3B
Nervous System Development and Function	quantity of neuronal progenitor cells	7.61E-03	1	ANGPT2
Tissue Morphology	quantity of neuronal progenitor cells	7.61E-03	1	ANGPT2
Cellular Assembly and Organization	removal of mitochondria	7.61E-03	1	BCL2
Cell-To-Cell Signaling and Interaction	response of fibrosarcoma cell lines	7.61E-03	1	JAK1
Behavior	spatial learning	7.61E-03	1	APP
Cell Death and Survival	survival of cd56+ natural killer cells	7.61E-03	1	BCL2
Hematological System Development and Function	survival of cd56+ natural killer cells	7.61E-03	1	BCL2
Small Molecule Biochemistry	synthesis of sulfur amino acid	7.61E-03	1	CDO1
Amino Acid Metabolism	synthesis of sulfur amino acid	7.61E-03	1	CDO1
Cellular Function and Maintenance	transmembrane potential of liposome	7.61E-03	1	BCL2
Cell Morphology	transmembrane potential of liposome	7.61E-03	1	BCL2
Infectious Disease	replication of Influenza A virus	7.73E-03	5	BCL2,CDC42BPA,JAK1,NTRK2,PAK3
Cellular Development	proliferation of melanoma cell lines	7.91E-03	3	JAK1,NRG1,VCAN
Cellular Growth and Proliferation	proliferation of melanoma cell lines	7.91E-03	3	JAK1,NRG1,VCAN
Cell Cycle	G1 phase of tumor cell lines	8.02E-03	4	BCL2,ESRRG,NRG1,PSEN1

Category	Function	p-value	Count	Genes
Gastrointestinal Disease	cholelithiasis	8.29E-03	2	APP,BAZ2B
Hepatic System Disease	cholelithiasis	8.29E-03	2	APP,BAZ2B
Infectious Disease	Bacterial Infection	8.57E-03	4	APP,GABRA3,NRG1,PSEN1
Cell Death and Survival	cell viability of myeloid cells	8.74E-03	2	APP,BCL2
Hematological System Development and Function	cell viability of myeloid cells	8.74E-03	2	APP,BCL2
Cell Death and Survival	cell death of endothelial cells	8.75E-03	3	ANGPT2,APP,BCL2
Cellular Development	proliferation of ovarian cancer cell lines	8.75E-03	3	APP,BCL2,NRG1
Cellular Growth and Proliferation	proliferation of ovarian cancer cell lines	8.75E-03	3	APP,BCL2,NRG1
Neurological Disease	astrocytoma	8.82E-03	6	ANGPT2,JD5,LGR5,PI15,RAPGEF2,TSPAN8
Cancer	astrocytoma	8.82E-03	6	ANGPT2,JD5,LGR5,PI15,RAPGEF2,TSPAN8
Carbohydrate Metabolism	glycolysis of cells	9.68E-03	2	BCL2,ESRRG
Cancer	cell viability of cancer cells	1.02E-02	2	APP,BCL2
Cell Death and Survival	cell viability of cancer cells	1.02E-02	2	APP,BCL2
Tumor Morphology	cell viability of cancer cells	1.02E-02	2	APP,BCL2
Cellular Movement	migration of breast cancer cell lines	1.02E-02	4	ANGPT2,CDH2,NRG1,SDCBP
Cellular Movement	invasion of tumor cell lines	1.06E-02	7	APP,BCL2,CDH2,L1CAM,NRG1,SDCBP,VCAN
Cell Cycle	arrest in G2/M phase transition	1.07E-02	2	BCL2,NRG1
Neurological Disease	complex partial seizure	1.07E-02	2	GABRA3,SCN3A
Cell Death and Survival	cell death of breast cancer cell lines	1.10E-02	5	ANGPT2,BCL2,NRG1,PLK2,PSEN1
Cancer	cell transformation	1.11E-02	3	L1CAM,NRG1,SDCBP
Cellular Movement	cell movement of ovarian cancer cell lines	1.12E-02	2	CDH2,NRG1
Neurological Disease	Creutzfeldt-Jakob disease	1.14E-02	1	APP
Psychological Disorders	Creutzfeldt-Jakob disease	1.14E-02	1	APP
Skeletal and Muscular Disorders	Creutzfeldt-Jakob disease	1.14E-02	1	APP
Infectious Disease	Creutzfeldt-Jakob disease	1.14E-02	1	APP
Cell-To-Cell Signaling and Interaction	adhesion of lymphoblastoid cell lines	1.14E-02	1	NRG1
Tissue Development	adhesion of lymphoblastoid cell lines	1.14E-02	1	NRG1
Cellular Development	angiogenesis of lung cell lines	1.14E-02	1	NRG1
Cardiovascular System Development and Function	angiogenesis of lung cell lines	1.14E-02	1	NRG1
Organismal Development	angiogenesis of lung cell lines	1.14E-02	1	NRG1
Respiratory System Development and Function	angiogenesis of lung cell lines	1.14E-02	1	NRG1
Cell Cycle	antiproliferative response of breast cancer cell lines	1.14E-02	1	NRG1
Cellular Growth and Proliferation	antiproliferative response of breast cancer cell lines	1.14E-02	1	NRG1
Cell Death and Survival	apoptosis of hippocampal neurons	1.14E-02	1	APP
Cell Death and Survival	apoptosis of photoreceptors	1.14E-02	1	BCL2
Neurological Disease	behavioral deficit	1.14E-02	1	APP
Psychological Disorders	behavioral deficit	1.14E-02	1	APP
Developmental Disorder	behavioral deficit	1.14E-02	1	APP
Gene Expression	binding of progesterone response element	1.14E-02	1	NRG1
Cell Death and Survival	cell death of skeletal muscle cells	1.14E-02	1	APP
Cell Signaling	clearance of Ca2+	1.14E-02	1	PSEN1
Vitamin and Mineral Metabolism	clearance of Ca2+	1.14E-02	1	PSEN1
Cell Death and Survival	delay in apoptosis of lymphoma cell lines	1.14E-02	1	BCL2
Cardiovascular System Development and Function	development of vein	1.14E-02	1	APP
Organismal Development	development of vein	1.14E-02	1	APP
Cell Morphology	frequency of micronuclei	1.14E-02	1	BCL2
Cellular Movement	haptotaxis of embryonic cell lines	1.14E-02	1	L1CAM
Embryonic Development	haptotaxis of embryonic cell lines	1.14E-02	1	L1CAM
Cellular Movement	haptotaxis of epithelial cell lines	1.14E-02	1	L1CAM
Hair and Skin Development and Function	haptotaxis of epithelial cell lines	1.14E-02	1	L1CAM
Cellular Movement	haptotaxis of kidney cell lines	1.14E-02	1	L1CAM
Renal and Urological System Development and Function	haptotaxis of kidney cell lines	1.14E-02	1	L1CAM
Cell Death and Survival	killing of macrophages	1.14E-02	1	APP
Small Molecule Biochemistry	metabolism of L-cysteine	1.14E-02	1	CDO1
Amino Acid Metabolism	metabolism of L-cysteine	1.14E-02	1	CDO1
Nervous System Development and Function	migration of astrocytes	1.14E-02	1	APP
Cellular Movement	migration of astrocytes	1.14E-02	1	APP
Cellular Movement	mobility of lung cancer cell lines	1.14E-02	1	NRG1
Neurological Disease	neurodegeneration of photoreceptors	1.14E-02	1	APP
Cellular Compromise	neurodegeneration of photoreceptors	1.14E-02	1	APP
Ophthalmic Disease	neurodegeneration of photoreceptors	1.14E-02	1	APP

Category	Function	p-value	Count	Molecules
Cardiovascular System Development and Function	quantity of microvascular endothelial cells	1.14E-02	1	BCL2
Tissue Morphology	quantity of microvascular endothelial cells	1.14E-02	1	BCL2
Cell Cycle	re-entry into cell cycle progression of fibroblasts	1.14E-02	1	BCL2
Connective Tissue Development and Function	re-entry into cell cycle progression of fibroblasts	1.14E-02	1	BCL2
Small Molecule Biochemistry	reduction of Cu2+	1.14E-02	1	APP
Small Molecule Biochemistry	reduction of hydrogen peroxide	1.14E-02	1	APP
Free Radical Scavenging	reduction of hydrogen peroxide	1.14E-02	1	APP
Cell-To-Cell Signaling and Interaction	response of neuroblastoma cell lines	1.14E-02	1	BCL2
Cell-To-Cell Signaling and Interaction	sensitization of tumor cells	1.14E-02	1	BCL2
Cancer	sensitization of tumor cells	1.14E-02	1	BCL2
Tumor Morphology	sensitization of tumor cells	1.14E-02	1	BCL2
Cell Signaling	sequestration of Ca2+	1.14E-02	1	BCL2
Molecular Transport	sequestration of Ca2+	1.14E-02	1	BCL2
Vitamin and Mineral Metabolism	sequestration of Ca2+	1.14E-02	1	BCL2
Cellular Development	sprouting of microvascular endothelial cells	1.14E-02	1	BCL2
Cell Morphology	sprouting of microvascular endothelial cells	1.14E-02	1	BCL2
Cardiovascular System Development and Function	sprouting of microvascular endothelial cells	1.14E-02	1	BCL2
Organismal Development	sprouting of microvascular endothelial cells	1.14E-02	1	BCL2
Nervous System Development and Function	survival of microglia	1.14E-02	1	APP
Cell Death and Survival	survival of microglia	1.14E-02	1	APP
Hematological System Development and Function	survival of microglia	1.14E-02	1	APP
Nervous System Development and Function	survival of retinal ganglion cells	1.14E-02	1	BCL2
Cell Death and Survival	survival of retinal ganglion cells	1.14E-02	1	BCL2
Neurological Disease	tauopathy	1.20E-02	7	APP,BCL2,GABRA3,NTRK2,PAK3,PSEN1,SCN3A
Psychological Disorders	tauopathy	1.20E-02	7	APP,BCL2,GABRA3,NTRK2,PAK3,PSEN1,SCN3A
Behavior	behavior	1.23E-02	3	APP,BCL2,PSEN1
Cell Cycle	G1/S phase transition	1.29E-02	3	ESRRG,NRG1,PLK2
Cancer	hepatocellular carcinoma	1.32E-02	5	CASD1,JAK1,NTRK2,PSEN1,TSPAN8
Gastrointestinal Disease	hepatocellular carcinoma	1.32E-02	5	CASD1,JAK1,NTRK2,PSEN1,TSPAN8
Hepatic System Disease	hepatocellular carcinoma	1.32E-02	5	CASD1,JAK1,NTRK2,PSEN1,TSPAN8
Cell Death and Survival	cell viability of brain cancer cell lines	1.33E-02	2	NTRK2,PTPRM
Cancer	pelvic cancer	1.36E-02	26	AGTPBP1,ANGPT2,APP,BAZ2B,BCL2,BTBD11,CDH2,DPT,EPHA6,ESRRG,FAM13A,JAK1,L1CAM,LGR5,NAV2,NTRK2,PCDH9,PCDHB10,PCDHB5,PI15,PTPRM,RAPGEF2,RBFOX2,SEMA6D,TRIB2,VCAN
Gastrointestinal Disease	diabetic nephropathy	1.37E-02	3	DPYSL3,GRIK2,PTPRM
Metabolic Disease	diabetic nephropathy	1.37E-02	3	DPYSL3,GRIK2,PTPRM
Organismal Injury and Abnormalities	diabetic nephropathy	1.37E-02	3	DPYSL3,GRIK2,PTPRM
Endocrine System Disorders	diabetic nephropathy	1.37E-02	3	DPYSL3,GRIK2,PTPRM
Renal and Urological Disease	diabetic nephropathy	1.37E-02	3	DPYSL3,GRIK2,PTPRM
Cellular Function and Maintenance	autophagy of brain cancer cell lines	1.38E-02	2	APP,HIVEP2
Cell Morphology	autophagy of brain cancer cell lines	1.38E-02	2	APP,HIVEP2
Cell Death and Survival	cell viability of embryonic cell lines	1.44E-02	2	APP,BCL2
Embryonic Development	cell viability of embryonic cell lines	1.44E-02	2	APP,BCL2
Cell Signaling	concentration of Ca2+	1.44E-02	2	APP,BCL2
Molecular Transport	concentration of Ca2+	1.44E-02	2	APP,BCL2
Vitamin and Mineral Metabolism	concentration of Ca2+	1.44E-02	2	APP,BCL2
Cancer	primary peritoneal cancer	1.44E-02	2	ANGPT2,BCL2
Cancer	breast or ovarian cancer	1.49E-02	14	AGTPBP1,ANGPT2,BCL2,CDC42BPA,CDH2,CHGB,ESRRG,GRIK2,L1CAM,LGR5,MAP1LC3B,NTRK2,PCDHB10,VCAN
Cell Death and Survival	cell viability of breast cancer cell lines	1.51E-02	3	ANGPT2,BCL2,NRG1
Cell-To-Cell Signaling and Interaction	action potential of neurons	1.52E-02	1	KCNMB4
Nervous System Development and Function	action potential of neurons	1.52E-02	1	KCNMB4
Cell-To-Cell Signaling and Interaction	activation of microglia	1.52E-02	1	APP
Nervous System Development and Function	activation of microglia	1.52E-02	1	APP
Hematological System Development and Function	activation of microglia	1.52E-02	1	APP
Cell-To-Cell Signaling and Interaction	adhesion of melanoma cells	1.52E-02	1	CDH2
Tissue Development	adhesion of melanoma cells	1.52E-02	1	CDH2
Cellular Compromise	adhesion of melanoma cells	1.52E-02	1	CDH2
Tumor Morphology	adhesion of melanoma cells	1.52E-02	1	CDH2
Cell-To-Cell Signaling and Interaction	adhesion of stomach cancer cell lines	1.52E-02	1	PVRL3
Tissue Development	adhesion of stomach cancer cell lines	1.52E-02	1	PVRL3
Cellular Development	adipogenesis of mesenchymal stem cells	1.52E-02	1	TNFRSF19
Hematological System Development and Function	adipogenesis of mesenchymal stem cells	1.52E-02	1	TNFRSF19

Category	Annotation	p-Value	#	Molecules
Connective Tissue Development and Function	adipogenesis of mesenchymal stem cells	1.52E-02	1	TNFRSF19
Cell Death and Survival	apoptosis of bone marrow cell lines	1.52E-02	1	BCL2
Cell Death and Survival	apoptosis of embryonic cancer cell lines	1.52E-02	1	NTRK2
Cell Death and Survival	apoptosis of melanocytes	1.52E-02	1	APP
Cell Cycle	apoptosis of microvascular smooth muscle cells	1.52E-02	1	APP
Cell Cycle	arrest in G2 phase of lymphoma cell lines	1.52E-02	1	BCL2
Cell-To-Cell Signaling and Interaction	arrest in G2/M phase transition of breast cancer cell lines	1.52E-02	1	NRG1
Tissue Development	binding of extracellular matrix	1.52E-02	1	APP
Cell Death and Survival	binding of extracellular matrix	1.52E-02	1	APP
Hematological System Development and Function	cell viability of thymocytes	1.52E-02	1	BCL2
Cellular Movement	cell viability of thymocytes	1.52E-02	1	BCL2
Cell Death and Survival	invasion of neuroblastoma cell lines	1.52E-02	1	BCL2
Cell Death and Survival	necroptosis of cervical cancer cell lines	1.52E-02	1	JAK1
Cell-To-Cell Signaling and Interaction	organization of synapse	1.52E-02	1	PAK3
Cellular Assembly and Organization	organization of synapse	1.52E-02	1	PAK3
Cellular Function and Maintenance	organization of synapse	1.52E-02	1	PAK3
Tissue Development	plasticity of synapse	1.52E-02	1	GRIK2
Cell-To-Cell Signaling and Interaction	plasticity of synapse	1.52E-02	1	GRIK2
Nervous System Development and Function	plasticity of synapse	1.52E-02	1	GRIK2
Cell Morphology	proliferation of Schwann cells	1.52E-02	1	NRG1
Nervous System Development and Function	proliferation of Schwann cells	1.52E-02	1	NRG1
Cellular Development	proliferation of Schwann cells	1.52E-02	1	NRG1
Cellular Growth and Proliferation	proliferation of Schwann cells	1.52E-02	1	NRG1
Cellular Development	proliferation of embryonic stem cells	1.52E-02	1	APP
Cellular Growth and Proliferation	proliferation of embryonic stem cells	1.52E-02	1	APP
Organismal Development	proliferation of embryonic stem cells	1.52E-02	1	APP
Embryonic Development	proliferation of embryonic stem cells	1.52E-02	1	APP
Cellular Development	sprouting of capillary vessel	1.52E-02	1	ANGPT2
Cell Morphology	sprouting of capillary vessel	1.52E-02	1	ANGPT2
Cardiovascular System Development and Function	sprouting of capillary vessel	1.52E-02	1	ANGPT2
Organismal Development	sprouting of capillary vessel	1.52E-02	1	ANGPT2
Free Radical Scavenging	synthesis of reactive oxygen species	1.52E-02	1	ANGPT2
Cell Death and Survival	cell death of embryonic cell lines	1.52E-02	4	ANGPT2,APP,BCL2,PSEN1
Embryonic Development	cell death of embryonic cell lines	1.54E-02	4	APP,BCL2,PSEN1,TNFRSF19
Cell Death and Survival	cell death of embryonic cell lines	1.54E-02	4	APP,BCL2,PSEN1,TNFRSF19
Renal and Urological System Development and Function	cell viability of kidney cell lines	1.56E-02	2	APP,BCL2
Cellular Development	cell viability of kidney cell lines	1.56E-02	2	APP,BCL2
Hematological System Development and Function	differentiation of macrophages	1.56E-02	2	APP,BCL2
Hematopoiesis	differentiation of macrophages	1.56E-02	2	APP,BCL2
Hereditary Disorder	X-linked hereditary disease	1.60E-02	4	IDS,L1CAM,PAK3,SCN3A
Cell Death and Survival	cell death of epithelial cell lines	1.67E-02	4	APP,BCL2,PSEN1,TNFRSF19
Cell Death and Survival	apoptosis of muscle cells	1.68E-02	2	APP,NRG1
Cellular Movement	migration of monocytes	1.68E-02	2	APP,JAK1
Hematological System Development and Function	migration of monocytes	1.68E-02	2	APP,JAK1
Inflammatory Response	migration of monocytes	1.68E-02	2	APP,JAK1
Immune Cell Trafficking	migration of monocytes	1.68E-02	2	APP,JAK1
Nutritional Disease	obesity	1.73E-02	4	ANGPT2,GABRA3,NTRK2,SCN3A
Cancer	fallopian tube cancer	1.74E-02	2	ANGPT2,BCL2
Organismal Injury and Abnormalities	fallopian tube cancer	1.74E-02	2	ANGPT2,BCL2
Reproductive System Disease	fallopian tube cancer	1.74E-02	2	ANGPT2,BCL2
Cell Cycle	arrest in interphase of tumor cell lines	1.75E-02	4	BCL2,ESRRG,NRG1,PSEN1
Cancer	prostatic adenocarcinoma	1.76E-02	3	ESRRG,FAM13A,PCDHB10
Organismal Injury and Abnormalities	prostatic adenocarcinoma	1.76E-02	3	ESRRG,FAM13A,PCDHB10
Reproductive System Disease	prostatic adenocarcinoma	1.76E-02	3	ESRRG,FAM13A,PCDHB10
Cellular Function and Maintenance	transmembrane potential of mitochondria	1.79E-02	3	APP,BCL2,TRIB2
Cell Morphology	transmembrane potential of mitochondria	1.79E-02	3	APP,BCL2,TRIB2
Gastrointestinal Disease	diabetes mellitus	1.79E-02	7	BCL2,DPYSL3,FGF14,GABRA3,GRIK2,PTPRM,TSPAN8
Metabolic Disease	diabetes mellitus	1.79E-02	7	BCL2,DPYSL3,FGF14,GABRA3,GRIK2,PTPRM,TSPAN8
Endocrine System Disorders	diabetes mellitus	1.79E-02	7	BCL2,DPYSL3,FGF14,GABRA3,GRIK2,PTPRM,TSPAN8
Cellular Movement	cell movement of cancer cells	1.80E-02	2	L1CAM,VCAN

Category	Annotation	p-value	Count	Genes
Neurological Disease	cerebrovascular dysfunction	1.82E-02	3	APP,GABRA3,PSEN1
Cardiovascular Disease	cerebrovascular dysfunction	1.82E-02	3	APP,GABRA3,PSEN1
Cellular Movement	migration of tumor cell lines	1.82E-02	7	ANGPT2,APP,CDH2,L1CAM,NRG1,PTPRM,SDCBP
Cell-To-Cell Signaling and Interaction	adhesion of breast cancer cell lines	1.87E-02	2	CDH2,NRG1
Tissue Development	adhesion of breast cancer cell lines	1.87E-02	2	CDH2,NRG1
Skeletal and Muscular Disorders	fibromyalgia	1.87E-02	2	GABRA3,SCN3A
Organismal Injury and Abnormalities	fibromyalgia	1.87E-02	2	GABRA3,SCN3A
Nervous System Development and Function	neuritogenesis	1.87E-02	2	APP,PTPRM
Cellular Assembly and Organization	neuritogenesis	1.87E-02	2	APP,PTPRM
Cellular Function and Maintenance	neuritogenesis	1.87E-02	2	APP,PTPRM
Tissue Development	neuritogenesis	1.87E-02	2	APP,PTPRM
Cellular Development	neuritogenesis	1.87E-02	2	APP,PTPRM
Cell Morphology	neuritogenesis	1.87E-02	2	APP,PTPRM
Cell Morphology	sprouting	1.87E-02	2	ANGPT2,BCL2
Tissue Development	aggregation of breast cancer cell lines	1.89E-02	1	NRG1
Cellular Development	angiogenesis of endothelial cell lines	1.89E-02	1	NRG1
Cardiovascular System Development and Function	angiogenesis of endothelial cell lines	1.89E-02	1	NRG1
Organismal Development	angiogenesis of endothelial cell lines	1.89E-02	1	NRG1
Psychological Disorders	apathetic behavior	1.89E-02	1	BCL2
Behavior	apathetic behavior	1.89E-02	1	BCL2
Cell Death and Survival	apoptosis of acute myeloblastic leukemia cells	1.89E-02	1	BCL2
Tumor Morphology	apoptosis of acute myeloblastic leukemia cells	1.89E-02	1	BCL2
Cell Death and Survival	apoptosis of germ cell tumor cell lines	1.89E-02	1	BCL2
Cell Death and Survival	apoptosis of granule cells	1.89E-02	1	BCL2
Cell Cycle	cell cycle progression of ovarian cancer cell lines	1.89E-02	1	NRG1
Nervous System Development and Function	cell viability of hippocampal neurons	1.89E-02	1	APP
Cell Death and Survival	cell viability of hippocampal neurons	1.89E-02	1	APP
Cell Morphology	elongation of T lymphocytes	1.89E-02	1	PAK3
Neurological Disease	gliosis	1.89E-02	1	APP
Organismal Injury and Abnormalities	gliosis	1.89E-02	1	APP
Cellular Movement	mobility of carcinoma cell lines	1.89E-02	1	NRG1
Cell Morphology	permeabilization of mitochondrial outer membrane	1.89E-02	1	BCL2
Hematological System Development and Function	quantity of lymphoblasts	1.89E-02	1	BCL2
Hematopoiesis	quantity of lymphoblasts	1.89E-02	1	BCL2
Tissue Morphology	quantity of lymphoblasts	1.89E-02	1	BCL2
Cell Death and Survival	survival of erythroblasts	1.89E-02	1	BCL2
Hematological System Development and Function	survival of erythroblasts	1.89E-02	1	BCL2
Cell Death and Survival	survival of intraepithelial T lymphocytes	1.89E-02	1	BCL2
Hematological System Development and Function	survival of intraepithelial T lymphocytes	1.89E-02	1	BCL2
Cell-To-Cell Signaling and Interaction	synthesis of dopamine	1.89E-02	1	APP
Small Molecule Biochemistry	synthesis of dopamine	1.89E-02	1	APP
Drug Metabolism	synthesis of dopamine	1.89E-02	1	APP
Cellular Function and Maintenance	cellular homeostasis	1.89E-02	7	APP,BCL2,HIVEP2,L1CAM,MAP1LC3B,RAPGEF2,TRIB2
Cancer	breast cancer	1.91E-02	12	AGTPBP1,BCL2,CDC42BPA,CDH2,CHGB,ESRRG,GRIK2,L1CAM,MAP1LC3B,NTRK2,PCDHB10,VCAN
Organismal Injury and Abnormalities	breast cancer	1.91E-02	12	AGTPBP1,BCL2,CDC42BPA,CDH2,CHGB,ESRRG,GRIK2,L1CAM,MAP1LC3B,NTRK2,PCDHB10,VCAN
Reproductive System Disease	breast cancer	1.91E-02	12	AGTPBP1,BCL2,CDC42BPA,CDH2,CHGB,ESRRG,GRIK2,L1CAM,MAP1LC3B,NTRK2,PCDHB10,VCAN
Cell Death and Survival	apoptosis of lymphoma cell lines	1.92E-02	3	BCL2,JAK1,PSEN1
Cell Cycle	arrest in G1 phase of tumor cell lines	1.99E-02	3	BCL2,ESRRG,PSEN1
Neurological Disease	Parkinson's disease	2.01E-02	4	APP,BCL2,GABRA3,NRG1
Psychological Disorders	Parkinson's disease	2.01E-02	4	APP,BCL2,GABRA3,NRG1
Skeletal and Muscular Disorders	Parkinson's disease	2.01E-02	4	APP,BCL2,GABRA3,NRG1
Psychological Disorders	depressive disorder	2.13E-02	4	APP,GABRA3,NRG1,PSEN1
Cancer	triple-negative breast cancer	2.17E-02	3	BCL2,L1CAM,NTRK2
Organismal Injury and Abnormalities	triple-negative breast cancer	2.17E-02	3	BCL2,L1CAM,NTRK2
Reproductive System Disease	triple-negative breast cancer	2.17E-02	3	BCL2,L1CAM,NTRK2
Cancer	thyroid carcinoma	2.21E-02	3	ANGPT2,BCL2,NTRK2
Endocrine System Disorders	thyroid carcinoma	2.21E-02	3	ANGPT2,BCL2,NTRK2
Cell Death and Survival	cell death of kidney cell lines	2.23E-02	4	APP,BCL2,PSEN1,TNFRSF19
Neurological Disease	Pick's disease	2.27E-02	1	PSEN1
Hereditary Disorder	Pick's disease	2.27E-02	1	PSEN1
Psychological Disorders	Pick's disease	2.27E-02	1	PSEN1

Category	Function / Disease	p-value	#	Molecules
Cancer	angiogenesis of tumor	2.27E-02	1	BCL2
Cardiovascular System Development and Function	angiogenesis of tumor	2.27E-02	1	BCL2
Cell Death and Survival	apoptosis of sympathetic neuron	2.27E-02	1	BCL2
Cell Cycle	arrest in G1 phase of cervical cancer cell lines	2.27E-02	1	PSEN1
Cell Death and Survival	cell death of pericytes	2.27E-02	1	APP
Nervous System Development and Function	cell viability of cortical neurons	2.27E-02	1	APP
Cell Death and Survival	cell viability of cortical neurons	2.27E-02	1	APP
Cell Death and Survival	cytolysis of leukemia cell lines	2.27E-02	1	BCL2
Cell Cycle	delay in cell cycle progression of lymphoblastoid cell lines	2.27E-02	1	BCL2
Cell Signaling	depletion of Ca2+	2.27E-02	1	BCL2
Molecular Transport	depletion of Ca2+	2.27E-02	1	BCL2
Vitamin and Mineral Metabolism	depletion of Ca2+	2.27E-02	1	BCL2
Cellular Development	differentiation of breast cancer cell lines	2.27E-02	1	NRG1
Cellular Development	differentiation of embryonic stem cell lines	2.27E-02	1	APP
Embryonic Development	differentiation of embryonic stem cell lines	2.27E-02	1	APP
Cellular Response to Therapeutics	drug resistance of breast cancer cell lines	2.27E-02	1	BCL2
Cardiovascular Disease	intracranial arteriovenous malformation	2.27E-02	1	ANGPT2
Developmental Disorder	intracranial arteriovenous malformation	2.27E-02	1	ANGPT2
Cellular Movement	migration of mesenchymal stem cells	2.27E-02	1	NRG1
Hematopoiesis	migration of mesenchymal stem cells	2.27E-02	1	NRG1
Inflammatory Response	migration of mesenchymal stem cells	2.27E-02	1	NRG1
Immune Cell Trafficking	migration of mesenchymal stem cells	2.27E-02	1	NRG1
Cellular Development	proliferation of B lymphoblastoid cell lines	2.27E-02	1	BCL2
Cellular Growth and Proliferation	proliferation of B lymphoblastoid cell lines	2.27E-02	1	BCL2
Cancer	sphere formation of breast cancer cell lines	2.27E-02	1	NRG1
Cancer	transformation of breast cancer cell lines	2.27E-02	1	NRG1
Cellular Function and Maintenance	transmembrane potential of cells	2.27E-02	1	BCL2
Cell Morphology	transmembrane potential of cells	2.27E-02	1	BCL2
Cell Death and Survival	cell viability of epithelial cell lines	2.55E-02	2	APP,BCL2
Hair and Skin Development and Function	cell viability of epithelial cell lines	2.55E-02	2	APP,BCL2
Cellular Growth and Proliferation	colony formation of breast cancer cell lines	2.55E-02	2	BCL2,NRG1
Neurological Disease	epileptic seizure	2.59E-02	3	CHGB,GABRA3,PLK2
Cardiovascular System Development and Function	angiogenesis	2.61E-02	4	ANGPT2,BCL2,NRG1,PTPRM
Cell Death and Survival	apoptosis of B lymphoblastoid cell lines	2.64E-02	1	BCL2
Cell Cycle	arrest in G1 phase of lymphoma cell lines	2.64E-02	1	BCL2
Cell-To-Cell Signaling and Interaction	cytotoxic reaction of ovarian cancer cell lines	2.64E-02	1	BCL2
Cancer	cytotoxic reaction of ovarian cancer cell lines	2.64E-02	1	BCL2
Inflammatory Response	cytotoxic reaction of ovarian cancer cell lines	2.64E-02	1	BCL2
Cellular Development	differentiation of erythroblasts	2.64E-02	1	BCL2
Hematological System Development and Function	differentiation of erythroblasts	2.64E-02	1	BCL2
Hematopoiesis	differentiation of erythroblasts	2.64E-02	1	BCL2
Dermatological Diseases and Conditions	idiopathic thrombocytopenic purpura	2.64E-02	1	BCL2
Hematological Disease	idiopathic thrombocytopenic purpura	2.64E-02	1	BCL2
Neurological Disease	myoclonus	2.64E-02	1	PSEN1
Cellular Development	proliferation of embryonic cancer cell lines	2.64E-02	1	NTRK2
Cellular Growth and Proliferation	proliferation of embryonic cancer cell lines	2.66E-02	4	ANGPT2,BCL2,NRG1,PLK2
Cell Death and Survival	apoptosis of breast cancer cell lines	2.68E-02	10	ANGPT2,APP,BCL2,JAK1,LGR5,NRG1,NTRK2,PLK2,PSEN1,XPR1
Cell Death and Survival	apoptosis of tumor cell lines	2.70E-02	2	NRG1,SDCBP
Cellular Movement	invasion of melanoma cell lines	2.70E-02	2	APP,CDC42BPA
Cellular Assembly and Organization	reorganization of cytoskeleton	2.70E-02	2	APP,CDC42BPA
Cellular Function and Maintenance	reorganization of cytoskeleton	2.70E-02	2	APP,CDC42BPA
Cell Morphology	reorganization of cytoskeleton	2.71E-02	3	BCL2,NRG1,TRIB2
Cell Morphology	morphology of tumor cell lines	2.71E-02	8	BCL2,GABRA3,LGR5,NRG1,PCDHB5,RGS7,SCN3A,TSPAN8
Cancer	skin cancer	2.71E-02	8	BCL2,GABRA3,LGR5,NRG1,PCDHB5,RGS7,SCN3A,TSPAN8
Dermatological Diseases and Conditions	skin cancer	2.75E-02	3	BCL2,NRG1,PSEN1
Gene Expression	binding of protein binding site	2.88E-02	6	ANGPT2,BCL2,DPT,ESRRG,NTRK2,VCAN
Cancer	benign neoplasia	2.95E-02	9	ANGPT2,FGF14,JAK1,LGR5,NRG1,PTPRM,RAPGEF2,TSPAN8,XPR1
Cell-To-Cell Signaling and Interaction	communication of cells	2.99E-02	4	CHGB,GABRA3,PLK2,SCN3A
Neurological Disease	epilepsy	3.00E-02	2	APP,BCL2
Cell Death and Survival	apoptosis of epithelial cells	3.00E-02	2	APP,BCL2
Molecular Transport	depletion of glutathione	3.01E-02	1	APP

Category	Function	p-value	Molecules
Drug Metabolism	depletion of glutathione	3.01E-02	1 APP
Infectious Disease	production of Influenza A virus	3.01E-02	1 BCL2
Small Molecule Biochemistry	secretion of aldosterone	3.01E-02	1 ANGPT2
Molecular Transport	secretion of aldosterone	3.01E-02	1 ANGPT2
Lipid Metabolism	secretion of aldosterone	3.01E-02	1 ANGPT2
Endocrine System Development and Function	secretion of aldosterone	3.01E-02	1 ANGPT2
Cellular Growth and Proliferation	proliferation of cells	3.01E-02	18 ANGPT2,APP,BCL2,CDH2,DPT,ESRRG,INSIG1,JAK1,L1CAM,NRG1,NTRK2,PSEN1,PTPRM,RBFOX2,SDCBP,TNFRSF19,TRIB2,VCAN
Neurological Disease	Alzheimer's disease	3.07E-02	6 APP,BCL2,GABRA3,NTRK2,PAK3,PSEN1
Psychological Disorders	Alzheimer's disease	3.07E-02	6 APP,BCL2,GABRA3,NTRK2,PAK3,PSEN1
Metabolic Disease	Alzheimer's disease	3.07E-02	6 APP,BCL2,GABRA3,NTRK2,PAK3,PSEN1
Small Molecule Biochemistry	oxidation of lipid	3.08E-02	2 APP,BCL2
Energy Production	oxidation of lipid	3.08E-02	2 APP,BCL2
Lipid Metabolism	oxidation of lipid	3.08E-02	2 APP,BCL2
Cell Death and Survival	apoptosis of embryonic cell lines	3.14E-02	3 APP,BCL2,TNFRSF19
Embryonic Development	apoptosis of embryonic cell lines	3.14E-02	3 APP,BCL2,TNFRSF19
Organismal Injury and Abnormalities	intracranial hemorrhage	3.16E-02	2 APP,GABRA3
Cell Cycle	G1/S phase transition of tumor cell lines	3.24E-02	2 ESRRG,NRG1
Neurological Disease	cerebellar ataxia	3.24E-02	2 FGF14,SCN3A
Neurological Disease	dyssomnia	3.24E-02	2 BCL2,GABRA3
Psychological Disorders	dyssomnia	3.24E-02	2 BCL2,GABRA3
Post-Translational Modification	phosphorylation of protein	3.25E-02	5 APP,CDC42BPA,JAK1,PSEN1,SDCBP
Free Radical Scavenging	production of reactive oxygen species	3.31E-02	3 ANGPT2,APP,BCL2
Small Molecule Biochemistry	accumulation of ceramide	3.38E-02	1 BCL2
Molecular Transport	accumulation of ceramide	3.38E-02	1 BCL2
Lipid Metabolism	accumulation of ceramide	3.38E-02	1 BCL2
Cell Death and Survival	apoptosis of heart cell lines	3.38E-02	1 BCL2
Cell Death and Survival	cell death of astrocytes	3.38E-02	1 APP
Cell Death and Survival	cell death of endometrial cancer cell lines	3.38E-02	1 BCL2
Cellular Movement	migration of peripheral blood monocytes	3.38E-02	1 APP
Hematological System Development and Function	migration of peripheral blood monocytes	3.38E-02	1 APP
Inflammatory Response	migration of peripheral blood monocytes	3.38E-02	1 APP
Immune Cell Trafficking	migration of peripheral blood monocytes	3.38E-02	1 APP
Cell Cycle	mitogenesis of gonadal cell lines	3.38E-02	1 NRG1
Reproductive System Development and Function	mitogenesis of gonadal cell lines	3.38E-02	1 NRG1
Small Molecule Biochemistry	quantity of inositol phosphate	3.38E-02	1 L1CAM
Molecular Transport	quantity of inositol phosphate	3.38E-02	1 L1CAM
Carbohydrate Metabolism	quantity of inositol phosphate	3.38E-02	1 L1CAM
Cellular Assembly and Organization	retraction of plasma membrane projections	3.38E-02	1 APP
Cellular Compromise	retraction of plasma membrane projections	3.38E-02	1 APP
Cell Death and Survival	apoptosis of epithelial cell lines	3.41E-02	3 APP,BCL2,TNFRSF19
Organismal Injury and Abnormalities	endometriosis	3.41E-02	5 ANGPT2,BCL2,JAK1,NTRK2,PLK2
Reproductive System Disease	endometriosis	3.41E-02	5 ANGPT2,BCL2,JAK1,NTRK2,PLK2
Cell Death and Survival	cell viability of lung cancer cell lines	3.49E-02	2 BCL2,NTRK2
Neurological Disease	X-linked mental retardation	3.65E-02	2 PAK3,SCN3A
Hereditary Disorder	X-linked mental retardation	3.65E-02	2 PAK3,SCN3A
Developmental Disorder	X-linked mental retardation	3.65E-02	2 PAK3,SCN3A
Neurological Disease	Multiple Sclerosis	3.69E-02	3 APP,BCL2,NTRK2
Skeletal and Muscular Disorders	Multiple Sclerosis	3.69E-02	3 APP,BCL2,NTRK2
Inflammatory Disease	Multiple Sclerosis	3.69E-02	3 APP,BCL2,NTRK2
Cell Death and Survival	apoptosis	3.70E-02	13 ANGPT2,APP,BCL2,CDH2,JAK1,LGR5,NRG1,NTRK2,PLK2,PSEN1,TNFRSF19,TRIB2,XPR1
Tissue Development	proliferation of endothelial cells	3.74E-02	3 ANGPT2,CDH2,PTPRM
Cellular Development	proliferation of endothelial cells	3.74E-02	3 ANGPT2,CDH2,PTPRM
Cellular Growth and Proliferation	proliferation of endothelial cells	3.74E-02	3 ANGPT2,CDH2,PTPRM
Cardiovascular System Development and Function	proliferation of endothelial cells	3.74E-02	3 ANGPT2,CDH2,PTPRM
Organismal Development	proliferation of endothelial cells	3.74E-02	3 ANGPT2,CDH2,PTPRM
Cell Death and Survival	apoptosis of mammary tumor cells	3.75E-02	1 BCL2
Tumor Morphology	apoptosis of mammary tumor cells	3.75E-02	1 BCL2
Cellular Movement	migration of glioma cells	3.75E-02	1 VCAN
Cancer	progressive, metastatic medullary thyroid cancer	3.75E-02	1 NTRK2
Endocrine System Disorders	progressive, metastatic medullary thyroid cancer	3.75E-02	1 NTRK2
Free Radical Scavenging	quantity of hydrogen peroxide	3.75E-02	1 BCL2

Category	Function/Disease	p-value	Count	Genes
Molecular Transport	quantity of hydrogen peroxide	3.75E-02	1	BCL2
Small Molecule Biochemistry	synthesis of hyaluronic acid	3.75E-02	1	NRG1
Carbohydrate Metabolism	synthesis of hyaluronic acid	3.75E-02	1	NRG1
Drug Metabolism	synthesis of hyaluronic acid	3.75E-02	1	NRG1
Small Molecule Biochemistry	synthesis of nucleotide	3.79E-02	3	APP,MRAP2,RGS13
Nucleic Acid Metabolism	synthesis of nucleotide	3.79E-02	3	APP,MRAP2,RGS13
Infectious Disease	tuberculosis	3.82E-02	2	GABRA3,NRG1
Cell Morphology	morphology of cells	3.85E-02	5	APP,BCL2,NRG1,PSEN1,TRIB2
Cell Death and Survival	apoptosis of hematopoietic cell lines	3.99E-02	2	BCL2,TRIB2
Cell Death and Survival	apoptosis of granulosa cells	4.11E-02	1	CDH2
Cell Death and Survival	apoptosis of thymocytes	4.11E-02	1	BCL2
Cellular Development	cell survival of carcinoma cell lines	4.11E-02	1	NTRK2
Hematological System Development and Function	differentiation of peripheral blood monocytes	4.11E-02	1	APP
Hematopoiesis	differentiation of peripheral blood monocytes	4.11E-02	1	APP
Cellular Movement	differentiation of peripheral blood monocytes	4.11E-02	1	APP
Respiratory System Development and Function	migration of lung cell lines	4.11E-02	1	NRG1
Cellular Compromise	migration of lung cell lines	4.11E-02	1	NRG1
Lipid Metabolism	peroxidation of lipid	4.11E-02	1	APP
Small Molecule Biochemistry	peroxidation of lipid	4.11E-02	1	APP
Lipid Metabolism	peroxidation of lipid	4.11E-02	1	APP
Small Molecule Biochemistry	quantity of nitric oxide	4.11E-02	1	APP
Cell Signaling	quantity of nitric oxide	4.11E-02	1	APP
Cell-To-Cell Signaling and Interaction	response of tumor cell lines	4.17E-02	2	BCL2,JAK1
Cell-To-Cell Signaling and Interaction	signal transduction	4.19E-02	8	ANGPT2,FGF14,JAK1,LGR5,PTPRM,RAPGEF2,TSPAN8,XPR1
Cancer	hemangioma	4.26E-02	2	ANGPT2,NTRK2
Psychological Disorders	Eating Disorders	4.35E-02	2	GABRA3,NTRK2
Nutritional Disease	Eating Disorders	4.35E-02	2	GABRA3,NTRK2
Cell Death and Survival	cell viability of carcinoma cell lines	4.35E-02	2	BCL2,NTRK2
Cellular Movement	migration of cells	4.36E-02	9	ANGPT2,APP,CDH2,JAK1,L1CAM,NRG1,PTPRM,SDCBP,VCAN
Cell Death and Survival	cell survival of lung cancer cell lines	4.48E-02	1	NTRK2
Hematological System Development and Function	coagulation of plasma	4.48E-02	1	APP
Organismal Functions	coagulation of plasma	4.48E-02	1	APP
Cell Cycle	entry into S phase of breast cancer cell lines	4.48E-02	1	NRG1
Small Molecule Biochemistry	exposure of phosphatidylserine	4.48E-02	1	BCL2
Carbohydrate Metabolism	exposure of phosphatidylserine	4.48E-02	1	BCL2
Lipid Metabolism	exposure of phosphatidylserine	4.48E-02	1	BCL2
Metabolic Disease	hyperglycemia	4.48E-02	1	BCL2
Endocrine System Disorders	hyperglycemia	4.48E-02	1	BCL2
Cellular Movement	invasion of bladder cancer cell lines	4.48E-02	1	CDH2
Cancer	locoregional medullary thyroid carcinoma	4.48E-02	1	NTRK2
Endocrine System Disorders	locoregional medullary thyroid carcinoma	4.48E-02	1	NTRK2
Cancer	metastatic medullary thyroid carcinoma	4.48E-02	1	NTRK2
Endocrine System Disorders	metastatic medullary thyroid carcinoma	4.48E-02	1	NTRK2
Cell Cycle	mitogenesis of breast cancer cell lines	4.48E-02	1	NRG1
Endocrine System Disorders	nodular goiter	4.48E-02	1	NTRK2
Cell Death and Survival	apoptosis of kidney cell lines	4.55E-02	3	APP,BCL2,TNFRSF19
Neurological Disease	bipolar disorder	4.68E-02	4	GABRA3,GRIK2,NRG1,SCN3A
Psychological Disorders	bipolar disorder	4.68E-02	4	GABRA3,GRIK2,NRG1,SCN3A
Hereditary Disorder	autosomal dominant disease	4.70E-02	5	GABRA3,APP,FGF14,PACS1,PSEN1
Psychological Disorders	Psychosis	4.72E-02	2	GABRA3,PSEN1
Cell-To-Cell Signaling and Interaction	adhesion of brain cancer cell lines	4.84E-02	1	L1CAM
Tissue Development	adhesion of brain cancer cell lines	4.84E-02	1	L1CAM
Cell-To-Cell Signaling and Interaction	adhesion of fibroblasts	4.84E-02	1	CDH2
Tissue Development	adhesion of fibroblasts	4.84E-02	1	CDH2
Connective Tissue Development and Function	adhesion of fibroblasts	4.84E-02	1	CDH2
Cell Death and Survival	apoptosis of beta islet cells	4.84E-02	1	BCL2
Cell Death and Survival	cell viability of lymphoblastoid cell lines	4.84E-02	1	BCL2
Cellular Movement	invasion of endothelial cell lines	4.84E-02	1	ANGPT2
Cellular Movement	invasion of stomach cancer cell lines	4.84E-02	1	SDCBP
Nervous System Development and Function	loss of neurons	4.84E-02	1	APP
Cell Death and Survival	loss of neurons	4.84E-02	1	APP

Cellular Movement	migration of neuroblastoma cell lines	4.84E-02	1	ANGPT2
Cellular Function and Maintenance	mitochondrial membrane potential	4.84E-02	1	BCL2
Cell Morphology	mitochondrial membrane potential	4.84E-02	1	BCL2
Cell Morphology	morphology of brain cancer cell lines	4.84E-02	1	BCL2
Cell Morphology	morphology of lung cancer cell lines	4.84E-02	1	TRIB2
Cellular Movement	migration of brain cancer cell lines	4.90E-02	2	CDH2, PTPRM

* Green highlight indicates neuronal function/disease terms.

APPENDIX II

Chapter 4 Additional Files

ADDITIONAL FILE 1

Supplementary Table S1. Exosomal proteins depleted from cells by depolarisation.

Cells Only	Cells and Exosomes	Exosomes Only
AKA12	MAP1B	FLNA
KALRN	PRKDC	FLNB
TRRAP	DYHC1	TPR
	CLH1	
	AHNAK	
	HTT	
	PLEC	

ADDITIONAL FILE 2
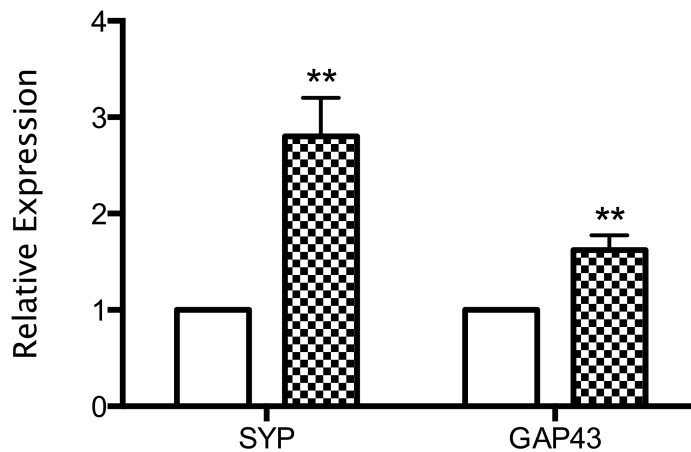
Figure S1. qPCR validation of neurite fractionation. Known neurite markers synaptophysin (SYP) and growth-associated protein 43 (GAP43) were probed by qPCR of mRNA extracted from neurite (chequered bars) and cell body (open bars) fractions. Differential expression was calculated by the **ΔΔ**Ct method, using the cell body as control and comparing the neurite expression in the same biological sample. Data shown are from t-tests conducted on triplicate samples, graphing mean±sem. Both transcripts were significantly enriched in the neurites, confirming the success of the fractionation procedure.

ADDITIONAL FILE 3

(a)

(b)
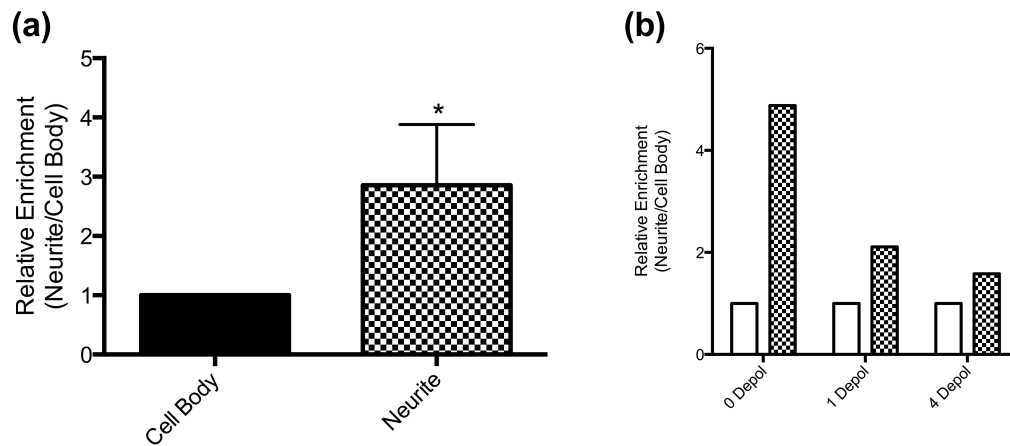
Figure S2. LAMP1 mRNA is enriched in neurites compared to cell bodies. Relative abundance of LAMP1 mRNA in neurites and cell bodies of SH-SY5Y neuroblastoma was compared by qPCR using the **ΔΔ**Ct method as already described. (a) Neurites contained significantly more LAMP1 mRNA than cell bodies (p=0.0139, 1-tailed t-test). (b) LAMP1 mRNA was depleted by 1 and 4 successive K^+ depolarisation/s.

ADDITIONAL FILE 4
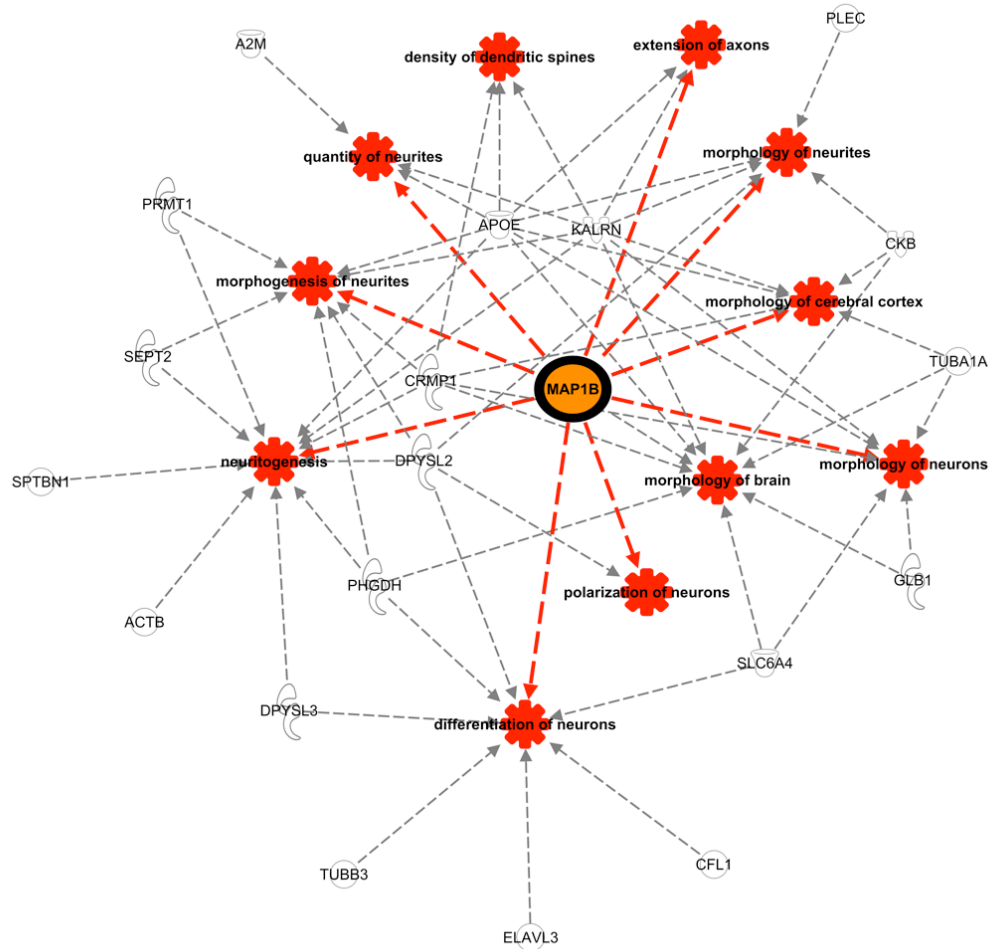
Figure S3. MAP1B-centred neuronal network connects exosome proteins. Functional analysis of exosomal proteins was carried out in Integrated Pathways Analysis (IPA) software. A number of these proteins were found to have strong association with many aspects of neuronal biology, including number, shape and connectivity.

ADDITIONAL FILE 5
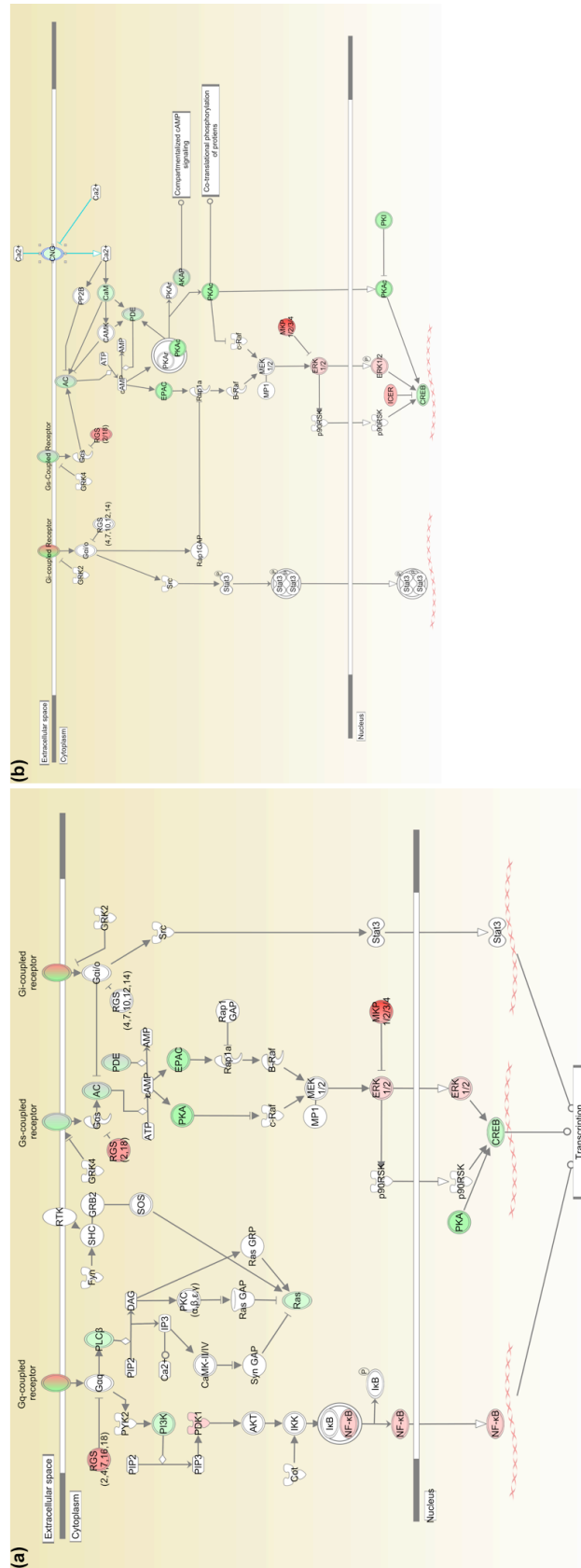
Figure S4. Involvement of genes from the "G-protein coupled receptor signalling" pathway in the response to LTP-inducing stimulation. (a) "G-protein coupled receptor signalling" and (b) "cAMP signalling" pathways were significantly over-represented by genes up- (red) and down- (green) regulated by LTP-inducing KCl stimulation.

ADDITIONAL FILE 6
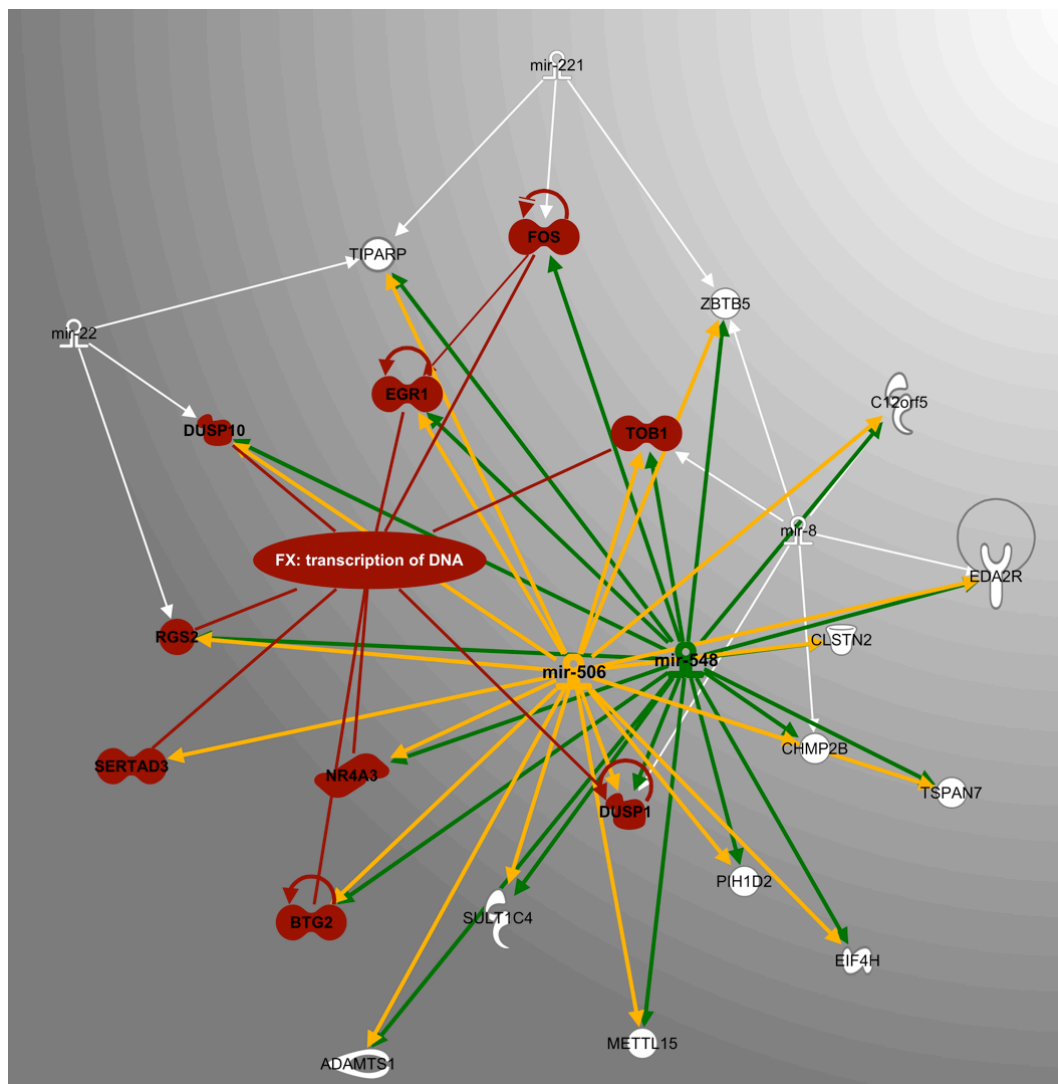
Figure S5. Late-phase LTP-associated "DNA Transcription" regulatory network. miRNA down-regulated by 4-stimuli compared to 1 were target matched with mRNAs up-regulated at least 1.5-fold in the same condition. Functional analysis of this module showed a highly connected network involved in DNA transcription (red), which could be tightly regulated by miR-506 (yellow) and miR-548 (green). In white, miRs-22, -221 and -8 could also assist in regulating some aspects of this network.

ADDITIONAL FILE 7

Figure S6. Neurite-specific "Neuronal Signalling" network. Integrated Pathways Analysis (IPA) software was used to analyse functional modular connectivity between miRNA and mRNAs responding to depolarisation in the neurites of SH-SY5Y. A miRNA target analysis was integrated with experimental mRNA expression data; negatively correlated pairings were then filtered based on functionality. This analysis revealed a highly connected network comprising 4 miRNA (red) and many neurotransmitter receptors with negatively correlated expression changes (mRNA up, miRNA down) in response to a single stimulus.

Goldie et al Supplementary Data S1.xls

Entries highlighted yellow indicate known co-chaperones and clients of the HSP90 complex (Finka and Goloubinoff, 2013)

"Previously Identified": Yes - protein was identified by Conde-Vancells et al (2008), or one of the 15 studies cited therein (see Reference).
Other - Another isoform or family member has been identified in exosomes previously.

"Reference": For proteins not found by Conde-Vancells et al (2008), indicates which of the 15 references cited in that paper did detect this protein.

Accession	Protein	Scores	Peptides	Previously Identified	Reference
14337_HUMAN	14-3-3 protein theta (14-3-3 protein T-cell) (HS1 protein) - Homo sapiens (Human)	76.6 (M:76.6)	1	Yes	1
14332_HUMAN	14-3-3 protein zeta/delta (Protein kinase C inhibitor protein 1) (KCIP-1) - Homo sapiens (Human)	121.2 (M:121.2)	2	Yes	
2AAA_HUMAN	Serine/threonine-protein phosphatase 2A 65 kDa regulatory subunit A alpha isoform OS=Homo sapiens GN=PPP2R1A PE=1 SV=4	193.5 (M:193.5)	1	No	
A16A1_HUMAN	Aldehyde dehydrogenase family 16 member A1 OS=Homo sapiens GN=ALDH16A1 PE=1 SV=2	99.8 (M:99.8)	2	Other	
A2MG_HUMAN	Alpha-2-macroglobulin OS=Homo sapiens GN=A2M PE=1 SV=3	453.2 (M:453.2)	2	No	
AATM_HUMAN	Aspartate aminotransferase, mitochondrial OS=Homo sapiens GN=GOT2 PE=1 SV=3	103.6 (M:103.6)	1	Yes	2
ACLY_HUMAN	ATP-citrate synthase (EC 2.3.3.8) (ATP-citrate (pro-S-)-lyase) (Citrate cleavage enzyme) - Homo sapiens (Human)	331.0 (M:331.0)	4	Yes	
ACPH_HUMAN	Acylamino-acid-releasing enzyme (EC 3.4.19.1) (AARE) (Acyl-peptide hydrolase) (APH) (Acylaminoacyl-peptidase) (Oxidized protein hydrolase) (OPH) (DNF15S2 protein) - Homo s	402.7 (M:402.7)	6	No	
ACTB_HUMAN	Actin, cytoplasmic 1 - Homo sapiens (Human)	1447.6 (M:1447.6)	19	Yes	
ACTN4_HUMAN	Alpha-actinin-4 (Non-muscle alpha-actinin 4) (F-actin cross-linking protein) - Homo sapiens (Human)	957.7 (M:95.7)	1	Yes	
ACTZ_HUMAN	Alpha-centractin (Centractin) (Centrosome-associated actin homolog) (Actin-RPV) (ARP1) - Homo sapiens (Human)	270.9 (M:270.9)	4	No	
ADT2_HUMAN	ADP/ATP translocase 2 OS=Homo sapiens GN=SLC25A5 PE=1 SV=7	387.0 (M:387.0)	4	No	
ADT3_HUMAN	ADP/ATP translocase 3 (Adenine nucleotide translocator 2) (ANT 3) (ADP/ATP carrier protein 3) (Solute carrier family 25 member 6) (ADP/ATP carrier protein, isoform T2) - Homo sa	395.7 (M:395.7)	4	No	
AGO2_HUMAN	Protein argonaute-2 OS=Homo sapiens GN=EIF2C2 PE=1 SV=3	39.4 (M:39.4)	1	No	
AHNK_HUMAN	Neuroblast differentiation-associated protein AHNAK OS=Homo sapiens GN=AHNAK PE=1 SV=2	552.7 (M:552.7)	6	No	
AKA12_HUMAN	A-kinase anchor protein 12 OS=Homo sapiens GN=AKAP12 PE=1 SV=4	438.4 (M:438.4)	4	No	
ALBU_HUMAN	Serum albumin precursor - Homo sapiens (Human)	545.6 (M:545.6)	7	Yes	
ALDOA_HUMAN	Fructose-bisphosphate aldolase A (EC 4.1.2.13) (Muscle-type aldolase) (Lung cancer antigen NY-LU-1) - Homo sapiens (Human)	173.5 (M:173.5)	1	Yes	
AMPL_HUMAN	Cytosol aminopeptidase (EC 3.4.11.1) (Leucine aminopeptidase) (LAP) (Leucyl aminopeptidase) (Leucine aminopeptidase 3) (Proline aminopeptidase) (EC 3.4.11.5) (Prolyl aminope	151.0 (M:151.0)	1	No	
ANM1_HUMAN	Protein arginine N-methyltransferase 1 OS=Homo sapiens GN=PRMT1 PE=1 SV=2	80.0 (M:80.0)	1	No	
ANO1_HUMAN	Anoctamin-1 OS=Homo sapiens GN=ANO1 PE=1 SV=1	96.2 (M:96.2)	1	No	
ANXA2_HUMAN	Annexin A2 (Annexin II) (Lipocortin II) (Calpactin I heavy chain) (Chromobindin-8) (p36) (Protein I) (Placental anticoagulant protein IV) (PAP-IV) - Homo sapiens (Human)	150.5 (M:150.5)	2	Yes	
ANXA5_HUMAN	Annexin A5 (Annexin V) (Lipocortin V) (Endonexin II) (Calphobindin I) (CBP-I) (Placental anticoagulant protein I) (PAP-I) (PP4) (Thromboplastin inhibitor) (Vascular anticoagulant-alp	237.7 (M:237.7)	2	Yes	2
AP2A2_HUMAN	AP-2 complex subunit alpha-2 (Adapter-related protein complex 2 alpha-2 subunit) (Alpha-adaptin C) (Adaptor protein complex AP-2 alpha-2 subunit) (Clathrin assembly protein com	172.6 (M:172.6)	2	Other	2
APOA1_HUMAN	Apolipoprotein A-I precursor (Apo-AI) (ApoA-I) [Contains: Apolipoprotein A-I(1-242)] - Homo sapiens (Human)	55.4 (M:55.4)	1	Other	
APOE_HUMAN	Apolipoprotein E precursor (Apo-E) - Homo sapiens (Human)	78.1 (M:78.1)	1	Yes	
ARF5_HUMAN	ADP-ribosylation factor 5 - Homo sapiens (Human)	40.4 (M:40.4)	1	Other	
ARP2_HUMAN	Actin-like protein 2 (Actin-related protein 2) - Homo sapiens (Human)	182.2 (M:182.2)	1	No	
ARP3_HUMAN	Actin-like protein 3 (Actin-related protein 3) - Homo sapiens (Human)	46.8 (M:46.8)	1	No	
ARPC4_HUMAN	Actin-related protein 2/3 complex subunit 4 (ARP2/3 complex 20 kDa subunit) (p20-ARC) - Homo sapiens (Human)	152.0 (M:152.0)	3	Yes	1, 2
ASAH1_HUMAN	Acid ceramidase OS=Homo sapiens GN=ASAH1 PE=1 SV=5	99.0 (M:99.0)	2	Yes	1
ASXL2_HUMAN	Putative Polycomb group protein ASXL2 - Homo sapiens (Human)	93.8 (M:93.8)	1	No	
AT131_HUMAN	Probable cation-transporting ATPase 13A1 (EC 3.6.3.-) - Homo sapiens (Human)	92.0 (M:92.0)	1	No	
AT1A3_HUMAN	Sodium/potassium-transporting ATPase alpha-3 chain (EC 3.6.3.9) (Sodium pump 3) (Na(+)/K(+) ATPase 3) (Alpha(III)) - Homo sapiens (Human)	314.3 (M:314.3)	3	Yes	2
AT2A2_HUMAN	Sarcoplasmic/endoplasmic reticulum calcium ATPase 2 (EC 3.6.3.8) (Calcium-transporting ATPase sarcoplasmic reticulum type, isoform) (SERCA2) (SR Ca(2+)ATPase 2) (Calcium-transporting ATPase	218.9 (M:218.9)	2	No	
AT2B1_HUMAN	Plasma membrane calcium-transporting ATPase 1 (EC 3.6.3.8) (PMCA1) (Plasma membrane calcium pump isoform 1) (Plasma membrane calcium ATPase isoform 1) - Homo sapiens (Human)	153.6 (M:153.6)	2	No	
ATPA_HUMAN	ATP synthase subunit alpha, mitochondrial precursor - Homo sapiens (Human)	330.5 (M:330.5)	3	Yes	
ATPB_HUMAN	ATP synthase subunit beta, mitochondrial precursor (EC 3.6.3.14) - Homo sapiens (Human)	357.7 (M:357.7)	3	Yes	
BACH_HUMAN	Cytosolic acyl coenzyme A thioester hydrolase (EC 3.1.2.2) (Long chain acyl-CoA thioester hydrolase) (CTE-II) (CTE-II) (Brain acyl-CoA hydrolase) (Acyl-CoA thioesterase 7) - Hom	169.6 (M:169.6)	2	No	
BDP1_HUMAN	Transcription factor TFIIIB component B'' homolog OS=Homo sapiens GN=BDP1 PE=1 SV=3	65.9 (M:65.9)	1	No	
BGAL_HUMAN	Beta-galactosidase OS=Homo sapiens GN=GLB1 PE=1 SV=2	268.9 (M:268.9)	2	Yes	1
BLMH_HUMAN	Bleomycin hydrolase (EC 3.4.22.40) (BLM hydrolase) (BMH) (BH) - Homo sapiens (Human)	118.7 (M:118.7)	2	No	
BRCA2_RAT	Breast cancer type 2 susceptibility protein homolog - Rattus norvegicus (Rat)	89.8 (M:89.8)	1	No	
BTF3_HUMAN	Transcription factor BTF3 (RNA polymerase B transcription factor 3) - Homo sapiens (Human)	43.6 (M:43.6)	1	No	
C1TC_HUMAN	C-1-tetrahydrofolate synthase, cytoplasmic (C1-THF synthase) [Includes: Methylenetetrahydrofolate dehydrogenase (EC 1.5.1.5); Methenyltetrahydrofolate cyclohydrolase (EC 3.5.4.	56.7 (M:56.7)	1	Yes	
CALM_HUMAN	Calmodulin (CaM) - Homo sapiens (Human)	84.8 (M:84.8)	1	Yes	
CAZA2_HUMAN	F-actin capping protein subunit alpha-2 (CapZ alpha-2) - Homo sapiens (Human)	94.3 (M:94.3)	1	No	
CC171_HUMAN	Coiled-coil domain-containing protein 171 OS=Homo sapiens GN=CCDC171 PE=2 SV=1	155.4 (M:155.4)	1	No	
CCD80_HUMAN	Coiled-coil domain-containing protein 80 OS=Homo sapiens GN=CCDC80 PE=1 SV=1	41.2 (M:41.2)	1	No	
CD81_HUMAN	CD81 antigen OS=Homo sapiens GN=CD81 PE=1 SV=1	67.0 (M:67.0)	1	Yes	1
CDCA2_HUMAN	Cell division cycle-associated protein 2 OS=Homo sapiens GN=CDCA2 PE=1 SV=2	93.3 (M:93.3)	1	No	
CE170_HUMAN	Centrosomal protein of 170 kDa OS=Homo sapiens GN=CEP170 PE=1 SV=1	42.4 (M:42.4)	1	No	
CENPF_HUMAN	Centromere protein F OS=Homo sapiens GN=CENPF PE=1 SV=2	236.2 (M:236.2)	1	No	
CG050_HUMAN	Uncharacterized protein C7orf50 OS=Homo sapiens GN=C7orf50 PE=1 SV=1	62.2 (M:62.2)	1	No	
CH60_HUMAN	60 kDa heat shock protein, mitochondrial precursor (Hsp60) (60 kDa chaperonin) (CPN60) (Heat shock protein 60) (HSP-60) (Mitochondrial matrix protein P1) (P60 lymphocyte prote	3021.2 (M:3021.2)	39	Yes	
CHD3_HUMAN	Chromodomain helicase-DNA-binding protein 3 (EC 3.6.1.-) (ATP-dependent helicase CHD3) (CHD-3) (Mi-2 autoantigen 240 kDa protein) (Mi2-alpha) (Zinc-finger helicase) (hZFH) -	42.1 (M:42.1)	1	No	
CLCA_HUMAN	Clathrin light chain A (Lca) - Homo sapiens (Human)	44.7 (M:44.7)	1	Yes	
CLCF_HUMAN	Cardiotrophin-like cytokine factor 1 precursor (B cell-stimulating factor 3) (BSF-3) (Novel neurotrophin-1) (NNT-1) - Homo sapiens (Human)	44.3 (M:44.3)	1	No	

Goldie et al Supplementary Data Data S1.xls

ID	Description	Mass	Count	Match	Notes
CLH1_HUMAN	Clathrin heavy chain 1 (CLH-17) - Homo sapiens (Human)	805.7 (M:805.7)	10	Yes	
COF1_HUMAN	Cofilin-1 (Cofilin, non-muscle isoform) (18 kDa phosphoprotein) (p18) - Homo sapiens (Human)	99.1 (M:99.1)	2	Yes	
COPA_HUMAN	Coatomer subunit alpha OS=Homo sapiens GN=COPA PE=1 SV=2	83.5 (M:83.5)	1	Other	
COPD_HUMAN	Coatomer subunit delta - Homo sapiens (Human)	53.7 (M:53.7)	1	Other	
CPSF5_HUMAN	Cleavage and polyadenylation specificity factor 5 (Cleavage and polyadenylation specificity factor 25 kDa subunit) (CPSF 25 kDa subunit) (Pre-mRNA cleavage factor Im 25 kDa sub	53.7 (M:53.7)	1	No	
CPT1A_HUMAN	Carnitine O-palmitoyltransferase I, liver isoform (EC 2.3.1.21) (CPT I) (CPT1-L) (Carnitine palmitoyltransferase 1A) - Homo sapiens (Human)	69.4 (M:69.4)	1	No	
CSEN_HUMAN	Calsenilin (DRE-antagonist modulator) (DREAM) (Kv channel-interacting protein 3) (KChIP3) (A-type potassium channel modulatory protein 3) - Homo sapiens (Human)	169.3 (M:169.3)	1	No	
CSN4_HUMAN	COP9 signalosome complex subunit 4 - Homo sapiens (Human)	117.9 (M:117.9)	1	No	
CSN8_HUMAN	COP9 signalosome complex subunit 8 (Signalosome subunit 8) (SGN8) (JAB1-containing signalosome subunit 8) (COP9 homolog) (hCOP9) - Homo sapiens (Human)	47.0 (M:47.0)	1	No	
CY561_HUMAN	Cytochrome b561 OS=Homo sapiens GN=CYB561 PE=2 SV=2	49.3 (M:49.3)	1	No	
CYTA_HUMAN	Cystatin-A (Stefin-A) (Cystatin-AS) - Homo sapiens (Human)	47.4 (M:47.4)	1	No	
DC1I2_HUMAN	Cytoplasmic dynein 1 intermediate chain 2 (Dynein intermediate chain 2, cytosolic) (DH IC-2) (Cytoplasmic dynein intermediate chain 2) - Homo sapiens (Human)	214.9 (M:214.9)	4	No	
DCA17_HUMAN	DDB1- and CUL4-associated factor 17 OS=Homo sapiens GN=DCAF17 PE=1 SV=1	46.7 (M:46.7)	1	No	
DCD_HUMAN	Dermcidin precursor (Preproteolysin) [Contains: Survival-promoting peptide; DCD-1] - Homo sapiens (Human)	107.8 (M:107.8)	2	No	
DCTN1_HUMAN	Dynactin subunit 1 - Homo sapiens (Human)	164.4 (M:164.4)	2	No	
DCTN2_HUMAN	Dynactin subunit 2 (Dynactin complex 50 kDa subunit) (50 kDa dynein-associated polypeptide) (p50 dynamitin) (DCTN-50) - Homo sapiens (Human)	156.0 (M:156.0)	2	No	
DDB1_HUMAN	DNA damage-binding protein 1 (Damage-specific DNA-binding protein 1) (UV-damaged DNA-binding factor) (DDB p127 subunit) (DDBa) (UV-damaged DNA-binding protein 1) (UV-D	123.8 (M:123.8)	2	No	
DDC_HUMAN	Aromatic-L-amino-acid decarboxylase (EC 4.1.1.28) (DDC) - Homo sapiens (Human)	147.7 (M:147.7)	3	No	
DHE3_HUMAN	Glutamate dehydrogenase 1, mitochondrial precursor (EC 1.4.1.3) (GDH) - Homo sapiens (Human)	230.3 (M:230.3)	6	No	
DHX9_HUMAN	ATP-dependent RNA helicase A (EC 3.6.1.-) (Nuclear DNA helicase II) (NDH II) (DEAH box protein 9) - Homo sapiens (Human)	405.0 (M:405.0)	1	No	
DJB11_HUMAN	DnaJ homolog subfamily B member 11 precursor - Homo sapiens (Human)	47.5 (M:47.5)	1	No	
DPYL1_HUMAN	Dihydropyrimidinase-related protein 1 (DRP-1) (Collapsin response mediator protein 1) (CRMP-1) - Homo sapiens (Human)	141.9 (M:141.9)	2	No	
DPYL2_HUMAN	Dihydropyrimidinase-related protein 2 (DRP-2) (Collapsin response mediator protein 2) (CRMP-2) (N2A3) - Homo sapiens (Human)	483.2 (M:483.2)	7	No	
DPYL4_HUMAN	Dihydropyrimidinase-related protein 4 (DRP-4) (Collapsin response mediator protein 3) (CRMP-3) (UNC33-like phosphoprotein 4) (ULIP4 protein) - Homo sapiens (Human)	84.9 (M:84.9)	1	No	
DX39B_HUMAN	Spliceosome RNA helicase DDX39B OS=Homo sapiens GN=DDX39B PE=1 SV=1	136.6 (M:136.6)	2	No	
DYHC1_HUMAN	Cytoplasmic dynein 1 heavy chain 1 OS=Homo sapiens GN=DYNC1H1 PE=1 SV=5	1622.9 (M:1622.9)	18	Yes	
ECHA_HUMAN	Trifunctional enzyme subunit alpha, mitochondrial precursor (TP-alpha) (78 kDa gastrin-binding protein) [Includes: Long-chain enoyl-CoA hydratase (EC 4.2.1.17); Long chain 3-hydr	173.0 (M:173.0)	7	No	
EF1A1_HUMAN	Elongation factor 1-alpha 1 (EF-1-alpha-1) (Elongation factor Tu) (EF-Tu) (Leukocyte receptor cluster member 7) - Homo sapiens (Human)	446.3 (M:446.3)	7	No	
EF1G_HUMAN	Elongation factor 1-gamma (EF-1-gamma) (eEF-1B gamma) - Homo sapiens (Human)	125.4 (M:125.4)	2	No	
EF2_HUMAN	Elongation factor 2 (EF-2) - Homo sapiens (Human)	261.6 (M:261.6)	2	No	
EIF3A_HUMAN	Eukaryotic translation initiation factor 3 subunit A OS=Homo sapiens GN=EIF3A PE=1 SV=1	141.3 (M:141.3)	2	Other	
ELAV4_HUMAN	ELAV-like protein 4 OS=Homo sapiens GN=ELAVL4 PE=1 SV=2	246.4 (M:246.4)	2	No	
EMAL4_HUMAN	Echinoderm microtubule-associated protein-like 4 OS=Homo sapiens GN=EML4 PE=1 SV=3	40.8 (M:40.8)	1	No	
ENOA_HUMAN	Alpha-enolase - Homo sapiens (Human)	230.2 (M:230.2)	2	Yes	
ENOG_HUMAN	Gamma-enolase - Homo sapiens (Human)	174.2 (M:174.2)	2	Other	
ENPL_HUMAN	Endoplasmin precursor (Heat shock protein 90 kDa beta member 1) (94 kDa glucose-regulated protein) (GRP94) (gp96 homolog) (Tumor rejection antigen 1) - Homo sapiens (Huma	970.7 (M:970.7)	11	Yes	1, 4
EXL1_CAEEL	Chloride intracellular channel exl-1 OS=Caenorhabditis elegans GN=exl-1 PE=2 SV=2	59.0 (M:59.0)	1	Yes	1, 5
F196A_HUMAN	Protein FAM196A OS=Homo sapiens GN=FAM196A PE=2 SV=1	70.9 (M:70.9)	1	No	
FA8_HUMAN	Coagulation factor VIII precursor (Procoagulant component) (Antihemophilic factor) (AHF) [Contains: Factor VIIIa heavy chain, 200 kDa isoform; Factor VIIIa heavy chain, 92 kDa iso	40.6 (M:40.6)	1	No	
FAS_HUMAN	Fatty acid synthase OS=Homo sapiens GN=FASN PE=1 SV=3	248.3 (M:248.3)	3	Yes	
FETUA_HUMAN	Alpha-2-HS-glycoprotein precursor (Fetuin-A) (Alpha-2-Z-globulin) (Ba-alpha-2-glycoprotein) [Contains: Alpha-2-HS-glycoprotein chain A; Alpha-2-HS-glycoprotein chain B] - Homo s	288.0 (M:288.0)	5	No	
FHDC1_HUMAN	FH2 domain-containing protein 1 OS=Homo sapiens GN=FHDC1 PE=2 SV=2	148.0 (M:148.0)	1	No	
FLNA_HUMAN	Filamin-A (Alpha-filamin) (Filamin-1) (Endothelial actin-binding protein) (Actin-binding protein 280) (ABP-280) (Nonmuscle filamin) - Homo sapiens (Human)	421.7 (M:421.7)	4	No	
FLNB_HUMAN	Filamin-B OS=Homo sapiens GN=FLNB PE=1 SV=2	152.6 (M:152.6)	5	No	
FRIH_HUMAN	Ferritin heavy chain (EC 1.16.3.1) (Ferritin H subunit) (Proliferation-inducing gene 15 protein) - Homo sapiens (Human)	133.7 (M:133.7)	2	Yes	
FRIL_HUMAN	Ferritin light chain (Ferritin L subunit) - Homo sapiens (Human)	120.3 (M:120.3)	1	Yes	
FSCN1_HUMAN	Fascin (Singed-like protein) (55 kDa actin-bundling protein) (p55) - Homo sapiens (Human)	177.0 (M:177.0)	2	No	
G3P_HUMAN	Glyceraldehyde-3-phosphate dehydrogenase - Homo sapiens (Human)	500.5 (M:500.5)	5	Yes	
G3PT_HUMAN	Glyceraldehyde-3-phosphate dehydrogenase, testis-specific (EC 1.2.1.12) (Spermatogenic cell-specific glyceraldehyde 3-phosphate dehydrogenase 2) (GAPDH-2) - Homo sapiens	121.6 (M:121.6)	1	No	
GANAB_HUMAN	Neutral alpha-glucosidase AB precursor (EC 3.2.1.84) (Glucosidase II subunit alpha) - Homo sapiens (Human)	116.8 (M:116.8)	1	No	
GBLP_HUMAN	Guanine nucleotide-binding protein subunit beta 2-like 1 (Guanine nucleotide-binding protein subunit beta-like protein 12.3) (Receptor of activated protein kinase C 1) (RACK1) (Rec	567.0 (M:567.0)	9	Yes	11
GDE_HUMAN	Glycogen debranching enzyme (Glycogen debrancher) [Includes: 4-alpha-glucanotransferase (EC 2.4.1.25) (Oligo-1,4-1,4-glucantransferase); Amylo-alpha-1,6-glucosidase (EC 3.2.	150.6 (M:150.6)	1	No	
GELS_HUMAN	Gelsolin precursor (Actin-depolymerizing factor) (ADF) (Brevin) (AGEL) - Homo sapiens (Human)	126.8 (M:126.8)	1	No	
GHITM_HUMAN	Growth hormone-inducible transmembrane protein (Dermal papilla-derived protein 2) (Transmembrane BAX inhibitor motif-containing protein 5) - Homo sapiens (Human)	42.2 (M:42.2)	1	No	
GIT1_HUMAN	ARF GTPase-activating protein GIT1 (G protein-coupled receptor kinase-interactor 1) (GRK-interacting protein 1) (Cool-associated and tyrosine-phosphorylated protein 1) (Cat-1) -	42.6 (M:42.6)	1	No	
H12_HUMAN	Histone H1.2 (Histone H1d) - Homo sapiens (Human)	164.8 (M:164.8)	2	Yes	
H15_HUMAN	Histone H1.5 (Histone H1a) - Homo sapiens (Human)	87.4 (M:87.4)	1	Yes	4
H1X_HUMAN	Histone H1x - Homo sapiens (Human)	44.7 (M:44.7)	1	No	
H2A1C_HUMAN	Histone H2A type 1-C - Homo sapiens (Human)	229.4 (M:229.4)	3	Yes	
H2A1H_HUMAN	Histone H2A type 1-H - Homo sapiens (Human)	176.1 (M:176.1)	1	Yes	
H2B1K_HUMAN	Histone H2B type 1-K (H2B K) (HIRA-interacting protein 1) - Homo sapiens (Human)	98.4 (M:98.4)	1	No	
H33_HUMAN	Histone H3.3 - Homo sapiens (Human)	104.8 (M:104.8)	1	Yes	
H4_HUMAN	Histone H4 - Homo sapiens (Human)	362.2 (M:362.2)	7	Yes	
HACD3_HUMAN	Very-long-chain (3R)-3-hydroxyacyl-[acyl-carrier protein] dehydratase 3 OS=Homo sapiens GN=PTPLAD1 PE=1 SV=2	123.0 (M:123.0)	2	No	
HBA_HUMAN	Hemoglobin subunit alpha (Hemoglobin alpha chain) (Alpha-globin) - Homo sapiens (Human)	142.2 (M:142.2)	2	Yes	
HBB_HUMAN	Hemoglobin subunit beta - Homo sapiens (Human)	41.3 (M:41.3)	1	Other	
HD_HUMAN	Huntingtin OS=Homo sapiens GN=HTT PE=1 SV=2	512.4 (M:512.4)	5	No	

Goldie et al Supplementary Data Data S1.xls

ID	Description	Mass	Count	Sel	Ref
HEMGN_HUMAN	Hemogen (Hemopoietic gene protein) (Negative differentiation regulator protein) (Erythroid differentiation-associated gene protein) (EDAG-1) - Homo sapiens (Human)	42.4 (M:42.4)	1	No	
HIF3A_HUMAN	Hypoxia-inducible factor 3-alpha OS=Homo sapiens GN=HIF3A PE=1 SV=2	42.3 (M:42.3)	1	No	
HNRH1_HUMAN	Heterogeneous nuclear ribonucleoprotein H (hnRNP H) - Homo sapiens (Human)	87.0 (M:87.0)	2	No	
HNRLL_HUMAN	Heterogeneous nuclear ribonucleoprotein L-like (Stromal RNA-regulating factor) (BLOCK24 protein) - Homo sapiens (Human)	67.4 (M:67.4)	1	No	
HNRPC_HUMAN	Heterogeneous nuclear ribonucleoproteins C1/C2 (hnRNP C1 / hnRNP C2) - Homo sapiens (Human)	241.7 (M:241.7)	2	No	
HNRPD_HUMAN	Heterogeneous nuclear ribonucleoprotein D0 (hnRNP D0) (AU-rich element RNA-binding protein 1) - Homo sapiens (Human)	116.1 (M:116.1)	1	No	
HNRPM_HUMAN	Heterogeneous nuclear ribonucleoprotein M (hnRNP M) - Homo sapiens (Human)	43.9 (M:43.9)	1	No	
HNRPQ_HUMAN	Heterogeneous nuclear ribonucleoprotein Q (hnRNP Q) (hnRNP-Q) (Synaptotagmin-binding, cytoplasmic RNA-interacting protein) (Glycine- and tyrosine-rich RNA-binding protein) (<77.6 (M:77.6)	77.6 (M:77.6)	1	No	
HNRPU_HUMAN	Heterogeneous nuclear ribonucleoprotein U OS=Homo sapiens GN=HNRNPU PE=1 SV=6	129.7 (M:129.7)	1	No	
HS90B_HUMAN	**Heat shock protein HSP 90-beta (HSP 84) (HSP 90) - Homo sapiens (Human)**	**306.8 (M:306.8)**	**1**	**Yes**	**14**
HSP74_HUMAN	Heat shock 70 kDa protein 4 OS=Homo sapiens GN=HSPA4 PE=1 SV=4	73.3 (M:73.3)	1	Yes	1, 8
IDH3A_HUMAN	Isocitrate dehydrogenase [NAD] subunit alpha, mitochondrial precursor (EC 1.1.1.41) (Isocitric dehydrogenase) (NAD(+)-specific ICDH) - Homo sapiens (Human)	119.2 (M:119.2)	1	Yes	
IF4A1_HUMAN	Eukaryotic initiation factor 4A-I (EC 3.6.1.-) (ATP-dependent RNA helicase eIF4A-1) (eIF4A-I) - Homo sapiens (Human)	109.1 (M:109.1)	1	No	
ILF2_HUMAN	Interleukin enhancer-binding factor 2 (Nuclear factor of activated T-cells 45 kDa) - Homo sapiens (Human)	168.4 (M:168.4)	3	No	
ILF3_HUMAN	Interleukin enhancer-binding factor 3 (Nuclear factor of activated T-cells 90 kDa) (NF-AT-90) (Double-stranded RNA-binding protein 76) (DRBP76) (Translational control protein 80) (<316.0 (M:316.0)	316.0 (M:316.0)	5	No	
IMB1_HUMAN	**Importin beta-1 subunit (Karyopherin beta-1 subunit) (Nuclear factor P97) (Importin 90) - Homo sapiens (Human)**	**137.1 (M:137.1)**	**1**	**Yes**	
IMDH1_HUMAN	Inosine-5'-monophosphate dehydrogenase 1 (EC 1.1.1.205) (IMP dehydrogenase 1) (IMPDH-I) (IMPD 1) - Homo sapiens (Human)	108.1 (M:108.1)	1	No	
INADL_HUMAN	InaD-like protein - Homo sapiens (Human)	205.0 (M:205.0)	1	No	
INO1_HUMAN	Inositol-3-phosphate synthase 1 OS=Homo sapiens GN=ISYNA1 PE=1 SV=1	78.2 (M:78.2)	1	No	
ITIH2_HUMAN	Inter-alpha-trypsin inhibitor heavy chain H2 OS=Homo sapiens GN=ITIH2 PE=1 SV=2	165.4 (M:165.4)	3	No	
KALRN_HUMAN	Kalirin OS=Homo sapiens GN=KALRN PE=1 SV=2	290.1 (M:290.1)	3	No	
KCRB_HUMAN	Creatine kinase B-type (EC 2.7.3.2) (Creatine kinase B chain) (B-CK) - Homo sapiens (Human)	306.4 (M:306.4)	4	Yes	8
KCRU_HUMAN	Creatine kinase, ubiquitous mitochondrial precursor (EC 2.7.3.2) (U-MtCK) (Mia-CK) (Acidic-type mitochondrial creatine kinase) - Homo sapiens (Human)	129.9 (M:129.9)	2	No	
KI26B_HUMAN	Kinesin-like protein KIF26B OS=Homo sapiens GN=KIF26B PE=1 SV=1	150.8 (M:150.8)	1	No	
KINH_HUMAN	Kinesin heavy chain (Ubiquitous kinesin heavy chain) (UKHC) - Homo sapiens (Human)	200.0 (M:200.0)	2	Yes	14
KPYM_HUMAN	Pyruvate kinase isozymes M1/M2 (EC 2.7.1.40) (Pyruvate kinase muscle isozyme) (Pyruvate kinase 2/3) (Cytosolic thyroid hormone-binding protein) (CTHBP) (THBP1) - Homo sapi	785.0 (M:785.0)	11	Yes	2, 4
LAMP1_HUMAN	Lysosome-associated membrane glycoprotein 1 OS=Homo sapiens GN=LAMP1 PE=1 SV=1	69.6 (M:69.6)	1	No	
LG3BP_HUMAN	Galectin-3-binding protein precursor (Lectin galactoside-binding soluble 3-binding protein) (Mac-2-binding protein) (Mac-2-binding antigen 90K) - Homo sa	243.1 (M:243.1)	3	Yes	1
LPPRC_HUMAN	Leucine-rich PPR motif-containing protein, mitochondrial precursor - Homo sapiens (Human)	424.9 (M:424.9)	4	Other	
LRP1_HUMAN	Prolow-density lipoprotein receptor-related protein 1 OS=Homo sapiens GN=LRP1 PE=1 SV=2	220.7 (M:220.7)	1	No	
LRP1B_HUMAN	Low-density lipoprotein receptor-related protein 1B precursor - Homo sapiens (Human)	98.8 (M:98.8)	1	No	
MAOM_HUMAN	NAD-dependent malic enzyme, mitochondrial precursor (EC 1.1.1.38) (NAD-ME) (Malic enzyme 2) - Homo sapiens (Human)	50.6 (M:50.6)	1	No	
MAP1A_HUMAN	Microtubule-associated protein 1A OS=Homo sapiens GN=MAP1A PE=1 SV=6	114.1 (M:114.1)	1	No	
MAP1B_HUMAN	Microtubule-associated protein 1B OS=Homo sapiens GN=MAP1B PE=1 SV=2	4962.6 (M:4962.6)	64	No	
MCCA_HUMAN	Methylcrotonoyl-CoA carboxylase subunit alpha, mitochondrial precursor (EC 6.4.1.4) (3-methylcrotonyl-CoA carboxylase 1) (MCCase subunit alpha) (3-methylcrotonyl-CoA:carbon	46.7 (M:46.7)	1	No	
MCM2_HUMAN	DNA replication licensing factor MCM2 (Minichromosome maintenance protein 2 homolog) (Nuclear protein BM28) - Homo sapiens (Human)	80.1 (M:80.1)	1	No	
MCM6_HUMAN	DNA replication licensing factor MCM6 (p105MCM) - Homo sapiens (Human)	82.2 (M:82.2)	1	No	
MCM7_HUMAN	DNA replication licensing factor MCM7 - Homo sapiens (Human)	126.0 (M:126.0)	1	No	
MDR1_HUMAN	Multidrug resistance protein 1 OS=Homo sapiens GN=ABCB1 PE=1 SV=3	56.2 (M:56.2)	1	No	
ML12B_HUMAN	Myosin regulatory light chain 12B OS=Homo sapiens GN=MYL12B PE=1 SV=2	165.4 (M:165.4)	2	No	
MMSA_HUMAN	Methylmalonate-semialdehyde dehydrogenase [acylating], mitochondrial precursor - Homo sapiens (Human)	78.2 (M:78.2)	1	Yes	
MPCP_HUMAN	Phosphate carrier protein, mitochondrial precursor (PTP) (Solute carrier family 25 member 3) - Homo sapiens (Human)	59.3 (M:59.3)	1	No	
MRP_HUMAN	MARCKS-related protein (MARCKS-like protein 1) (Macrophage myristoylated alanine-rich C kinase substrate) (Mac-MARCKS) (MacMARCKS) - Homo sapiens (Human)	61.4 (M:61.4)	1	No	
MTMR5_HUMAN	Myotubularin-related protein 5 OS=Homo sapiens GN=SBF1 PE=1 SV=3	122.2 (M:122.2)	1	No	
MTMRD_HUMAN	Myotubularin-related protein 13 (SET-binding factor 2) - Homo sapiens (Human)	42.4 (M:42.4)	1	No	
MYH10_HUMAN	Myosin-10 OS=Homo sapiens GN=MYH10 PE=1 SV=3	728.4 (M:728.4)	10	Yes	
NASP_HUMAN	Nuclear autoantigenic sperm protein (NASP) - Homo sapiens (Human)	117.0 (M:117.0)	1	No	
NH2L1_HUMAN	NHP2-like protein 1 (High mobility group-like nuclear protein 2 homolog 1) (U4/U6.U5 tri-snRNP 15.5 kDa protein) (OTK27) (hSNU13) - Homo sapiens (Human)	72.2 (M:72.2)	1	No	
NIF3L_HUMAN	NIF3-like protein 1 OS=Homo sapiens GN=NIF3L1 PE=1 SV=2	94.1 (M:94.1)	1	No	
NNTM_HUMAN	NAD(P) transhydrogenase, mitochondrial precursor (EC 1.6.1.2) (Pyridine nucleotide transhydrogenase) (Nicotinamide nucleotide transhydrogenase) - Homo sapiens (Human)	145.1 (M:145.1)	2	Yes	
NP1L1_HUMAN	Nucleosome assembly protein 1-like 1 - Homo sapiens (Human)	41.8 (M:41.8)	1	No	
NP1L4_HUMAN	Nucleosome assembly protein 1-like 4 (Nucleosome assembly protein 2) (NAP2) - Homo sapiens (Human)	53.8 (M:53.8)	1	No	
NPL4_HUMAN	Nuclear protein localization protein 4 homolog (Protein NPL4) - Homo sapiens (Human)	71.1 (M:71.1)	1	No	
NPM_HUMAN	Nucleophosmin (NPM) (Nucleolar phosphoprotein B23) (Numatrin) (Nucleolar protein NO38) - Homo sapiens (Human)	119.7 (M:119.7)	1	Yes	1
NUCL_HUMAN	Nucleolin (Protein C23) - Homo sapiens (Human)	470.2 (M:470.2)	6	No	
NWD1_HUMAN	NACHT and WD repeat domain-containing protein 1 OS=Homo sapiens GN=NWD1 PE=2 SV=3	81.6 (M:81.6)	1	No	
ODO2_HUMAN	Dihydrolipoyllysine-residue succinyltransferase component of 2-oxoglutarate dehydrogenase complex, mitochondrial OS=Homo sapiens GN=DLST PE=1 SV=4	167.6 (M:167.6)	2	No	
OR8J2_HUMAN	Olfactory receptor 8J2 OS=Homo sapiens GN=OR8J2 PE=3 SV=2	83.3 (M:83.3)	1	No	
OXA1_YEAST	Inner membrane protein OXA1, mitochondrial precursor (Oxidase assembly protein 1) (Cytochrome oxidase biogenesis protein OXA1) - Saccharomyces cerevisiae (Baker's yeast)	42.2 (M:42.2)	1	No	
P85B_HUMAN	Phosphatidylinositol 3-kinase regulatory subunit beta OS=Homo sapiens GN=PIK3R2 PE=1 SV=2	76.8 (M:76.8)	1	No	
PA2G4_HUMAN	Proliferation-associated protein 2G4 - Homo sapiens (Human)	202.3 (M:202.3)	2	No	
PAIRB_HUMAN	Plasminogen activator inhibitor 1 RNA-binding protein (PAI-1 RNA-binding protein 1) (PAI-RBP1) (SERPINE1 mRNA-binding protein 1) - Homo sapiens (Human)	124.1 (M:124.1)	2	No	
PCD16_HUMAN	Protocadherin-16 precursor (Cadherin-19) (Cadherin-1) (Dachsous-1) - Homo sapiens (Human)	615.9 (M:615.9)	6	No	
PD1L2_HUMAN	Programmed cell death 1 ligand 2 OS=Homo sapiens GN=PDCD1LG2 PE=1 SV=2	44.6 (M:44.6)	1	No	
PDIA6_HUMAN	Protein disulfide-isomerase A6 precursor (EC 5.3.4.1) (Protein disulfide isomerase P5) (Thioredoxin domain-containing protein 7) - Homo sapiens (Human)	78.7 (M:78.7)	1	Yes	
PECA1_HUMAN	Platelet endothelial cell adhesion molecule precursor (PECAM-1) (EndoCAM) (GPIIA') (CD31 antigen) - Homo sapiens (Human)	67.1 (M:67.1)	1	No	
PGK1_HUMAN	**Phosphoglycerate kinase 1 (EC 2.7.2.3) (Primer recognition protein 2) (PRP 2) - Homo sapiens (Human)**	**107.2 (M:107.2)**	**1**	**Yes**	**5**

Goldie et al Supplementary Data Data S1.xls

Gene	Description	Mass	Count	Detected	Note
PHB_HUMAN	Prohibitin - Homo sapiens (Human)	48.7 (M:48.7)	1	Yes	
PLCE1_HUMAN	1-phosphatidylinositol-4,5-bisphosphate phosphodiesterase epsilon 1 (EC 3.1.4.11) (Phospholipase C-epsilon-1) (PLC-epsilon-1) (Phosphoinositide-specific phospholipase C epsilon 1) - Homo sapiens (Human)	148.4 (M:148.4)	1	Other	
PLEC_HUMAN	Plectin OS=Homo sapiens GN=PLEC PE=1 SV=3	322.0 (M:322.0)	1	No	
PPIA_HUMAN	Peptidyl-prolyl cis-trans isomerase A (EC 5.2.1.8) (PPIase A) (Cyclophilin A) (Rotamase A) (Cyclosporin A-binding protein) - Homo sapiens (Human)	75.5 (M:75.5)	1	Yes	1, 2
PRC2C_HUMAN	Protein PRRC2C OS=Homo sapiens GN=PRRC2C PE=1 SV=4	166.1 (M:166.1)	1	Yes	
PRDX1_HUMAN	Peroxiredoxin-1 (EC 1.11.1.15) (Thioredoxin peroxidase 2) (Thioredoxin-dependent peroxide reductase 2) (Proliferation-associated gene protein) (PAG) (Natural killer cell-enhancing ...	155.5 (M:155.5)	2	Other	
PRDX2_HUMAN	Peroxiredoxin-2 (EC 1.11.1.15) (Thioredoxin peroxidase 1) (Thioredoxin-dependent peroxide reductase 1) (Thiol-specific antioxidant protein) (TSA) (PRP) (Natural killer cell-enhanci...	332.6 (M:332.6)	3	No	
PRDX3_HUMAN	Thioredoxin-dependent peroxide reductase, mitochondrial precursor (EC 1.11.1.15) (Peroxiredoxin-3) (PRX III) (Antioxidant protein 1) (AOP-1) (Protein MER5 homolog) (HBC189) - 1269.2 (M:269.2)	-1269.2 (M:269.2)	3	No	
PRDX4_HUMAN	Peroxiredoxin-4 (EC 1.11.1.15) (Prx-IV) (Thioredoxin-dependent peroxide reductase AO372) (Thioredoxin-dependent peroxide reductase A0372) (Antioxidant enzyme AOE372) - Homo sapie	76.5 (M:76.5)	3	No	
PRKDC_HUMAN	**DNA-dependent protein kinase catalytic subunit - Homo sapiens (Human)**	3361.2 (M:3361.2)	39	No	
PRS7_HUMAN	26S protease regulatory subunit 7 (Proteasome 26S subunit ATPase 2) (Protein MSS1) - Homo sapiens (Human)	127.5 (M:127.5)	1	No	
PRS8_HUMAN	26S protease regulatory subunit 8 (Proteasome 26S subunit ATPase 5) (Proteasome subunit p45) (p45/SUG) (Thyroid hormone receptor-interacting protein 1) (TRIP1) - Homo sapie	241.3 (M:241.3)	3	No	
PRUN2_HUMAN	Protein prune homolog 2 OS=Homo sapiens GN=PRUNE2 PE=1 SV=3	92.9 (M:92.9)	1	No	
PSA1_HUMAN	Proteasome subunit alpha type 1 (EC 3.4.25.1) (Proteasome component C2) (Macropain subunit C2) (Multicatalytic endopeptidase complex subunit C2) - Homo sapiens (Human)	615.2 (M:615.2)	7	No	
PSA2_HUMAN	Proteasome subunit alpha type 2 (EC 3.4.25.1) (Proteasome component C3) (Macropain subunit C3) (Multicatalytic endopeptidase complex subunit C3) - Homo sapiens (Human)	968.5 (M:968.5)	7	No	
PSA3_HUMAN	Proteasome subunit alpha type 3 (EC 3.4.25.1) (Proteasome component C8) (Macropain subunit C8) (Multicatalytic endopeptidase complex subunit C8) - Homo sapiens (Human)	623.3 (M:623.3)	13	No	
PSA4_HUMAN	Proteasome subunit alpha type 4 (EC 3.4.25.1) (Proteasome component C9) (Macropain subunit C9) (Multicatalytic endopeptidase complex subunit C9) (Proteasome subunit L) - Ho	654.1 (M:654.1)	7	No	
PSA5_HUMAN	Proteasome subunit alpha type 5 (EC 3.4.25.1) (Proteasome zeta chain) (Macropain zeta chain) (Multicatalytic endopeptidase complex zeta chain) - Homo sapiens (Human)	767.8 (M:767.8)	9	No	
PSA6_HUMAN	Proteasome subunit alpha type 6 (EC 3.4.25.1) (Proteasome iota chain) (Macropain iota chain) (Multicatalytic endopeptidase complex iota chain) (27 kDa prosomal protein) (PROS-	-617.9 (M:617.9)	11	No	
PSA7_HUMAN	Proteasome subunit alpha type 7 (EC 3.4.25.1) (Proteasome subunit RC6-1) (Proteasome subunit XAPC7) - Homo sapiens (Human)	682.9 (M:682.9)	8	No	
PSB1_HUMAN	Proteasome subunit beta type 1 precursor (EC 3.4.25.1) (Proteasome component C5) (Macropain subunit C5) (Multicatalytic endopeptidase complex subunit C5) (Proteasome gamm	711.6 (M:711.6)	7	No	
PSB2_HUMAN	Proteasome subunit beta type 2 (EC 3.4.25.1) (Proteasome component C7-I) (Macropain subunit C7-I) (Multicatalytic endopeptidase complex subunit C7-I) - Homo sapiens (Human)	609.9 (M:609.9)	9	No	
PSB3_HUMAN	Proteasome subunit beta type 3 (EC 3.4.25.1) (Proteasome theta chain) (Proteasome chain 13) (Proteasome component C10-II) - Homo sapiens (Human)	471.5 (M:471.5)	6	Yes	1
PSB4_HUMAN	Proteasome subunit beta type 4 precursor (EC 3.4.25.1) (Proteasome beta chain) (Macropain beta chain) (Multicatalytic endopeptidase complex beta chain) (Proteasome chain 3) (	748.1 (M:748.1)	6	No	
PSB5_HUMAN	**Proteasome subunit beta type-5 OS=Homo sapiens GN=PSMB5 PE=1 SV=3**	1041.2 (M:1041.2)	10	No	
PSB6_HUMAN	Proteasome subunit beta type 6 precursor (EC 3.4.25.1) (Proteasome delta chain) (Macropain delta chain) (Multicatalytic endopeptidase complex delta chain) (Proteasome subunit Y	323.2 (M:323.2)	13	No	
PSB7_HUMAN	Proteasome subunit beta type 7 precursor (EC 3.4.25.1) (Proteasome subunit Z) (Macropain chain Z) (Multicatalytic endopeptidase complex chain Z) - Homo sapiens (Human)	388.7 (M:388.7)	5	No	
PSD11_HUMAN	26S proteasome non-ATPase regulatory subunit 11 (26S proteasome regulatory subunit S9) (26S proteasome regulatory subunit p44.5) - Homo sapiens (Human)	262.4 (M:262.4)	4	No	
PSD13_HUMAN	26S proteasome non-ATPase regulatory subunit 13 OS=Homo sapiens GN=PSMD13 PE=1 SV=2	135.8 (M:135.8)	3	No	
PSDE_HUMAN	26S proteasome non-ATPase regulatory subunit rpn11 (26S proteasome-associated PAD1 homolog 1) - Homo sapiens (Human)	81.9 (M:81.9)	2	No	
PSMD1_HUMAN	26S proteasome non-ATPase regulatory subunit 1 - Homo sapiens (Human)	264.0 (M:264.0)	4	No	
PSMD2_HUMAN	26S proteasome non-ATPase regulatory subunit 2 (26S proteasome regulatory subunit RPN1) (26S proteasome regulatory subunit S2) (26S proteasome subunit p97) (Tumor necros	384.7 (M:384.7)	5	No	
PSMD3_HUMAN	26S proteasome non-ATPase regulatory subunit 3 (26S proteasome regulatory subunit p58) (Proteasome subunit S3) - Homo sapiens (Human)	87.8 (M:87.8)	1	No	
PSME1_HUMAN	Proteasome activator complex subunit 1 - Homo sapiens (Human)	248.4 (M:248.4)	3	No	
PSME2_HUMAN	Proteasome activator complex subunit 2 OS=Homo sapiens GN=PSME2 PE=1 SV=4	190.1 (M:190.1)	2	No	
PSME3_HUMAN	Proteasome activator complex subunit 3 (Proteasome activator 28-gamma subunit) (PA28gamma) (PA28g) (Activator of multicatalytic protease subunit 3) (11S regulator complex su	58.7 (M:58.7)	1	Yes	1
PTBP1_HUMAN	Polypyrimidine tract-binding protein 1 (PTB) (Heterogeneous nuclear ribonucleoprotein I) (hnRNP I) (57 kDa RNA-binding protein PPTB-1) - Homo sapiens (Human)	53.3 (M:53.3)	1	Yes	
PUR6_HUMAN	Multifunctional protein ADE2 [Includes: Phosphoribosylaminoimidazole-succinocarboxamide synthase (EC 6.3.2.6) (SAICAR synthetase); Phosphoribosylaminoimidazole carboxylas	80.9 (M:80.9)	1	No	
PURA_HUMAN	Transcriptional activator protein Pur-alpha (Purine-rich single-stranded DNA-binding protein alpha) - Homo sapiens (Human)	43.0 (M:43.0)	1	No	
PZP_HUMAN	Pregnancy zone protein OS=Homo sapiens GN=PZP PE=1 SV=4	213.1 (M:213.1)	1	No	
RAB7A_HUMAN	Ras-related protein Rab-7a OS=Homo sapiens GN=RAB7A PE=1 SV=1	108.5 (M:108.5)	1	Yes	
RABP2_HUMAN	Cellular retinoic acid-binding protein 2 (Cellular retinoic acid-binding protein II) (CRABP-II) (CRABP-II) (Retinoic acid-binding protein II, cellular) - Homo sapiens (Human)	151.8 (M:151.8)	2	No	
RALY_HUMAN	RNA-binding protein Raly (hnRNP associated with lethal yellow homolog) (Autoantigen p542) - Homo sapiens (Human)	174.6 (M:174.6)	2	No	
RAP1B_HUMAN	Ras-related protein Rap-1b precursor (GTP-binding protein smg p21B) - Homo sapiens (Human)	42.2 (M:42.2)	1	Yes	
RB11A_HUMAN	Ras-related protein Rab-11A (Rab-11) (YL8) - Homo sapiens (Human)	76.1 (M:76.1)	1	No	
RBP2_HUMAN	E3 SUMO-protein ligase RanBP2 (Ran-binding protein 2) (Nuclear pore complex protein Nup358) (Nucleoporin Nup358) (358 kDa nucleoporin) (p270) - Homo sapiens (Human)	104.9 (M:104.9)	1	No	
REF_HEVBR	Rubber elongation factor protein (REF) (Allergen Hev b 1) - Hevea brasiliensis (Para rubber tree)	44.8 (M:44.8)	1	No	
RL10_HUMAN	60S ribosomal protein L10 OS=Homo sapiens GN=RPL10 PE=1 SV=4	177.3 (M:177.3)	2	No	
RL10A_HUMAN	60S ribosomal protein L10a (CSA-19) - Homo sapiens (Human)	336.8 (M:336.8)	4	No	
RL11_HUMAN	60S ribosomal protein L11 (CLL-associated antigen KW-12) - Homo sapiens (Human)	198.5 (M:198.5)	3	Yes	
RL12_HUMAN	60S ribosomal protein L12 - Homo sapiens (Human)	403.1 (M:403.1)	5	No	
RL13_HUMAN	60S ribosomal protein L13 (Breast basic conserved protein 1) - Homo sapiens (Human)	255.5 (M:255.5)	4	No	
RL13A_HUMAN	60S ribosomal protein L13a (Ribosomal protein L13) - Homo sapiens (Human)	187.9 (M:187.9)	2	Yes	
RL14_HUMAN	60S ribosomal protein L14 OS=Homo sapiens GN=RPL14 PE=1 SV=4	277.7 (M:277.7)	3	No	
RL15_HUMAN	60S ribosomal protein L15 - Homo sapiens (Human)	177.9 (M:177.9)	1	No	
RL17_HUMAN	60S ribosomal protein L17 (L23) - Homo sapiens (Human)	142.6 (M:142.6)	1	No	
RL18_HUMAN	60S ribosomal protein L18 - Homo sapiens (Human)	394.0 (M:394.0)	5	Yes	2
RL18A_HUMAN	60S ribosomal protein L18a - Homo sapiens (Human)	133.3 (M:133.3)	1	No	
RL19_HUMAN	60S ribosomal protein L19 - Homo sapiens (Human)	191.5 (M:191.5)	2	No	
RL21_HUMAN	60S ribosomal protein L21 - Homo sapiens (Human)	183.0 (M:183.0)	3	No	
RL22_HUMAN	60S ribosomal protein L22 (Epstein-Barr virus small RNA-associated protein) (EBER-associated protein) (EAP) (Heparin-binding protein HBp15) - Homo sapiens (Human)	292.0 (M:292.0)	4	No	
RL23_HUMAN	60S ribosomal protein L23 (Ribosomal protein L17) - Homo sapiens (Human)	386.7 (M:386.7)	5	No	
RL23A_HUMAN	60S ribosomal protein L23a - Homo sapiens (Human)	189.1 (M:189.1)	2	No	
RL24_HUMAN	60S ribosomal protein L24 (Ribosomal protein L30) - Homo sapiens (Human)	162.9 (M:162.9)	3	No	
RL26L_HUMAN	60S ribosomal protein L26-like 1 - Homo sapiens (Human)	93.4 (M:93.4)	1	No	
RL27_HUMAN	60S ribosomal protein L27 - Homo sapiens (Human)	200.9 (M:200.9)	3	No	
RL27A_HUMAN	60S ribosomal protein L27a - Homo sapiens (Human)	237.4 (M:237.4)	3	No	

Goldie et al Supplementary Data Data S1.xls

Accession	Description	Score	Count	Match	Extra
RL28_HUMAN	60S ribosomal protein L28 - Homo sapiens (Human)	224.6 (M:224.6)	5	No	
RL29_HUMAN	60S ribosomal protein L29 (Cell surface heparin-binding protein HIP) - Homo sapiens (Human)	99.3 (M:99.3)	1	No	
RL3_HUMAN	60S ribosomal protein L3 (HIV-1 TAR RNA-binding protein B) (TARBP-B) - Homo sapiens (Human)	302.1 (M:302.1)	5	No	
RL30_HUMAN	60S ribosomal protein L30 - Homo sapiens (Human)	327.2 (M:327.2)	3	No	
RL31_HUMAN	60S ribosomal protein L31 - Homo sapiens (Human)	216.3 (M:216.3)	2	No	
RL32_HUMAN	60S ribosomal protein L32 - Homo sapiens (Human)	166.6 (M:166.6)	2	No	
RL35_HUMAN	60S ribosomal protein L35 - Homo sapiens (Human)	104.7 (M:104.7)	2	No	
RL36_HUMAN	60S ribosomal protein L36 - Homo sapiens (Human)	85.7 (M:85.7)	1	No	
RL4_HUMAN	60S ribosomal protein L4 - Homo sapiens (Human)	467.1 (M:467.1)	5	No	
RL6_HUMAN	60S ribosomal protein L6 (TAX-responsive enhancer element-binding protein 107) (TAXREB107) (Neoplasm-related protein C140) - Homo sapiens (Human)	260.3 (M:260.3)	1	Yes	
RL7_HUMAN	60S ribosomal protein L7 - Homo sapiens (Human)	317.4 (M:317.4)	2	Yes	
RL7L_HUMAN	60S ribosomal protein L7a (Surfeit locus protein 3) (PLA-X polypeptide) - Homo sapiens (Human)	427.7 (M:427.7)	6	No	
RL8_HUMAN	60S ribosomal protein L8 - Homo sapiens (Human)	191.1 (M:191.1)	1	No	
RL9_HUMAN	60S ribosomal protein L9 - Homo sapiens (Human)	239.7 (M:239.7)	4	No	
RLA0_HUMAN	60S acidic ribosomal protein P0 (L10E) - Homo sapiens (Human)	529.6 (M:529.6)	7	No	15
RLA1_HUMAN	60S acidic ribosomal protein P1 - Homo sapiens (Human)	45.6 (M:45.6)	1	No	
RLA2_HUMAN	60S acidic ribosomal protein P2 (Renal carcinoma antigen NY-REN-44) - Homo sapiens (Human)	298.8 (M:298.8)	4	Yes	
RM23_HUMAN	Mitochondrial 39S ribosomal protein L23 (L23mt) (MRP-L23) (L23 mitochondrial-related protein) (Ribosomal protein L23-like) - Homo sapiens (Human)	40.1 (M:40.1)	1	No	
RM43_HUMAN	39S ribosomal protein L43, mitochondrial precursor (L43mt) (MRP-L43) (Mitochondrial ribosomal protein bMRP36a) - Homo sapiens (Human)	81.8 (M:81.8)	1	No	
RM49_HUMAN	Mitochondrial 39S ribosomal protein L49 (L49mt) (MRP-L49) (Protein NOF1) (Neighbor of FAU) (NOF) - Homo sapiens (Human)	115.2 (M:115.2)	1	No	
RO60_HUMAN	60 kDa SS-A/Ro ribonucleoprotein (60 kDa Ro protein) (60 kDa autoantigen) (Ro 60 kDa autoantigen) (TROVE domain family member 2) (Sjoegren syndrome typ 123.8 (M:123.8		1	No	
ROA1_HUMAN	Heterogeneous nuclear ribonucleoprotein A1 OS=Homo sapiens GN=HNRNPA1 PE=1 SV=5	178.7 (M:178.7)	1	No	
ROA2_HUMAN	Heterogeneous nuclear ribonucleoproteins A2/B1 (hnRNP A2 / hnRNP B1) - Homo sapiens (Human)	126.9 (M:126.9)	2	No	
RS10_HUMAN	40S ribosomal protein S10 - Homo sapiens (Human)	181.4 (M:181.4)	2	No	
RS11_HUMAN	40S ribosomal protein S11 - Homo sapiens (Human)	132.3 (M:132.3)	2	No	
RS12_HUMAN	40S ribosomal protein S12 OS=Homo sapiens GN=RPS12 PE=1 SV=3	381.0 (M:381.0)	5	No	
RS13_HUMAN	40S ribosomal protein S13 - Homo sapiens (Human)	314.7 (M:314.7)	4	No	
RS14_HUMAN	40S ribosomal protein S14 - Homo sapiens (Human)	430.5 (M:430.5)	5	No	
RS15_HUMAN	40S ribosomal protein S15 (RIG protein) - Homo sapiens (Human)	261.3 (M:261.3)	1	No	
RS15A_HUMAN	40S ribosomal protein S15a - Homo sapiens (Human)	290.8 (M:290.8)	3	No	
RS16_HUMAN	40S ribosomal protein S16 - Homo sapiens (Human)	529.8 (M:529.8)	5	No	
RS17_HUMAN	40S ribosomal protein S17 - Homo sapiens (Human)	246.8 (M:246.8)	4	No	
RS18_HUMAN	40S ribosomal protein S18 (Ke-3) (Ke3) - Homo sapiens (Human)	650.1 (M:650.1)	10	Yes	2
RS19_HUMAN	40S ribosomal protein S19 - Homo sapiens (Human)	322.8 (M:322.8)	4	No	
RS2_HUMAN	40S ribosomal protein S2 (S4) (LLRep3 protein) - Homo sapiens (Human)	229.0 (M:229.0)	4	No	
RS20_HUMAN	40S ribosomal protein S20 - Homo sapiens (Human)	185.6 (M:185.6)	3	No	
RS23_HUMAN	40S ribosomal protein S23 - Homo sapiens (Human)	116.8 (M:116.8)	1	No	
RS24_HUMAN	40S ribosomal protein S24 - Homo sapiens (Human)	232.0 (M:232.0)	3	No	
RS25_HUMAN	40S ribosomal protein S25 - Homo sapiens (Human)	238.1 (M:238.1)	4	No	
RS26_HUMAN	40S ribosomal protein S26 - Homo sapiens (Human)	149.3 (M:149.3)	2	No	
RS3_HUMAN	40S ribosomal protein S3 - Homo sapiens (Human)	522.3 (M:522.3)	9	Yes	
RS3A_HUMAN	40S ribosomal protein S3a - Homo sapiens (Human)	426.2 (M:426.2)	2	No	
RS4X_HUMAN	40S ribosomal protein S4, X isoform (Single copy abundant mRNA protein) (SCR10) - Homo sapiens (Human)	407.0 (M:407.0)	3	Yes	
RS5_HUMAN	40S ribosomal protein S5 - Homo sapiens (Human)	318.1 (M:318.1)	5	No	
RS6_HUMAN	40S ribosomal protein S6 (Phosphoprotein NP33) - Homo sapiens (Human)	412.1 (M:412.1)	4	Yes	
RS7_HUMAN	40S ribosomal protein S7 - Homo sapiens (Human)	134.7 (M:134.7)	1	No	
RS8_HUMAN	40S ribosomal protein S8 - Homo sapiens (Human)	306.2 (M:306.2)	5	No	
RS9_HUMAN	40S ribosomal protein S9 - Homo sapiens (Human)	266.8 (M:266.8)	4	No	
RSSA_HUMAN	40S ribosomal protein SA (p40) (34/67 kDa laminin receptor) (Colon carcinoma laminin-binding protein) (NEM/1 CHD4) (Multidrug resistance-associated protein MGr1-Ag) - Homo sa 600.4 (M:600.4		7	Yes	
RUVB1_HUMAN	RuvB-like 1 (EC 3.6.1.-) (49 kDa TATA box-binding protein-interacting protein) (TIP49a) (Pontin 52) (Nuclear matrix protein 238) (NMP 238) (54 kDa TBP-interacting protein) (TIP49a)	101.2 (M:101.2)	1	No	
RUVB2_HUMAN	RuvB-like 2 (EC 3.6.1.-) (48 kDa TATA box-binding protein-interacting protein) (TIP49b) (Repressing pontin 52) (Repin 52) (51 kDa erythrocyte cyto 378.8 (M:378.8		4	Yes	
SCAM3_HUMAN	Secretory carrier-associated membrane protein 3 OS=Homo sapiens GN=SCAMP3 PE=1 SV=3	49.7 (M:49.7)	1	No	
SEP11_HUMAN	Septin-11 - Homo sapiens (Human)	131.4 (M:131.4)	1	No	
SEPT2_HUMAN	Septin-2 (Protein NEDD5) - Homo sapiens (Human)	455.9 (M:455.9)	5	No	
SEPT7_HUMAN	Septin-7 (CDC10 protein homolog) - Homo sapiens (Human)	136.8 (M:136.8)	1	No	
SEPT9_HUMAN	Septin-9 (MLL septin-like fusion protein) (MLL septin-like fusion protein MSF-A) (Ovarian/Breast septin) (Ov/Br septin) (Septin D1) - Homo sapiens (Human)	85.2 (M:85.2)	1	No	
SERA_HUMAN	D-3-phosphoglycerate dehydrogenase (EC 1.1.1.95) (3-PGDH) - Homo sapiens (Human)	106.9 (M:106.9)	3	No	
SF3B3_HUMAN	Splicing factor 3B subunit 3 (Spliceosome-associated protein 130) (SAP 130) (SF3b130) (Pre-mRNA-splicing factor SF3b 130 kDa subunit) (STAF130) - Homo sapiens (Human)	307.8 (M:307.8)	2	No	
SMC2_HUMAN	Structural maintenance of chromosomes protein 2 OS=Homo sapiens GN=SMC2 PE=1 SV=2	72.8 (M:72.8)	1	No	
SMD1_HUMAN	Small nuclear ribonucleoprotein Sm D1 (snRNP core protein D1) (Sm-D1) (Sm-D autoantigen) - Homo sapiens (Human)	120.6 (M:120.6)	2	Yes	1
SMD3_HUMAN	Small nuclear ribonucleoprotein Sm D3 (snRNP core protein D3) (Sm-D3) - Homo sapiens (Human)	77.6 (M:77.6)	1	No	
SND1_HUMAN	Staphylococcal nuclease domain-containing protein 1 (p100 co-activator) (EBNA2 coactivator p100) - Homo sapiens (Human)	141.8 (M:141.8)	1	Yes	
SPT19_HUMAN	Spermatogenesis-associated protein 19, mitochondrial precursor (Spermatogenic cell-specific gene 1 protein) (Spergen-1) - Homo sapiens (Human)	40.2 (M:40.2)	1	No	
SPTB2_HUMAN	Spectrin beta chain, brain 1 (Spectrin, non-erythroid beta chain 1) (Beta-II spectrin) (Fodrin beta chain) - Homo sapiens (Human)	239.4 (M:239.4)	2	Yes	
SRSF3_HUMAN	Serine/arginine-rich splicing factor 3 OS=Homo sapiens GN=SRSF3 PE=1 SV=1	146.8 (M:146.8)	1	No	
SSBP_HUMAN	Single-stranded DNA-binding protein, mitochondrial OS=Homo sapiens GN=SSBP1 PE=1 SV=1	96.5 (M:96.5)	2	No	
STAR9_HUMAN	StAR-related lipid transfer protein 9 OS=Homo sapiens GN=STARD9 PE=1 SV=3	151.9 (M:151.9)	1	No	

Goldie et al Supplementary Data S1.xls

ID	Description	Mass	Count	Exosome	Ref
SYDC_HUMAN	Aspartyl-tRNA synthetase, cytoplasmic (EC 6.1.1.12) (Aspartate--tRNA ligase) (AspRS) (Cell proliferation-inducing gene 40 protein) - Homo sapiens (Human)	71.7 (M:71.7)	1	Other	
SYG_HUMAN	Glycine--tRNA ligase OS=Homo sapiens GN=GARS PE=1 SV=3	104.7 (M:104.7)	1	Other	
SYHC_HUMAN	Histidyl-tRNA synthetase, cytoplasmic (EC 6.1.1.21) (Histidine--tRNA ligase) (HisRS) - Homo sapiens (Human)	72.9 (M:72.9)	1	Other	
SYIM_HUMAN	Isoleucyl-tRNA synthetase, mitochondrial precursor (EC 6.1.1.5) (Isoleucine--tRNA ligase) (IleRS) - Homo sapiens (Human)	50.9 (M:50.9)	1	Other	
SYNE2_HUMAN	Nesprin-2 - Homo sapiens (Human)	396.7 (M:396.7)	1	No	
SZT2_HUMAN	Protein SZT2 OS=Homo sapiens GN=SZT2 PE=2 SV=3	101.7 (M:101.7)	1	No	
TAF6L_HUMAN	TAF6-like RNA polymerase II p300/CBP-associated factor-associated factor 65 kDa subunit 6L (PCAF-associated factor 65 alpha) (PAF65-alpha) - Homo sapiens (Human)	73.9 (M:73.9)	1	No	
TAF9_HUMAN	Transcription initiation factor TFIID subunit 9 (Transcription initiation factor TFIID 31 kDa subunit) (TAFII-31) (TAFII-32) (STAF31/32) - Homo sapiens (Human)	47.9 (M:47.9)	1	No	
TAGL2_HUMAN	Transgelin-2 (SM22-alpha homolog) - Homo sapiens (Human)	98.2 (M:98.2)	1	No	
TBA1A_HUMAN	Tubulin alpha-1A chain OS=Homo sapiens GN=TUBA1A PE=1 SV=1	1093.2 (M:1093.2)	13	Yes	5
TBA1B_HUMAN	Tubulin alpha-1B chain OS=Homo sapiens GN=TUBA1B PE=1 SV=1	1043.3 (M:1043.3)	1	No	
TBB2B_HUMAN	Tubulin beta-2B chain - Homo sapiens (Human)	1005.4 (M:1005.4)	2	No	
TBB3_HUMAN	Tubulin beta-3 chain (Tubulin beta-III) (Tubulin beta-4) - Homo sapiens (Human)	1059.3 (M:1059.3)	2	Yes	
TBB4B_HUMAN	Tubulin beta-4B chain OS=Homo sapiens GN=TUBB4B PE=1 SV=1	1156.4 (M:1156.4)	4	No	
TBB5_HUMAN	Tubulin beta chain (Tubulin beta-5 chain) - Homo sapiens (Human)	1164.6 (M:1164.6)	16	Yes	
TCPA_HUMAN	T-complex protein 1 subunit alpha (TCP-1-alpha) (CCT-alpha) - Homo sapiens (Human)	410.6 (M:410.6)	3	Yes	
TCPB_HUMAN	T-complex protein 1 subunit beta (TCP-1-beta) (CCT-beta) - Homo sapiens (Human)	859.4 (M:859.4)	9	Yes	
TCPD_HUMAN	T-complex protein 1 subunit delta (TCP-1-delta) (CCT-delta) (Stimulator of TAR RNA-binding) - Homo sapiens (Human)	540.5 (M:540.5)	7	Yes	
TCPE_HUMAN	T-complex protein 1 subunit epsilon (TCP-1-epsilon) (CCT-epsilon) - Homo sapiens (Human)	154.1 (M:154.1)	1	Yes	
TCPG_HUMAN	T-complex protein 1 subunit gamma (TCP-1-gamma) (hTRiC5) - Homo sapiens (Human)	552.2 (M:552.2)	6	Yes	
TCPH_HUMAN	T-complex protein 1 subunit eta (TCP-1-eta) (CCT-eta) (HIV-1 Nef-interacting protein) - Homo sapiens (Human)	373.3 (M:373.3)	4	No	
TCPQ_HUMAN	T-complex protein 1 subunit theta (TCP-1-theta) (CCT-theta) (Renal carcinoma antigen NY-REN-15) - Homo sapiens (Human)	699.1 (M:699.1)	7	Yes	2
TCPZ_HUMAN	T-complex protein 1 subunit zeta (TCP-1-zeta) (CCT-zeta) (CCT-zeta-1) (Tcp20) (HTR3) (Acute morphine dependence-related protein 2) - Homo sapiens (Human)	396.3 (M:396.3)	5	Yes	2
TECR_HUMAN	Trans-2,3-enoyl-CoA reductase OS=Homo sapiens GN=TECR PE=1 SV=1	58.4 (M:58.4)	1	No	
TERA_HUMAN	Transitional endoplasmic reticulum ATPase (TER ATPase) (15S Mg(2+)ATPase p97 subunit) (Valosin-containing protein) (VCP) - Homo sapiens (Human)	2957.4 (M:2957.4)	36	Yes	
THB_HUMAN	Thyroid hormone receptor beta OS=Homo sapiens GN=THRB PE=1 SV=2	57.0 (M:57.0)	1	No	
TM198_HUMAN	Transmembrane protein 198 OS=Homo sapiens GN=TMEM198 PE=2 SV=1	40.4 (M:40.4)	1	No	
TPIS_HUMAN	Triosephosphate isomerase OS=Homo sapiens GN=TPI1 PE=1 SV=3	259.2 (M:259.2)	4	Yes	1, 5
TPM4_HUMAN	Tropomyosin alpha-4 chain (Tropomyosin-4) (TM30p1) - Homo sapiens (Human)	69.2 (M:69.2)	1	No	
TPP2_HUMAN	Tripeptidyl-peptidase 2 (EC 3.4.14.10) (Tripeptidyl-peptidase II) (TPP-II) (Tripeptidyl aminopeptidase) - Homo sapiens (Human)	383.0 (M:383.0)	4	Other	
TPR_HUMAN	Nucleoprotein TPR OS=Homo sapiens GN=TPR PE=1 SV=3	396.6 (M:396.6)	2	No	
TPX2_HUMAN	Targeting protein for Xklp2 (Restricted expression proliferation-associated protein 100) (p100) (Differentially expressed in cancerous and noncancerous lung cells 2) (DIL-2) (Protein l68.1	68.1 (M:68.1)	1	No	
TR56_HUMAN	Tripartite motif-containing protein 56 (RING finger protein 109) - Homo sapiens (Human)	41.2 (M:41.2)	1	No	
TRPM7_HUMAN	Transient receptor potential cation channel subfamily M member 7 (EC 2.7.11.1) (Long transient receptor potential channel 7) (LTrpC7) (Channel-kinase 1) - Homo sapiens (Human)	41.5 (M:41.5)	1	No	
TRRAP_HUMAN	Transformation/transcription domain-associated protein - Homo sapiens (Human)	174.2 (M:174.2)	2	No	
TRY1_HUMAN	Trypsin-1 precursor (EC 3.4.21.4) (Trypsin I) (Cationic trypsinogen) (Serine protease 1) - Homo sapiens (Human)	83.7 (M:83.7)	1	No	
TRYP_PIG	Trypsin precursor - Sus scrofa (Pig)	180.4 (M:180.4)	3	No	
TSN_HUMAN	Translin - Homo sapiens (Human)	98.8 (M:98.8)	2	No	
UBR5_HUMAN	E3 ubiquitin-protein ligase UBR5 OS=Homo sapiens GN=UBR5 PE=1 SV=2	130.1 (M:130.1)	3	No	
UGPA_HUMAN	UTP--glucose-1-phosphate uridylyltransferase OS=Homo sapiens GN=UGP2 PE=1 SV=5	173.0 (M:173.0)	3	No	
VATB2_HUMAN	Vacuolar ATP synthase subunit B, brain isoform (EC 3.6.3.14) (V-ATPase B2 subunit) (Vacuolar proton pump B isoform 2) (Endomembrane proton pump B isoform 2) - Homo sapiens (Human) - Hk 155.6	155.6 (M:155.6)	2	Other	
VATE1_HUMAN	V-type proton ATPase subunit E 1 OS=Homo sapiens GN=ATP6V1E1 PE=1 SV=1	82.3 (M:82.3)	1	No	
VGF_HUMAN	Neurosecretory protein VGF OS=Homo sapiens GN=VGF PE=1 SV=2	235.1 (M:235.1)	1	No	
VTI1A_HUMAN	Vesicle transport through interaction with t-SNAREs homolog 1A OS=Homo sapiens GN=VTI1A PE=1 SV=2	78.1 (M:78.1)	1	Yes	6
XPOT_HUMAN	Exportin-T (tRNA exportin) (Exportin(tRNA)) - Homo sapiens (Human)	66.7 (M:66.7)	1	No	
Y5087_PSEA7	UPF0307 protein PSPA7_5087 OS=Pseudomonas aeruginosa (strain PA7) GN=PSPA7_5087 PE=3 SV=1	40.6 (M:40.6)	1	No	
YBOX1_HUMAN	Nuclease sensitive element-binding protein 1 (Y-box-binding protein 1) (Y-box transcription factor) (YB-1) (CCAAT-binding transcription factor I subunit A) (CBF-A) (Enhancer factor I subunit A)	123.4 (M:123.4)	2	No	
ZPBP1_HUMAN	Zona pellucida-binding protein 1 precursor (Sp38) - Homo sapiens (Human)	67.3 (M:67.3)	1	No	
ZSC12_HUMAN	Zinc finger and SCAN domain-containing protein 12 OS=Homo sapiens GN=ZSCAN12 PE=2 SV=1	99.9 (M:99.9)	1	No	

Identified proteins were compared to the exosome compositions reported for the following sources:

1.- Urine.
Pisitkun T, Shen R-F, Knepper MA (2004) Identification and proteomic profiling of exosomes in human urine. Proceedings of the National Academy of Sciences 101:13368-13373.

2.- Dentritic Cells.
Segura E, Nicco C, Lombard B, Veron P, Raposo G, Batteux F, Amigorena S, et al. (2005) ICAM-1 on exosomes from mature dendritic cells is critical for efficient naive T-cell priming. Blood 106:216-223.

3.- Dentritic Cells.
Thery C, Regnault A, Garin J, Wolfers J, Zitvogel L, Ricciardi-Castagnoli P, Raposo G, et al. (1999) Molecular characterization of dendritic cell-derived exosomes. Selective accumulation of the heat shock protein hsc73. J Cell Biol 147:599-610.

4.- Intestinal Epithelial cells.
Van Niel G, Mallegol J, Bevilacqua C, Candalh C, Brugiere S, Tomaskovic-Crook E, Heath JK, et al. (2003) Intestinal epithelial exosomes carry MHC class II/peptides able to inform the immune system in mice. Gut 52:1690-1697.

5.- Schwann-immortalized cells (Mov Cells).

Fevrier B, Vilette D, Archer F, Loew D, Faigle W, Vidal M, Laude H, et al. (2004) Cells release prions in association with exosomes. Proc Natl Acad Sci U S A 101:9683-9688.

6.- Microglial cell line N9

Potolicchio I, Carven GJ, Xu X, Stipp C, Riese RJ, Stern LJ, Santambrogio L (2005) Proteomic analysis of microglia-derived exosomes: metabolic role of the aminopeptidase CD13 in neuropeptide catabolism. J Immunol 175:2237-2243.

7.- Human B-Cells.

Wubbolts R, Leckie RS, Veenhuizen PT, Schwarzmann G, Mobius W, Hoernschemeyer J, Slot JW, et al. (2003) Proteomic and biochemical analyses of human B cell-derived exosomes. Potential implications for their function and multivesicular body formation. J Biol Chem 278:10963-10972.

8.- Mast Cells.

Skokos D, Le Panse S, Villa I, Rousselle JC, Peronet R, David B, Namane A, et al. (2001) Mast cell-dependent B and T lymphocyte activation is mediated by the secretion of immunologically active exosomes. J Immunol 166:868-876.

9.- Mast Cell line MC/9.

Valadi H, Ekstrom K, Bossios A, Sjostrand M, Lee JJ, Lotvall JO (2007) Exosome-mediated transfer of mRNAs and microRNAs is a novel mechanism of genetic exchange between cells. Nat Cell Biol 9:654-659.

10.- Pleural fluid.

Bard MP, Hegmans JP, Hemmes A, Luider TM, Willemsen R, Severijnen LA, van Meerbeeck JP, et al. (2004) Proteomic analysis of exosomes isolated from human malignant pleural effusions. Am J Respir Cell Mol Biol 31:114-121.

11.- Mesothelioma Cells.

Hegmans JP, Bard MP, Hemmes A, Luider TM, Kleijmeer MJ, Prins JB, Zitvogel L, et al. (2004) Proteomic analysis of exosomes secreted by human mesothelioma cells. Am J Pathol164:1807-1815.

12.- Ram Epididymal Fluid.

Gatti JL, Metayer S, Belghazi M, Dacheux F, Dacheux JL (2005) Identification, proteomic profiling, and origin of ram epididymal fluid exosome-like vesicles. Biol Reprod 72:1452-1465.

13.- Adipocytes (3T3-L1 cells).

Aoki N, Jin-no S, Nakagawa Y, Asai N, Arakawa E, Tamura N, Tamura T, et al. (2007) Identification and characterization of microvesicles secreted by 3T3-L1 adipocytes: redox- and hormone-dependent induction of milk fat globule-epidermal growth factor 8-associated microvesicles. Endocrinology 148:3850-3862.

14.- Synovial fibroblasts.

Zhang HG, Liu C, Su K, Yu S, Zhang L, Zhang S, Wang J, et al. (2006) A membrane form of TNF-alpha presented by exosomes delays T cell activation-induced cell death. J Immunol 176:7385-7393.

15.- IMCD cells from rat kidneys.

Barile M, Pisitkun T, Yu MJ, Chou CL, Verbalis MJ, Shen RF, Knepper MA (2005) Large scale protein identification in intracellular aquaporin-2 vesicles from renal inner medullary collecting duct. Mol Cell Proteomics 4:1095-1106.

ADDITIONAL FILE 9

Supplementary Data S2. Gene Ontology analysis of proteins identified in exosomes by mass spectrometry.

GO id	Description	q-value	Occurrences in Sample	Occurrences in Genome
GO:0051084	'de novo' posttranslational protein folding	5.96E-35	20	37
GO:0006458	'de novo' protein folding	9.48E-34	20	42
GO:0006457	protein folding	9.39E-28	22	111
GO:0051352	negative regulation of ligase activity	1.84E-20	16	71
GO:0051444	negative regulation of ubiquitin-protein ligase activity	1.84E-20	16	71
GO:0031397	negative regulation of protein ubiquitination	2.39E-19	16	83
GO:0072431	signal transduction involved in mitotic cell cycle G1/S transition DNA damage checkpoint	2.45E-19	15	67
GO:0051436	negative regulation of ubiquitin-protein ligase activity involved in mitotic cell cycle	2.45E-19	15	67
GO:0072413	signal transduction involved in mitotic cell cycle checkpoint	2.45E-19	15	67
GO:0006977	DNA damage response, signal transduction by p53 class mediator resulting in cell cycle arrest	2.45E-19	15	67
GO:0000502	proteasome complex	2.45E-19	13	37
GO:0072474	signal transduction involved in mitotic cell cycle G1/S checkpoint	2.45E-19	15	67
GO:0072422	signal transduction involved in DNA damage checkpoint	2.51E-19	15	68
GO:0072401	signal transduction involved in DNA integrity checkpoint	2.51E-19	15	68
GO:0072404	signal transduction involved in G1/S transition checkpoint	2.51E-19	15	68
GO:0072395	signal transduction involved in cell cycle checkpoint	2.99E-19	15	69
GO:0002479	antigen processing and presentation of exogenous peptide antigen via MHC class I, TAP-dependent	4.52E-19	15	71
GO:0051438	regulation of ubiquitin-protein ligase activity	4.71E-19	16	92
GO:0051437	positive regulation of ubiquitin-protein ligase activity involved in mitotic cell cycle	5.09E-19	15	72
GO:0031400	negative regulation of protein	6.07E-19	18	146

	modification process			
GO:0051340	regulation of ligase activity	6.32E-19	16	95
GO:0042590	antigen processing and presentation of exogenous peptide antigen via MHC class I	6.32E-19	15	74
GO:0031571	mitotic cell cycle G1/S transition DNA damage checkpoint	6.32E-19	15	74
GO:0006521	regulation of cellular amino acid metabolic process	6.32E-19	14	56
GO:0019884	antigen processing and presentation of exogenous antigen	7.27E-19	15	75
GO:0002478	antigen processing and presentation of exogenous peptide antigen	7.27E-19	15	75
GO:0051439	regulation of ubiquitin-protein ligase activity involved in mitotic cell cycle	1.33E-18	15	78
GO:0000216	M/G1 transition of mitotic cell cycle	1.47E-18	15	79
GO:0071158	positive regulation of cell cycle arrest	1.47E-18	15	79
GO:0051443	positive regulation of ubiquitin-protein ligase activity	1.47E-18	15	79
GO:0051351	positive regulation of ligase activity	2.53E-18	15	82
GO:0031575	mitotic cell cycle G1/S transition checkpoint	2.53E-18	15	82
GO:0033238	regulation of cellular amine metabolic process	2.81E-18	14	63
GO:0031145	anaphase-promoting complex-dependent proteasomal ubiquitin-dependent protein catabolic process	2.89E-18	15	83
GO:0071779	G1/S transition checkpoint	4.13E-18	15	85
GO:0031398	positive regulation of protein ubiquitination	4.93E-18	16	110
GO:0031396	regulation of protein ubiquitination	6.58E-18	17	140
GO:0002474	antigen processing and presentation of peptide antigen via MHC class I	9.52E-18	15	90
GO:2000045	regulation of G1/S transition of mitotic cell cycle	1.86E-17	15	94
GO:0048002	antigen processing and presentation of peptide antigen	2.15E-17	15	95
GO:0051248	negative regulation of protein metabolic process	5.31E-17	19	232
GO:0007093	mitotic cell cycle checkpoint	8.89E-17	16	132
GO:0019882	antigen processing and presentation	1.31E-16	15	107
GO:0032269	negative regulation of cellular protein metabolic process	1.43E-16	18	205

GO:0030330	DNA damage response, signal transduction by p53 class mediator	2.57E-16	15	112
GO:0072331	signal transduction by p53 class mediator	4.97E-16	15	117
GO:0000077	DNA damage checkpoint	1.54E-15	15	126
GO:0042770	signal transduction in response to DNA damage	1.89E-15	15	128
GO:0000084	S phase of mitotic cell cycle	1.89E-15	15	128
GO:0090068	positive regulation of cell cycle process	2.09E-15	15	129
GO:2000602	regulation of interphase of mitotic cell cycle	2.30E-15	15	130
GO:0031570	DNA integrity checkpoint	2.86E-15	15	132
GO:0051320	S phase	3.97E-15	15	135
GO:0000209	protein polyubiquitination	1.60E-14	15	148
GO:0010565	regulation of cellular ketone metabolic process	6.35E-14	14	128
GO:0000082	G1/S transition of mitotic cell cycle	1.16E-13	15	169
GO:0007346	regulation of mitotic cell cycle	1.75E-13	17	260
GO:0043161	proteasomal ubiquitin-dependent protein catabolic process	6.51E-13	15	190
GO:0000075	cell cycle checkpoint	7.10E-13	16	235
GO:0010498	proteasomal protein catabolic process	1.08E-12	15	197
GO:0006414	translational elongation	2.06E-12	12	97
GO:0071156	regulation of cell cycle arrest	2.44E-12	16	255
GO:0044257	cellular protein catabolic process	1.98E-11	16	292
GO:0006511	ubiquitin-dependent protein catabolic process	8.02E-11	15	265
GO:0019941	modification-dependent protein catabolic process	9.30E-11	15	268
GO:0043632	modification-dependent macromolecule catabolic process	1.08E-10	15	271
GO:0051603	proteolysis involved in cellular protein catabolic process	1.99E-10	15	283
GO:0044445	cytosolic part	6.24E-08	10	134
GO:0000184	nuclear-transcribed mRNA catabolic process, nonsense-mediated decay	2.89E-07	9	113
GO:0006415	translational termination	8.06E-07	8	87
GO:0022626	cytosolic ribosome	8.71E-07	8	88
GO:0006612	protein targeting to membrane	1.18E-06	9	133
GO:0034623	cellular macromolecular complex disassembly	1.61E-06	9	138
GO:0003735	structural constituent of ribosome	1.68E-06	8	96
GO:0032984	macromolecular complex disassembly	2.02E-06	9	142
GO:0006614	SRP-dependent cotranslational protein targeting to membrane	3.09E-06	8	104

GO:0045047	protein targeting to ER	3.21E-06	8	105
GO:0006613	cotranslational protein targeting to membrane	3.21E-06	8	105
GO:0072599	establishment of protein localization in endoplasmic reticulum	3.21E-06	8	105
GO:0070972	protein localization in endoplasmic reticulum	4.92E-06	8	111
GO:0071845	cellular component disassembly at cellular level	5.62E-06	10	217
GO:0072594	establishment of protein localization to organelle	6.16E-06	9	163
GO:0022411	cellular component disassembly	6.25E-06	10	220
GO:0000956	nuclear-transcribed mRNA catabolic process	6.35E-06	9	164
GO:0043624	cellular protein complex disassembly	7.00E-06	8	117
GO:0044391	ribosomal subunit	8.44E-06	8	120
GO:0043241	protein complex disassembly	8.91E-06	8	121
GO:0006402	mRNA catabolic process	9.62E-06	9	173
GO:0022625	cytosolic large ribosomal subunit	1.31E-05	6	50
GO:0006401	RNA catabolic process	2.99E-05	9	198
GO:0006413	translational initiation	3.67E-05	8	146
GO:0019083	viral transcription	3.98E-05	8	148
GO:0019080	viral genome expression	3.98E-05	8	148
GO:0030705	cytoskeleton-dependent intracellular transport	4.26E-05	5	32
GO:0005840	ribosome	4.79E-05	8	152
GO:0015934	large ribosomal subunit	6.61E-05	6	66
GO:0019058	viral infectious cycle	7.61E-05	9	223
GO:0007411	axon guidance	7.91E-05	10	294
GO:0022415	viral reproductive process	1.58E-04	9	244
GO:0051131	chaperone-mediated protein complex assembly	0.002885291	3	12
GO:0050750	low-density lipoprotein particle receptor binding	0.002885291	3	12
GO:0070325	lipoprotein particle receptor binding	0.008698574	3	17
GO:0051082	unfolded protein binding	0.01332208	4	53
GO:0008135	translation factor activity, nucleic acid binding	0.018816276	4	58
GO:0051301	cell division	0.022195081	5	115
GO:0034381	plasma lipoprotein particle clearance	0.027637205	3	25
GO:0000086	G2/M transition of mitotic cell cycle	0.04454137	5	134
GO:0009615	response to virus	0.074237843	5	150
GO:0006913	nucleocytoplasmic transport	0.082173792	6	236
GO:0051169	nuclear transport	0.087043929	6	239

APPENDIX III

Chapter 5 Additional Files

ADDITIONAL FILE 1
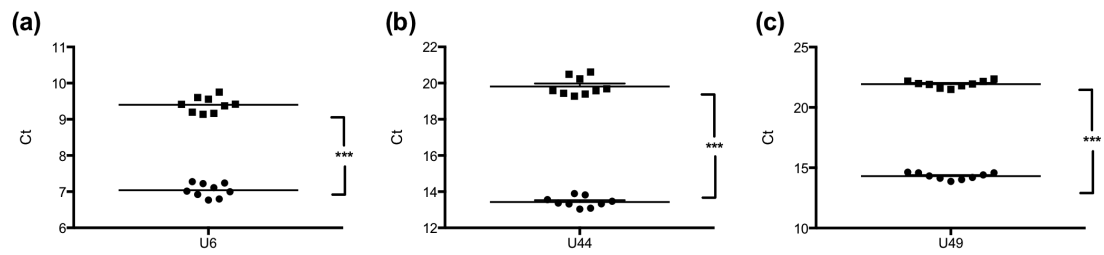
Supplementary Figure S1. Compartmental reference gene expression qPCR. Cycle detection threshold for (a) U6, (b) U44 and (c) U49. ■, cytoplasm; •, nucleus. ***, p<0.001. Results demonstrated consistency between experimental replicates, but significantly different expression between compartments.

ADDITIONAL FILE 2
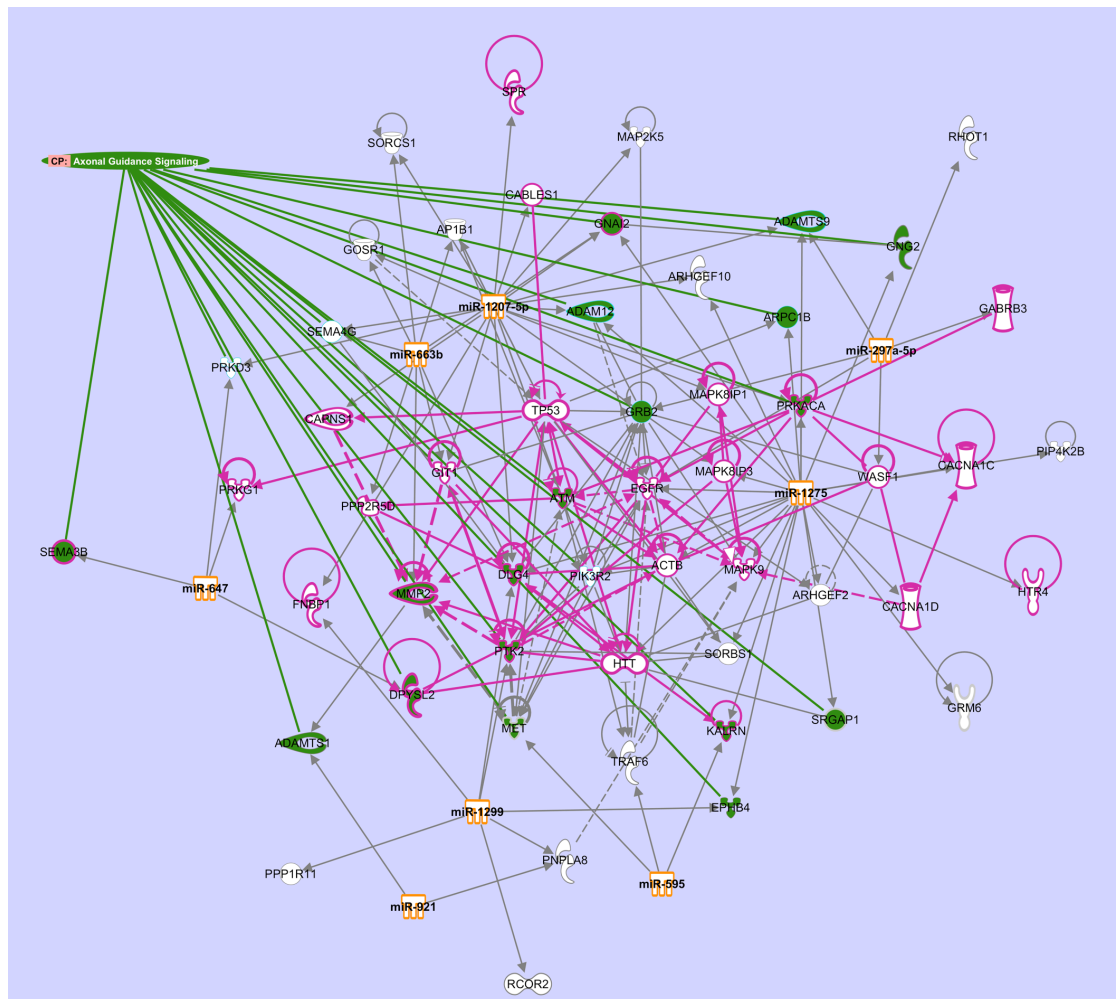
Supplementary Figure S2. "Axon Guiding Signalling" is enriched in nuclear Ago2 RIP-seq. Ago2-associated mRNA identified by RIP-seq were filtered for predicted targets of nucleus-enriched miRNA. Core analysis identified significant enrichment of "Axonal Guidance Signaling" (green) and "Nervous System Development and Function" (pink). Network generated using IPA software.

ADDITIONAL FILE 3

Supplementary Table S1. Nuclear enrichment of miRNA in SH-SY5Y.

Mature miRNA	Raw Expression Cytoplasm	Raw Expression Nucleus	Nuclear % of total
hsa-miR-768-5p	632.4299	10223.281	94.1742194
hsa-miR-768-3p	380.70798	5669.1206	93.70712781
hsa-miR-1299	6.865166	93.65542	93.170388
hsa-miR-297	7.3870163	94.01574	92.71517208
hsa-miR-1201	5.3476424	66.47131	92.55399554
hsa-miR-663b	45.643597	537.6604	92.17498984
hsa-miR-647	9.583795	79.09322	89.19247
hsa-miR-1248	3.388134	25.204283	88.15023578
hsa-miR-595	19.243858	142.33234	88.0899178
hsa-miR-148b*	4.166365	27.230688	86.73007623
hsa-miR-921	30.8864	160.05347	83.82401748
hsa-miR-32*	5.997028	28.369547	82.54982348
hsa-miR-593*	35.417072	147.32124	80.61869369
hsa-miR-125b-1*	7.8984885	31.823034	80.11534301
hsa-miR-1291	9.81671	36.088696	78.61535088
hsa-miR-1183	55.099842	198.55347	78.27749949
hsa-miR-300	4.4833255	16.116777	78.23639227
hsa-miR-1305	3.3115141	11.634234	77.84310241
hsa-miR-34b	5.869924	20.129953	77.42326243
hsa-miR-664*	165.62343	508.84592	75.44389082
hsa-miR-335*	4.313956	13.230105	75.41073301
hsa-miR-1279	5.3603215	15.512283	74.31886615
hsa-miR-1275	367.72522	1039.6671	73.87187533
hsa-miR-1322	4.12467	11.567449	73.71502217
hsa-miR-648	9.128713	23.488218	72.01234843
hsa-miR-574-5p	289.71848	742.6009	71.93518928
hsa-miR-554	4.4645925	11.400543	71.85909632
hsa-miR-584	7.407421	18.506092	71.41483287
hsa-miR-206	7.712482	18.785023	70.89355394
hsa-miR-640	6.592426	15.7988	70.55799446
hsa-miR-650	14.3974085	33.674038	70.04997863
hsa-miR-34c-3p	16.528984	34.26302	67.45750768
hsa-miR-601	6.52156	13.159968	66.86456458
hsa-miR-513a-5p	13.817599	27.282816	66.38087718
hsa-miR-99a*	6.326794	12.380191	66.17950995
hsa-miR-612	9.381312	18.279535	66.08450927
hsa-miR-622	3.218372	6.266047	66.06674589
hsa-miR-1273	8.719127	16.911835	65.98205327
hsa-miR-610	4.3348923	7.9906883	64.83011681
hsa-miR-564	30.666649	56.267475	64.72426754
hsa-miR-187*	30.398596	54.79749	64.31925758

hsa-miR-1306	31.652609	56.807774	64.21832246
hsa-miR-567	3.6247628	6.469873	64.09218845
hsa-miR-519e*	16.60502	29.345072	63.86292328
hsa-miR-221	55.121487	96.3623	63.61228611
hsa-miR-548l	3.1469505	5.495529	63.58741146
hsa-miR-453	3.1778023	5.505877	63.40488645
hsa-miR-31*	3.7469432	6.4586463	63.285382
hsa-miR-661	4.480894	7.623651	62.98172298
hsa-miR-608	13.722169	22.91511	62.54588393
hsa-miR-1282	2.6801555	4.386671	62.07412903
hsa-miR-630	4.6057277	7.5185857	62.01246579
hsa-miR-890	4.0902286	6.5216846	61.45625654
hsa-miR-1207-5p	2468.3574	3914.0564	61.32564454
hsa-miR-525-5p	4.190682	6.6362367	61.29386286
hsa-miR-765	38.466484	60.401913	61.093246
hsa-miR-324-5p	1886.2516	2914.5996	60.71005908
hsa-miR-337-3p	9.185412	14.087007	60.53091
hsa-miR-518d-3p	2.522268	3.8646328	60.50873375
hsa-miR-548c-5p	3.9660928	6.050573	60.40506013
hsa-miR-708*	6.542236	9.964146	60.36541503
hsa-miR-101*	7.586657	11.477868	60.20537097
hsa-miR-551b	48.60094	72.86701	59.98867191
hsa-miR-16-1*	9.591605	14.336322	59.91460104
hsa-miR-623	10.543012	15.634034	59.72421029
hsa-miR-33a*	3.1147358	4.517444	59.18943367
hsa-miR-192*	5.318157	7.6770988	59.07616532
hsa-miR-574-3p	1809.9048	2608.1238	59.03365587
hsa-miR-559	3.8197925	5.4907017	58.97325729
hsa-miR-452*	3.2060583	4.556457	58.69820315
hsa-miR-892a	3.30435	4.6420264	58.41689553
hsa-miR-583	4.011557	5.628515	58.38664898
hsa-miR-520c-5p	4.3596997	6.1051383	58.33953951
hsa-miR-582-3p	3.296154	4.5728936	58.11241503
hsa-miR-1234	28.34774	39.325138	58.11063333
hsa-miR-194*	14.054751	19.485975	58.0964616
hsa-miR-1204	2.917802	4.0212646	57.95108812
hsa-miR-1268	1735.3385	2385.5664	57.8893825
hsa-miR-211	5.611794	7.697965	57.83699765
hsa-miR-523	3.3382447	4.5559754	57.71279927
hsa-miR-1257	3.4385707	4.683028	57.661406
hsa-miR-1255b	6.1577396	8.332136	57.50315758
hsa-miR-520d-3p	3.4191885	4.6262474	57.50151337
hsa-miR-520d-5p	3.1700528	4.2831607	57.46730186
hsa-miR-1203	8.64974	11.571727	57.22496296
hsa-miR-122	2.921875	3.8751326	57.0123329
hsa-miR-659	41.95262	55.57088	56.98204023
hsa-miR-223	4.9931083	6.605541	56.95095031
hsa-miR-1289	3.2395904	4.2801175	56.91866701

hsa-miR-545	2.8832896	3.796396	56.83495044
hsa-miR-1182	39.060856	51.38503	56.81300972
hsa-miR-1246	182.69478	240.2253	56.80158294
hsa-miR-1200	3.1585228	4.1377378	56.71038943
hsa-miR-582-5p	2.8488748	3.7186584	56.62184395
hsa-miR-548d-5p	3.410385	4.438947	56.55190786
hsa-miR-28-3p	2.3852904	3.1044319	56.5498896
hsa-miR-657	4.274651	5.5456696	56.47137019
hsa-miR-519e	3.3373387	4.32068	56.42033755
hsa-miR-34c-5p	2.5835934	3.3444107	56.41714553
hsa-miR-613	3.436903	4.415497	56.23117773
hsa-miR-619	3.7575119	4.823458	56.21110499
hsa-miR-938	5.9119854	7.5669723	56.13915014
hsa-miR-371-3p	3.889109	4.9764905	56.13258866
hsa-miR-518d-5p	3.2682116	4.149583	55.94092616
hsa-miR-942	2.5239007	3.203126	55.92999942
hsa-miR-373	2.5912197	3.2747746	55.82641974
hsa-miR-631	7.3690605	9.291798	55.77022337
hsa-miR-1264	3.1065953	3.8910236	55.60496585
hsa-miR-1249	9.356734	11.693383	55.55020431
hsa-miR-518c	2.733483	3.408376	55.49420786
hsa-miR-195*	73.34733	91.03884	55.38108224
hsa-miR-219-2-3p	4.0832343	5.0679097	55.38006724
hsa-miR-662	5.065678	6.2644134	55.29005176
hsa-miR-200a	2.9892318	3.6700394	55.11172754
hsa-miR-105*	3.1712615	3.883487	55.04784472
hsa-miR-1298	3.2394285	3.9581263	54.9926525
hsa-miR-31	85.92651	104.12655	54.78814706
hsa-miR-513c	2.637334	3.1937132	54.7708343
hsa-miR-1197	2.6786785	3.2347877	54.70205782
hsa-miR-517*	3.728997	4.4925	54.6433332
hsa-miR-367*	3.4134655	4.109936	54.62869421
hsa-miR-770-5p	3.6922958	4.436167	54.57571879
hsa-miR-219-5p	2.6098216	3.1167853	54.42638816
hsa-miR-220c	5.7874875	6.8990893	54.38101553
hsa-miR-21*	9.199001	10.964189	54.3772538
hsa-miR-590-5p	24.69986	29.345154	54.29761569
hsa-miR-1258	3.8264787	4.527631	54.19645136
hsa-miR-625*	5.610435	6.636768	54.19007099
hsa-miR-620	2.9156625	3.4464567	54.1715204
hsa-miR-611	3.6524668	4.3074503	54.11426081
hsa-miR-135a	2.570999	3.0285199	54.08535901
hsa-miR-384	2.385206	2.7937984	53.94470026
hsa-miR-509-3p	3.5192115	4.1074696	53.8565799
hsa-miR-188-5p	139.63348	162.67561	53.81102169
hsa-miR-1253	3.9888973	4.6460595	53.80524313
hsa-miR-548j	3.1183698	3.6224606	53.73908532
hsa-miR-556-3p	2.6174233	3.0319834	53.66905873

hsa-miR-651	2.8599033	3.312765	53.66828151
hsa-miR-888	2.7373154	3.1691906	53.65592789
hsa-miR-1297	2.3681152	2.7233057	53.48812745
hsa-miR-639	6.2302403	7.164414	53.48711389
hsa-miR-548n	2.8945506	3.3177521	53.40615646
hsa-miR-607	2.862131	3.2787774	53.3923841
hsa-miR-224	3.6241558	4.1475096	53.36706338
hsa-let-7f-1*	6.5078316	7.430555	53.31000792
hsa-miR-431*	4.596212	5.231693	53.23304407
hsa-miR-593	4.870609	5.5384965	53.20818873
hsa-miR-200a*	3.1143503	3.539381	53.19392744
hsa-miR-542-5p	30.794899	34.946175	53.1572925
hsa-miR-454*	4.392967	4.963557	53.04915586
hsa-miR-1272	7.49785	8.471614	53.04883119
hsa-miR-558	2.6641395	3.0009592	52.97276109
hsa-miR-1207-3p	3.2574425	3.6652577	52.94549228
hsa-miR-571	3.1748924	3.570325	52.93120723
hsa-miR-875-5p	2.8811414	3.2312949	52.86427116
hsa-miR-645	3.1614268	3.5426452	52.84318546
hsa-miR-20a	22147.1	24815.264	52.84074711
hsa-miR-548e	2.8982785	3.2436092	52.81127494
hsa-miR-380	3.1891062	3.5633698	52.77130641
hsa-miR-516a-5p	2.9188411	3.2564204	52.73331988
hsa-miR-649	3.335304	3.7208922	52.73226671
hsa-miR-127-5p	4.435023	4.9468493	52.72774071
hsa-miR-548a-5p	2.6069486	2.9074504	52.72470128
hsa-miR-520b	2.9625893	3.292999	52.64091628
hsa-miR-216b	3.7474804	4.147573	52.5338182
hsa-miR-524-5p	4.482926	4.9397435	52.4240344
hsa-miR-616*	3.4697669	3.8229425	52.42142927
hsa-miR-142-3p	2.8239126	3.108936	52.40207883
hsa-miR-576-3p	3.3360138	3.6620731	52.32963169
hsa-miR-1263	8.8666315	9.71306	52.27783249
hsa-miR-1283	3.0169086	3.2998774	52.23981626
hsa-miR-573	3.7883189	4.139318	52.21376877
hsa-miR-802	2.896886	3.1621857	52.18927678
hsa-miR-325	3.5479076	3.8726857	52.18835669
hsa-miR-518e	3.7743251	4.118309	52.17914511
hsa-miR-875-3p	3.4712346	3.7845821	52.15928484
hsa-miR-493	5.715385	6.213001	52.08584799
hsa-miR-136*	2.5562398	2.767109	51.98060664
hsa-miR-147b	3.6865857	3.9817035	51.92427406
hsa-miR-568	3.016991	3.2580004	51.92039626
hsa-let-7a*	2.9226923	3.1536725	51.90064461
hsa-miR-618	3.7010784	3.9824693	51.83112613
hsa-miR-19b-2*	2.9883366	3.210801	51.79431733
hsa-miR-1259	4.0792994	4.3824115	51.79108045
hsa-miR-1256	4.790755	5.1463256	51.78910997

hsa-miR-150	5.0852675	5.4555054	51.75621799
hsa-miR-520e	3.3477771	3.5858955	51.71711598
hsa-miR-923	9101.707	9734.614	51.68001756
hsa-miR-221*	4.0695853	4.3413005	51.61525912
hsa-miR-33a	3.3727195	3.5978107	51.61459167
hsa-miR-519c-3p	3.7692604	4.01959	51.60697399
hsa-miR-132*	18.078497	19.270647	51.59595358
hsa-miR-520c-3p	3.421252	3.630685	51.48493244
hsa-miR-1284	6.09176	6.463759	51.48141626
hsa-miR-200b	3.5025787	3.7157977	51.476918
hsa-miR-183*	4.767676	5.040652	51.39155216
hsa-miR-519b-5p	2.8489125	3.0042865	51.32725711
hsa-miR-219-1-3p	9.018294	9.504196	51.3116541
hsa-miR-323-5p	14.265897	14.972653	51.20860303
hsa-miR-17*	1137.8087	1193.6232	51.19700044
hsa-miR-635	6.7392044	7.0447564	51.10836067
hsa-miR-924	2.5877779	2.6931963	50.99809615
hsa-miR-524-3p	2.6782057	2.7809374	50.94091415
hsa-miR-1265	2.7921307	2.8870814	50.83594959
hsa-miR-96	3.5496995	3.6691716	50.8274985
hsa-miR-17	28200.74	28995.975	50.69517541
hsa-miR-130a*	3.7931728	3.898547	50.68498465
hsa-miR-208b	3.6553793	3.751401	50.64820135
hsa-miR-433	4.162376	4.2701726	50.63916975
hsa-miR-200b*	5.7268033	5.864204	50.59270388
hsa-miR-220a	3.632107	3.7149916	50.56406348
hsa-miR-302a*	3.9422448	4.0262766	50.52727348
hsa-miR-621	5.052355	5.1588864	50.52163785
hsa-miR-1267	10.576594	10.79539	50.51187573
hsa-miR-106a	26101.924	26631.123	50.50177169
hsa-miR-526b	4.445262	4.527101	50.45606157
hsa-miR-371-5p	41.443954	42.179478	50.43978343
hsa-miR-130a	4143.551	4214.8184	50.42632358
hsa-miR-1321	8.454694	8.584232	50.38012372
hsa-miR-155	3.2222548	3.262654	50.31148626
hsa-miR-526b*	2.7157676	2.7452452	50.26989133
hsa-miR-302d	3.0181458	3.0461304	50.23073322
hsa-miR-519a*	2.607608	2.6296413	50.21035183
hsa-miR-106b	23379.49	23562.635	50.19507532
hsa-miR-302d*	3.795952	3.8203924	50.16044705
hsa-miR-548b-5p	3.2936203	3.310623	50.12872557
hsa-miR-217	2.812524	2.8244598	50.10587045
hsa-miR-1826	15385.52	15449.406	50.10359357
hsa-miR-450b-5p	4.667299	4.678017	50.05734424
hsa-miR-302a	2.6088722	2.6127436	50.0370709
hsa-miR-141	2.9668043	2.948818	49.84797626
hsa-miR-877*	16.881926	16.77402	49.83969252
hsa-miR-93	27809.85	27627.72	49.83573414

hsa-miR-492	4.9874964	4.9536586	49.82980951
hsa-miR-190	2.7018137	2.6827343	49.82283193
hsa-miR-617	3.650381	3.6234455	49.81484642
hsa-miR-577	2.8833935	2.8587215	49.78516627
hsa-miR-518f*	3.2712584	3.242691	49.78072135
hsa-miR-526a	5.3062987	5.2503085	49.73480968
hsa-miR-92a	27539.588	27213.69	49.70239407
hsa-miR-373*	17.401028	17.162962	49.65561557
hsa-miR-517a	3.0697553	3.016674	49.56393727
hsa-miR-521	3.8164062	3.7477138	49.54593264
hsa-miR-516b*	2.8252592	2.7735033	49.53779161
hsa-miR-222	75.8617	74.404144	49.51500755
hsa-miR-548m	3.2913883	3.2252429	49.49248777
hsa-miR-107	22732.686	22172.178	49.37589389
hsa-miR-499-3p	4.1370482	4.0244765	49.31035129
hsa-miR-191	17980.83	17451.248	49.25268001
hsa-miR-522	3.5907679	3.4843795	49.24815418
hsa-miR-552	5.5400066	5.36936	49.21788952
hsa-miR-16	21772.672	21100.967	49.21664569
hsa-let-7a	27118.63	26278.791	49.21359592
hsa-miR-26a	19085.176	18417.084	49.10926435
hsa-miR-203	10.358785	9.994086	49.10406006
hsa-miR-888*	3.0911977	2.9803555	49.08720062
hsa-miR-513a-3p	3.5532658	3.4163523	49.01778334
hsa-miR-1251	3.2913492	3.162255	48.99982865
hsa-miR-1266	17.90788	17.170723	48.94927828
hsa-miR-223*	2.807967	2.6861722	48.89159343
hsa-miR-496	3.714285	3.5516255	48.88066678
hsa-miR-141*	3.9366086	3.76356	48.8763324
hsa-miR-127-3p	7.0982704	6.785166	48.87238148
hsa-miR-103	25237.303	24046.85	48.7922558
hsa-miR-541*	10.906415	10.368959	48.73690587
hsa-miR-1293	3.0283318	2.8747005	48.69870863
hsa-miR-624*	3.2986565	3.1285775	48.67688807
hsa-miR-633	3.6889808	3.4912815	48.62331422
hsa-miR-205	3.1871598	3.0086021	48.55903355
hsa-miR-450a	2.9657066	2.7947636	48.51624091
hsa-miR-340*	3.4034946	3.2063065	48.50836586
hsa-miR-511	2.7642157	2.603205	48.50011105
hsa-miR-518a-3p	3.3465164	3.1428173	48.43050836
hsa-miR-92a-2*	5.1606674	4.8408017	48.40090642
hsa-miR-512-5p	4.0303006	3.778115	48.38516792
hsa-miR-581	3.0627563	2.8706045	48.38075075
hsa-miR-135b	3.075987	2.8821828	48.37362641
hsa-miR-646	3.1531422	2.9541428	48.37080307
hsa-miR-934	3.8929617	3.6460524	48.36245631
hsa-miR-544	3.5599186	3.3303945	48.33444361
hsa-miR-376b	4.2792397	4.0026875	48.3303874

hsa-miR-580	3.8000863	3.549648	48.29627651
hsa-miR-25	13719.228	12774.609	48.2172854
hsa-miR-548k	3.3749483	3.139725	48.19466542
hsa-miR-590-3p	2.784127	2.5872595	48.16744243
hsa-miR-510	7.707245	7.1607804	48.16228253
hsa-miR-18a	10299.919	9552.46	48.11745736
hsa-miR-497*	3.397333	3.143677	48.06103339
hsa-let-7i*	31.507704	29.127253	48.03706383
hsa-miR-655	3.7595193	3.4735744	48.02335687
hsa-miR-23b	26421.889	24411.932	48.02301208
hsa-miR-302f	3.1396685	2.898997	48.00724597
hsa-miR-886-5p	4.399567	4.0422225	47.88347897
hsa-miR-578	2.8769958	2.6390364	47.84302021
hsa-miR-20b	10304.625	9439.018	47.80788429
hsa-miR-515-3p	2.8723247	2.62736	47.77292051
hsa-miR-586	3.3801386	3.0867043	47.73123992
hsa-miR-374a*	5.259968	4.8000264	47.71400668
hsa-miR-587	3.1764057	2.897768	47.70637363
hsa-miR-668	17.36867	15.834969	47.69046248
hsa-miR-200c*	3.9052255	3.559974	47.68759361
hsa-miR-450b-3p	2.993779	2.7275324	47.67320304
hsa-miR-1245	3.9821618	3.6279736	47.67291788
hsa-miR-512-3p	4.260385	3.878906	47.65655878
hsa-miR-144*	5.374865	4.8916645	47.64671937
hsa-miR-519a	3.2064798	2.916232	47.62974472
hsa-miR-190b	3.093375	2.8103218	47.60274613
hsa-miR-29a*	3.1420438	2.8477147	47.54306371
hsa-miR-493*	3.500108	3.1667125	47.49959145
hsa-miR-100*	3.6103735	3.2580488	47.43518464
hsa-miR-624	3.175623	2.8565586	47.35531503
hsa-miR-146a*	3.4873874	3.1357453	47.34534913
hsa-miR-185*	56.465794	50.716785	47.31812341
hsa-miR-302e	3.3850715	3.0356362	47.27884124
hsa-miR-513b	3.7666438	3.3743303	47.25308134
hsa-miR-33b	2.8897297	2.5874913	47.2409512
hsa-miR-24	23655.766	21179.133	47.23805221
hsa-miR-886-3p	8.870412	7.9264417	47.19003833
hsa-miR-506	3.0699904	2.7366095	47.12929334
hsa-miR-130b	10085.375	8957.337	47.03813721
hsa-miR-23a	18273.408	16211.88	47.01100365
hsa-miR-181a	7701.815	6827.775	46.99220694
hsa-miR-136	3.3223932	2.945058	46.98972367
hsa-miR-891b	3.030986	2.6855495	46.97862018
hsa-miR-1205	2.8775558	2.5486643	46.96942352
hsa-miR-525-3p	3.0113728	2.665569	46.95431262
hsa-ApmiR-218-1*	3.5492313	3.1372058	46.91894582
hsa-miR-27b	12020.3125	10614.913	46.89554783
hsa-miR-632	5.237619	4.6251435	46.8950104

hsa-miR-302b*	3.8714244	3.4181817	46.89117153
hsa-miR-144	2.6514537	2.3325925	46.80118134
hsa-miR-142-5p	3.3428752	2.9347134	46.74905584
hsa-miR-519d	3.0182552	2.6477396	46.73035704
hsa-miR-1	3.569641	3.1311638	46.7281751
hsa-let-7b	23489.084	20566.055	46.68253345
hsa-miR-671-3p	51.56505	44.857098	46.52157096
hsa-miR-124	9663.6045	8397.491	46.494915
hsa-miR-1185	4.2818704	3.7096741	46.41998928
hsa-miR-1261	3.606088	3.1119373	46.32220275
hsa-miR-1302	4.1243834	3.5589752	46.32056611
hsa-miR-508-5p	10.589528	9.114369	46.25668212
hsa-miR-1276	16.997414	14.627948	46.25385158
hsa-miR-1286	8.19825	7.0539894	46.24887674
hsa-miR-196b	3.353296	2.8835971	46.23451218
hsa-miR-208a	3.848818	3.3073132	46.21649754
hsa-miR-15b*	3.9764357	3.411403	46.17592693
hsa-miR-597	3.5997307	3.08338	46.1368985
hsa-miR-585	3.5098183	2.9989555	46.07558339
hsa-miR-548d-3p	3.4418309	2.940689	46.07410625
hsa-miR-29b	21.558142	18.409243	46.06066421
hsa-miR-892b	3.4537413	2.9483716	46.05310225
hsa-miR-298	17.684969	15.095778	46.05074436
hsa-miR-27a	6704.2554	5721.891	46.04718805
hsa-let-7f-2*	3.148966	2.6872451	46.04434374
hsa-miR-599	2.9292924	2.4978106	46.02475022
hsa-miR-220b	4.2173824	3.5933197	46.00507936
hsa-miR-101	24.00448	20.431744	45.97992845
hsa-miR-548a-3p	8.468829	7.2083206	45.97979087
hsa-miR-579	3.4952424	2.953388	45.79868618
hsa-miR-138	3600.6326	3038.1096	45.76333149
hsa-miR-19b	16652.049	14046.669	45.75653289
hsa-miR-125a-5p	13925.739	11730.472	45.72176305
hsa-miR-609	4.5577216	3.8305705	45.66567848
hsa-miR-518c*	7.3899	6.1926637	45.5927455
hsa-miR-555	3.56691	2.9767673	45.49074112
hsa-miR-449a	3.3514416	2.7890415	45.42055494
hsa-let-7c	20489.117	17014.72	45.36794462
hsa-miR-199a-3p	10460.374	8681.306	45.35289483
hsa-miR-643	8.299049	6.8839583	45.33988665
hsa-miR-26a-2*	4.1422777	3.4331005	45.31919608
hsa-miR-181a*	7.5571294	6.2602882	45.30722296
hsa-miR-199b-3p	10427.594	8636.328	45.30194784
hsa-miR-520f	3.3676414	2.7873814	45.28628879
hsa-miR-641	60.43385	49.994785	45.27338856
hsa-miR-30d*	4.6543574	3.8499382	45.27051247
hsa-miR-542-3p	4.448405	3.6746228	45.23710728
hsa-miR-576-5p	4.164822	3.4384086	45.22299508

hsa-miR-15b	12492.32	10306.829	45.20707769
hsa-miR-377	4.003966	3.3015594	45.19263461
hsa-miR-345	4294.2495	3535.5667	45.15516852
hsa-miR-606	5.589599	4.5983396	45.13513264
hsa-miR-372	4.8431277	3.9718914	45.05822795
hsa-miR-889	3.4919436	2.862881	45.0505117
hsa-miR-30e	249.34102	204.28271	45.03351489
hsa-miR-876-5p	3.9035428	3.1947062	45.00696158
hsa-miR-182*	3.7450988	3.0599258	44.96568315
hsa-miR-431	3.3888009	2.767707	44.95579385
hsa-miR-600	3.8845527	3.1661298	44.90529534
hsa-miR-1324	4.6002517	3.7447014	44.87384597
hsa-miR-96*	3.423793	2.7857406	44.86231623
hsa-miR-34b*	10.033456	8.162114	44.85769888
hsa-miR-515-5p	3.6291256	2.950598	44.84379861
hsa-miR-561	3.523814	2.864322	44.83814997
hsa-miR-448	3.2552357	2.644411	44.8232095
hsa-miR-147	2.9908972	2.4296367	44.82283009
hsa-miR-634	9.737343	7.90015	44.79179666
hsa-miR-556-5p	3.7645156	3.0525658	44.77819203
hsa-miR-626	3.6242237	2.9331799	44.73081236
hsa-miR-920	8.592895	6.94873	44.71044694
hsa-miR-1208	28.558182	23.085054	44.70102145
hsa-miR-452	4.295917	3.4642384	44.64135345
hsa-miR-664	9.899732	7.9809494	44.63448132
hsa-miR-378*	8.251946	6.647589	44.61608366
hsa-miR-520a-5p	3.0901012	2.4892614	44.61551576
hsa-miR-361-5p	11465.151	9235.22	44.61378977
hsa-miR-202*	5.447723	4.385235	44.59731243
hsa-miR-1237	18.096575	14.507001	44.49512225
hsa-let-7i	8590.974	6881.6504	44.47629712
hsa-miR-143	4757.453	3807.661	44.45546201
hsa-miR-604	4.137121	3.3058746	44.41591501
hsa-let-7d	14033.391	11195.368	44.37542092
hsa-miR-514	3.6575105	2.90911	44.30147897
hsa-miR-517b	3.1241486	2.482011	44.27292794
hsa-miR-181d	2749.0999	2177.0361	44.19358499
hsa-miR-591	4.340592	3.4346695	44.17432777
hsa-miR-1227	6.9475174	5.476904	44.08176303
hsa-miR-519b-3p	6.2724304	4.9345155	44.0308675
hsa-miR-199a-5p	5071.175	3977.961	43.95956697
hsa-miR-548c-3p	4.20713	3.3001058	43.9590002
hsa-miR-1252	3.5729873	2.8002408	43.93755811
hsa-miR-451	4.513478	3.527753	43.87080784
hsa-miR-499-5p	4.6911893	3.6601017	43.8267772
hsa-miR-549	3.7694595	2.9362898	43.78764652
hsa-miR-518f	4.570228	3.5558262	43.75833723
hsa-miR-1179	3.5373437	2.7514098	43.7512744

hsa-miR-412	6.9167075	5.360126	43.66049275
hsa-miR-644	3.6553924	2.8325608	43.65877362
hsa-miR-509-3-5p	4.9035316	3.7837975	43.55536042
hsa-miR-523*	4.517999	3.478803	43.5024276
hsa-miR-1290	13.778359	10.607621	43.49885057
hsa-miR-30c	6574.3438	5060.5747	43.4947155
hsa-miR-29b-1*	18.79127	14.46062	43.48811451
hsa-miR-516b	3.4656603	2.6666784	43.48550415
hsa-miR-302b	3.3438606	2.5709386	43.46620254
hsa-miR-449b	3.9528627	3.038867	43.46373688
hsa-miR-656	4.3375473	3.3245306	43.38941268
hsa-miR-545*	5.1539326	3.9399767	43.32544531
hsa-miR-1827	4.7210183	3.596571	43.24054567
hsa-miR-181b	6536.9434	4971.7007	43.19970847
hsa-miR-342-3p	9746.556	7406.7847	43.17983785
hsa-miR-149*	4853.676	3687.5615	43.17362092
hsa-miR-99b	10797.437	8201.2	43.16730721
hsa-miR-1181	49.17155	37.338676	43.16099694
hsa-miR-548g	4.894737	3.7165768	43.15923082
hsa-miR-548h	4.3678203	3.31621	43.15716975
hsa-miR-548f	3.6826026	2.7945817	43.14500824
hsa-let-7g*	37.81726	28.665335	43.11705191
hsa-miR-548i	4.361241	3.3044393	43.10692816
hsa-miR-215	4.308076	3.2601032	43.07645358
hsa-miR-665	191.99348	144.76271	42.98739394
hsa-miR-1308	9893.656	7452.6387	42.96386536
hsa-miR-1206	4.2217097	3.1532876	42.75645769
hsa-miR-411*	21.586021	16.08784	42.70292339
hsa-miR-520h	3.886547	2.8934937	42.67664204
hsa-miR-34a	2708.0789	2016.1216	42.67646134
hsa-miR-222*	4.5615673	3.395012	42.66924104
hsa-miR-106a*	3.3045971	2.457721	42.65160231
hsa-miR-145	7395.7036	5485.266	42.58426322
hsa-miR-148a*	7.0693603	5.2428803	42.58266607
hsa-miR-566	5.7547507	4.257769	42.52445066
hsa-miR-519c-5p	4.242604	3.1349556	42.49312469
hsa-miR-126*	3.8267748	2.825554	42.4746594
hsa-miR-153	195.0334	143.96571	42.46787256
hsa-miR-1274a	5.6004386	4.1293583	42.44033398
hsa-miR-7-2*	9.71978	7.1630273	42.42793969
hsa-miR-548o	3.3828638	2.4926972	42.42483739
hsa-miR-15a*	38.331287	28.200617	42.38660748
hsa-miR-944	7.144875	5.2549014	42.37900129
hsa-miR-518a-5p	5.190266	3.8123329	42.34702603
hsa-miR-516a-3p	3.7375634	2.7441301	42.33662237
hsa-miR-936	28.011124	20.564854	42.33543996
hsa-miR-548p	3.8830745	2.8501675	42.32979447
hsa-miR-605	13.371555	9.787105	42.26110233

hsa-miR-491-3p	3.935405	2.8789237	42.24808968
hsa-miR-10a*	4.1738095	3.0484712	42.20925947
hsa-miR-522*	3.9422925	2.8774107	42.19260891
hsa-miR-429	3.6850493	2.6819248	42.12243929
hsa-miR-455-5p	4.2260685	3.0749404	42.11665048
hsa-miR-369-5p	3.9693956	2.8879874	42.11500801
hsa-miR-196a	3.6287386	2.6372669	42.08848684
hsa-miR-539	8.43481	6.1032157	41.98104905
hsa-miR-320c	14189.629	10266.234	41.97862083
hsa-miR-338-3p	15.202235	10.986487	41.95121473
hsa-miR-1294	7.2176814	5.204737	41.89793672
hsa-miR-615-5p	14.008475	10.095328	41.88271867
hsa-miR-1295	3.8764875	2.7900093	41.85120587
hsa-miR-588	5.4109206	3.890702	41.82820748
hsa-miR-1233	12.981563	9.3216	41.79496872
hsa-miR-504	5.5793343	4.0051365	41.78776881
hsa-miR-320a	15371.7295	10998.757	41.70858585
hsa-miR-425	7851.2896	5575.145	41.52364471
hsa-miR-527	5.167888	3.6574929	41.44289002
hsa-miR-1243	6.590529	4.6560936	41.39992748
hsa-miR-210	3213.9978	2270.5806	41.39936444
hsa-miR-518b	4.4984603	3.169276	41.33261599
hsa-miR-1238	35.93812	25.263243	41.27888949
hsa-miR-16-2*	13.439743	9.396085	41.14624177
hsa-miR-125b	7945.5903	5553.01	41.13767262
hsa-miR-520a-3p	4.938909	3.4505959	41.12991102
hsa-miR-488	4.5527186	3.1754606	41.08937588
hsa-miR-320b	16240.847	11228.737	40.87698234
hsa-miR-30b	3479.0618	2402.4988	40.84798174
hsa-miR-381	75.8661	52.33984	40.8248167
hsa-miR-483-5p	294.70743	203.30542	40.82332815
hsa-miR-380*	5.2414165	3.609587	40.78166956
hsa-miR-369-3p	3.904998	2.6854222	40.74735933
hsa-miR-337-5p	7.9960475	5.479612	40.66303397
hsa-miR-19a*	3.8829224	2.6577854	40.63452277
hsa-miR-155*	5.6413236	3.860359	40.62816201
hsa-miR-216a	3.9659405	2.6996136	40.500963
hsa-miR-151-5p	10537.483	7154.777	40.44015293
hsa-miR-638	12662.414	8591.204	40.42231304
hsa-miR-365	5.974645	4.0399933	40.34088081
hsa-miR-424	3.966941	2.6729705	40.25611637
hsa-miR-1178	4.1596313	2.786174	40.11304492
hsa-miR-186*	3.8625596	2.5826144	40.07051478
hsa-miR-376a*	3.7822	2.520605	39.9917973
hsa-miR-508-3p	3.8673623	2.5735362	39.95616761
hsa-miR-146a	8.069615	5.362516	39.92304721
hsa-miR-143*	37.310337	24.761805	39.89197763
hsa-miR-520g	4.305188	2.8469613	39.80567492

hsa-miR-362-3p	19.207586	12.634624	39.67885395
hsa-miR-488*	6.4201865	4.219933	39.660579
hsa-miR-1236	14.296849	9.39478	39.65442815
hsa-miR-767-3p	13.5478735	8.864188	39.55097125
hsa-miR-302c*	6.398643	4.1635556	39.4194027
hsa-miR-658	42.499714	27.622915	39.39229803
hsa-let-7g	4822.756	3134.2605	39.3898957
hsa-miR-379*	6.5605245	4.2583847	39.36057343
hsa-miR-507	3.9622052	2.5686483	39.33097412
hsa-miR-575	64.91419	42.081123	39.32987513
hsa-miR-517c	5.0982327	3.2976859	39.27724954
hsa-miR-653	4.600092	2.9532154	39.09830811
hsa-miR-553	5.1060414	3.262904	38.98823381
hsa-miR-562	4.2026696	2.676555	38.90780074
hsa-miR-122*	4.596584	2.9196393	38.8444992
hsa-miR-708	7822.0835	4967.0376	38.8379902
hsa-miR-603	8.5528965	5.430737	38.83637969
hsa-miR-302c	4.280043	2.7051468	38.72689043
hsa-miR-30a	615.6221	388.6366	38.69885319
hsa-miR-99a	4628.558	2921.4666	38.69479578
hsa-miR-374b*	5.789959	3.648667	38.65676
hsa-miR-296-3p	537.3803	338.02127	38.61328122
hsa-miR-1262	8.995952	5.6463904	38.56207051
hsa-miR-140-3p	3604.8557	2257.2546	38.50583637
hsa-miR-432	52.99394	33.11374	38.4561981
hsa-miR-518e*	4.3468566	2.7155964	38.45117837
hsa-miR-1278	5.9230056	3.6850863	38.35398681
hsa-miR-95	32.557064	20.205027	38.29459109
hsa-miR-29c*	53.275665	32.883316	38.16585992
hsa-miR-367	4.233122	2.610379	38.14391201
hsa-miR-138-2*	40.14981	24.658813	38.04866059
hsa-miR-375	3826.7937	2340.0747	37.94591595
hsa-miR-1287	9.064453	5.5342045	37.90899608
hsa-miR-320d	10423.91	6346.7954	37.84453455
hsa-miR-486-3p	64.286064	38.916634	37.70893083
hsa-miR-18b	2318.6946	1403.2552	37.70215278
hsa-miR-93*	5303.596	3207.827	37.68849228
hsa-miR-614	6.0681863	3.6696854	37.68467601
hsa-miR-193a-3p	21.666315	13.082127	37.64809657
hsa-miR-509-5p	7.4148526	4.469438	37.60794944
hsa-miR-32	5.8875847	3.5341187	37.51040072
hsa-miR-137	1112.6227	667.2181	37.48751574
hsa-miR-654-3p	174.40724	104.34808	37.43357436
hsa-miR-570	7.200482	4.306048	37.4226461
hsa-miR-1228	66.75829	39.919277	37.42049816
hsa-miR-145*	6.602522	3.9442818	37.39788731
hsa-miR-299-5p	32.621754	19.482431	37.39129784
hsa-miR-876-3p	4.4673877	2.6547158	37.27432212

hsa-miR-410	20.896404	12.234689	36.92811764
hsa-miR-15a	2452.536	1427.0962	36.78431682
hsa-miR-485-3p	98.0187	56.92505	36.73917147
hsa-miR-301a	992.2229	575.17413	36.69613499
hsa-miR-1226*	82.242546	47.48749	36.60485379
hsa-miR-23a*	89.07064	51.40034	36.59142977
hsa-miR-1228*	5564.5923	3209.8206	36.58159966
hsa-miR-569	4.1250553	2.3734403	36.52291924
hsa-miR-922	5.381914	3.0936415	36.50075207
hsa-let-7f	5297.2363	3043.2263	36.48750011
hsa-let-7b*	60.443523	34.68594	36.46182676
hsa-miR-125a-3p	419.30136	239.21082	36.32595224
hsa-miR-873	144.09044	81.96584	36.25904133
hsa-miR-1825	43.063076	24.461578	36.22614342
hsa-miR-363	1705.6382	958.2046	35.97076374
hsa-miR-146b-3p	7.4377236	4.1577992	35.85693609
hsa-miR-1224-5p	212.3891	118.50297	35.8131792
hsa-miR-154*	18.077402	10.05644	35.74499352
hsa-miR-106b*	2137.2578	1185.9603	35.68710402
hsa-miR-214	6609.267	3657.4504	35.62434084
hsa-miR-186	12.825709	7.0726643	35.54393213
hsa-miR-30d	3162.215	1741.2155	35.51014948
hsa-miR-421	3220.1897	1766.4113	35.42315297
hsa-miR-483-3p	63.781067	34.978695	35.41796202
hsa-miR-495	162.80894	89.05856	35.3592901
hsa-miR-376c	160.07329	87.44773	35.32941566
hsa-let-7e	14878.8125	8101.4453	35.25393566
hsa-miR-299-3p	51.76652	28.150625	35.2247631
hsa-miR-132	3294.2664	1789.2266	35.1967948
hsa-let-7e*	92.178856	50.035244	35.18304022
hsa-miR-10b	2523.8643	1359.8872	35.01478403
hsa-miR-432*	9.844659	5.3002605	34.99695393
hsa-miR-497	954.1976	513.4554	34.98479545
hsa-miR-1277	4.386895	2.359952	34.97859074
hsa-miR-563	7.7883124	4.153627	34.78184624
hsa-miR-1323	16.250906	8.652286	34.74368266
hsa-miR-589	54.996784	29.213501	34.69113185
hsa-miR-22*	16.666784	8.818276	34.60174706
hsa-miR-204	6.121811	3.2362518	34.58249714
hsa-miR-543	210.94055	111.30194	34.53980883
hsa-miR-423-3p	6008.9478	3162.955	34.48526515
hsa-miR-758	63.930157	33.62547	34.4679964
hsa-miR-338-5p	250.85864	130.48222	34.21669002
hsa-miR-18b*	8.195367	4.259317	34.19851519
hsa-miR-1304	14.637303	7.5628333	34.06660751
hsa-miR-128	2147.9683	1106.7109	34.00368614
hsa-miR-199b-5p	389.52896	199.8553	33.90916819
hsa-miR-642	8.610816	4.41462	33.89230119

hsa-miR-744	2459.0354	1253.9127	33.77135005
hsa-miR-769-5p	978.85205	498.99512	33.76500156
hsa-miR-7	336.09988	171.27107	33.7565779
hsa-miR-548b-3p	5.7590203	2.9271376	33.69887623
hsa-miR-933	95.66571	48.510548	33.64669653
hsa-miR-935	1852.5963	936.7695	33.58360169
hsa-miR-195	3552.36	1795.7402	33.57716073
hsa-miR-184	22.6047	11.374095	33.4740976
hsa-miR-92b	3238.6301	1625.625	33.41981386
hsa-miR-377*	20.77823	10.42332	33.40641731
hsa-miR-196a*	6.263415	3.122507	33.26798369
hsa-miR-596	46.975697	23.413834	33.26323342
hsa-miR-340	26.964125	13.397609	33.193839
hsa-miR-185	4409.517	2188.3547	33.16758494
hsa-miR-376a	60.821056	30.087952	33.09677738
hsa-miR-424*	118.152374	58.315388	33.04591577
hsa-miR-335	14.979299	7.3926606	33.0443141
hsa-miR-503	206.67104	101.64292	32.96734277
hsa-miR-126	2205.6152	1081.2194	32.89546118
hsa-miR-24-1*	14.831882	7.2496743	32.83135573
hsa-miR-1224-3p	27.974443	13.622742	32.74919204
hsa-miR-139-5p	1713.3131	832.02985	32.68832006
hsa-miR-19b-1*	59.287434	28.64018	32.57245215
hsa-miR-187	69.1202	33.06917	32.36067509
hsa-miR-744*	109.31112	52.253696	32.34224957
hsa-miR-487a	214.22939	102.29443	32.31808273
hsa-miR-652	2328.2744	1111.4795	32.31276226
hsa-miR-1260	72.61321	34.534145	32.23051563
hsa-miR-1229	48.803143	23.191439	32.21275595
hsa-miR-140-5p	402.69092	191.08788	32.18166091
hsa-miR-22	1478.6045	700.2229	32.13760301
hsa-miR-627	14.474841	6.765982	31.85367158
hsa-miR-1255a	13.76887	6.4180646	31.79316091
hsa-miR-151-3p	2723.9238	1269.1023	31.78297031
hsa-miR-592	1345.8695	625.6677	31.73501875
hsa-miR-411	109.74756	50.847046	31.66173962
hsa-miR-182	114.2431	52.822018	31.6176223
hsa-miR-532-5p	1298.3613	600.2607	31.61559805
hsa-miR-100	522.8905	240.40733	31.49587495
hsa-miR-490-3p	487.9979	224.25957	31.4857449
hsa-miR-181a-2*	2184.8474	1003.25464	31.46871171
hsa-miR-494	940.9046	427.87183	31.25943877
hsa-miR-663	3579.1963	1626.3912	31.24318245
hsa-miR-34a*	187.81563	85.01151	31.15947702
hsa-miR-214*	672.46674	302.91742	31.05621687
hsa-miR-9*	740.9289	332.93002	31.00314332
hsa-miR-551b*	85.930565	38.510906	30.94700319
hsa-miR-1184	52.97337	23.732065	30.93922223

hsa-miR-26a-1*	5.3226695	2.3803518	30.9015347
hsa-miR-885-5p	601.827	268.69217	30.86573843
hsa-miR-326	95.05505	42.315533	30.80392619
hsa-miR-19a	1403.7738	624.6968	30.79644339
hsa-miR-133b	10.487533	4.663998	30.7823546
hsa-miR-129-5p	185.12183	82.247284	30.76169972
hsa-miR-29c	80.8379	35.721928	30.6468606
hsa-miR-329	126.11017	55.58017	30.59060267
hsa-miR-541	12.303983	5.3981423	30.49431754
hsa-miR-197	2092.545	917.51416	30.48159891
hsa-miR-30c-2*	33.97245	14.822426	30.37701336
hsa-miR-625	509.4021	221.86601	30.33989955
hsa-miR-20a*	34.32558	14.933715	30.31654229
hsa-miR-152	2242.7832	975.2171	30.30506554
hsa-miR-1307	2584.8445	1123.2617	30.29205852
hsa-miR-301b	179.97856	78.12046	30.26763139
hsa-miR-1288	10.534538	4.5602584	30.21079768
hsa-miR-382	390.59628	168.70827	30.16393662
hsa-miR-1271	2490.4084	1074.1149	30.13347956
hsa-miR-192	311.59622	134.18007	30.10031556
hsa-miR-671-5p	980.2797	421.8363	30.08569191
hsa-miR-99b*	1365.4532	586.8093	30.05790973
hsa-miR-330-5p	92.52128	39.752354	30.05312003
hsa-miR-138-1*	397.49033	170.48048	30.01571155
hsa-miR-181c	813.0976	348.1464	29.98046922
hsa-miR-1250	191.3039	81.87384	29.97090466
hsa-miR-29b-2*	266.52118	114.03231	29.96485724
hsa-miR-1202	641.04987	273.59927	29.91302982
hsa-miR-339-5p	3321.1982	1416.4404	29.89760342
hsa-miR-943	99.69102	42.49708	29.88793014
hsa-miR-129*	40.08797	17.072344	29.86747763
hsa-miR-636	76.66967	32.603943	29.8369772
hsa-miR-1269	171.49512	72.76605	29.79026507
hsa-miR-324-3p	2218.2615	940.0103	29.76343898
hsa-miR-331-3p	1001.8779	424.1207	29.74201377
hsa-miR-370	264.17496	111.818184	29.73942099
hsa-miR-30e*	228.07176	96.346306	29.69819381
hsa-miR-181c*	586.7198	247.23146	29.64579249
hsa-miR-24-2*	334.3285	140.34834	29.56713456
hsa-miR-629*	318.87527	133.46513	29.50546314
hsa-miR-1226	309.7229	129.56133	29.49373575
hsa-miR-939	332.73032	139.15495	29.48914892
hsa-miR-1180	1962.0685	818.5161	29.43683497
hsa-miR-154	59.267292	24.54339	29.28432202
hsa-miR-125b-2*	499.06763	206.39946	29.25713516
hsa-miR-629	606.5737	250.68318	29.24248097
hsa-miR-1281	310.90738	128.31776	29.21457547
hsa-miR-660	327.54877	135.1198	29.20444758

hsa-miR-550	195.1991	79.6067	28.96834783
hsa-miR-766	756.5275	306.55756	28.83659752
hsa-miR-33b*	40.554043	16.41497	28.81385711
hsa-miR-484	902.0052	364.77283	28.79532336
hsa-miR-202	22.089617	8.929849	28.78788758
hsa-miR-193b*	52.8458	21.349073	28.7743238
hsa-miR-212	303.25534	122.51069	28.77418144
hsa-miR-891a	38.750557	15.635132	28.74861436
hsa-miR-502-5p	36.958496	14.888626	28.71639818
hsa-miR-29a	856.5	343.88718	28.64802172
hsa-miR-487b	1081.8497	433.3369	28.59957315
hsa-miR-30c-1*	82.18042	32.815083	28.53597066
hsa-miR-637	67.16569	26.788177	28.51205369
hsa-miR-188-3p	12.082149	4.8050065	28.45361671
hsa-miR-887	744.5825	295.98254	28.44440555
hsa-miR-218	1839.7618	731.08496	28.43751605
hsa-miR-191*	151.29471	60.037632	28.4091074
hsa-miR-149	5297.1733	2101.8694	28.40731545
hsa-miR-331-5p	293.52988	116.35721	28.38762499
hsa-miR-654-5p	28.267822	11.202819	28.38266295
hsa-miR-330-3p	1869.8148	740.3151	28.36315158
hsa-miR-7-1*	260.75085	103.06677	28.3292409
hsa-miR-628-5p	26.714376	10.548638	28.30860112
hsa-miR-362-5p	808.7078	319.12466	28.29539593
hsa-miR-339-3p	1215.1195	479.41953	28.29203232
hsa-miR-194	645.00226	254.0509	28.25760604
hsa-miR-760	113.66238	44.480946	28.12698273
hsa-miR-124*	145.80684	56.72968	28.00960538
hsa-miR-505	507.35245	196.97809	27.96671148
hsa-miR-425*	1005.52997	390.35107	27.96449402
hsa-miR-10b*	356.82495	137.25322	27.77965681
hsa-miR-490-5p	1397.1348	537.33496	27.77686016
hsa-miR-551a	131.39317	50.49712	27.76240557
hsa-miR-489	113.07363	43.427612	27.74905262
hsa-miR-328	293.80484	112.30932	27.6546181
hsa-miR-1280	387.67264	147.38832	27.54607998
hsa-miR-198	92.7539	35.22388	27.52343415
hsa-let-7d*	105.246185	39.83841	27.45874571
hsa-miR-877	813.2449	307.5566	27.44077341
hsa-miR-491-5p	464.95657	175.20142	27.36846571
hsa-miR-150*	197.69627	73.95208	27.22346004
hsa-miR-502-3p	814.3129	304.0321	27.18589523
hsa-miR-628-3p	302.96664	112.68337	27.11015693
hsa-miR-1225-3p	23.288248	8.658171	27.10216441
hsa-miR-498	40.952465	15.189921	27.05606598
hsa-miR-27b*	719.6982	266.65915	27.0347405
hsa-miR-374b	411.51248	152.36098	27.0204205
hsa-miR-30a*	218.10283	80.699524	27.00766005

hsa-miR-148a	184.0973	67.92228	26.95119165
hsa-miR-10a	10.158043	3.7315404	26.86574746
hsa-miR-105	779.78973	286.1954	26.84797301
hsa-miR-9	146.54149	53.517597	26.75089535
hsa-miR-146b-5p	254.7885	92.72709	26.68285759
hsa-miR-589*	501.18466	182.18494	26.65979581
hsa-miR-409-3p	611.6479	221.88708	26.6200082
hsa-miR-1254	95.390625	34.55958	26.59447902
hsa-miR-21	254.30336	92.10258	26.58804869
hsa-miR-27a*	123.75695	44.773777	26.5671298
hsa-miR-139-3p	91.41864	32.901733	26.46527854
hsa-miR-500*	806.8135	290.13004	26.44894923
hsa-miR-18a*	1327.5199	476.57788	26.41641076
hsa-miR-296-5p	29.223566	10.47038	26.37777559
hsa-miR-885-3p	136.9282	48.912388	26.31954006
hsa-miR-378	374.83838	133.52217	26.26525013
hsa-miR-501-3p	541.23627	192.77397	26.26311726
hsa-miR-20b*	231.12207	82.25411	26.24772247
hsa-miR-323-3p	58.38815	20.771545	26.24005183
hsa-miR-557	35.016495	12.449454	26.22817886
hsa-miR-486-5p	1249.3412	443.42178	26.19514871
hsa-miR-675	2291.3833	809.06757	26.09515854
hsa-miR-500	589.19336	207.49188	26.04439866
hsa-miR-423-5p	989.8256	345.8602	25.89382922
hsa-miR-193b	1086.9585	379.6605	25.8867845
hsa-miR-1296	532.92285	186.11589	25.88398645
hsa-miR-454	234.58423	81.6499	25.81944586
hsa-miR-129-3p	156.37105	54.205524	25.74147873
hsa-miR-422a	165.26031	57.13754	25.6915883
hsa-miR-183	16.60586	5.7205596	25.62237789
hsa-miR-501-5p	313.9296	107.47678	25.50430774
hsa-miR-616	17.757753	6.0729127	25.48360493
hsa-miR-550*	562.6246	191.15251	25.35928824
hsa-miR-769-3p	501.6558	170.2212	25.33517296
hsa-miR-940	117.03887	39.67597	25.31730243
hsa-miR-98	175.18718	59.189175	25.253902
hsa-miR-1231	329.1135	110.88386	25.20102848
hsa-miR-615-3p	379.44247	127.822754	25.19840666
hsa-miR-455-3p	357.856	119.92273	25.10005625
hsa-miR-134	264.4685	88.40867	25.05366669
hsa-miR-1247	73.05303	24.204203	24.88678965
hsa-miR-148b	493.11063	163.29478	24.87712281
hsa-miR-200c	61.29306	20.254953	24.83807055
hsa-miR-218-2*	540.53925	176.72583	24.63884482
hsa-miR-130b*	164.5981	53.63681	24.57755728
hsa-miR-135a*	392.41373	124.69599	24.11402942
hsa-miR-92b*	383.83472	121.76681	24.08355252
hsa-miR-874	614.94147	193.81795	23.96484606

hsa-miR-379	486.32065	152.74449	23.90123955
hsa-miR-941	344.6631	108.20435	23.89316123
hsa-miR-767-5p	668.34955	208.60313	23.78727322
hsa-miR-133a	15.286804	4.722302	23.60076457
hsa-miR-346	767.073	234.57372	23.41880778
hsa-miR-1225-5p	736.13544	225.11067	23.41863001
hsa-miR-409-5p	111.967384	34.163166	23.3785242
hsa-miR-92a-1*	286.09787	85.921265	23.09592624
hsa-miR-1303	171.91893	51.587677	23.08105236
hsa-miR-361-3p	39.726677	11.8517065	22.97804952
hsa-miR-26b	163.5984	48.732555	22.95122489
hsa-miR-26b*	18.657608	5.503636	22.77877745
hsa-miR-720	167.36076	49.14256	22.69829396
hsa-miR-532-3p	682.23413	197.67317	22.46522673
hsa-miR-135b*	17.927763	5.17342	22.3946107
hsa-miR-937	21.20896	6.110401	22.36655901
hsa-miR-1301	2243.9705	640.3619	22.20139052
hsa-miR-23b*	372.55435	104.15783	21.84920679
hsa-miR-1270	333.5906	92.33719	21.67907147
hsa-miR-1292	130.29216	35.05202	21.19942776
hsa-miR-193a-5p	170.92229	45.8644	21.15646491
hsa-miR-505*	1158.1102	304.45657	20.81659287
hsa-miR-1285	331.3991	87.08072	20.8088218
hsa-miR-28-5p	37.09463	9.643445	20.6329529
hsa-miR-485-5p	65.90208	17.015638	20.52111227
hsa-let-7c*	27.7213	7.1033173	20.39740233
hsa-miR-1244	363.41016	92.60647	20.3076958
hsa-miR-1274b	25.604078	6.467405	20.16559384
hsa-miR-342-5p	617.91864	153.23999	19.87139663
hsa-miR-25*	1114.6824	273.0684	19.67704865
hsa-miR-383	25.511606	6.1408715	19.40091893
hsa-miR-1300	553.7117	130.3384	19.05392602
hsa-miR-374a	27.848215	5.8543243	17.37057332
hsa-miR-602	152.74074	30.534098	16.66027826
hsa-miR-572	340.56937	67.493095	16.53989298
hsa-miR-30b*	212.2274	40.460518	16.01205088
hsa-miR-598	321.70288	57.216015	15.0998052
hsa-miR-363*	33.397717	4.503005	11.88105335

ADDITIONAL FILE 4

Supplementary Table S2 - Ago1 Unique Genes

ABHD10	ADAT1	ADRA2A	ARHGAP35
ASXL2	ATP8B2	ATPAF1	B4GALT1
B4GALT3	BCL2L2	BEGAIN	BRWD3
BTAF1	C12orf43	C14orf101	C15orf41
C1orf21	C20orf27	C5orf22	C9orf3
CAMK2N2	CCDC102A	CDK16	CDON
CERS5	CHRNA10	CNNM1	CNTNAP1
COPS7B	CREBBP	CRTC3	CTNS
CTTNBP2NL	CYB5R1	CYTH2	DTNB
EGLN3	ENG	ERBB4	FAM105A
FAM120C	FAM160B2	FAM193B	FAM3A
FANCA	FBXL16	FBXL19	FLNA
FMNL3	FOXJ2	FSTL4	GABPA
GDF11	GPCPD1	GPKOW	GPSM1
GRIPAP1	GTPBP1	HK1	HLCS
ICA1L	IGFBP5	INO80D	ISCA1
KAT2A	KAT7	KCNK3	KITLG
KLHL12	L2HGDH	LDLRAD2	LEMD2
LIN28A	LMO7	LPPR2	LRFN4
LRP1	LUZP1	MAGED2	MANSC1
MAP3K9	MBD6	MBNL2	MICALL1
MKL1	MLLT3	MLXIP	MMS22L
MRAP2	MTMR3	MTMR6	MYH11
MYO19	NACC2	NCOA1	NFIX
NINJ1	NLGN2	NOL6	NR1D1
NRN1	NRXN1	NUP43	PAM
PDPK1	PFKFB2	PHF19	PIGO
PITPNM3	PLCB3	PLD5	PLEKHG7
PLEKHM3	POLR2F	PPP1R16B	PRKACA
PRKRIR	PRMT6	PTBP1	PTDSS1
PTPLA	RAB3D	RAD51D	RALBP1
RALGPS1	RASA4	RBM23	RNF121
RNF185	SAR1B	SARM1	SCAI
SH3BGRL2	SH3GLB2	SH3KBP1	SHARPIN
SLC16A2	SLC1A4	SLC25A23	SLC25A44
SLC2A4RG	SMYD5	SNAP91	SOCS2
SOX12	SPATA2	SPRED1	SPTLC2
STAG3L4	STAT5B	STYX	SYVN1
TAPT1	TBC1D4	TCF20	TET3
TLN1	TMEM199	TMEM214	TMEM64
TMEM91	TMOD2	TNK2	TPP1
TRIM46	TRIM66	TSC1	TSKU
TTC1	TULP4	U2AF2	UBE2W

ULK2	UNC119B	VAMP2	VPS53
VSIG10L	WBP1	WBP2	WDR52
WDR5B	XPO4	ZC3H18	ZFX
ZNF365	ZNF507	ZNF740	ZSCAN22
ZYX			

Supplementary Table S2 – Ago2 Unique Genes

ACBD4	ACTR1A	ADAMTS19	ADAMTS5
ADCY9	ADPGK	AGAP2	AK4
AKAP5	ANKH	ANKRD40	ANKRD54
ANKS6	AP3M1	APBA1	APBB1
APBB2	ARC	ARF6	ARFGEF2
ARHGAP26	ARHGAP28	ARL4C	ARRDC3
ASB7	ATG13	ATP2B2	ATP5S
ATP6V0A1	ATP6V0A2	ATXN1	ATXN7L3
BAI1	BBS4	BCAR3	BCL2L11
BCL7A	BSN	BTG2	C17orf85
C1orf115	C1orf198	C20orf112	C21orf91
C3orf70	CABP7	CADM3	CAMK2D
CAMK2G	CAMTA2	CAPN12	CASKIN2
CC2D1A	CCDC120	CCDC6	CCDC86
CCDC92	CDC42EP4	CDH11	CDK14
CDK18	CDK2AP2	CDK5RAP2	CECR6
CELF3	CELSR3	CHD1	CHIC1
CLCF1	CLCN5	CLEC16A	CLTB
CNIH2	CNOT6L	CPD	CPEB2
CRTAP	CRY2	CSRP1	CWF19L1
CYB5RL	DAGLA	DCAF15	DCHS1
DCLK1	DCTN5	DCUN1D3	DFFA
DIP2B	DISP2	DNAL1	DOLPP1
DPF2	DRG2	DTX3L	DUSP3
DVL3	DZIP1	EBF1	EDEM1
EFNB1	EHD2	EIF1AD	ELK1
ENC1	ENDOD1	EPB41L4B	EPHB4
EPHX1	EPS8L2	ETS1	ETV5
ETV6	FAM134A	FAM134C	FAM161B
FAM196A	FAM53C	FAM76A	FAM84A
FAM91A1	FAT3	FBXL20	FBXO24
FBXO32	FBXO41	FBXO46	FGD6
FGFR2	FHL3	FNBP1	FNDC3B
FOXN2	FOXO4	FSCN3	FUT9
G6PD	GAL3ST3	GALNT10	GALNT7
GAS7	GATA4	GCH1	GCLC
GIT1	GJB7	GMEB1	GNG12
GNG2	GNS	GOT1	GPR124
GPRC5B	GRHL1	GRIA2	GRIA3
GRIA4	GSTM3	GTDC1	GTPBP3
HCFC2	HDX	HEG1	HIF3A

HIP1R	HIST2H2BE	HOXD9	HS6ST1
HUNK	ICK	IGDCC4	IGF1R
IGSF10	IKZF4	IP6K1	IQSEC1
ITGA3	ITGA4	ITGB3	ITGB8
JHDM1D	JUN	KALRN	KCMF1
KCNA3	KCNG1	KCNH4	KCNJ14
KCTD15	KCTD5	KDM6A	KIAA0355
KIAA1522	KIF1C	KIFC2	KLHL15
LDOC1L	LEMD3	LENG8	LHFPL3
LIMD1	LMO4	LPCAT3	LPIN2
LRP3	LRRC14	LYST	LZTFL1
MAP1A	MAP1LC3A	MAP2K4	MAP6
MAPK8IP3	MARCH4	MARCH9	MBD5
MCTP2	MEST	METTL17	MFI2
MINK1	MMAA	MMP11	MOCS1
MOSPD2	MPPED2	MSI1	MTHFD1
MTUS2	MXD1	MYO1C	NACC1
NCALD	NCOA5	NDFIP2	NDRG1
NECAB3	NEURL1B	NEUROD1	NFASC
NFRKB	NIPA2	NKD1	NLE1
NMNAT2	NOVA1	NR3C1	NT5M
OAF	OPA1	ORMDL2	PAG1
PARD6B	PATL1	PBX1	PBX2
PCBP4	PCDH7	PDK3	PEAR1
PEX5L	PGAP3	PHC2	PHF15
PHF21B	PHLDA3	PIM1	PKDCC
PLAGL2	PLEKHA4	POLDIP3	POLI
POMT2	POU2F2	PPIL6	PPP1R9B
PPT2	PRELID2	PRKCI	PRR12
PRSS23	PSKH1	PTGFRN	PTK2B
PTPN14	PTPRO	PTPRU	R3HDM2
RAB1B	RABGGTA	RAP1GAP	RAPGEF2
RARA	RASAL2	RASGRP2	RBM18
RERE	RGMB	RHOBTB2	RIC8B
RIMKLA	RND2	RNF114	RNF220
ROBO1	ROBO2	RPS6KA2	RTN4R
RUNX1T1	SAP30L	SCAF1	SCN8A
SCNM1	SELT	SEMA4D	SEMA6A
SENP5	SESN2	SETD1A	SETD8
SFMBT1	SH2B3	SH3GLB1	SH3PXD2B
SHANK2	SHB	SHC3	SHISA5
SHROOM2	SIPA1L3	SKAP2	SLC12A5
SLC1A2	SLC35E4	SLC8A2	SLC9A6
SLCO3A1	SLMO1	SMARCD1	SMG5
SMURF1	SNX19	SNX21	SORCS3
SORL1	SOX6	SPATS2L	SPRY4
SPTB	SRC	SRF	SRGAP3
STAG1	STC2	STIM1	STK40

STS	STX1A	STXBP4	STXBP5L
SYNGAP1	SYNGR3	SYNPO2L	SYT13
TAOK3	TBC1D12	TBC1D20	TCEAL8
TCTA	THAP6	THTPA	TMC6
TMEM127	TMEM151A	TMEM201	TMEM222
TMEM231	TMEM63B	TMEM63C	TMUB2
TNFRSF12A	TNK1	TNKS2	TP53RK
TRAF3	TRIM39	TRIM59	TRIM62
TRIP10	TSC22D3	TSHZ2	TSPAN33
TSPAN9	TTLL5	TXLNG	UBAP1
UBE2L6	UBE3B	UBE4A	UPF1
USP31	USP46	USP50	UVRAG
VAMP3	VANGL1	VASH2	VASP
VAV3	VCPIP1	VPS37C	VSTM2L
WDFY2	WDR37	WDTC1	WIZ
WWP2	ZBTB34	ZC3H4	ZC3H7B
ZCCHC24	ZDHHC22	ZDHHC7	ZFHX2
ZFP36L1	ZMYM3	ZNF26	ZNF275
ZNF282	ZNF385A	ZNF502	ZNF609
ZNF689	ZNF81	ZNHIT6	

Supplementary Table S2 – Ago1/2 Common Genes

AAK1	ABCC1	ABCC5	ABHD2
ABL2	ACACA	ACLY	ACSL4
ACVR2A	ADAM12	ADAMTS4	ADCY1
ADIPOR2	AEBP2	AFAP1	AFF3
AFF4	AK3	AKNA	AKT3
ALCAM	AMOTL1	ANKRD28	ANKRD52
ANTXR1	AP1G1	AP2B1	AP2M1
APBA2	APPBP2	ARFIP2	ARG2
ARHGAP39	ARHGEF12	ARID1A	ARID2
ARL3	ARMC8	ARNT	ASB6
ASH1L	ASPH	ASXL1	ATCAY
ATF7	ATG7	ATG9A	ATP1B3
ATP2B1	ATP6V1G1	ATRN	AZIN1
BACH2	BAHD1	BAZ2A	BCAP31
BCL2	BCLAF1	BICD2	BMPR2
BMS1	BNIP2	BOC	BRD2
BRD7	BRPF3	BSDC1	BTRC
C16orf52	C16orf72	C17orf96	C1GALT1
C5orf63	C6orf106	C6orf89	CACHD1
CACNA1B	CACNA2D1	CACNA2D2	CADM1
CADM2	CALM1	CALM3	CALU
CAMK1	CAMSAP1	CAPRIN1	CARM1
CBL	CBLL1	CBX5	CBX6
CCDC85C	CCDC88A	CCNJ	CCNT2
CCNY	CD276	CDK13	CDK6
CELF5	CENPO	CEP170	CEP350

CFL1	CGGBP1	CHCHD3	CHURC1
CIC	CISD1	CISD3	CLCN3
CLN6	CLVS1	CNBP	CNOT2
CNTNAP2	COG5	COMMD10	COPS2
CPEB4	CPLX1	CPLX2	CPSF2
CPT2	CRCP	CREBZF	CRELD1
CRIM1	CSNK1E	CSNK1G1	CSRNP3
CSTF2T	CTDSPL	CUX1	CUX2
DCK	DCP1A	DCP2	DCUN1D5
DCX	DDAH1	DDHD1	DDT
DDX3X	DDX42	DENND5A	DENND5B
DHDDS	DIEXF	DIP2A	DIP2C
DMWD	DNAJA1	DNAJB1	DNMT3A
DPP8	DPYSL2	DPYSL3	DUSP16
DUSP8	DYRK1B	EAF1	EEF1A1
EEF2K	EFNB3	EIF2B1	EIF4A2
EIF4G2	EIF4H	ELAVL1	ELAVL3
ELN	ENAH	ENOSF1	EPB41L5
EPM2AIP1	EPT1	ERC1	ERRFI1
ESRRG	ETF1	EXOC5	EXOC7
FAF2	FAM120A	FAM131A	FAM168B
FAM192A	FAM3C	FAM8A1	FBLIM1
FBXO11	FBXO45	FBXW2	FGF2
FKBP3	FNDC3A	FOXJ3	FOXN3
FOXO3	FRMD4A	FSTL1	FXR1
G3BP2	GAB2	GABRB3	GALNT2
GATAD2B	GBF1	GDE1	GDPD1
GGA2	GGA3	GGCX	GIGYF1
GJC1	GLCCI1	GLG1	GLUL
GNAI2	GNB2	GORASP2	GPATCH8
GPD2	GPM6B	GPR137C	GPR161
GRB2	GRK5	GSK3B	H1F0
H2AFX	HAND1	HDAC8	HECTD1
HELZ	HIF1AN	HIPK1	HIPK2
HIVEP1	HM13	HMGA1	HNRNPA1
HNRNPA3	HNRNPF	HNRNPUL2	HPCAL4
HSF2	IL6ST	IMPDH1	INSIG2
INTS6	IPO7	ISL1	ITCH
ITM2C	ITPR2	KANK2	KCNAB1
KCNH1	KDM2A	KDM5C	KDM6B
KIAA0930	KIF1A	KIF1B	KIF3A
KLF12	KLF6	KLHDC3	KLHL24
KLHL5	KMO	KPNA1	KPNA4
KPNA6	KRIT1	LAMP1	LAMTOR3
LCOR	LHFPL2	LHFPL4	LIN7C
LMBRD1	LMO3	LPHN1	LRCH1
LRP8	LRRC59	LRRC8D	LSAMP
LUC7L3	M6PR	MAP1B	MAP3K13

MAP3K2	MAP3K3	MAP4	MAP4K4
MAP7D1	MAPK1IP1L	MAPRE2	Mar-05
MARCKS	MARK2	MAT2A	MBTD1
MCC	MCL1	MCRS1	MED1
MED13L	MED17	MED29	MEGF9
MEIS1	MEIS2	METTL8	MEX3A
MIER1	MIER3	MKLN1	MLL2
MLL3	MLL4	MLLT4	MLLT6
MRPL49	MTHFR	MTX3	MXD3
MXD4	MYSM1	NAA25	NAMPT
NAPG	NARG2	NDUFA4	NEFL
NEK9	NEO1	NFAT5	NFATC3
NFE2L1	NFIB	NFYA	NIPA1
NIPBL	NIT1	NKRF	NLGN4X
NLK	NLN	NONO	NOTCH3
NPEPPS	NR1H2	NR2C2	NRARP
NRBF2	NRCAM	NSD1	NUBPL
NUDT16	NUFIP2	ODC1	OLA1
ONECUT2	ORC2	ORMDL3	OSBPL7
OSBPL8	OST4	OTUD5	PAIP2
PAPD5	PAPOLG	PCBP2	PCNX
PDAP1	PDE3A	PDGFRA	PDGFRB
PDHA1	PDSS2	PFKM	PGM3
PHC3	PHF13	PHF17	PHF21A
PHIP	PICALM	PITPNB	PKN2
PMEPA1	POGK	POLDIP2	POLR1D
POP4	POU2F1	PPM1A	PPP1CB
PPP1CC	PPP1R11	PPP1R12A	PPP2R1A
PPP2R3A	PPP2R5C	PPP2R5D	PRCD
PRDM2	PRKAR2B	PRPF4	PRRC2B
PRRC2C	PSIP1	PTCH1	PTPN11
PTTG1IP	PUM1	PURB	PVRL1
QKI	QRICH1	QSER1	RAB11FIP4
RAB15	RAB1A	RAB22A	RAD23B
RALGAPB	RAP1A	RASA1	RASL11B
RBFOX2	RBM12	RBM14	RBM17
RBM39	RBM8A	RBMS1	RBMS2
RBMS3	RC3H1	RCC1	REEP3
RGAG4	RGS5	RHOF	RIC3
RIC8A	RICTOR	RIMBP2	RLIM
RNF141	RNF144A	RNF165	RNF169
RNF182	RNF20	RNF41	RNF44
RNF8	RORA	RPN2	RRP15
RTN3	RYK	SBK1	SBNO1
SDC1	SEC62	SEC63	SECISBP2L
SEPN1	Sep-10	Sep-11	Sep-06
SERBP1	SERTAD2	SET	SETD6
SGK494	SH3PXD2A	SIPA1L2	SKIV2L2

SKP1	SLAIN2	SLC11A2	SLC12A2
SLC25A25	SLC26A2	SLC2A1	SLC2A12
SLC30A7	SLC30A9	SLC35C2	SLC38A2
SLC44A1	SLC50A1	SLC6A6	SLC7A14
SMAD2	SMAD4	SMAD5	SMAD9
SMARCA5	SMC1A	SMCR8	SMEK1
SMG1	SMPD3	SNTB2	SNX27
SOCS4	SOCS7	SPAG9	SPARC
SPEN	SPNS2	SRCIN1	SRGAP1
SRPK1	SRRM2	SSH1	SSH2
SSPN	SSR1	SSR2	SSR3
SSX2IP	ST8SIA2	STAT3	STIM2
STK16	STK35	STRN	SUPT16H
SURF4	SV2A	SYNC	SYNCRIP
SYNPO2	SYNRG	SYP	TAF9B
TANC2	TAOK1	TBL1XR1	TCEA1
TCEANC2	TCEB3	TCF12	TCF19
TEAD1	TEAD3	TFAP2B	TFDP2
THAP5	THSD7A	THY1	TLK1
TM9SF3	TMBIM6	TMEM115	TMEM120B
TMF1	TNPO1	TNRC6A	TNRC6B
TNRC6C	TOB2	TPM4	TRAK2
TRIT1	TSPYL5	TTC28	TTYH3
TUB	TUSC2	TWF1	U2SURP
UBE2G2	UBE2N	UBE2QL1	UBE2R2
UBE2Z	UBN2	UBR5	UBTD2
UBTF	UGGT1	ULK1	UNC5C
UNK	UPF3B	URM1	USF2
USP34	USP37	USP38	USP45
USP47	USP7	VANGL2	VAT1
VAV2	VCP	VMA21	VPS13D
WAC	WASF2	WDR1	WDR82
WHSC1	XRRA1	XYLT1	YAF2
YIPF5	YKT6	YOD1	YPEL5
YTHDF3	YWHAQ	ZBTB4	ZBTB44
ZCCHC3	ZFAND3	ZFAND5	ZFHX3
ZFHX4	ZFP106	ZFP14	ZFP36L2
ZFP90	ZFP91	ZFYVE27	ZHX3
ZKSCAN1	ZMAT3	ZMYM2	ZMYND11
ZNF24	ZNF260	ZNF280D	ZNF395
ZNF398	ZNF618	ZNF644	ZNF654
ZNF704	ZNF710	ZNF711	ZNRF1
ZSWIM6			

BIBLIOGRAPHY

1.   Carroll AP, Tran N, Tooney PA, Cairns MJ (2012) Alternative mRNA fates identified in microRNA-associated transcriptome analysis. BMC Genomics 13: 561. doi:10.1186/1471-2164-13-561.

2.   Lugli G, Larson J, Demars MP, Smalheiser NR (2012) Primary microRNA precursor transcripts are localized at post-synaptic densities in adult mouse forebrain. J Neurochem: n/a–n/a. doi:10.1111/j.1471-4159.2012.07921.x.

3.   Lugli G, Larson J, Martone ME, Jones Y, Smalheiser NR (2005) Dicer and eIF2c are enriched at postsynaptic densities in adult mouse brain and are modified by neuronal activity in a calpain-dependent manner. J Neurochem 94: 896–905. doi:10.1111/j.1471-4159.2005.03224.x.

4.   Castanotto D, Lingeman R, Riggs AD, Rossi JJ (2009) CRM1 mediates nuclear-cytoplasmic shuttling of mature microRNAs. Proc Natl Acad Sci USA 106: 21655–21659. doi:10.1073/pnas.0912384106.

5.   Piriyapongsa J, Jordan IK, Conley AB, Ronan T, Smalheiser NR (2011) Transcription factor binding sites are highly enriched within microRNA precursor sequences. Biol Direct 25: 3181–3182. doi:10.1093/bioinformatics/btp554.

6.   Konopka G, Friedrich T, Davis-Turak J, Winden K, Oldham MC, et al. (2012) Human-Specific Transcriptional Networks in the Brain. Neuron 75: 601–617. doi:10.1016/j.neuron.2012.05.034.

7.   Schratt GM, Tuebing F, Nigh EA, Kane CG, Sabatini ME, et al. (2006) A brain-specific microRNA regulates dendritic spine development. Nature 439: 283–289. doi:10.1038/nature04367.

8.   Hansen T, Olsen L, Lindow M, Jakobsen KD, Ullum H, et al. (2007) Brain expressed microRNAs implicated in schizophrenia etiology. PLoS ONE 2: e873. doi:10.1371/journal.pone.0000873.

9.   Lin S, Cheung WKC, Chen S, Lu G, Wang Z, et al. (2010) Computational identification and characterization of primate-specific microRNAs in human genome. Comput Biol Chem 34: 232–241. doi:10.1016/j.compbiolchem.2010.08.001.

10.   Biedler JL, Helson L, Spengler BA (1973) Morphology and growth, tumorigenicity, and cytogenetics of human neuroblastoma cells in continuous culture. Cancer Res 33: 2643–2652.

11.   Påhlman S, Hoehner JC, Nånberg E, Hedborg F, Fagerström S, et al. (1995) Differentiation and survival influences of growth factors in human

neuroblastoma. Eur J Cancer 31A: 453–458.

12.   Redfern CP, Lovat PE, Malcolm AJ, Pearson AD (1994) Differential effects of 9-cis and all-trans retinoic acid on the induction of retinoic acid receptor-beta and cellular retinoic acid-binding protein II in human neuroblastoma cells. Biochem J 304 (Pt 1): 147–154.

13.   Encinas M, Iglesias M, Liu Y, Wang H, Muhaisen A, et al. (2000) Sequential treatment of SH-SY5Y cells with retinoic acid and brain-derived neurotrophic factor gives rise to fully differentiated, neurotrophic factor-dependent, human neuron-like cells. J Neurochem 75: 991–1003.

14.   Meyerson G, Pfenninger KH, Påhlman S (1992) A complex consisting of pp60c-src/pp60c-srcN and a 38 kDa protein is highly enriched in growth cones from differentiated SH-SY5Y neuroblastoma cells. J Cell Sci 103 (Pt 1): 233–243.

15.   Meyerson G, Parrow V, Gestblom C, Johansson I, Påhlman S (1994) Protein synthesis and mRNA in isolated growth cones from differentiating SH-SY5Y neuroblastoma cells. J Neurosci Res 37: 303–312. doi:10.1002/jnr.490370303.

16.   Goodall AR, Danks K, Walker JH, Ball SG, Vaughan PF (1997) Occurrence of two types of secretory vesicles in the human neuroblastoma SH-SY5Y. J Neurochem 68: 1542–1552.

17.   Ou XM, Partoens PM, Wang JM, Walker JH, Danks K, et al. (1998) The storage of noradrenaline, neuropeptide Y and chromogranins in and stoichiometric release from large dense cored vesicles of the undifferentiated human neuroblastoma cell line SH-SY5Y. Int J Mol Med 1: 105–112.

18.   Fauré J, Lachenal G, Court M, Hirrlinger J, Chatellard-Causse C, et al. (2006) Exosomes are released by cultured cortical neurones. Mol Cell Neurosci 31: 642–648. doi:10.1016/j.mcn.2005.12.003.

19.   Stoorvogel W (2012) Functional transfer of microRNA by exosomes. Blood 119: 646–648. doi:10.1182/blood-2011-11-389478.

20.   Koles K, Nunnari J, Korkut C, Barria R, Brewer C, et al. (2012) Mechanism of Evenness Interrupted (Evi)-Exosome Release at Synaptic Boutons. Journal of Biological Chemistry 287: 16820–16834. doi:10.1074/jbc.M112.342667.

21.   Beitzinger M, Peters L, Zhu JY, Kremmer E, Meister G (2007) Identification of human microRNA targets from isolated argonaute protein complexes. RNA Biol 4: 76–84.

22.   Rüdel S, Flatley A, Weinmann L, Kremmer E, Meister G (2008) A multifunctional human Argonaute2-specific monoclonal antibody. RNA 14: 1244–1253. doi:10.1261/rna.973808.

23. Höck J, Meister G (2008) The Argonaute protein family. Genome Biol 9: 210. doi:10.1186/gb-2008-9-2-210.

24. Jeffries CD, Fried HM, Perkins DO (2011) Nuclear and cytoplasmic localization of neural stem cell microRNAs. RNA 17: 675–686. doi:10.1261/rna.2006511.

25. Steward O, Levy WB (1982) Preferential localization of polyribosomes under the base of dendritic spines in granule cells of the dentate gyrus. J Neurosci 2: 284–291.

26. Rao A, Steward O (1991) Evidence that protein constituents of postsynaptic membrane specializations are locally synthesized: analysis of proteins synthesized within synaptosomes. J Neurosci 11: 2881–2895.

27. Steward O, Pollack A, Rao A (1991) Evidence that protein constituents of postsynaptic membrane specializations are locally synthesized: time course of appearance of recently synthesized proteins in synaptic junctions. J Neurosci Res 30: 649–660. doi:10.1002/jnr.490300408.

28. Torre ER, Steward O (1992) Demonstration of local protein synthesis within dendrites using a new cell culture system that permits the isolation of living axons and dendrites from their cell bodies. J Neurosci 12: 762–772.

29. Kang H, Schuman EM (1996) A requirement for local protein synthesis in neurotrophin-induced hippocampal synaptic plasticity. Science 273: 1402–1406.

30. Feig S, Lipton P (1993) Pairing the cholinergic agonist carbachol with patterned Schaffer collateral stimulation initiates protein synthesis in hippocampal CA1 pyramidal cell dendrites via a muscarinic, NMDA-dependent mechanism. J Neurosci 13: 1010–1021.

31. Goodman CS, Shatz CJ (1993) Developmental mechanisms that generate precise patterns of neuronal connectivity. Cell 72 Suppl: 77–98.

32. Lo DC (1995) Neurotrophic factors and synaptic plasticity. Neuron 15: 979–981.

33. Kang H, Jia LZ, Suh KY, Tang L, Schuman EM (1996) Determinants of BDNF-induced hippocampal synaptic plasticity: role of the Trk B receptor and the kinetics of neurotrophin delivery. Learn Mem 3: 188–196.

34. Dotti CG, Sullivan CA, Banker GA (1988) The establishment of polarity by hippocampal neurons in culture. J Neurosci 8: 1454–1468.

35. Kleiman R, Banker G, Steward O (1994) Development of subcellular mRNA compartmentation in hippocampal neurons in culture. J Neurosci 14: 1130–1140.

36.   Steward O, Wallace CS, Lyford GL, Worley PF (1998) Synaptic activation causes the mRNA for the IEG Arc to localize selectively near activated postsynaptic sites on dendrites. Neuron 21: 741–751.

37.   Dahm R, Kiebler M, Macchi P (2007) RNA localisation in the nervous system. Semin Cell Dev Biol 18: 216–223. doi:10.1016/j.semcdb.2007.01.009.

38.   Zhang HL, Eom T, Oleynikov Y, Shenoy SM, Liebelt DA, et al. (2001) Neurotrophin-induced transport of a beta-actin mRNP complex increases beta-actin levels and stimulates growth cone motility. Neuron 31: 261–275.

39.   Ainger K, Avossa D, Diana AS, Barry C, Barbarese E, et al. (1997) Transport and localization elements in myelin basic protein mRNA. J Cell Biol 138: 1077–1087.

40.   Huang F, Chotiner JK, Steward O (2005) The mRNA for elongation factor 1alpha is localized in dendrites and translated in response to treatments that induce long-term depression. J Neurosci 25: 7199–7209. doi:10.1523/JNEUROSCI.1779-05.2005.

41.   Blichenberg A, Schwanke B, Rehbein M, Garner CC, Richter D, et al. (1999) Identification of a cis-acting dendritic targeting element in MAP2 mRNAs. J Neurosci 19: 8818–8829.

42.   Mori Y, Imaizumi K, Katayama T, Yoneda T, Tohyama M (2000) Two cis-acting elements in the 3' untranslated region of alpha-CaMKII regulate its dendritic targeting. Nat Neurosci 3: 1079–1084. doi:10.1038/80591.

43.   Schratt GM, Nigh EA, Chen WG, Hu L, Greenberg ME (2004) BDNF regulates the translation of a select group of mRNAs by a mammalian target of rapamycin-phosphatidylinositol 3-kinase-dependent pathway during neuronal development. J Neurosci 24: 7366–7377. doi:10.1523/JNEUROSCI.1739-04.2004.

44.   Kim J, Krichevsky A, Grad Y, Hayes GD, Kosik KS, et al. (2004) Identification of many microRNAs that copurify with polyribosomes in mammalian neurons. Proc Natl Acad Sci USA 101: 360–365. doi:10.1073/pnas.2333854100.

45.   Zhu Y, Kalbfleisch T, Brennan MD, Li Y (2009) A MicroRNA gene is hosted in an intron of a schizophrenia-susceptibility gene. Schizophr Res 109: 86–89. doi:10.1016/j.schres.2009.01.022.

46.   Bicker S, Schratt G (2008) microRNAs: tiny regulators of synapse function in development and disease. J Cell Mol Med 12: 1466–1476. doi:10.1111/j.1582-4934.2008.00400.x.

47.   Filipowicz W, Bhattacharyya SN, Sonenberg N (2008) Mechanisms of post-transcriptional regulation by microRNAs: are the answers in sight? Nat Rev

Genet 9: 102–114. doi:10.1038/nrg2290.

48.   Konecna A, Heraud J, Schoderboeck L, Raposo A, Kiebler M (2009) What are the roles of microRNAs at the mammalian synapse? Neurosci Lett. doi:10.1016/j.neulet.2009.06.050.

49.   Bartel DP (2009) MicroRNAs: target recognition and regulatory functions. Cell 136: 215–233. doi:10.1016/j.cell.2009.01.002.

50.   Jinek M, Doudna JA (2009) A three-dimensional view of the molecular machinery of RNA interference. Nature 457: 405–412. doi:10.1038/nature07755.

51.   Potenza N, Papa U, Russo A (2009) Differential expression of Dicer and Argonaute genes during the differentiation of human neuroblastoma cells. Cell Biol Int 33: 734–738. doi:10.1016/j.cellbi.2009.04.002.

52.   Barbato C, Ciotti MT, Serafino A, Calissano P, Cogoni C (2007) Dicer expression and localization in post-mitotic neurons. Brain Res 1175: 17–27. doi:10.1016/j.brainres.2007.07.088.

53.   Beveridge NJ, Tooney PA, Carroll AP, Tran N, Cairns MJ (2009) Down-regulation of miR-17 family expression in response to retinoic acid induced neuronal differentiation. Cell Signal 21: 1837–1845. doi:10.1016/j.cellsig.2009.07.019.

54.   Le MTN, Xie H, Zhou B, Chia PH, Rizk P, et al. (2009) MicroRNA-125b promotes neuronal differentiation in human cells by repressing multiple targets. Mol Cell Biol 29: 5290–5305. doi:10.1128/MCB.01694-08.

55.   Giraldez AJ, Cinalli RM, Glasner ME, Enright AJ, Thomson JM, et al. (2005) MicroRNAs regulate brain morphogenesis in zebrafish. Science 308: 833–838. doi:10.1126/science.1109020.

56.   De Pietri Tonelli D, Pulvers JN, Haffner C, Murchison EP, Hannon GJ, et al. (2008) miRNAs are essential for survival and differentiation of newborn neurons but not for expansion of neural progenitors during early neurogenesis in the mouse embryonic neocortex. Development 135: 3911–3921. doi:10.1242/dev.025080.

57.   Berdnik D, Fan AP, Potter CJ, Luo L (2008) MicroRNA processing pathway regulates olfactory neuron morphogenesis. Curr Biol 18: 1754–1759. doi:10.1016/j.cub.2008.09.045.

58.   Li X, Cassidy JJ, Reinke CA, Fischboeck S, Carthew RW (2009) A microRNA imparts robustness against environmental fluctuation during development. Cell 137: 273–282. doi:10.1016/j.cell.2009.01.058.

59.   Stark KL, Xu B, Bagchi A, Lai W-S, Liu H, et al. (2008) Altered brain microRNA biogenesis contributes to phenotypic deficits in a 22q11-deletion mouse model. Nat Genet 40: 751–760. doi:10.1038/ng.138.

60.   Beveridge NJ, Gardiner E, Carroll AP, Tooney PA, Cairns MJ (2010) Schizophrenia is associated with an increase in cortical microRNA biogenesis. Mol Psychiatry 15: 1176–1189. doi:10.1038/mp.2009.84.

61.   Gardiner E, Beveridge NJ, Wu JQ, Carr V, Scott RJ, et al. (2012) Imprinted DLK1-DIO3 region of 14q32 defines a schizophrenia-associated miRNA signature in peripheral blood mononuclear cells. Mol Psychiatry 17: 827–840. doi:10.1038/mp.2011.78.

62.   Santarelli DM, Beveridge NJ, Tooney PA, Cairns MJ (2011) Upregulation of dicer and microRNA expression in the dorsolateral prefrontal cortex Brodmann area 46 in schizophrenia. Biol Psychiatry 69: 180–187. doi:10.1016/j.biopsych.2010.09.030.

63.   Cheng L-C, Pastrana E, Tavazoie M, Doetsch F (2009) miR-124 regulates adult neurogenesis in the subventricular zone stem cell niche. Nat Neurosci 12: 399–408. doi:10.1038/nn.2294.

64.   Yoo A, Staahl B, Chen L, Crabtree G (2009) MicroRNA-mediated switching of chromatin-remodelling complexes in neural development. Nature. doi:10.1038/nature08139.

65.   Xu X-L, Li Y, Wang F, Gao F-B (2008) The steady-state level of the nervous-system-specific microRNA-124a is regulated by dFMR1 in Drosophila. J Neurosci 28: 11883–11889. doi:10.1523/JNEUROSCI.4114-08.2008.

66.   Lugli G, Torvik VI, Larson J, Smalheiser NR (2008) Expression of microRNAs and their precursors in synaptic fractions of adult mouse forebrain. J Neurochem 106: 650–661. doi:10.1111/j.1471-4159.2008.05413.x.

67.   Siegel G, Obernosterer G, Fiore R, Oehmen M, Bicker S, et al. (2009) A functional screen implicates microRNA-138-dependent regulation of the depalmitoylation enzyme APT1 in dendritic spine morphogenesis. Nat Cell Biol 11: 705–716. doi:10.1038/ncb1876.

68.   Edbauer D, Neilson JR, Foster KA, Wang C-F, Seeburg DP, et al. (2010) Regulation of Synaptic Structure and Function by FMRP-Associated MicroRNAs miR-125b and miR-132. Neuron 65: 373–384. doi:10.1016/j.neuron.2010.01.005.

69.   Fiore R, Khudayberdiev S, Christensen M, Siegel G, Flavell SW, et al. (2009) Mef2-mediated transcription of the miR379-410 cluster regulates activity-dependent dendritogenesis by fine-tuning Pumilio2 protein levels. EMBO J 28: 697–710. doi:10.1038/emboj.2009.10.

70.   Rajasethupathy P, Fiumara F, Sheridan R, Betel D, Puthanveettil SV, et al. (2009) Characterization of small RNAs in Aplysia reveals a role for miR-124 in constraining synaptic plasticity through CREB. Neuron 63: 803–817. doi:10.1016/j.neuron.2009.05.029.

71.   Ashraf SI, McLoon AL, Sclarsic SM, Kunes S (2006) Synaptic protein synthesis associated with memory is regulated by the RISC pathway in Drosophila. Cell 124: 191–205. doi:10.1016/j.cell.2005.12.017.

72.   Eulalio A, Behm-Ansmant I, Izaurralde E (2007) P bodies: at the crossroads of post-transcriptional pathways. Nat Rev Mol Cell Biol 8: 9–22. doi:10.1038/nrm2080.

73.   Jakymiw A, Pauley KM, Li S, Ikeda K, Lian S, et al. (2007) The role of GW/P-bodies in RNA processing and silencing. J Cell Sci 120: 1317–1323. doi:10.1242/jcs.03429.

74.   Eulalio A, Behm-Ansmant I, Schweizer D, Izaurralde E (2007) P-body formation is a consequence, not the cause, of RNA-mediated gene silencing. Mol Cell Biol 27: 3970–3981. doi:10.1128/MCB.00128-07.

75.   Kiebler MA, Bassell GJ (2006) Neuronal RNA granules: movers and makers. Neuron 51: 685–690. doi:10.1016/j.neuron.2006.08.021.

76.   Katahira J, Miki T, Takano K, Maruhashi M, Uchikawa M, et al. (2008) Nuclear RNA export factor 7 is localized in processing bodies and neuronal RNA granules through interactions with shuttling hnRNPs. Nucleic Acids Res 36: 616–628. doi:10.1093/nar/gkm556.

77.   Barbee SA, Estes PS, Cziko A-M, Hillebrand J, Luedeman RA, et al. (2006) Staufen- and FMRP-containing neuronal RNPs are structurally and functionally related to somatic P bodies. Neuron 52: 997–1009. doi:10.1016/j.neuron.2006.10.028.

78.   Zeitelhofer M, Karra D, Macchi P, Tolino M, Thomas S, et al. (2008) Dynamic interaction between P-bodies and transport ribonucleoprotein particles in dendrites of mature hippocampal neurons. J Neurosci 28: 7555–7562. doi:10.1523/JNEUROSCI.0104-08.2008.

79.   Kedersha N, Stoecklin G, Ayodele M, Yacono P, Lykke-Andersen J, et al. (2005) Stress granules and processing bodies are dynamically linked sites of mRNP remodeling. J Cell Biol 169: 871–884. doi:10.1083/jcb.200502088.

80.   Hong X, Hammell M, Ambros V, Cohen S (2009) Immunopurification of Ago1 miRNPs selects for a distinct class of microRNA targets. Proc Natl Acad Sci USA. doi:10.1073/pnas.0908149106.

81.   Cougot N, Bhattacharyya SN, Tapia-Arancibia L, Bordonné R, Filipowicz W, et al. (2008) Dendrites of mammalian neurons contain specialized P-body-like structures that respond to neuronal activation. J Neurosci 28: 13793–13804. doi:10.1523/JNEUROSCI.4155-08.2008.

82.   Goldie BJ, Cairns MJ (2011) Post-Transcriptional Trafficking and Regulation of Neuronal Gene Expression. Mol Neurobiol. doi:10.1007/s12035-011-8222-0.

83. Krichevsky AM, Sonntag K-C, Isacson O, Kosik KS (2006) Specific microRNAs modulate embryonic stem cell-derived neurogenesis. 24: 857–864. doi:10.1634/stemcells.2005-0441.

84. Smirnova L, Gräfe A, Seiler A, Schumacher S, Nitsch R, et al. (2005) Regulation of miRNA expression during neural cell specification. Eur J Neurosci 21: 1469–1477. doi:10.1111/j.1460-9568.2005.03978.x.

85. Bayés À, van de Lagemaat LN, Collins MO, Croning MDR, Whittle IR, et al. (2010) Characterization of the proteome, diseases and evolution of the human postsynaptic density. Nat Neurosci 14: 19–21. doi:10.1038/nn.2719.

86. Somel M, Liu X, Tang L, Yan Z, Hu H, et al. (2011) MicroRNA-Driven Developmental Remodeling in the Brain Distinguishes Humans from Other Primates. PLoS Biol 9: e1001214. doi:10.1371/journal.pbio.1001214.g006.

87. Stio M, Celli A, Treves C (2001) Synergistic anti-proliferative effects of vitamin D derivatives and 9-cis retinoic acid in SH-SY5Y human neuroblastoma cells. J Steroid Biochem Mol Biol 77: 213–222.

88. Sidell N, Lucas CA, Kreutzberg GW (1984) Regulation of acetylcholinesterase activity by retinoic acid in a human neuroblastoma cell line. Exp Cell Res 155: 305–309.

89. Sarkanen J-R, Nykky J, Siikanen J, Selinummi J, Ylikomi T, et al. (2007) Cholesterol supports the retinoic acid-induced synaptic vesicle formation in differentiating human SH-SY5Y neuroblastoma cells. J Neurochem 102: 1941–1952. doi:10.1111/j.1471-4159.2007.04676.x.

90. McAllister AK, Lo DC, Katz LC (1995) Neurotrophins regulate dendritic growth in developing visual cortex. Neuron 15: 791–803.

91. Righi M, Tongiorgi E, Cattaneo A (2000) Brain-derived neurotrophic factor (BDNF) induces dendritic targeting of BDNF and tyrosine kinase B mRNAs in hippocampal neurons through a phosphatidylinositol-3 kinase-dependent pathway. J Neurosci 20: 3165–3174.

92. Tongiorgi E, Righi M, Cattaneo A (1997) Activity-dependent dendritic targeting of BDNF and TrkB mRNAs in hippocampal neurons. J Neurosci 17: 9492–9505.

93. Miyata S, Mori Y, Fujiwara T, Ikenaka K, Matsuzaki S, et al. (2005) Local protein synthesis by BDNF is potentiated in hippocampal neurons exposed to ephrins. Brain Res Mol Brain Res 134: 333–337. doi:10.1016/j.molbrainres.2004.10.034.

94. Kaplan DR, Matsumoto K, Lucarelli E, Thiele CJ (1993) Induction of TrkB by retinoic acid mediates biologic responsiveness to BDNF and differentiation of human neuroblastoma cells. Eukaryotic Signal Transduction Group. Neuron 11: 321–331.

95. Påhlman S, Ruusala AI, Abrahamsson L, Odelstad L, Nilsson K (1983) Kinetics and concentration effects of TPA-induced differentiation of cultured human neuroblastoma cells. Cell Differ 12: 165–170.

96. Huang D, Sherman B, Lempicki R (2008) Bioinformatics enrichment tools: paths toward the comprehensive functional analysis of large gene lists. Nucleic Acids Res. doi:10.1093/nar/gkn923.

97. Luchtman DW, Song C (2010) Why SH-SY5Y cells should be differentiated. Neurotoxicology 31: 164–5–authorreply165–6. doi:10.1016/j.neuro.2009.10.015.

98. Cheung Y-T, Lau WK-W, Yu M-S, Lai CS-W, Yeung S-C, et al. (2009) Effects of all-trans-retinoic acid on human SH-SY5Y neuroblastoma as in vitro model in neurotoxicity research. Neurotoxicology 30: 127–135. doi:10.1016/j.neuro.2008.11.001.

99. Labelle C, Leclerc N (2000) Exogenous BDNF, NT-3 and NT-4 differentially regulate neurite outgrowth in cultured hippocampal neurons. Brain Res Dev Brain Res 123: 1–11.

100. Bamji SX, Rico B, Kimes N, Reichardt LF (2006) BDNF mobilizes synaptic vesicles and enhances synapse formation by disrupting cadherin-beta-catenin interactions. J Cell Biol 174: 289–299. doi:10.1083/jcb.200601087.

101. Luikart BW, Nef S, Virmani T, Lush ME, Liu Y, et al. (2005) TrkB has a cell-autonomous role in the establishment of hippocampal Schaffer collateral synapses. J Neurosci 25: 3774–3786. doi:10.1523/JNEUROSCI.0041-05.2005.

102. Cheng P-L, Song A-H, Wong Y-H, Wang S, Zhang X, et al. (2011) Self-amplifying autocrine actions of BDNF in axon development. Proceedings of the National Academy of Sciences 108: 18430–18435. doi:10.1073/pnas.1115907108.

103. Dong Q, Ji Y-S, Cai C, Chen Z-Y (2012) LIM kinase 1 (LIMK1) interacts with tropomyosin-related kinase B (TrkB) and Mediates brain-derived neurotrophic factor (BDNF)-induced axonal elongation. Journal of Biological Chemistry 287: 41720–41731. doi:10.1074/jbc.M112.405415.

104. Agholme L, Lindström T, Kågedal K, Marcusson J, Hallbeck M (2010) An in vitro model for neuroscience: differentiation of SH-SY5Y cells into cells with morphological and biochemical characteristics of mature neurons. J Alzheimers Dis 20: 1069–1082. doi:10.3233/JAD-2010-091363.

105. Hüttelmaier S, Zenklusen D, Lederer M, Dictenberg J, Lorenz M, et al. (2005) Spatial regulation of beta-actin translation by Src-dependent phosphorylation of ZBP1. Nature 438: 512–515. doi:10.1038/nature04115.

106. Caudy AA, Myers M, Hannon GJ, Hammond SM (2002) Fragile X-related

protein and VIG associate with the RNA interference machinery. Genes Dev 16: 2491–2496. doi:10.1101/gad.1025202.

107.   Eulalio A, Huntzinger E, Izaurralde E (2008) Getting to the root of miRNA-mediated gene silencing. Cell 132: 9–14. doi:10.1016/j.cell.2007.12.024.

108.   Banerjee S, Neveu P, Kosik KS (2009) A coordinated local translational control point at the synapse involving relief from silencing and MOV10 degradation. Neuron 64: 871–884. doi:10.1016/j.neuron.2009.11.023.

109.   Géraldine M, Stéphanie D, Bénédicte L, Isabelle D, Monique L, et al. (2010) DHA enhances the noradrenaline release by SH-SY5Y cells. Neurochem Int 56: 94–100. doi:10.1016/j.neuint.2009.09.006.

110.   Huang YY, Kandel ER (1994) Recruitment of long-lasting and protein kinase A-dependent long-term potentiation in the CA1 region of hippocampus requires repeated tetanization. Learn Mem 1: 74–82.

111.   Miranda KC, Bond DT, McKee M, Skog J, Păunescu TG, et al. (2010) Nucleic acids within urinary exosomes/microvesicles are potential biomarkers for renal disease. Kidney Int 78: 191–199. doi:10.1038/ki.2010.106.

112.   Dun MD, Anderson AL, Bromfield EG, Asquith KL, Emmett B, et al. (2012) Investigation of the expression and functional significance of the novel mouse sperm protein, a disintegrin and metalloprotease with thrombospondin type 1 motifs number 10 (ADAMTS10). Int J Androl 35: 572–589. doi:10.1111/j.1365-2605.2011.01235.x.

113.   Dun MD, Smith ND, Baker MA, Lin M, Aitken RJ, et al. (2011) The chaperonin containing TCP1 complex (CCT/TRiC) is involved in mediating sperm-oocyte interaction. Journal of Biological Chemistry 286: 36875–36887. doi:10.1074/jbc.M110.188888.

114.   Huang DW, Sherman BT, Tan Q, Kir J, Liu D, et al. (2007) DAVID Bioinformatics Resources: expanded annotation database and novel algorithms to better extract biology from large gene lists. Nucleic Acids Res 35: W169–W175. doi:10.1093/nar/gkm415.

115.   Lakkaraju A, Rodriguez-Boulan E (2008) Itinerant exosomes: emerging roles in cell and tissue polarity. Trends Cell Biol 18: 199–209. doi:10.1016/j.tcb.2008.03.002.

116.   Théry C, Zitvogel L, Amigorena S (2002) Exosomes: composition, biogenesis and function. Nat Rev Immunol 2: 569–579. doi:10.1038/nri855.

117.   Kawakami S-I, Muramoto K, Ichikawa M, Kuroda Y (2003) Localization of microtubule-associated protein (MAP) 1B in the postsynaptic densities of the rat cerebral cortex. Cellular and molecular neurobiology 23: 887–894.

118.   Kitamura C, Shirai K, Inoue M, Tashiro T (2007) Changes in the subcellular

distribution of microtubule-associated protein 1B during synaptogenesis of cultured rat cortical neurons. Cellular and molecular neurobiology 27: 57–73. doi:10.1007/s10571-006-9117-x.

119.   Tortosa E, Montenegro-Venegas C, Benoist M, Härtel S, González-Billault C, et al. (2011) Microtubule-associated protein 1B (MAP1B) is required for dendritic spine development and synaptic maturation. Journal of Biological Chemistry 286: 40638–40648. doi:10.1074/jbc.M111.271320.

120.   Zervas M, Opitz T, Edelmann W, Wainer B, Kucherlapati R, et al. (2005) Impaired hippocampal long-term potentiation in microtubule-associated protein 1B-deficient mice. J Neurosci Res 82: 83–92. doi:10.1002/jnr.20624.

121.   Noam Y, Phan L, McClelland S, Manders EM, Ehrengruber MU, et al. (2012) Distinct regional and subcellular localization of the actin-binding protein filamin A in the mature rat brain. J Comp Neurol 520: 3013–3034. doi:10.1002/cne.23106.

122.   Arbuckle MI, Komiyama NH, Delaney A, Coba M, Garry EM, et al. (2010) The SH3 domain of postsynaptic density 95 mediates inflammatory pain through phosphatidylinositol-3-kinase recruitment. EMBO Rep 11: 473–478. doi:10.1038/embor.2010.63.

123.   Konopka W, Kiryk A, Novak M, Herwerth M, Parkitna JR, et al. (2010) MicroRNA loss enhances learning and memory in mice. J Neurosci 30: 14835–14842. doi:10.1523/JNEUROSCI.3030-10.2010.

124.   Krol J, Busskamp V, Markiewicz I, Stadler MB, Ribi S, et al. (2010) Characterizing light-regulated retinal microRNAs reveals rapid turnover as a common property of neuronal microRNAs. Cell 141: 618–631. doi:10.1016/j.cell.2010.03.039.

125.   Hillebrand J, Pan K, Kokaram A, Barbee S, Parker R, et al. (2010) The Me31B DEAD-Box Helicase Localizes to Postsynaptic Foci and Regulates Expression of a CaMKII Reporter mRNA in Dendrites of Drosophila Olfactory Projection Neurons. Front Neural Circuits 4: 121. doi:10.3389/fncir.2010.00121.

126.   Smalheiser NR (2007) Exosomal transfer of proteins and RNAs at synapses in the nervous system. Biol Direct 2: 35. doi:10.1186/1745-6150-2-35.

127.   Valadi H, Ekström K, Bossios A, Sjöstrand M, Lee JJ, et al. (2007) Exosome-mediated transfer of mRNAs and microRNAs is a novel mechanism of genetic exchange between cells. Nat Cell Biol 9: 654–659. doi:10.1038/ncb1596.

128.   Nazarenko I, Rana S, Baumann A, McAlear J, Hellwig A, et al. (2010) Cell surface tetraspanin Tspan8 contributes to molecular pathways of exosome-induced endothelial cell activation. Cancer Res 70: 1668–1678. doi:10.1158/0008-5472.CAN-09-2470.

129.   Park M, Salgado JM, Ostroff L, Helton TD, Robinson CG, et al. (2006) Plasticity-induced growth of dendritic spines by exocytic trafficking from recycling endosomes. Neuron 52: 817–830. doi:10.1016/j.neuron.2006.09.040.

130.   Morel L, Regan M, Higashimori H, Ng SK, Esau C, et al. (2013) Neuronal Exosomal miRNA-dependent Translational Regulation of Astroglial Glutamate Transporter GLT1. Journal of Biological Chemistry 288: 7105–7116. doi:10.1074/jbc.M112.410944.

131.   Korkut C, Li Y, Koles K, Brewer C, Ashley J, et al. (2013) Regulation of Postsynaptic Retrograde Signaling by Presynaptic Exosome Release. Neuron 77: 1039–1046. doi:10.1016/j.neuron.2013.01.013.

132.   Sheen VL, Feng Y, Graham D, Takafuta T, Shapiro SS, et al. (2002) Filamin A and Filamin B are co-expressed within neurons during periods of neuronal migration and can physically interact. Hum Mol Genet 11: 2845–2854.

133.   Lécuyer E, Yoshida H, Parthasarathy N, Alm C, Babak T, et al. (2007) Global analysis of mRNA localization reveals a prominent role in organizing cellular architecture and function. Cell 131: 174–187. doi:10.1016/j.cell.2007.08.003.

134.   Makeyev EV, Zhang J, Carrasco MA, Maniatis T (2007) The MicroRNA miR-124 promotes neuronal differentiation by triggering brain-specific alternative pre-mRNA splicing. Mol Cell 27: 435–448. doi:10.1016/j.molcel.2007.07.015.

135.   Politz JCR, Hogan EM, Pederson T (2009) MicroRNAs with a nucleolar location. RNA 15: 1705–1715. doi:10.1261/rna.1470409.

136.   Hwang H-W, Wentzel EA, Mendell JT (2007) A hexanucleotide element directs microRNA nuclear import. Science 315: 97–100. doi:10.1126/science.1136235.

137.   Parisi C, Giorgi C, Batassa EM, Braccini L, Maresca G, et al. (2011) Ago1 and Ago2 differentially affect cell proliferation, motility and apoptosis when overexpressed in SH-SY5Y neuroblastoma cells. FEBS Lett 585: 2965–2971. doi:10.1016/j.febslet.2011.08.003.

138.   Castanotto D, Lingeman R, Riggs AD, Rossi JJ (2009) CRM1 mediates nuclear-cytoplasmic shuttling of mature microRNAs. Proc Natl Acad Sci USA {106}: {21655–21659}. doi:{10.1073/pnas.0912384106}.

139.   Hansen TB, Wiklund ED, Bramsen JB, Villadsen SB, Statham AL, et al. (2011) miRNA-dependent gene silencing involving Ago2-mediated cleavage of a circular antisense RNA. EMBO J 30: 4414–4422. doi:10.1038/emboj.2011.359.

140.   Janas MM, Khaled M, Schubert S, Bernstein JG, Golan D, et al. (2011) Feed-Forward Microprocessing and Splicing Activities at a MicroRNA–

Containing Intron. PLoS Genetics 7: e1002330.
doi:10.1371/journal.pgen.1002330.g005.

141.   Ballarino M, Pagano F, Girardi E, Morlando M, Cacchiarelli D, et al. (2009)
Coupled RNA processing and transcription of intergenic primary miRNAs.
Mol Cell Biol. doi:10.1128/MCB.00664-09.

142.   Goldie BJ, Dun MD, Lin M, Smith ND, Verrills NM, et al. (2014) Activity-
associated miRNA are packaged in Map1b-enriched exosomes released
from depolarized neurons. Nucleic Acids Res. doi:10.1093/nar/gku594.

143.   Meister G (2013) Argonaute proteins: functional insights and emerging
roles. Nat Rev Genet 14: 447–459. doi:10.1038/nrg3462.

144.   Rybak A, Fuchs H, Smirnova L, Brandt C, Pohl EE, et al. (2008) A feedback
loop comprising lin-28 and let-7 controls pre-let-7 maturation during
neural stem-cell commitment. Nat Cell Biol 10: 987–993.
doi:10.1038/ncb1759.

145.   Khudayberdiev SA, Zampa F, Rajman M, Schratt G (2013) A comprehensive
characterization of the nuclear microRNA repertoire of post-mitotic
neurons. Front Mol Neurosci 6: 43. doi:10.3389/fnmol.2013.00043.

146.   Komatsu M, Li HO, Tsutsui H, Itakura K, Matsumura M, et al. (1997) MAZ, a
Myc-associated zinc finger protein, is essential for the ME1a1-mediated
expression of the c-myc gene during neuroectodermal differentiation of
P19 cells. Oncogene 15: 1123–1131. doi:10.1038/sj.onc.1201283.

147.   Tsutsui H, Geltinger C, Murata T, Itakura K, Wada T, et al. (1999) The DNA-
binding and transcriptional activities of MAZ, a myc-associated zinc finger
protein, are regulated by casein kinase II. Biochem Biophys Res Commun
262: 198–205. doi:10.1006/bbrc.1999.1130.

148.   Bossone SA, Asselin C, Patel AJ, Marcu KB (1992) MAZ, a zinc finger
protein, binds to c-MYC and C2 gene sequences regulating transcriptional
initiation and termination. Proc Natl Acad Sci USA 89: 7452–7456.

149.   Höck J, Weinmann L, Ender C, Rüdel S, Kremmer E, et al. (2007) Proteomic
and functional analysis of Argonaute-containing mRNA-protein complexes
in human cells. EMBO Rep 8: 1052–1060. doi:10.1038/sj.embor.7401088.

150.   Cassola A, Noé G, Frasch AC (2010) RNA recognition motifs involved in
nuclear import of RNA-binding proteins. RNA Biol 7: 339–344.

151.   Meseguer S, Mudduluru G, Escamilla JM, Allgayer H, Barettino D (2010)
Micro-RNAs-10a and -10b contribute to retinoic acid-induced
differentiation of neuroblastoma cells and target the alternative splicing
regulatory factor SFRS1 (SF2/ASF). Journal of Biological Chemistry.
doi:10.1074/jbc.M110.167817.

152.   Wu H, Sun S, Tu K, Gao Y, Xie B, et al. (2010) A splicing-independent

function of SF2/ASF in microRNA processing. Mol Cell 38: 67–77. doi:10.1016/j.molcel.2010.02.021.

153. Chen L (2009) A global comparison between nuclear and cytosolic transcriptomes reveals differential compartmentalization of alternative transcript isoforms. Nucleic Acids Res. doi:10.1093/nar/gkp1136.

154. Guidi M, Muiños-Gimeno M, Kagerbauer B, Martí E, Estivill X, et al. (2010) Overexpression of miR-128 specifically inhibits the truncated isoform of NTRK3 and upregulates BCL2 in SH-SY5Y neuroblastoma cells. BMC Mol Biol 11: 95. doi:10.1186/1471-2199-11-95.

155. Laneve P, Di Marcotullio L, Gioia U, Fiori ME, Ferretti E, et al. (2007) The interplay between microRNAs and the neurotrophin receptor tropomyosin-related kinase C controls proliferation of human neuroblastoma cells. Proc Natl Acad Sci USA 104: 7957–7962. doi:10.1073/pnas.0700071104.

156. Kim DH, Villeneuve LM, Morris KV, Rossi JJ (2006) Argonaute-1 directs siRNA-mediated transcriptional gene silencing in human cells. Nat Struct Mol Biol 13: 793–797. doi:10.1038/nsmb1142.

157. Caudron-Herger M, Müller-Ott K, Mallm J-P, Marth C, Schmidt U, et al. (2011) Coding RNAs with a non-coding function: Maintenance of open chromatin structure. nucleus 2: 410–424. doi:10.4161/nucl.2.5.17736.

158. Baltz AG, Munschauer M, Schwanhäusser B, Vasile A, Murakawa Y, et al. (2012) The mRNA-bound proteome and its global occupancy profile on protein-coding transcripts. Mol Cell 46: 674–690. doi:10.1016/j.molcel.2012.05.021.

159. Castello A, Fischer B, Eichelbaum K, Horos R, Beckmann BM, et al. (2012) Insights into RNA biology from an atlas of mammalian mRNA-binding proteins. Cell 149: 1393–1406. doi:10.1016/j.cell.2012.04.031.

160. Ugai H, Li HO, Komatsu M, Tsutsui H, Song J, et al. (2001) Interaction of Myc-associated zinc finger protein with DCC, the product of a tumor-suppressor gene, during the neural differentiation of P19 EC cells. Biochem Biophys Res Commun 286: 1087–1097. doi:10.1006/bbrc.2001.5469.

161. Diederichs S, Haber DA (2007) Dual Role for Argonautes in MicroRNA Processing and Posttranscriptional Regulation of MicroRNA Expression. Cell 131: 1097–1108. doi:10.1016/j.cell.2007.10.032.

162. Yang JS, Maurin T, Lai EC (2012) Functional parameters of Dicer-independent microRNA biogenesis. RNA 18: 945–957. doi:10.1261/rna.032938.112.

163. Schaefer A, Im HI, Veno MT, Fowler CD, Min A, et al. (2010) Argonaute 2 in dopamine 2 receptor-expressing neurons regulates cocaine addiction. Journal of Experimental Medicine 207: 1843–1851. doi:10.1038/ng1744.

164. Wang Y, Zhu W, Levy DE (2006) Nuclear and cytoplasmic mRNA quantification by SYBR green based real-time RT-PCR. Methods 39: 356–362. doi:10.1016/j.ymeth.2006.06.010.

165. Smyth GK (2004) Linear models and empirical bayes methods for assessing differential expression in microarray experiments. Stat Appl Genet Mol Biol 3: Article3. doi:10.2202/1544-6115.1027.

166. Kim D, Pertea G, Trapnell C, Pimentel H, Kelley R, et al. (2013) TopHat2: accurate alignment of transcriptomes in the presence of insertions, deletions and gene fusions. Genome Biol 14: R36. doi:10.1186/gb-2013-14-4-r36.

167. Anders S, Pyl PT, Huber W (2014) HTSeq–A Python framework to work with high-throughput sequencing data. bioRxiv.

168. Chang JT, Nevins JR (2006) GATHER: a systems approach to interpreting genomic signatures. Bioinformatics 22: 2926–2933. doi:10.1093/bioinformatics/btl483.

169. Lau CS, Wong DTW (2012) Breast Cancer Exosome-like Microvesicles and Salivary Gland Cells Interplay Alters Salivary Gland Cell-Derived Exosome-like Microvesicles In Vitro. PLoS ONE 7: e33037. doi:10.1371/journal.pone.0033037.

170. Alvarez-Erviti L, Seow Y, Yin H, Betts C, Lakhal S, et al. (2011) Delivery of siRNA to the mouse brain by systemic injection of targeted exosomes. Nat Biotechnol: 1–7. doi:10.1038/nbt.1807.

171. Shaw G, Morse S, Ararat M, Graham FL (2002) Preferential transformation of human neuronal cells by human adenoviruses and the origin of HEK 293 cells. FASEB J 16: 869–871. doi:10.1096/fj.01-0995fje.

172. Shan G, Li Y, Zhang J, Li W, Szulwach KE, et al. (2008) A small molecule enhances RNA interference and promotes microRNA processing. Nat Biotechnol 26: 933–940. doi:10.1038/nbt.1481.

173. Kondo T, Asai M, Tsukita K, Kutoku Y, Ohsawa Y, et al. (2013) Modeling Alzheimer's disease with iPSCs reveals stress phenotypes associated with intracellular Aβ and differential drug responsiveness. Cell Stem Cell 12: 487–496. doi:10.1016/j.stem.2013.01.009.

174. Egawa N, Kitaoka S, Tsukita K, Naitoh M, Takahashi K, et al. (2012) Drug screening for ALS using patient-specific induced pluripotent stem cells. Sci Transl Med 4: 145ra104. doi:10.1126/scitranslmed.3004052.

175. Morizane A, Doi D, Kikuchi T, Okita K, Hotta A, et al. (2013) Direct Comparison of Autologous and Allogeneic Transplantation of iPSC-Derived Neural Cells in the Brain of a Nonhuman Primate. Stem Cell Reports 1: 283–292. doi:10.1016/j.stemcr.2013.08.007.

176.   Lee RC, Ambros V (2001) An extensive class of small RNAs in Caenorhabditis elegans. Science 294: 862–864. doi:10.1126/science.1065329.